UNIVERSITY
of
GLASGOW

Exploring links between parasitism, plasticity, metabolism and microbiome in the European eel, *Anguilla anguilla*.

A thesis submitted for the degree of Doctor of Philosophy

Michele De Noia

Institute of Biodiversity, Animal Health and Comparative Medicine, School of Medical, Veterinary and Life Sciences, University of Glasgow, G12 8QQ

January 2022

Table of Contents

List of Tables

List of Figures

Acknowledgement

My first thank you needs to go to my supervisor Martin Llewellyn. We started our journey together long 7 years ago, meeting a lost Italian in the clyster (also known as cloister) of a genetic building in Bangor and dreaming about ambitious projects. Since that day he not only became my supervisor but also my scientific mentor and friend. I cannot thank him enough for the support, help, learning experiences and adventures we lived together. He gave me the courage to start a new chapter after my master in a new country and he is doing the same after my PhD, pushing me always to learn more and aiming for the best! We will not be working together anymore but we will always have a special connection and I will never be thanking him enough for what he did for me. I would also like to thank my second supervisor Colin Adams for the knowledge on Loch Lomond he pass to me which allowed me to understand the ecology of this beautiful place.

Thanks to all the members of the "Llewellyn Lab". We experienced the same struggles, the same excitement for a new piece of equipment, the same lab away day always with a good intention at the beginning and a drunk pub crew at the end. I want to thank Raminta, that my phone always calls Ramona, for the amazing support and laughs together, the crazy time in the Salmosim lab and the great trip in US, maybe not the best microbiome conference but for sure the best pan cakes! A thank you to Bach for his constant support in stats and for his encouraging words making me feel less shit in R than I actually am. I also want to thank Elle because she is always been kind and respectful, of great support and availability. A special thank goes to my pal Toni, which introduced me to the Scottish world and taught me the real meaning of "Gimme a shout if you need me". A special thank goes to Maria de la O for all the Raffaella Carrà singing while doing boring lab jobs and all the coffee and cakes that appeared on my desk when most needed. To Paddy who thought me that PhD is not always so serious and to the rest of the lab members which are a bunch of wonderful people.

A big thank goes to the "GK". The Graham Kerr is one of the most welcoming and inclusive Institute I've ever been. From the minute I stepped in the department I felt part of it. I loved all the possibilities the institute offered me, from seminars to conferences, from invited speakers to Friday pub plan. A special thank you go

to Neil Metcalf for the support in the respirometry set up and interpretation of the data, to Maria for the lab chat, to Dan Haydon for the stats drop-in support, to everyone else to be so kind.

I want to thank all the lab technicians and staff members in the Burrishoole Catchment. Without them, my field work would have not been possible. Thanks to Cat and Liz for the help handling all the sampling, thanks to Russell for transferring me his 30+ years of knowledge in eels, thanks to Joshka and Phill to be a great guide in the sea of possible stats and finally thanks to Phill for his support, supervision in the field, great encouragement and always a kind word.

I want to separately thank special friends, who supported me over this journey in different ways. I want to thank Chiara for the amazing time we spent walking during the pandemic, for the food exchange thru the window, for the Vicenza exploration, to keep up with food intake in Terlizzi and for being an amazing friend. Thank Eleni and Chris who are the sweetest couple, for the dinners and aperitif and drink, anything involving good food and moaning about how much better food is in our own country. A thank goes to the fitness group, coach Marco, Hans, Teteh and Agnes that during the pandemic kept me fit and part of the group, Diana and Sara, which tried to not keep me fit with all the coffee and biscuits on Thursday at 11 am. I enjoyed every single minute of swearing in front of the laptop while doing jumping jacks for the joy of my downstair neighbour.

Now a special thank goes to the Italian part of the family in Glasgow, because yes, every Italian has tons of Italian friends abroad. I want to thank the “Nduja, ragu and haggis” group, a clash of Italian culture in the Scottish land. Thank to Peppino, Brunello and Fabri for the amazing chat, the dancing and the always favourite sentence: “Ma raga allora quando andiamo da Paesano?”. To Pheega who showed me that perseverance can bring you very far, for the shit chat and endless memes, for the honesty and evening on the couch with the intent of watching a movie but only watching trailers. To Fabiolino for all the walks and hikes, for the dinners and porcini hunting, for the support and friendship that we built and that will always be dear to me. A special thanks go to my far apart Italian friends Hana, MeravigliosaMarika, Phrau, Risi and Lucrezia for all the zoom aperitif during Covid, for the pub quiz, Cluedo and the amazing surprise for my 30th birthday. Now you

can call me LORD. A special mention goes to Alisce, the S is not a spelling mistake, because even if we are km away I know she will always be there when I need her and likewise. She is been thru all the PhD struggle before me so I felt understood when I needed to share any little piece of achievement, she always believes in me, we have a rare connection that is rare and precious.

The massive thank you goes to Gattini, Martina Donald Elliott and Poppy, and Jo. You are my family here and with you I feel at home. Thank Martina because she is a joy, she believes in me like no one else does and with her everything seems light and easy, sparkling with life and prosecco. Thank Donald because he is the calm of the group, he always has the right answer and gives you 110% of his time in anything you need, a naturally caring person. Thank Elliott because he is the happiest bambino I've met, because every time he calls me Chele my heart melts and because he is a cheeky wee monkey. Thank Poppy, she is my favourite gattina, and don't believe anyone saying you are fat! In my eyes you are skinny and the scale is broken. Thank Jo for all the infinite support, for the walks with Duca, for dreaming of going to Istanbul for our birthdays in the middle of a pandemic, for the laugh and crazy times and for believing in me every minute. I would also like to thank Jamie, who entered my life one year ago and showed me what an amazing person he is. He showed me parts of Scotland that I would have never imagined to explore, a passion for nature which is rare to find, a great creative mind, a kind soul and a big heart.

Last but not least I want to thank my parents, Giulio and Ena. They are always supporting me in every decision, they care about me and everything they do is for my own good. The past few years have not been the easiest but they never made me worry about anything happening back home and never made me feel far. Thank to my grandma, Nunzia or for me "LaNo'", for taking care of me in her way, sewing table cloths and gifting tea spoons, telling me her diabetes is low and asking me to make her favourite soup. This thesis is dedicated to them.

Author's Declaration

I declare that, with the exception of the aid listed below, this dissertation is the result of my own work and has not been submitted for any other degree at the University of Glasgow or any other institution.

All amplicon sequencing was carried out by Novogene (UK) Company Limited. All field work in Ireland was done by me with the support of field technician Dr Elizabeth Ryan, Dr Catherin Waters; post doc Dr Joshka Kaufmann and Dr Karl Phillips; senior researcher Dr Russell Poole and supervised in the field by Prof Philip McGinnity. All field work in Scotland was done by me with the supervision of Prof Colin Adams. Respirometry design, set up and material was supported by Prof Neil Metcalf. All of the resulting data and all statistical analyses in the thesis were performed by me with limited support from Dr Bachar Cheaib. All the research performed in this thesis was overseen by Dr Martin Llewellyn. Part of chapter 1 is published in *Parasitology* Manuscript DOI: 10.1017/S0031182021002146.

Impact of Covid-19

The Covid-19 outbreak affected everyone's life in a different manner. Fortunately, it did not cause any health-related issues to my loved ones. I contracted the virus in July 2021 with severe symptoms which lasted two months. I personally encountered difficulties in the data collection and analysis with initial poor productivity and reduced quality of work from home. Although most of the data were collected in the field before January 2020, the relevant laboratory work to analyse the collected material was delayed when labs closed in the first lockdown. Once access to campus was allowed again, the restriction and the limited number of people allowed to work at the same time in the laboratory slowed down the analysis of the sample. The shift in the sample processing resulted in a delay in the data analysis. On top of it, the translation from face to face meetings to online influenced the quality and promptness of feedback and support from colleagues and external help, stretching the time to get consistent results. As compensation for this delay, I received a three-month extension to my thesis project deadline by the Covid-19 Disruption mitigation plan offered by the University of Glasgow. This extension was very helpful as it enabled me to carry out and finish sample processing, analysis and finalize the writing process.

1 Introduction

1.1 *Anguilla anguilla* life history traits

The European eel, *Anguilla anguilla*, (Linnaeus, 1758) is a semelparous facultative catadromous fish (van Ginneken & Maes, 2005). The range of distribution of *A. anguilla* extends all around Europe, North Africa and East Asia. Eels have several life cycle stages and their breeding area is located in the the Sargasso Sea, performing approx. 6000 km migration to reach the spawning ground (**Figure 1-1**). The exact site where the reproduction occurs is still one of the unsolved mysteries of this species. After spawning, it is thought that adults die and the larvae called leptocephalus migrate back towards the continental shelf, following the gulf stream and oceanic currents (Zenimoto et al., 2011). The leptocephalus are thought to be planktivorous and their migration takes on average two years (Davey & Jellyman, 2005). Once the eels reach the coastline they metamorphose into glass eels that have an elongate and transparent body. The transitioning phase between salt water and fresh water is called elvers, it is a short life stage where eels adapt to freshwater. At this stage, they are sexually undifferentiated and the sexual determination and maturation is thought to relate to the yellowing phase and environmental factors (Davey & Jellyman, 2005). The yellow phase represents the main growing phase, where daily migration between fresh and salt water can occur for feeding or escape predation (Schneebauer et al., 2017). The duration of their residential yellow freshwater stage is highly debated. The minimum that had been recorded for this phase is in males three years and in females three years (Fazio et al., 2012). However, fifteen year-old males and twenty year-old for females have been recorded (C. Durif et al. 2009). Eels are carnivores and usually feed on worms, small fish, copepods and also crustaceans and bivalves (van Ginneken & Maes, 2005). Yellow eels start the metamorphose into silver eels predicting the imminent migration. The triggers to start the metamorphosis are still unknown but some study suggests to be related with the lunar cycle, with full moon increasing the luminosity of the water (Cresci et al., 2019; C. Durif et al., 2005; Sandlund et al., 2017). The new moon, the darkest night in the lunar phase, is the most productive in terms of silver eel's escape once the migration run started (Sandlund et al., 2017). One of the easiest features to distinguish a yellow eel during the silvering phase is the change in the abdomen coloration (Han et al.,

2001). The silvering phase includes gonad differentiation and development, regression of the digestive tract (C. Durif et al., 2009). Eels upregulate gonadotropin and growth hormone levels to stimulate vitellogenesis and gonads maturation (Palstra et al., 2010). Other physical changes involve the increasing of pectoral fin length and the ocular diameter. Silvering does happen at different times across Europe, between August and October in relation to the latitude and potentially the lunar cycle. Differential departures based on location may maximise the size of the spawning population in the Sargasso Sea by compensating for different distances traveled (Righton et al., 2016). During migration eels stop feeding, the digestive tract atrophies and sexual maturation reaches completion. To enable migration and the associated aerobic effort they rely on lipid reserves accumulated during the yellow-phase (Baillon et al., 2015). Energy is also invested in daily vertical migration up to 1000m to avoid predation (Simon et al., 2018). The importance of an efficient swim bladder during the migration is traditionally thought to be essential for the successful migration, even if recent study found that the swim bladder can have a peripherical impact on diving capacity (Righton et al., 2016). European eel have an extraordinary swimming capacity and energetics among the anguillids species (Tudorache et al., 2007). Study comparing the swimming performance of New Zealand short finned eel, *Anguilla autralis*, and *A. anguilla* revealed that European eel have a higher critical swimming speed and optimal swimming speed with a lower minimum cost of transport possibly revealing an adaptation to a longer migration distance (Tudorache et al., 2015).

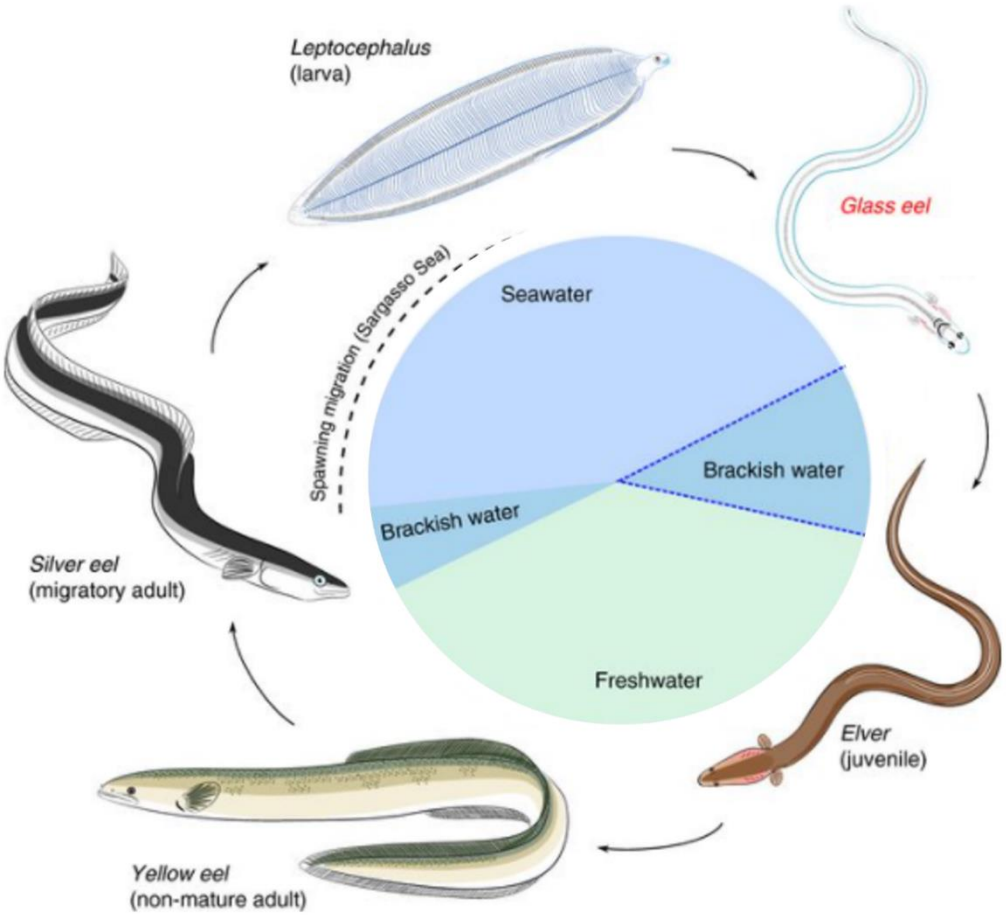

Figure 1-1. European eel life cycle. Source: Cresci *et al.*, 2019.

1.2 Anguillid phenotypic plasticity

Despite their extensive geographic range, consistent with the reproductive ecology of *A. anguilla*, the genetic data indicate that the entire species represents a single panmictic population (Jacobsen et al., 2014). Although recent studies outline that only part of the European population contributes to spawning, based on changes in allele frequencies observed in the genetic profiling of the adults, differences in the population from a genetic point of view are small (Pujolar et al., 2011). With a catastrophic decline of the eel population in recent past decades, low genetic diversity is expected within populations (Baltazar-Soares et al., 2016). The genetic uniformity of *A. anguilla* populations, set against the astonishing diversity of habitats they exploit, means that phenotypic plasticity has a key role in enabling survival (De Meyer et al., 2016). The same is also true of the American eel, *Anguilla rostrata* (Pavey et al., 2015). In many freshwater

catchments two different *A. anguilla* 'ecomorphs' are observed among yellow eels (Barry et al., 2016; Lammens & Visser, 1989; Meyer et al., 2017; Proman & Reynolds, 2000). One morphotype is characterised by a narrow head, living in the benthic environment and as feeding preference for invertebrates, the other one is a broad head morph with a bigger mouth gap, living in the water column and with piscivorous habits (Barry, 2015). A bimodal distribution of the two ecotypes has been shown, based on the jaw length, head width and head height. The distribution of the morphotype trait values is, however, not discrete and there is overlap at the extremes (Ide et al., 2011). The presence of ecomorphs in any given freshwater catchment may be explained by the interaction between local population density and prey diversity, with both phenotypes having different prey preferences (Ide et al., 2011). However, other studies suggest ecomorphs are established earlier in development and highlight bimodal trait distributions in marine glass eels, albeit less prominent ones (De Meyer et al., 2015). A recent study supported the hypothesis that the diet induces the morphological plasticity of the head shape (De Meyer et al., 2016). The hard feeders (broad head) develop a specific region in the post orbital part of the cranium to allow them to crush harder prey items. By contrast, soft feeders (narrow head) are more advantageous to slide in the benthic substrate and have increased hydrodynamics. Specialization in diet requirement of eels is an advantage to avoid competition for the same prey, however there may be a trade-off as different prey have different energetic content. Narrow head eels grow slower compared to the broad headed individuals, are less aggressive and have lower lipid content (Churcher et al., 2015). The developmental mechanisms that underpin ecomorph diversity in *A. anguilla* are not clear. The polymorphism in head shape in Japanese eels, *Anguilla japonica*, is mainly explained by somatic growth (S. H. Lee et al., 2018). The two ecotypes in *A. japonica* are defined by simple growth rate between lakes with different salinity (Kaifu, Yokouchi, et al., 2013). Growth rate may also underpin the developmental differences estuarine and lake morphotypes in the American eel, *A. rostrata*. Some genetic differences have been identified between *A. rostrata* ecomorphs (Pavey et al., 2015), and these presumably arise in single generation through differential mortality.

1.3 European eel conservation status and conservation challenges

The complex life cycle and a series of threats have lead the European eel to be listed as Critically Endangered by the International Union for Conservation of Nature IUCN (IUCN 2014). Since the early 1980s, the recruitment of the glass eels dropped by 98% (Aalto et al., 2016). In the last 15 years, the eel population declined by 90% (ICES, 2020; Magnusson & Dekker, 2021). The synergetic interaction of multiple threats is likely to be driving the collapse of this species. Barriers to migration such as dams and hydropower turbines, for example, are not only causing a physical barrier but also habitat loss (Henderson et al., 2012). The presence of pollutants in the water of streams and lakes can be toxic for the eels, with an effect on their migratory ability and gamete production. Also, climate change is related to the decline of the population in relation to the glass eels recruitments and ocean current modification (Baltazar-Soares et al., 2016). Another anthropogenic driver of the decline of the eel is the overfishing of the glass stage; fishing quotas and trades are now in place but illegal trade is a major concern associated with a managing estimation problem (Jacoby & Gollock, 2014). One of the more recent threats for *A. anguilla* survival is the introduction in the 1980's of the nematode parasite, *Anguillicola crassus* (F. S. Lefebvre & Crivelli, 2004). *A. crassus* lives in the swim bladders of *A. anguilla, A rostrata and A. japonica* , and eels are their definitive host where parasite reproduction occurs. *A. crassus* are transmitted via the zooplankton and intermediate hosts include copepods, as well as small fish such as sticklebacks. The presence of *A. crassus* may be impacting eels ability to cope with high water pressure during the migration to the spawning area (Simon et al., 2018). Environmental Management Plans (EMP) has been enacted to reduce the anthropogenic impact at National and local levels (Affairs, 2018) Passages to facilitate migration in river beds have been implemented to allow a higher percentage of silver eels to escape and start the migration process (IUCN 2014). In addition to those plans, the European eel was included in the CITES Appendix II in 2017 to ensure limit their trade and to control transportation via the issue of special permits (Musing et al., 2018). Most European States applied a restriction on the minimum landing size for yellow-eels fishing. In the UK, silver eels are protected by laws that mean this life stage needs to be released if it is caught by anglers (British Sea Fishing). There is no regulation for

glass eels, but the minimum landing size for yellow is 300mm (European Council, 2007). Improvements to stock assessment and the estimation of population size are required to better understand the actual status of the European eel and the possibility for recovery due to effective management (Åström & Dekker, 2007). Various models based on the stock dynamics have been developed showing that recovery is possible but will take several decades, based on the little knowledge we have on the eels marine phase (Righton & Walker, 2013). The most effective, beneficial and achievable management measure is likely a large reduction of mortality due to fishing or anthropogenic sources. However, an initial increase in the recruitment observed is not translating into a long term recovery (Åström & Dekker, 2007). Sadly many studies are providing evidence of a collapse across multiple European populations (Arai, 2014; Davey & Jellyman, 2005; Henderson et al., 2012; Magnusson & Dekker, 2021; Schabuss, Kennedy, Konecny, Grillitsch, Reckendorfer, et al., 2005; Schabuss, Kennedy, Konecny, Grillitsch, Schiemer, et al., 2005a). There is genuine concern that the European eel is in terminal decline (Aalto et al., 2016; Arai, 2014; Henderson et al., 2012).

1.4 *Anguillicola crassus* biology, epidemiology and detection

The parasite nematode, *Angullicola crassus* (Kuwahara, Niimi & Itagaki 1974), is a significant threat to eel health status, migration success and survival of the eel population. *A. crassus* is originally from East Asia but was introduced to Europe around the 1980s with the commercial trade of Japanese eels (F. S. Lefebvre & Crivelli, 2004). *A. crassus* is listed as one of the 100 “worst” exotic species that threaten European species and ecosystems (F. Lefebvre et al., 2012). The life cycle of the parasite involves several potential intermediate hosts. *A crassus* is a freshwater parasite with the adult stage found in the eel’s swim bladder (**Figure 1-2**). Adults' worms feed on the swim bladder wall, and a single eel may harbor up to 100 worms (Becerra-Jurado et al., 2014a). Adult parasites reproduce in the swim bladder lumen and the eggs or newly hatched L2 larvae pass through the pneumatic duct to the gut where they are expelled with faeces. L2 larvae are ingested by the intermediate host, usually small crustacean (copepods) or small fish (sticklebacks). In the intermediate hosts, the L2 larvae develop in L3 larvae. When the eels feed on infected prey, the parasite larvae penetrate the intestine

and crawl up to the swim bladder. In the swim bladder, they molt into L4 larvae before reaching sexual maturation (Dangel et al., 2015).

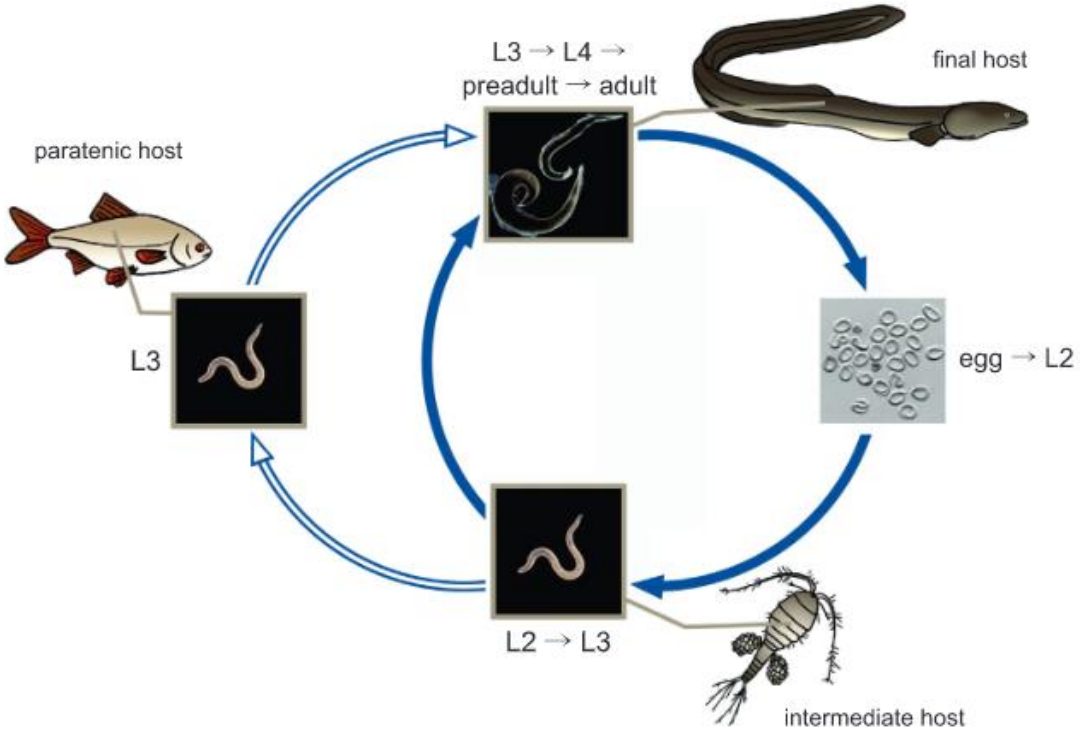

Figure 1-2. Life cycle of *Anguillicola crassus*. The basic life cycle is described by blue arrows and includes eels as final hosts and copepods as intermediate hosts. Additional paratenic hosts (e.g. fish) are integrated into the life cycle with a white arrow. Source (Dangel et al., 2015).

A. crassus is considered a highly successful nematode species due to the fast growth rate and the numerous production of L2 larvae, even when found as co-infections alongside its sister species *Aanguillicola novaezelandiae* (Grabner et al., 2012). The parasite in Europe evolved genetic differences compared to the original Asian population, leading to higher infectivity and changes in the developmental dynamics, with a faster plastic adaptation to exposure to different environments (Weclawski et al., 2013). The first detection of *A. crassus* occurred in 1982 in North Germany and Italy, then 1987 in Sweden and Austria, 1993 Norway (Aguilar et al., 2005a; Didžiulis, 2013; Schabuss, Kennedy, Konecny, Grillitsch, Reckendorfer, et al., 2005; Wielgoss et al., 2008). In Ireland a well-established parasite population is present on the North Coast (Becerra-Jurado et al., 2014b). On the West Coast, *A. crassus* was discovered more recently, as the first site in Burrishoole Catchment was in 2011 (Pers. Comm. R. Poole). A catchment in the

early stages of colonisation represents a valuable site to study disease epidemiology, as well as to exploit the presence of sympatric non-infected controls. Currently, the only reliable method to detect the parasite is a post-mortem dissection of the eel. One of the first methods aimed to detect the inflammation status of the swim bladder using x-ray radiography (Beregi et al., 1998). With this method, the eels need to be anesthetized and immobilized, pictures from the different perspectives taken to evaluate the status of the animal. Results from this method give a good match with the presence or absence of the parasite in the dissection but cannot detect any swim bladder damage that needs validation with pathological findings obtained from fish dissections separately. An ultrasound technique was also proposed for parasitic detection, however, this technique is not able to differentiate between a worm-free eel and a mildly infected eel, making it an unsuitable replacement for a post mortem dissection (Frisch et al., 2016). Anal redness was also suggested as an indicator of infection, although this measure is qualitative, subjective and non-specific (Crean et al., 2003). All methods currently deployed to detect the nematode parasite in the eels are not accurate, they require specific expertise and/or lack in precision. Molecular PCR based tools had been used to access the correct identification of the nematode fish parasites species (Selim & El-ashram, 2012). The DNA-based technique using 18S ribosomal DNA primers has been used to detect the presence of different species of Anisakidae nematode in sardine, *Sardina pilchardus* (Santos et al., 2006). The developed methodology was able to detect a specific nematode with a precision of 1 part of nematode to 100 00 part of fish. More studies have been published showing the efficiency of molecular tools to detect parasites in a range of fish species (Gilbey et al., 2006; Herrero et al., 2011; Paoletti et al., 2018; Thapana et al., 2018). A recent study proposed a molecular detection *A. crassus* using microsatellite DNA of the parasite present the eel's faeces (Jousseaume et al., 2021). Although these authors provided evidence that a non-lethal protocol for molecular detection is possible, their assay showed low sensitivity (70% based on a small 51 animals sample size).

1.5 Impact of *A. crassus* on silver eels migration

The process of migration and silvering in the European eel is still relatively obscure. It is known that the presence of the parasite influences the silvering

phase (Fazio et al., 2012). Infected eels can have an altered modulation of the freshwater rod opsin genes, a different allocation of the gut mass, differential genes expression in the liver and alteration of the sexual maturation (Fazio et al., 2012). Those alterations are partially explained by the accumulation of cortisol after the infection, but it is not clear if the accumulation of cortisol is simply a stress response or a plastic response to mitigate the impact of parasitic infection (Fazio et al. 2012). The cortisol increase can also induce the mobilization of lipid, reducing the lipid accumulation mechanisms (Sancho et al., 2017) Parasite infection can reduce swim bladder elasticity and increase the energetic demand for the buoyancy because *A. crassus* feeds on the organ's wall (Pelster, 2015). During the fresh water stage, the swim bladder is thought to possess minimal function because eels are primarily benthic animals, not experiencing critical depth changes (Barry et al., 2014). Recent work suggests no impact of the parasite on the migratory and diving behaviour in the first part of the migration. Vertical movements and migration speed appear to be comparable in infected and un-infected eels, but the study is based only on three satellite tagged silver eels in the Baltic sea and does not consider the deep daily vertical migration that is thought to occur beyond the continental shelf, or the endurance necessary to complete their 6000 km journey (Simon et al., 2018). All European eels, independently from where they start the migration, converge in the Azores region on a westerly route to the Sargasso Sea. The migration takes longer than previously assumed. Instead of taking 4-6 months, the migration may take up to a year and involve reducing the average migration speed to arrive in the Sargasso spawning area before the spawning event (Righton et al., 2016; van den Thillart et al., 2009).

1.6 Importance of fish physiology

Measurement of metabolic rate variation in animals can provide insights into behavioural ecology, physiology and responses to environmental changes (Clark et al., 2013b; Clarke & Johnston, 1999; de Eyto et al., 2015). Significant standing variation in metabolic rate exists in fish populations (Robertsen et al., 2019). Measurement of oxygen consumption is now widely deployed to understand adaptation and resilience in different fishes (Cooper et al., 2018; Pilakouta et al., 2020). Standard metabolic rate (SMR) consists of the minimum rate of energy

needed to maintain resting metabolism, whereas the maximum metabolic rate is the upper limit for the capacity to perform oxygen-consuming physiological activities (Killen et al., 2021). Aerobic scope (AS) is the difference between SMR and MMR and represents an individual's total capacity for simultaneous oxygen-consuming tasks above basal metabolism (Holt & Jørgensen, 2015). The variability in metabolic rate can be interspecific (between species) as well as intraspecific (within species) (Glazier, 2005). Understanding the driver in metabolic differences is essential to understand the evolution of the morphology, physiology, behaviour and life histories (Lovegrove, 2003). Individual differences in SMR have been linked to several fitness measures with controversial results. In some cases, SMR is positively associated with growth (Auer et al., 2015), reproduction (Lapointe et al., 2018) and survival (Reid et al., 2012). However, the converse can also be true, and the adaptive role of intraspecific metabolic rate variation depends heavily on its biological context of growth (Norin & Malte, 2011), reproduction (Alves et al., 2013) and survival (Artacho & Nespolo, 2009). The same is also true for Aerobic Scope (AS) and Maximum Metabolic Rate (MMR). AS and MMR can be linked to differences in geographic distributions (Naya et al., 2007), ability to cope with environmental extremes (Pilakouta et al., 2020) and migratory effort (Kraskura et al., 2020). In juveniles of Atlantic salmon, there is negative correlation between SMR and growth rate and strong correlation with dominance, important to acquire good feeding territories (Reid et al., 2011). In adult salmon SMR is correlated with body size, energy stored and reproduction status (Rosenfeld et al., 2015; Seppänen et al., 2009). Salinity has also a strong impact on metabolic rate because the energetic cost of maintaining physiological stability in a hyperosmotic environment is higher compare to a hypoosmotic environment. Fish in salt water maintain hypoosmotic state by actively drinking and secreting ions from the intestine, kidney, and gill epithelia (McKenzie et al., 2001). Adults of sockeye salmon, *Oncorhynchus nerka Walbaum*, have significantly higher SMR and active metabolic rates in salt water, especially considering the transitioning period between environments after the migration (Wagner et al., 2006). Contrasting are the results in rainbow trout, *Oncorhynchus mykiss*, where gill metabolism was estimated to be higher in fresh water, caused by the increase of gill ventilation to ensure the adequate uptake of oxygen (Rosewarne et al., 2016a). Once again this highlights the importance of species specific studies to better understand the impact of environmental factor on metabolic rates. Little is known about anguillid

metabolism. The European eel, *Anguilla anguilla*, for a fixed mass, showed a higher values of critical swimming speed and optimal swimming speed compared to New Zealand short-finned eels (Tudorache et al., 2015). Both species recorded similar SMR, MMR and AS indicating very similar swimming physiology traits but the European eel has a better swimming capacity and performance possibly showing evolutionary adaptation to the long migration (Tudorache et al., 2015). In the European eel the cumulative organ mass (liver, heart, spleen and intestine) was found to explain 38% of the variation in SMR, showing the effect of body mass on metabolic traits (Boldsen et al., 2013). At the present there is no data available on the effect of salinity, parasite infection status or environmental factors on metabolic rates of the European eel in the wild.

1.7 Microbiome influence on fish health

The gut microbiome in teleosts is an understudied topic compared to humans or mice. However, with the rise of next generation sequencing), numerous studies are revealing the importance of fish gut microbiota in all life functions (Piazzon et al., 2017). Many factors can influence the abundance of certain microbial species and their composition, such as diet and stress (Sandoval-Motta et al., 2018). Alteration in the microbiome can increase complex carbohydrate digestion, detoxify phytochemicals and decrease the capacity for thermogenesis (Wang et al., 2020). Microbiome changes can also lead to behavioural adaptations increasing explorative capabilities (Alberdi et al., 2016). In anadromous species such as the Atlantic salmon, *Salmo salar*, salinity gradient is one of the main drivers of the changing in the microbiome composition and richness (Dehler et al., 2017). Fresh water fish harbour an increased number of unique and higher abundant Operational Taxonomic Units (OTUs), while salt water fish microbiome was dominated by *Mycoplasma* spp. (Dehler et al., 2017). During the marine stage, the temperature is recognized to be an important factor for the gut microbial composition because temperature can regulate a series of biological processes such as immune responses, metabolic rates and enzyme activity (Anti Vasemägi et al., 2017). In anguillids little is known about their microbiome composition and function. A recent paper characterized the differences in gut microbiome composition based on the 16S rDNA sequencing in three different species of wild anguillids, *Anguilla japonica*, *A. marmorata* and A. *bicolor pacifica* (Hsu et al.,

2018). The gut microbiome of Japanese eels, *Anguilla japonica*, were characterised by Gram-negative bacteria (*Bradyrhizobium*, *Cetobacterium*) recognized as important for nitrogen fixation, vitamin B12 and acetic acid production, and Gram-positive bacteria (*Clostridium*) used in aquaculture as probiotic for his suppresses inflammation and has anti-oxidation ability (Godoy-Vitorino et al., 2017; Lin et al., 2019). In the Giant Mottled eel, *A. marmorata*, and Shortfin eel, *A. bicolor pacifica*, the most represented genus in the gut microbiome were *Acinetobacter, Mycoplasma*, *Shewanella* and *Bacteroides*. *Bacterioides* is associated with the production of anti-inflammatory substances to maintain the balance of immune system (Gerhauser, 2018). Acinetobacter has the ability to produce e inhibitory substances against potential bacterial pathogens including *Vibrio* species (Osimani et al., 2019). *Shewanella* is associated with the prevention of pathogens infection producing the digestive enzymes (Ramírez & Romero, 2017). The mucus secreted by the eels represents the first barrier for protection and exchange with the environment. In eels, the microbiome composition in the mucus reflects the changes in the salinity of the environment (Carda-Diéguez et al., 2017). Higher alpha diversity was detected in the resident bacteria living on the section of the mucus closer to the skin compared to the one associated with the most distant part of the mucus. Bacteria diversity and richness in the mucus was higher compared to the environment, characterized by bacteria with particular abilities to attach to a substrate and resistance innate genes. The skin mucosal microbiome was dominated by Gammaproteobacteria and *Vibrio*, which were not found in the water biome composition (Carda-Diéguez et al., 2017). Only one study is available in the literature that investigates the gut microbiome composition of European eels between elver, yellow and silver stage and in a farmed setting (W. Huang et al., 2018a). The main group characterizing the elver and silver eel gut microbiome are Proteobacteria (*Aeromonas*), while in yellow eels there is a shift towards the dominance of *Cetobacterium* and *Plesiomonas*. One of the main drivers in microbial differentiation in farmed eels is thought to be diet composition; Proteobacteria are associated with carbohydrates digestion and metabolism in starch based feed in aquaculture fish (Parata et al., 2020; Piazzon et al., 2017; Wang et al., 2020). Nothing has been done to study the effect of diet and salinity preferences in the gut microbiome in wild European eels.

1.8 Aims and objective of the thesis

The overall purpose of my PhD is to understand the biology, physiology and microbial ecology of the European Eel in the context of infection with the nematode swim-bladder parasite, *Anguillicola crassus*. Each chapter represents an objective:

1.8.1 Chapter 2: Towards an in-situ non-lethal rapid test to accurately detect the presence of the nematode parasite, *Anguillicoloides crassus*, in European eel, *Anguilla anguilla*

A. crassus is an invasive and emerging parasite introduced into Europe in the early 1980s. It is unlikely to be the primary cause of the eel collapse since the 1980s but in conjunction with low recruitment may contribute to declining adult stocks. The presence of the parasite can affect the speed and migratory behaviour due to his energetic demand. Currently, accurate detection of the parasite can only be achieved via post-mortem dissection. This chapter aims to develop a rapid, non-lethal and portable, *in situ* PCR-based approach to detect *A. crassus* in the European eel using parasite DNA traces in faecal material. The test can be used to assess the parasite spread in Europe, can offer managers the opportunity to engage in infection control by assessing the disease status of adult eels and can be used as tools for the conservation management of the European eel.

1.8.2 Chapter 3: Do diet and salinity induce ecotype-specific phenotypic plasticity between life stages of the European eel, *Anguilla anguilla*?

The population of European eel is widely accepted to be panmictic. In genetically uniform species, phenotypic plasticity enables some level of adaptation to local environmental conditions. In eels two different cranial ecomorphs have been independently reported in many water systems across Europe supporting the hypothesis that trophic ecology induces morphological plasticity. The aim of the chapter is to improve the existing methodology to assess head morphological differentiation, to better understand the environmental factor driving head differentiation and to capture the differences between head morphology between silver and yellow eel life stages from the same catchment across different years.

1.8.3 Chapter 4: Metabolic rate and migratory phenotype in European eels, *Anguilla anguilla*

The capacity to provide oxygen for vital processes and important activities, such as reproduction, digestion and locomotion, is essential for animal fitness. How energy is distributed between all life processes is crucial to understanding evolutionary strategies and local adaptation to stressors. In fish the most commonly used measure for energy expenditure capacity is metabolic rate. This chapter aims to understand the main drivers affecting the metabolism of different life stages of the European eel. We are interested in linking the effect of the nematode parasite *A. crassus* to the eel metabolism, especially its impact on migration in silver eels. This chapter explores the importance of the amount of stored fat in metabolism and the effect of daily migration from freshwater to saltwater on basal and maximum metabolism.

1.8.4 Chapter 5: Body mass, salinity and parasitic infection induce microbial community changes in European eel, *Anguilla anguilla*.

The microbiome can play an important role in the digestion process, nutrient absorption and disease control. Fish are constantly surrounded by the water environment which plays a key role in the microbiome composition, as does diet and temperature in shaping abundance and composition of microbial diversity. Parasite infection can also cause dysbiosis in bacterial community, inducing acting as a driver of opportunistic pathogen colonization. For all these reasons, is important to characterize the microbiome community and its interaction with physiological and ecological traits. The aim of this chapter is to characterize the microbial composition of gut compartments in yellow and silver eels, to understand the influence of *A. crassus* infection on immune status and to reveal the main environmental and ecological drivers in the European eel microbiome.

1.8.5 Chapter 6: Contributions, Discussion and Conclusion

The main results and contributions in this thesis are summarised and are discussed in this chapter. Future work is proposed that might build upon the results conducted in this thesis. These future perspectives include implementation of the rapid test for *A. crassus* detection, introducing genetic differentiation in head

morphology plasticity and including environmental factors in both microbiome characterization and metabolic profiling.

2 Chapter 2 Towards an *in-situ* non-lethal rapid test to accurately detect the presence of the nematode parasite, *Anguillicoloides crassus*, in European eel, *Anguilla anguilla*

Accepted for publication in *Parasitology* 18/12/2021

De Noia M.[1], Poole R.[3], Kaufmann J.[2,3], Waters C.[2,3], Adams C.[1], McGinnity P.[2,3], Llewellyn M.[1]

[1] Institute of Biodiversity Animal Health and Comparative Medicine, University of Glasgow, G20 6NB, Glasgow, UK;

[2] School of Biological, Earth and Environmental Sciences, University College Cork, T23 N73K, Cork, Ireland

[3] Marine Institute, Foras na Mara, F28 PF65, Newport, Ireland.

Abstract

Anguillicoloides crassus is an invasive nematode parasite of the critically endangered European eel, *Anguilla anguilla*, and possibly one of the primary drivers of eel population collapse. The presence of the parasite has been shown to impact many features of eel physiology and life history. Early detection of the parasite is vital to limit the spread of *A. crassus*, and to assess its potential impact on spawning biomass. However, until recently, accurate diagnosis of infection could only be achieved via necropsy. To support *A. anguilla* fisheries management in the context of *A. crassus* we developed a rapid, non-lethal, minimally invasive and *in-situ* DNA-based method to infer the presence of the parasite in the swim bladder. Screening of 131 wild eels was undertaken between 2017 and 2019 in Ireland and the UK to validate the procedure. DNA extractions and PCR were conducted using both a Qiagen Stool kit at Glasgow University and *in situ* using Whatman qualitative filter paper No. 1 and a miniPCR DNA Discovery System™. Primers were specifically designed to target the cytochrome oxidase mtDNA gene region and *in situ* extraction and amplification takes approximately 3h for up to 16 individuals. Our *in situ* diagnostic procedure demonstrated Positive Predictive

Values at 96% and Negative Predictive Values at 87% by comparison to necropsy data. Our method could be a valuable tool in the hands of fisheries managers to enable infection control and help protect this iconic but critically endangered species.

2.1 Introduction

Anguillicoloides crassus, (Kuwahara, Niimi & Itagaki 1974) is a nematode parasite of the *Anguilla japonica* that also infects other Anguilla species, including the European eel *Anguilla anguilla* (F. Lefebvre et al., 2012). *A. crassus* originates from East Asia, having been introduced into Europe in the early 1980s as a result of the trade in live Japanese eels, *Anguilla japonica* (Temminck & Schlegel, 1847) (Laetsch et al., 2012a; Weclawski et al., 2013). *A. crassus* is now well established in the Western Hemisphere and can be found in almost all European rivers and lakes, where it can tolerate salinities up to 12 ppt (Aguilar et al., 2005a; Becerra-Jurado et al., 2014b). While A. *crassus* was unlikely to have been the primary cause of the *Anguilla anguilla* recruitment collapse since the 1980s, in conjunction with low recruitment, infections of the parasite may have contributed to declining adult stocks (Henderson et al., 2012) and to the quality of emigrating silver eels, thereby potentially impacting on effective spawner biomass and the ability of the stock to recover (Kirk, 2003).

Anguillicoloides crassus reproduces sexually in the swim bladder of the eels. The eggs hatch in the female worm inside the swim bladder and L2 larvae migrate to the intestinal tract via the pneumatic duct to be excreted with the faeces (Didžiulis, 2013). As part of its life cycle *A. crassus* is then trophically transmitted to various intermediate hosts including several zooplankton species (especially copepods of the orders Cyclopoidea and Calanoidea) as well as planktivorous fish such as the three-spined sticklebacks, Gasterosteus aculeatus, Linnaeus, 1758 (Kuwahara, 1999). In the intermediate host, the parasite develops into the infectious phase L4 larvae, which, once ingested, parasitize the eel as the final host. The parasite migrates from the gut system perforating the connective tissue and muscles reaching the swim bladder (Heitlinger et al., 2009). The number of parasites found in the swim bladder can vary from less than ten to greater than 70 individuals per eel (Jousseaume et al., 2021). The presence of the parasite has

been shown to detrimentally affect many features of eel physiology and life history (Newbold et al., 2015). Adult nematodes feed on blood supplied to the swim bladder wall and can result in increased eel mortality as a consequence of damage caused to the organ (Schneebauer et al., 2017). The swim bladder wall becomes thicker, opaque and less elastic due to the perforation caused by the parasite feeding habit with an impact on buoyancy control (Barry et al., 2014; Newbold et al., 2015; Weclawski et al., 2013). *A. crassus* infection is also thought to alter the physiological mechanisms involved in silvering – the process by which freshwater sub-adults adapt to life in the ocean. In this respect, infected eels have also been found to silver faster as a result of an over-production of cortisol, which seems to have a stimulatory effect on GTH2 synthesis (Di Biase et al., 2017; Muñoz et al., 2015). Moreover, cortisol is the key hormone produced during fasting, typical of the silvering phase stage (Fazio et al., 2012). During the silvering phase occur a normal increase of erythropoiesis but the parasite, due to their blood feeding behaviour, increases erythropoiesis in infected eels prior to their silvering (Churcher et al., 2015). The presence of the parasite may impact the eel's migration speed in rivers (Newbold et al., 2015) and in the ocean as the energy demand increases (Pelster, 2015), due to the reduction of the swim bladder elasticity. The presence of the parasite appears not to affect the speed and migratory behaviour during the first phase of the migration in shallow water (Simon et al., 2018). However, where deep diving is required in the ocean, damage to the integrity of the swim bladder is believed to seriously impact on an infected eel's chances of survival (F. Lefebvre et al., 2012; Righton et al., 2016).

Currently, accurate detection of the parasite can only be achieved via post-mortem dissection and thus requires the eel to be dissected. However, several non-lethal techniques are under development (Frisch et al., 2016). Anal redness can be used as an indicator for the presence or absence of the parasite, but this approach lacks both specificity and objectivity (Crean et al., 2003). A radio diagnostic method has been developed to detect inflammation caused by the nematode's feeding habits (Beregi et al., 1998). The method uses X-ray to scan the pneumatic duct and can detect swim bladder damage and parasite presence. The quality of the images has a large margin of error so the accuracy of detection can be low and swim bladder alterations can be caused by other factors (Beregi et al., 1998). Frisch et al. 2016 made improvements to the method developed by

Beregi et al. (1998). Using compound radiography, they were able to detect small alterations to the thickness of the swim bladder wall and to inflations of the lumen. However, to perform a full body scan using this method, the animal has also to be euthanized. Recently, attempts have been made to develop a molecular test for *A. crassus* infection based in nuclear microsatellite markers (Jousseaume et al., 2021), however, reported sensitivity and specificity were below 71%, and the test, which involves fine-scale size discrimination of microsatellite locus sizes between target and off-target nematode species, is not easily transferred to field conditions. Finally, it is not clear from this molecular study whether faeces could be sampled non-lethally (Jousseaume et al., 2021).

To support the assessment of eel stocks and ultimately fisheries management in the context of *A. crassus*, sensitive, specific and rapid non-lethal and in situ methods for pathogen detection are urgently required. Screening of translocated eel populations could, for example, limit the spread of the pathogen. Furthermore, non-lethal screening of silver eels alongside satellite tagging studies could reveal the impact of infection on migratory and breeding success. Several non-lethal and/or molecular methods have been proposed to detect parasites in various fish species related to the food health safety chain and conservation management (Cavallero et al., 2017; Levsen et al., 2018). A non-lethal qPCR based eDNA approach has also been optimized to detect the cestode Schistocephalus solidus in samples taken by needle from the intra-peritoneal cavity of a fish (Berger & Aubin-Horth, 2018).

In the current study, we developed an alternate, rapid, non-lethal and portable, in situ PCR-based approach to detect *A. crassus* in the European eel using parasite DNA traces in faecal material. We tested the specificity and sensitivity of two different DNA extraction methods, the former lab-based extraction protocol, the latter more suited to the field. Using necropsy data, we were also able to explore any link between host condition and parasite infection load.

2.2 Materials and methods

2.2.1 Sample collection

The study was conducted at two different locations in UK and Ireland. In the Burrishoole catchment, Ireland 53°55'27.6"N 9°34'27.0"W, yellow eel (feeding stage) were collected from Loughs Feeagh (freshwater) and Furnace (tidal brackish water) using unbaited fyke nets deployed overnight in chains of 10 nets set at different lake depths in summer 2017, 2018 and 2019. Eels undergoing silvering were collected in autumn 2019 using permanent downstream river Wolf-type traps. The study was carried out under a Health Products Regulatory Authority (HPRA) license number AE19130-P096. In Lough Neagh, UK-Northern Ireland 54°36'05.5"N 6°24'55.5"W, yellow eels were collected with baited long lines fished overnight in the lake in summer 2018. Between capture and the procedures, eels were kept in holding tanks at the Marine Institute of the Burrishoole catchment. Under mild anaesthesia, colonic irrigation with 2ml 0.09 % sterile saline solution was performed to collect faecal material using a 5 ml syringe and a modified (needle removed) Terumo Surflo Winged Infusion Set (Figure 1). Each colonic irrigation procedure lasted less than 30 seconds. The eels were then euthanized with an overdose of MS-222 (10 min in a 100 mg/L Tricaine methane sulfonate solution, FVG Ireland) followed by a cervical separation of the spinal cord. A total number of 131 eels were sampled and weight and length were recorded to the nearest 0.1 cm and gram (Appendix 1, Supplementary 2.1). A drop of the collected wash material was placed on 1 cm^2 of Whatman qualitative filter paper No. 1 and air dried for 5 minutes at room temperature. The air-dried paper was used to perform instant *in situ* DNA extraction or preserved at -80◦C. The remaining wash was stored in 100% ethanol (1 wash: 9 ETOH) at -20◦C. Subsequently, all eels were dissected, swim bladder inspected and the number of *A. crassus* present counted. *A. crassus* were collected and stored in 100% ethanol before being stored at -20◦C. An eel was considered infected if at least one parasite, regardless of its lifecycle stage, was found in the swim bladder.

2.2.2 DNA collection and extraction methods development

2.2.2.1 DNA extraction

A total of 131 eels were sampled and faecal material was collected from all. DNA was extracted from faecal wash of 104 eels using the Qiagen stool. The Whatman extraction protocol was used *in situ* for eels sampled in 2019 (N= 55). To enable direct comparison between the two protocols, DNA was extracted from 28 eels caught in 2019 (14 in Lough Furnace and 14 in Lough Feeagh) using both Qiagen and Whattman extraction methods for each eel. DNA concentrations for Qiagen extractions are included in Appendix 1, Supplementary material 2.3.

2.2.2.2 Laboratory genomic DNA extraction

DNA from 200 µl of stored faecal material was centrifuged for 5 min at 12000 rpm to concentrate the pellet. For each sample, 180 µl of supernatant was removed and the remaining material was extracted with a slight modification to the suggested protocol of the QIAamp Stool Kit (Qiagen). ATL tissue lysis buffer volume was increased to 350 µl, proteinase K up to 20 µl AL lysis buffer up to 300µl and Ethanol 100% up to 400µl.

2.2.2.3 In situ genomic DNA extraction

A small sample of the filter paper (were faecal material had been previously deposited) of 1mm diameter was removed by a punch from the Whatman qualitative filter paper No. 1 and DNA was extracted using adjusted extraction protocol of DNA from Whatman™ FTA™ cards (Santos et al., 2006) (Figure 1) (Appendix 1, Supplementary material 2.2).

2.2.2.4 Primer design, PCR conditions and species specificity

A pair of specific customised primers were designed using all 467 cytochrome c oxidase subunit 1 (COI) gene sequences available for *A. crassus* (NCBI). All sequences were aligned to build a consensus sequence using BioEdit version 7.0.5.3 (Thomas A. Hall, 2017). The obtained consensus sequence was used to identify a conserved region within *A. crassus* suitable for primer design (**Table 1**). The designed primer pair was assayed for cross-reactivity *in silico* against common fish nematode parasites *Camallanus* sp. (NCBI Accession: EU598889),

Contracaecum sp. (NCBI Accession: FJ866816) and *Capillaria* sp (NCBI Accession: AJ288168) (Pouder et al., 2009). The total length of the expected amplicon is 187 bp. The same PCR conditions and mastermix were used to test the efficiency and specificity of the primer using a mini PCR DNA Discovery System. The PCR Mastermix was made with of 10 µl of Q5® High-Fidelity DNA Polymerase, 1 µl of FWD Primer [10 nM], 1 µl of RV primer [10 nM], 0.5 µl MgCl2 (0.5 M), 6,5 µl of RNA and DNA free water and 1 µl of extracted DNA. The total volume of the PCR reaction was 20 µl per sample. The cycle used for the PCR started with 5 minutes at 95 °C, followed by 35 cycles of 95 °C for 30 seconds, 60 °C for 30 seconds and 72 °C for 30 seconds and a last step of 10 minutes at 72 °C. 5 µl of PCR products was visualized on a 2% agarose gel using SYBR safe staining (Invitrogen). Each sample was amplified in technical triplicate alongside negative controls (ddH_20) and a positive control of either 20ng/ul DNA (Qiagen extraction) or *A. crassus* tissue crushed onto Whatman FTA card. Species specificity of the primer set was confirmed using a series of parasites collected in the same study system, various non-nematode parasites (*Anisakis* sp.) and other animal taxa, including the European eel, to assay cross-reactivity (*Lepeophtheirus salmonis*, *Anguilla anguilla*, *Neoparamoeba perurans*, *Scombrus scombrus*, *Diphyllobothrium* sp., *Schistocephalus* sp., *Dentitruncus truttae*). For each organism 1 µl of DNA was used. To identify amplicons as *A. crassus*, a subset of positive amplifications were Sanger-sequenced at MRC PPU DNA Sequencing and Services, Dundee, UK.

Table 1. Primer name, direction of amplification, primer size expressed in base pairs and specific designed sequence

Primer Name	Direction	Primer size bp	Primer sequence
AcrasCO1_fwd	5′ -> 3′	26	CCATTCTGGTATAAGTGTTGATCTCG
AcrasCO1_rev	3′ -> 5′	30	ACAACCTCATATGTTCTARAGTAATAGAT

2.2.2.5 Sensitivity, Specificity, PPV and NPV

Several parameters were calculated to assay the validity of the test. Here *sensitivity* is defined the ability of the test to correctly classify an individual as infected (i.e. a true positive). The ability of a test to correctly classify an

individual as non-infected (i.e. a true negative) is called the test's *specificity*. The Positive Predictive Value (PPV) is the percentage of eels with a positive test that are actually infected on dissection and the Negative Predictive Value (NPV) is the percentage of eels with a negative test that do not have the parasite on dissection. Positive and negative predictive values are directly related to the prevalence of the disease in the population (Stojanović et al., 2014) (**Table 2**).

Table 2. The criteria for Specificity, Sensitivity NPV (Negative Predictive Value) and PPV (Positive Predictive Value) as applied to a rapid test for *A. crassus*. Animals that are infected and test positive are considered True Positive (TP). Animals that are infected and test negative are described as False Negative (FN). Animals that have no visible parasites, but test positive are False Positive (FP), and those that have no visible parasites but test negative are True Negative (TN).

		Dissection result		
	Infected	Not Infected		
Test result: Positive	True Positive (TP)	False Positives (FP)	Sensitivity=(TP/(TP+FN)	PPV=(TP)/(TP+FP)
Test result: Negative	False Negatives (FN)	True Negatives (TN)	Specificity=(TN)/(TN+FP)	NPV=(TN)/(TN+RN)

2.2.3 Biological validation of eel infection status

2.2.3.1 Eggs count in faecal wash

Nematode larvated and unlarvated eggs and L2 larvae were counted with a modified McMaster Salt Flotation Technique. 200 µg of faecal material was diluted in 1,5 ml of distilled water. After mechanical homogenisation, the suspension was poured through a 250-micron aperture sieve and the filtrate was collected. After thorough mixing, the solution was transferred to a centrifuge tube and spun for five minutes at 2500 rpm. The supernatant was discarded and the remaining faecal pellet covered and homogenised with 300 µl of saturated sodium chloride solution, mixed by inverting slowly six times. Then, using a Pasteur pipette, the mixture was transferred to a McMaster slide. Each chamber holds 0.15 ml beneath the gridded area. The preparation is then examined using the 25x objective of a stereoscopic microscope, the number of eggs present in the grids of both

chambers was counted to give an estimate of the numbers of eggs/gram of faecal material.

2.2.3.2 *A. crassus* count in swim bladder necropsy

All dissected eels were checked for *A. crassus*, and where present, they were counted. The swim bladder was extracted whole from the animal and stored at 4°C until the procedure was completed for all the specimens. The swim bladder was then opened and nematodes were counted and classified into adults and larval stages. A Mann-Whitney test was performed in R studio between years of infection to test if there was a significant change in the parasitic load.

2.3 Results

2.3.1 Rapid test *in-situ*

The *in situ* non-lethal test was performed on 55 eels collected in 2019. Individuals were anally catheterised to enable colonic irrigation with a soft silicon tube without causing internal lesions. The amount of saline solution used (between 0.5 ml and 2 ml) varied in approximate proportion to the size of the tested animals. The procedure was deployed to minimize the invasiveness of the collection of the faecal material. *In-situ* DNA extraction took 20 minutes for 16 samples, PCR reaction was undertaken over a period of 2 hours and electrophoresis with gel visualization took a further 17 minutes. Thus, the test can be performed for 16 individuals in approximately 3 hours (**Figure 2-1**).

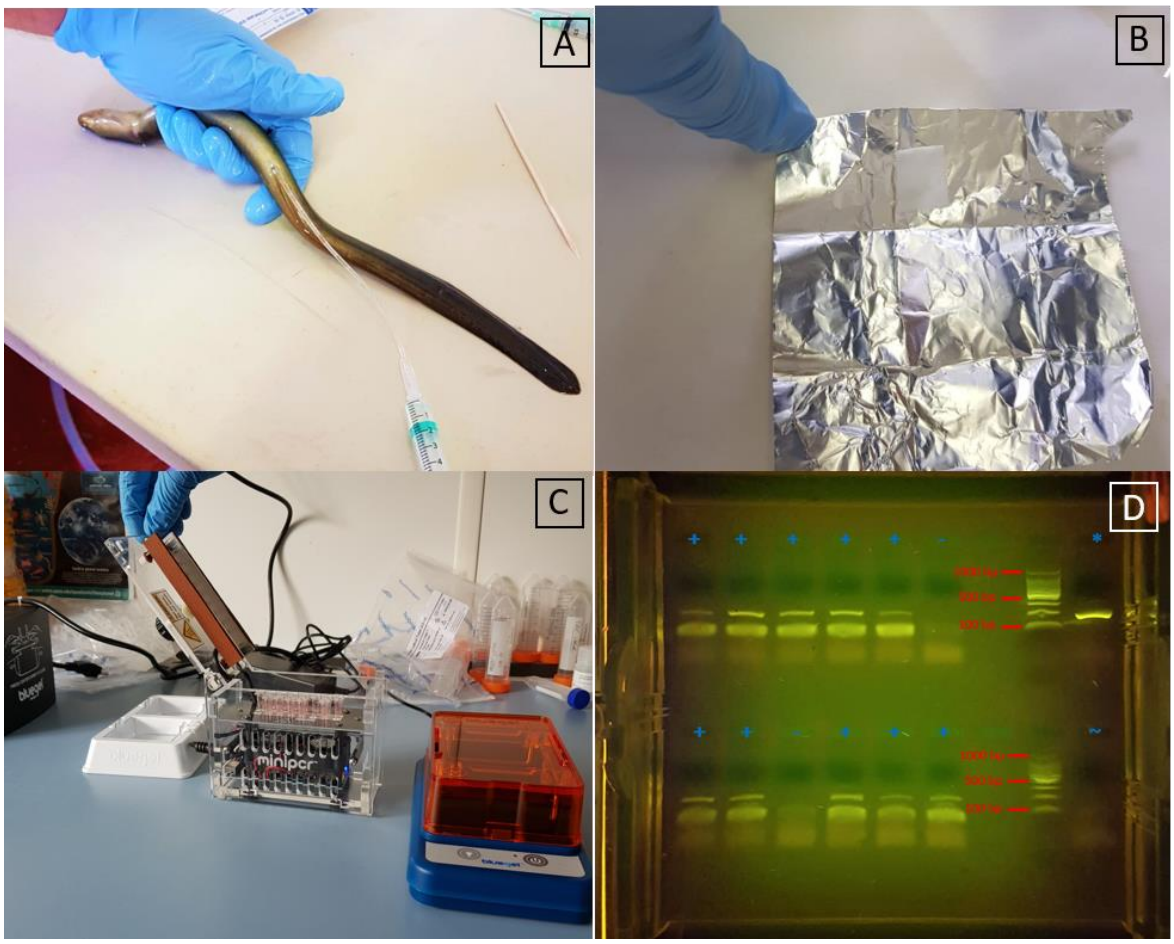

Figure 2-1. Experimental procedure for rapid, in situ and non-lethal molecular detection of *A. crassus* from the European eel. A) Colonic irrigation with sterile saline solution (9 ‰) on an anesthetized yellow eel. B) Collection of a drop of faecal material on a piece of Whatman qualitative filter paper No. 1. C) In situ DNA extraction and diagnostic PCR with MiniPCR thermocycler. D) In situ visualization on electrophoresis agarose gel 2 % on amplified target CO1 gene. "+" Positive amplification from faecal extracted DNA, "-" Negative amplification from faecal extracted DNA, "*" Positive control, "~" Negative control. The amplified fragment can be visualized around 187 bp. The band below represents resultant primer dimer.

2.3.2 Comparison of different DNA extraction methods

The DNA Whatman paper extraction method provides a rapid and more reliable assessment of infection compared to the method based on the Qiagen Stool and Blood kit. Both specificity ($p<0.001$) and sensitivity ($p<0.001$) were shown to be significantly higher using the Whatman protocol (**Figure 2-2**, **Table 3**). The resulting improvement of using the Whatman test in specificity was 46%, in sensitivity 45%, in PPV is 30% and in NPV 41%. Additionally, the time for DNA

extraction from 1 sample using the Whatman paper as compared to a Qiagen extraction was reduced from c.80 minutes to c.20 minutes.

Table 3. Relative *A. crassus* detection for the two different extractions methods across the 3 sampling seasons. For 2019 the same samples were tested with both methods. 2018n considers samples collected in Lough Neagh and 2019s silver eels collected in the Burrishoole catchment.

Extraction Method	Year	Number of samples	Observed Infected	Test Positive	Test Negative	False Positive	False Negative
Qiagen	2017	12	8	3	2	3	4
Qiagen	2018	23	12	4	8	2	9
Qiagen	2018n	41	28	20	10	4	7
Qiagen	2019	28	18	16	4	6	2
Whatman paper	2019	28	18	19	9	2	1
Whatman paper	2019s	27	23	22	4	0	1

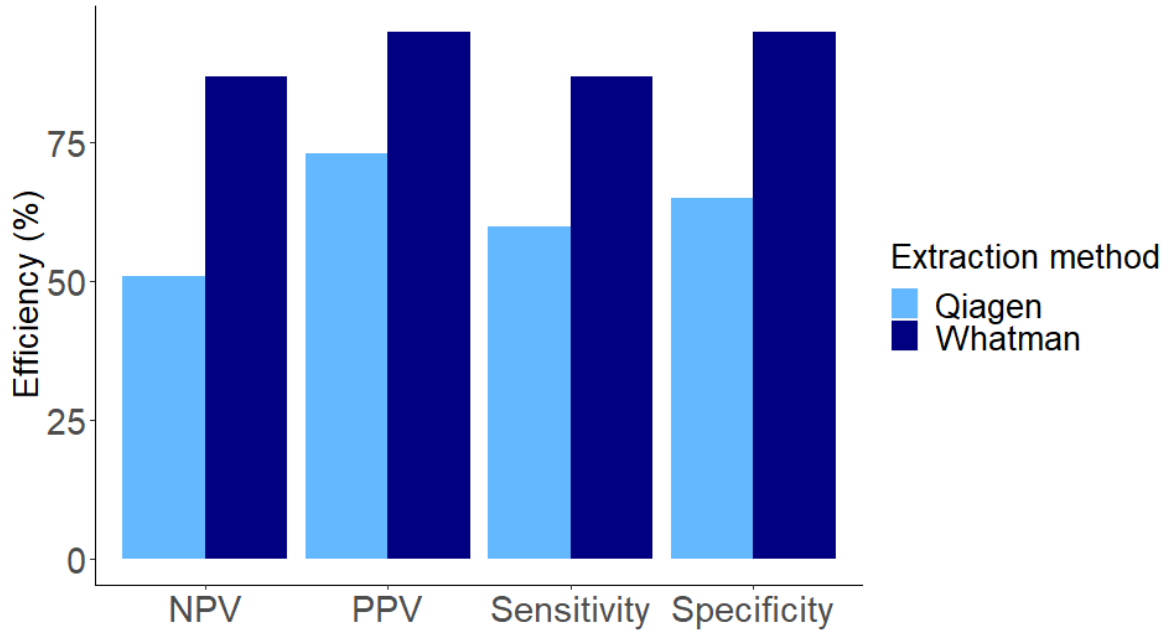

Figure 2-2. Relative *A. crassus* parasite detection efficiency for the two DNA extraction methods. The Whatman DNA extraction method (dark blue bar) performs better in all the categories with an average improvement of 41% over the Qiagen method (pale blue bar). NPV= Negative predictive value, PPV = Positive predictive value. A Welch two-sample T-test indicates both sensitivity ($p<0.005$) and specificity ($p<0.005$) were significantly improved by using the Whatman protocol.

2.3.3 Parasite count in swim bladder and eggs count in faecal material.

Faecal material from all 131 samples was tested to detect the presence of eggs and/or L2 larvae using the McMaster floatation protocol. All 131 collected swim bladders were then screened under the microscope and the number of nematode eggs was reported (Appendix 1, Supplementary material 2.1). No eggs or larvae were detected in any samples. The number of nematodes in the swim bladder showed an increasing trend in infection across the three sampling years and a significant increase in the silver eels collected in 2019 (**Figure 2-3**).

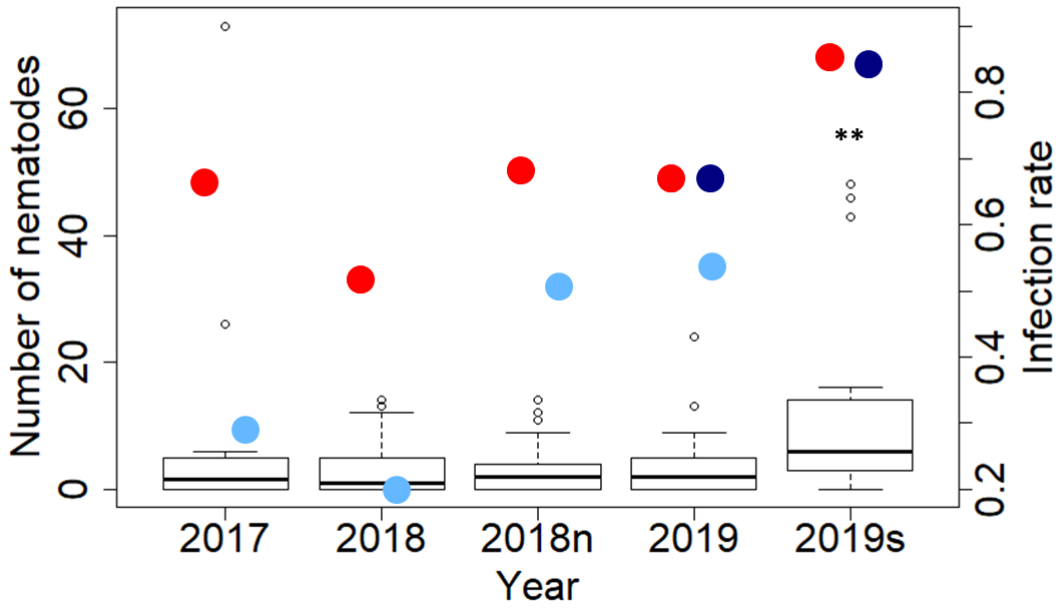

Figure 2-3. Number of *A. crassus* counted in dissected animals and infection rate in different years of sampling. Infection prevalence represents the number of animals infected compared to the total number of animals. The dark line in each box stands for the mean number of nematode per cohort of sampling. Red dots show the actual infection rate based on average parasite load in dissected animals, each empty dot stands for a single dissected eel. Light blue dots indicate the infection rate derived from the extraction using Qiagen Blood and Stool kit. Dark Blue dots indicate the infection rate observed with Whatman. A Mann-Whitney test shows that silver eels in 2019 were significantly more infected than other eels (P value < 0.05). “2018n” refers to samples collected in Lough Neagh and ”2019s” to silver eels collected in the Burrishoole system.

2.4 Discussion

Our study represents the first attempt to develop a sensitive, non-lethal and, importantly, i*n situ* method to establish *A. crassus* infection in *A. anguilla* via the detection of parasite DNA in faecal material. High values for NPV (87%) and PPV (95%) suggest the test may have a useful role in both veterinary and fisheries management contexts. We found inter-annual differences in the prevalence of infected eels in the three years we sampled in the Burrishoole catchment with the total number of infected animals significantly higher in 2019.

Sensitivity is a key consideration for any molecular test. Mitochondrial genes are the major target genes in PCR-based detection systems because they are highly conserved and present in multiple copies (Paoletti et al., 2018). High target copy numbers may explain the high sensitivity of the test we deployed. The mitochondrial gene COI has been widely used to detect the presence of nematode parasites in commercially important fish species (Godínez-González et al., 2017; Herrero et al., 2011; Paoletti et al., 2018; Santos et al., 2006). The use of microsatellites is also a well-established method for parasite detection (Vieira et al., 2016), although these nuclear markers can suffer from lower sensitivity than their mitochondrial counterparts, which may contribute to their poorer performance in detecting *A. crassus* in eels (Jousseaume et al. in 2021).

Some improvement in detection sensitivity and specificity was achieved here by adopting a more 'crude' nucleic acid extraction approach using a Whatman paper. Nucleic acid extraction is increasingly recognised as a major rate limiting step in molecular diagnostics, however, paper-based options offer several advantages in terms of speed and cost (Zou et al., 2017), as seems to be the case in our study. Nonetheless, our final protocol did show both false positives and false negatives, albeit at a low rate. False negatives likely relate to issues with template purification and PCR amplification, or potentially the reduced biomass of younger worms (Barry et al., 2014). Similarly juvenile, un-mated worms are likely to shed less genetic material in the form of larvae. False positives could indicate the presence of early infections, not yet detectable via necropsy – and further investigation of such cases is warranted. It is not clear whether the DNA we are detecting originates from embryonated eggs, cellular material or free DNA shed from the worms. Our inability to microscopically detect the presence of *A. crassus*

larvae or eggs in faecal material suggests DNA or cellular fragments from worms are the likely source. However, our use of ethanol as fixative for storing samples could have played a role in our low success in detecting eggs or larvae (Crawley et al., 2016).

The test we present relies on a simple PCR, not qPCR. Nonetheless, validation against 'real' infection levels assayed via necropsy reveals excellent specificity and sensitivity. Point-of-care qPCR for viral pathogens can now deliver a result in less than 20 minutes (Melchers et al., 2017). Similarly, several mobile qPCR instruments have been brought to the market and have been successfully deployed to deliver veterinary diagnoses in remote locations on actionable timescales for cattle (Hole & Nfon, 2019). However, the cost of such approaches may be prohibitive in respect to their application to the detection of pathogens fish. Our experimental set-up, which fits in a carry-on suitcase and can be performed in the field powered with a portable battery shows that standard PCR, using low-cost reagents and equipment may be just as portable, and informative epidemiologically, as 'higher-end' devices, although benchmarking against a portable qPCR device could be a focus of future study.

Stocking, as part of eel population enhancement, is likely a major contributor to *A. crassus* dispersal, as are translocations associated with the trade in live eels (Laetsch et al., 2012a; Weclawski et al., 2013). Screening of such individuals and early detection with a non-lethal method could be a powerful tool to avoid the spread of the parasite. However, there remains a need to clarify whether our approach has enough sensitivity to detect infection in glass eels and elvers. *A. crassus* is known to infect the elvers or European eels (Haenen et al., 1989) and natural infection has been detected in late-stage glass eels as well as elvers of the American eel *Anguilla rostrata* (Hein et al., 2016). Both juvenile stages are a major component of stocking biomass. Advances in sample pooling designs and detection algorithms during the recent coronavirus epidemic can achieve individual-level identification using a seven-fold lower number of tests than the number of individuals (Shental et al., 2020). Such algorithms could also be adapted to screen large cohorts of eels, but regulation and legislation may be required before the industry agrees to bear the associated cost.

The increase in parasite load we noted from 2017 to 2019 follows a trend that is also found all over Europe, where the parasite is established and is fast colonizing all the freshwater basins (Aguilar et al., 2005a; Schabuss, Kennedy, Konecny, Grillitsch, Schiemer, et al., 2005b; Selim & El-ashram, 2012; Wielgoss et al., 2008). *A. crassus* has a very recent history in the Burrishoole catchment. First detection occurred in 2010 in a yellow eel in brackish water and in 2016 for the first time in a silver eel from freshwater (R. Poole, pers. comm.). In contrast to the rising burdens across much of Europe, in some lakes where the parasite had been detected since first discovery there is stabilization and even a slight decline in nematode abundance and intensities (Wielgoss et al., 2008). There is a possibility of an increased resistance towards the parasites in the long term (Schabuss, Kennedy, Konecny, Grillitsch, Schiemer, et al., 2005b). Although some evidence of increasing tolerance of *A. anguilla* to parasite infection, the overall impact of the parasite on the eel's mortality has been severe and is likely a contributor to the European population's steep decline impeding a recovery (Kirk, 2003; Molnar et al., 1993; Schabuss, Kennedy, Konecny, Grillitsch, Schiemer, et al., 2005b). Treatment of infected eels with anti-helminthic has not been trialed and a single vaccination study aimed at reducing the development of adults from irradiated L3 larvae was unsuccessful and revealed the antibody response is not a key element in resistance of *A. anguilla* against *A. crassus* (Knopf & Lucius, 2008). Infection control via physically blocking transmission, which requires extensive diagnostic testing, therefore represents the only feasible route to reducing population-wide parasite burden.

In this study, we developed potentially useful tool that can be deployed for specific parasite screening for the European eel. The cost per sample is low and the time to run a test comprising 16 samples is under 3 hours. Our test offers managers the opportunity to engage in infection control by assessing the disease status of adult eels before allowing transfers between river systems, although further work is required to establish whether it can survey juveniles. Nonetheless, the rapid test represents an important contribution to the conservation and management of this critically endangered species.

3 Chapter 3 Do diet and salinity induce ecotype-specific phenotypic plasticity between life stages of the European eel, *Anguilla anguilla* ?

Abstract

The European eel, *Anguilla anguilla*, population is considered to be panmictic across his range of distribution. Despite a lack of genetic subdivision across the population, many freshwater catchments are inhabited by two distinct yellow eel ecomorphs. These include a broad head morph with a bigger mouth gap, living in the water column with distinct piscivorous habits and a narrow head morph living in the benthic environment and feeding prevalently on zooplankton and benthic invertebrates. Less apparent dimorphic head shape distribution has also been recorded in glass eels but not in silver eels. The two different morphs exhibit differential fat content allocation which is essential for the transition into silvering. For this study, we collected 307 yellow and silver eels across four lakes in Ireland and Scotland and we implemented a fixed-landmark morphometric methodology to assay ecomorph diversity. We detected a strong difference between head morphology in silver and yellow eels (P value < 0.01). Silver eels showed little variation in head shape, while yellow eels showed greater variability in head morphology but with no evidence of distinct ecomorphs. Eighty per cent of the variation in head shape was explained by the jaw position and size. We also detected a strong influence of salinity in shaping the head morphology, probably linked with food availability across different lakes. Our study demonstrates the importance of jaw size in shaping the European eel's head morphology, consistent with previous studies asserting that diet and prey availability shape this plastic phenotypic trait. However, we did not find any evidence of clear head shape dimorphism. Our improved methodology can be further used to assess the impact of diet and head morphs into fat deposition and eels health status in the conservation management plan to ensure the migration success.

3.1 Introduction

3.1.1 Phenotypic plasticity in the animal realm

Phenotypic plasticity can be defined as the ability of an organism to develop more than one phenotype from the same genotype in response to different environmental conditions (S. A. Kelly et al., 2012). Variation can occur within or across populations and can affect morphs differentiation, behavioural traits and mating (Cogliati et al., 2018). Horn size in the dung beetle, *Onthophagus taurus*, is an example of polymorphism determined by nutritional conditions at the larval stage and body size. The amount of food available to larvae explained 39% of the variation in adult body size and males exceeding a critical body size develop a pair of long, curved horns on their heads, while those smaller than this critical body size remain essentially hornless (Moczek & Emlen, 1999). Plumage signals in birds affect their mating behaviour. The trade-off between the cost of the plumage and the success of the reproduction as shown in the Pied flycatcher, *Ficedula hypoleuca*, is a plastic character responding to conditions in the breeding areas where higher costs of breeding stimulate plumage patching, to ensure a higher breeding success (Moreno et al., 2019). Plasticity in foraging strategies is also an evolutionary response to available resources. The spider, *Parawixia bistriata*, produces two types of webs in response to different prey availability and temporal prey fluctuations (Sandoval, 1994). A similar mechanism is recorded in the tiger snake, *Notechis scutatus*, in which the size of the prey available and geographical confinement shapes their head morphology (Aubret et al., 2004). Phenotypic plasticity can also be latent and occur in specific generations when mostly needed, as showed in the Mexican tetra, *Astyanax mexicanus*, where fish exhibited a derived cave morph in experimental conditions only when exposed to cave conditions (Bilandžija et al., 2020). The role of plasticity can be considered as a mechanism that allows for the expression of traits effecting fitness, which may then be selected under natural selection and play a role in species evolution. (R. J. Sommer, 2020). Plasticity can enable a population/individual to change its expressed phenotype more rapidly that it may do through evolution, which takes many generations.

3.1.2 Morphological adaptation in fish

Morphological adaptation and plasticity in fish is a topic that has been investigated for many years. Bony fish are the largest and most diverse vertebrate clade on the planet (Volff, 2005). Bony fish occur in diverse habitats, allowing the study of adaptation to diverse and sometimes extreme environments (Sleezer et al., 2021). The Antarctic notothenioid group of fishes provide an example of an elevated rate of morphological evolution facilitating evolutionary potential and niche colonization in extreme conditions (Y. Hu et al., 2016). Fish can be used to study the maternal effect on plastic traits; egg size is a commonly studied factor for its relationship with fecundity, maternal fitness, genetics and offspring survival (Cogliati et al., 2018). Bony fish also represent a great model for research in laboratory conditions for their low maintenance requirements in experimental conditions (Oufiero & Whitlow, 2016a). Caudal fin development and regeneration in lab reared zebrafish, *Danio rerio*, is a plastic trait associated with water flow rate, with an increase of fish rays in the caudal fin with the increase of water flow speed (Dagenais et al., 2021). Phenotypic plasticity plays a key role in the East African cichlid, *Astatoreochromis alluaudi*, pharyngeal jaws evolution related to acellular bones and their differentiation was influenced by the ingestion of either hard-shelled snails, or soft, pulverised snails in a laboratory experiment (Gunter & Meyer, 2014). Growth rate and timing of migration are essential for fish survival, in chinook salmon, *Oncorhynchus tshawytsch*, is been shown the importance of absolute egg size in body morphology and its consequences on migration timing (Cogliati et al., 2018). Body shape morphology in freshwater western rainbowfish, *Melanotaenia australis*, has been shown to be affected by water flow matching inhabiting arid regions in nature, allowing them to colonize a variety of freshwater habitats in extreme hydrological conditions (Kelley et al., 2017).

3.1.3 Cranial morphology adaptation

Cranial morphology is recognized as a plastic character in fish, on which depends on the prey target and the position of the fish within the trophic network (Day et al., 2015). Across species, researchers have suggested that feeding ecology differences are the critical driver of head morphology (Wintzer & Motta, 2005). In salmonids like the arctic charr, *Salvelinus alpinus*, three different morphs living in sympatry are known and it has been shown that selective pressures could have

been working on traits related to their trophic niche such as habitat and diet (Simonsen et al., 2017). The body shape and the head conformation often reflects the adaptation to the habitat they are found (Pakkasmaa et al., 1998). In brown trout, *Salmo trutta*, the prey availability shapes the characters of their skull and visceral bones (Marić et al., 2011). Diet variation between and within trout subpopulations determine variation in the length of the premaxilar and maxilar bones (Bridcut & Giller, 1995; Westley et al., 2013). In Atlantic salmon, *Salmo salar*, the shape of the kype, an elongation of the lower jaw forming a hook at the tip, is recognized to be a sexual trait in natural selection and varies across populations (Perry et al., 2019). The European whitefish, *Coregonus lavaretus*, have evolved different ecomorphs adapted to different trophic niches and habitats to avoid competition for food. They are associated with the three main habitats of the lakes where they are found: the littoral, the pelagic and the profundal zones (Bitz-Thorsen et al., 2019) In Arctic charr, *Salvelinus alpinus*, head morphology and ecomorph differentiation is associated with lake size, predicting phenotypic extremes of profundal and pelagic and piscivorous ecomorphology (Bitz-Thorsen et al., 2019; Doenz et al., 2019). The differences in head morphology are found not only during the reproduction phase but also in the juvenile parr life stage, where differences in morphology are associated with environmental adaptation over geographical distances (Solem & Berg, 2011). In threespine sticklebacks, *Gasterosteus aculeatus*, divergent body shape is associated with opportunistic expansion into new habitat to reduce intraspecific competitions (Walker, 1997). Tropical cichlids, *Geophagus sp.*, develop longer and shallower heads when consuming nauplii in comparison with fish feeding on other larvae (Stauffer & van Snik Gray, 2004). Studies suggest that feeding on tougher prey leads to larger and more powerful jaws in anguillid species (Pavey et al., 2015). In the Japanese eel, *Anguilla japonica*, shows a dimorphism in head shape between animals living in fresh or brackish water where slow-growing fish in freshwater become broad-head and the fast-growing fish in brackish water become narrow-head (Kaifu, Yokouchi, et al., 2013).

3.1.4 Phenotypic plasticity in anguillids

The European eel population has been widely recognized as panmictic, despite its huge geographic distribution (van Ginneken & Maes, 2005). Though recent studies

outline that only part of the European population contributes to spawning, differences in the population from a genetic point of view are small (Pujolar et al., 2011). In addition, the drastic decline of the eels population across the past decades is likely to have reduced overall genetic low diversity (Baltazar-Soares et al., 2016). The fact that eels colonising freshwater ecosystems from west Africa to northern Norway interbreed every generation theoretically severely limits their capacity for adaptation and evolution. In the American eel, *Anguilla rostrata* which demonstrates similar patterns of distribution, spawning and migration, differential mortality is thought to drive some genetic specialisation (Pavey et al., 2015). However, overall *A. anguilla,* is thought to rely almost entirely on phenotypic plasticity to enable some level of adaptation to local environmental conditions. For example, *A. anguilla* is thought to occur with two different morphotypes. The two different morphology ecotypes have been independently reported in many water systems across Europe (De Meyer et al., 2016). Studies about differences in eels head morphology are reported in Scotland (Barry et al., 2016), Germany (Amin et al., 2008), Belgium (Ide et al., 2011). Netherlands (Lammens & Visser, 1989) and across different life stages (De Meyer et al., 2015; Meyer et al., 2017). One is characterised by a narrow head, living in the benthic environment and feeding predominantly on zooplankton, the other one is a broad head morph with a bigger mouth gape, partially living in the water column and with piscivorous foraging habits (Barry, 2015). A bimodal distribution of the two ecotypes has been shown, based on the jaw length, head width and head height. The distribution is not discrete and the tails of the bimodal pattern overlap (Ide et al., 2011). Differences in the distribution of such traits among populations are proposed to be explained by the interaction between the population density and the prey diversity (Ide et al., 2011). In contrast, other studies highlight the presence of the two morphs in the glass eel prior to the freshwater feeding stage. However, the presence of the bimodal distribution of the head shape with an overlapping of the two distribution shows probably a transition between those (De Meyer, Herrel, et al., 2017). A recent study supported the hypothesis that diet induces the morphological plasticity of the head shape (De Meyer, Herrel, et al., 2017). The hard prey feeders (broad head) develop a specific region in the post orbital part of the cranium to allow them to crush harder preys. By contrast, soft prey feeders (narrow head) are thought to have better hydrodynamics and slide in the benthic substrate (van Ginneken & Maes, 2005). Specialization in diet

requirement avoids competition for the same prey. However, the different prey types exploited by eel morphotypes are thought to have different energetic contents (De Meyer et al., 2016). Narrow head eels grow slower compared to the broad head morph, they are less aggressive and have lower lipid content (Barry, 2015). Different environments with different qualities of prey can regulate the gene expression and adaptive developmental plasticity, as shown in tiger snakes (Aubret et al., 2004). Presumably similar processes are at play in *A. anguilla*. The polymorphism in head shape observed Japanese eels, *Anguilla japonica*, is associated with bimodal somatic growth and is mainly explained by phenotypic plasticity (S. H. Lee et al., 2018). Mouth width, snout-eye and growth rate are not significantly different between the two morphs of fish coming from freshwater and brackish water. In contrast, the somatic growth rate is statistically different between ecotypes (Kaifu, Miyazaki, et al., 2013). These results suggest a possible differentiation process of head-shape polymorphism in which slow and fast somatic growth, mainly found in the fresh water environment, lead to broad and narrow heads respectively in *A. japonica* (Kaifu, Yokouchi, et al., 2013). In American eels, *Anguilla rostrata*, although there is evidence of panmixia for both nuclear and mitochondrial markers, genetic differences had been found correlated with habitat ecotypes. Eels have the capacity to choose salinity habitats, and if these choices are due to genetic differences, the mechanism has the potential to result in the genotype-habitat associations observed (Pavey et al., 2015). American eels may migrate periodically between habitats of different salinity to result in divergent ecotypes associated with distinct habitat use, creating divergent natural selection of phenotypes between habitats despite the panmictic nature of the population (Jessop, 2010).

3.1.5 Aims of the study

The overall aim of this study is to establish the presence of distinct ecomorphs previous reported in *A. anguilla* among different life stages of European eels sampled in Burrishoole and Loch Lomond catchments. To achieve this the following objectives are relevant:

1) Implement the already existing fixed landmark technique to address head morphology in the European eel, with the intent of including post cranial development between morphs across the two catchments.

2) Better understand drivers in shaping the head morphological differences between the two sites of sampling

3) Try to capture the differences between head morphology across life stages from the same catchment across different years

3.2 Materials and methods

3.2.1 Sample collection

The data was collected over three years of sampling from 2017 to 2019 in four locations across Ireland and Scotland. A total of 106 yellow eels and 48 silver eels were collected from Lough Feeagh, a freshwater lake in the Burrishoole catchment, Ireland, 53°56′56″N, 9°34′32″W. Ninety-seven yellow eels were collected from Lough Furnace, a brackish water lake located in the same catchment and connected to Lough Feeagh with two streams with traps, 53°55'0.1128"N, 9°34'15.2688"W. Seventeen yellow eels were samples in the Bunaveela, a freshwater lake located in the County Mayo, Ireland, part of the Burrishoole catchment too 54°1'25.5"N, 9°32'46.3"W. Finally 39 yellow eels were collected in the freshwater Loch Lomond, Scotland, 56°6'40.924"N 4°37'43.897" W (**Figure 3-1) (Table 4).** All animals were collected using unbaited fyke nets, deployed overnight in chains of 10 nets set at different lake depths. Eels were mildly anaesthetized with MS-222 and a head picture was taken with a Canon EOS 90D including a scale bar in mm. The study was carried out under a Health Products Regulatory Authority (HPRA) license number AE19130-P096 (Appendix 2, Supplementary material 3.1).

Figure 3-1. Map indicating sampling sites of collection for all the eels. Red star indicates sampling area in Loch Lomond in Scotland and yellow stars respectively in Bunaveela, Lough Feeagh and Lough Furnace in Ireland.

Table 4. European eel samples collection for head digitalization.

Lake	Life Stage	Year	Individuals	Cuntry	Salinity
Feeagh	Yellow	2017	22	Ireland	Freshwater
Feeagh	Yellow	2018	31	Ireland	Freshwater
Feeagh	Yellow	2019	51	Ireland	Freshwater
Furnace	Yellow	2017	12	Ireland	Brackish
Furnace	Yellow	2018	64	Ireland	Brackish
Furnace	Yellow	2019	21	Ireland	Brackish
Loch Lomond	Yellow	2019	38	Scotland	Freshwater
Feeagh	Silver	2017	22	Ireland	Freshwater
Feeagh	Silver	2019	25	Ireland	Freshwater
Buunaveela	Yellow	2017	17	Ireland	Freshwater

3.2.2 Fixed landmark

All the acquired photos were edited using PhotoShop CS4 (version 11.0) to increase brightness and sharpness when needed to highlight head shape features. Edited

images were digitalized into TPS files using 'tpsUtil' version 1.78 (Rohlf, 2015). TPS files were used for placing landmarks to generate coordinate data using the software 'tpsDig2' version 2.31 (Rohlf, 2015). A scale was drawn using the reference scales within each image. Landmark number and position were chosen based on previous studies (Barry, 2015). 13 fixed landmarks were placed in a specific sequence in each image in succession (**Figure 3-2A**). Landmarks were placed onto specific features of the eels' heads. 307 images in total were used, one per individual.

3.3 Statistical analysis

3.3.1 Data standardization

All analyses were performed in R Studio version 3.4.1. We ran a Generalized Procrustes Analysis (Rohlf & Slice, 1990) using R package Geomorph version 3.0.3 (D. C. Adams & Otárola-Castillo, 2013). Data pattern and distribution were visualized using OLS-centering and projection of the data using gm.prcomp function. To remove non-shape effects from the landmark coordinates, a procrustes superimposition was performed to standardise position, scale, and orientation of the specimens. In order to control for common allometric effects, shape data were then regressed against centroid size of the head to obtain the residual shape component for subsequent analyses (**Figure 3-2B)** (Ivanović & Arntzen, 2014). Shape variation was further assessed by producing deformation grids to compare the shapes corresponding to the extremes variations (Dean et al., 2021).

3.3.2 Morphological variability between lakes and life stages

The resulting Procrustes shape coordinates were used to identify the morphological variabilities patterns using allometry covariation. Allometry models were created procD.allometry function. Variables considered in the model are country of origin, lake of sampling, water-type and life stage. The best fitted model was selected using reveal.model.designs function of RRPP, which does pairwise comparison of the allometric model with ANOVA. Predictors for the allometric variabilities were visualized using PCA based on the model residuals.

3.4 Results

3.4.1 Head morphology continuum

GPA adjusted coordinates of the eel head configurations in the yellow and silver eel groups were plotted to visualise the differences in average head shape configurations alongside the variability of head shape configurations. (fig. 2A). Implementing the number of the published fixed landmark from 9 to 13 allowed us to include in the analysis a post cranial development. PCA was then performed on acquired digitalized coordinates to visualize any trend of clustering of the data. There is no evidence of separation of groups by head morphology but data formed a continuum across all the sampled animals (**Figure 3-3**).

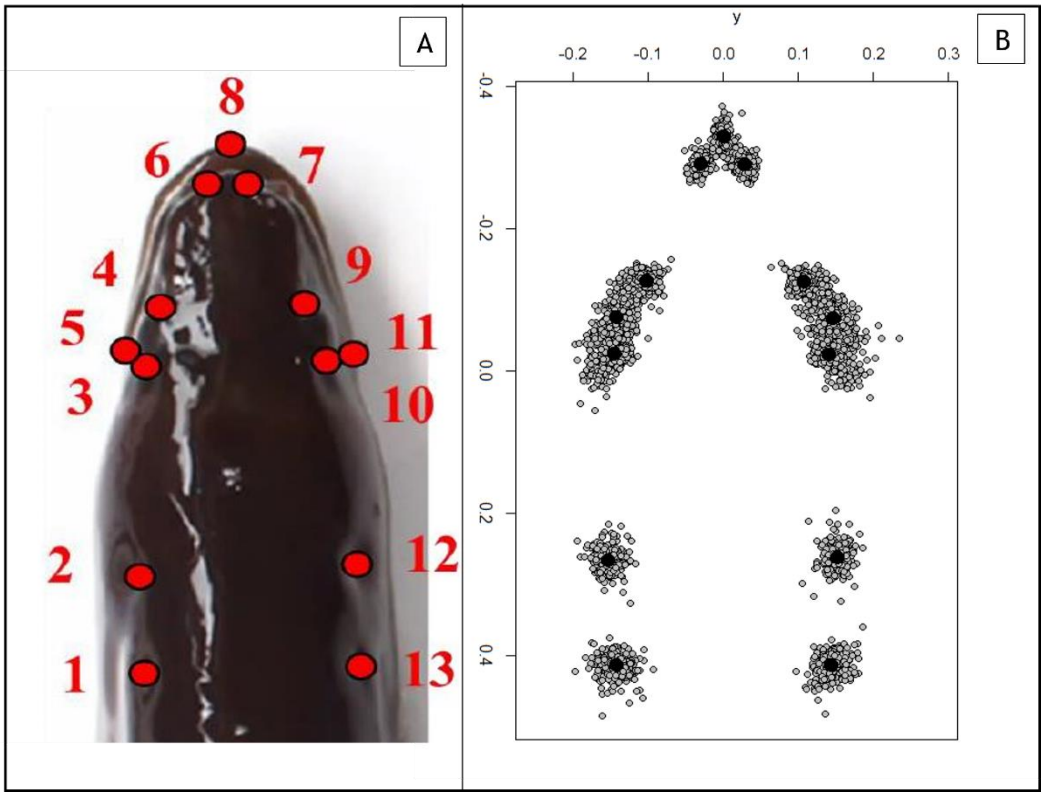

Figure 3-2 Landmark placing for coordinate acquisition over imposed an eel head shot. **A**: Landamark placed on the eel head picture: the four dimples on the back of the head [1, 2, 12, 13], ends of eyes [3-4, 9-10], end of jaws [5, 11], nostrils [6, 7], the tip of the jaw [8]. **B**: Representation of the Procrustes superimposition analysis. Black dots represent centroids, the average configurations of each group, with the grey data points representing each data sample

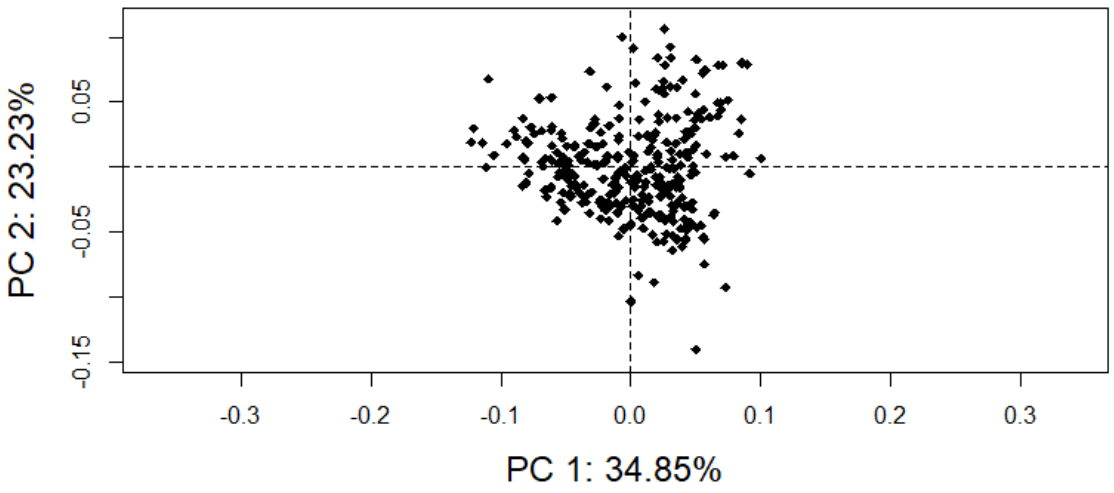

Figure 3-3 Principal components analysis on Procrustes shape variability across for all the aligned digitalized eel's head photographs. There are no clearly separated clusters of morphology across all samples.

3.4.2 Head shape trajectory

Trajectory analysis across all eels in all sites revealed substantial variation in the head morphology mainly linked to the jaw shape and mouth gap opening (**Figure 3-4A**). Vectors between the minimum and maximum variations of shape differences were plotted for both silver and yellow eels. The positions of the jaw landmarks explain the largest proportion of variation in the shapes. Post cranial, the tip of the mouth and nostril landmarks are not contributing significantly to the variation in head shape (**Figure 3-4B**).

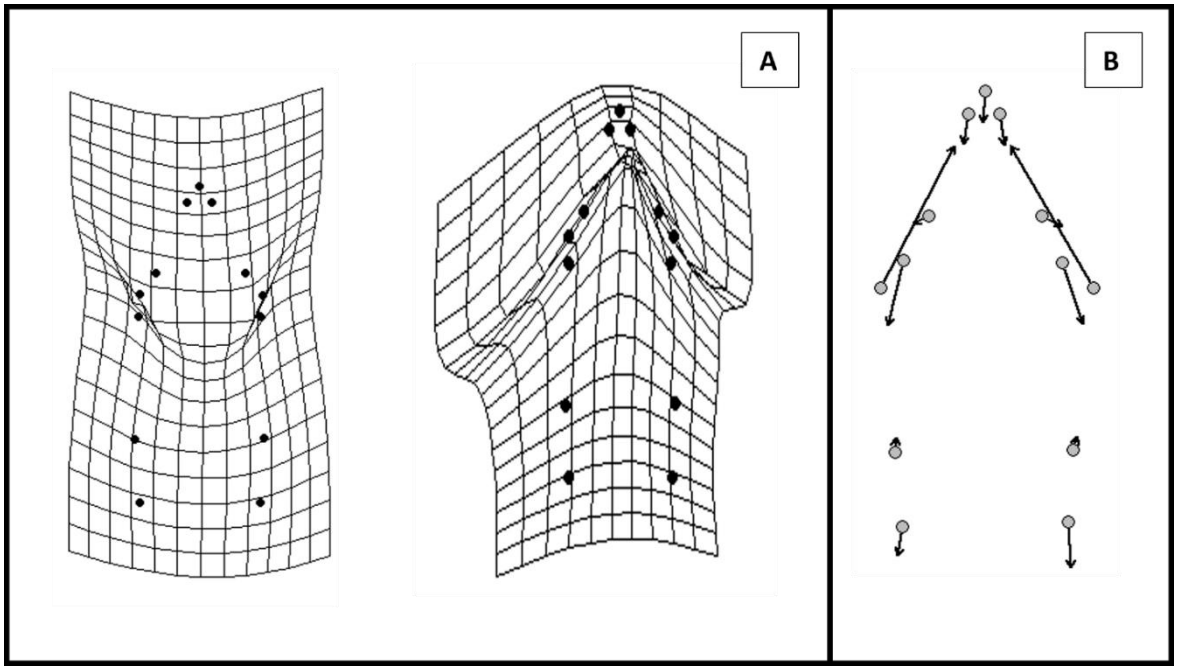

Figure 3-4 Trajectory analysis across all eels in all sites A: Deformation grids to compare the shapes corresponding to the extremes of the digitalized individual eel head morphology. **B**: Vectors between the minimum and maximum variations of shape differences across all samples.

3.4.3 Geographical Differences and life stage differences among yellow and silver eels

The allometry model showed an effect of geographical location and life stage on head morphology. PCA based on trajectory analysis of the allometric model shows that PCA1 and PC2 combined, explain more than 80% in shape variability (**Figure 3-5A**). The two principal components are associated with the jaw landmark (P value < 0.05). There is a strong effect of life stage on head morphology (Rsq 0.129, P value < 0.01) (**Figure 3-5A**). Silver eels tend to have a relatively smaller jaw, with landmarks marking the jawline falling before the landmark of the eye pupil. Yellow eels have a broader jaw with the landmark of the jaw varying between extreme configurations. There is also a smaller but significant effect of the lake of origin on head shape morphology (Rse 0.025, P value < 0.01). Lough Bunaveela, Furnace and Lomond appear to have a similar head shape compared to Lough Feeagh which covers the full range of morphological variation from a graphical interpretation of the PCA (**Figure 3-5B**). The salinity of the water also impacts morphologic variation (Rsq 0.05092, P value <0.01) (**Figure 3-5C**). Eels coming

from brackish water environment have a jaw variation less pronounced than samples coming from freshwater.

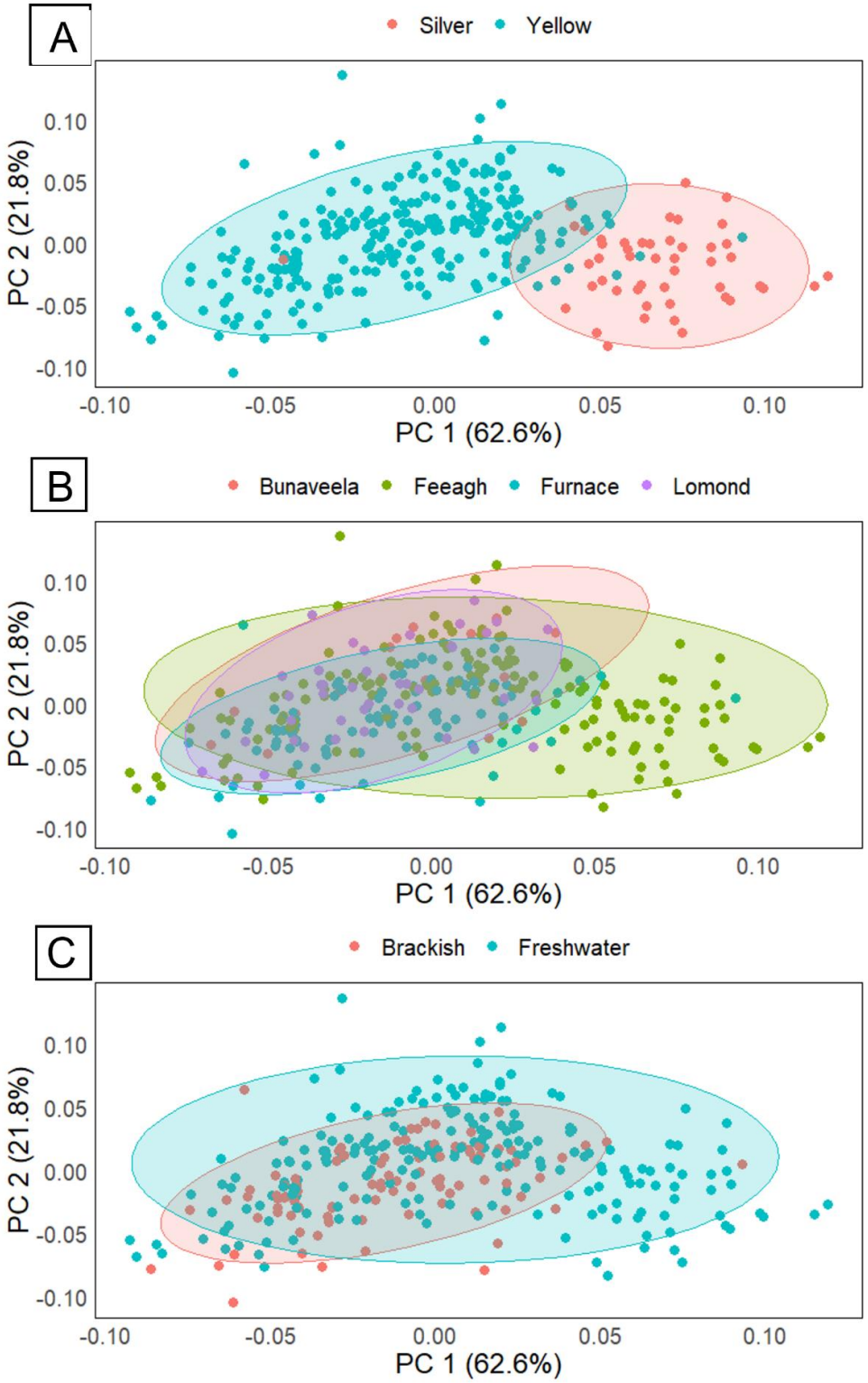

Figure 3-5 Principal component analysis based on the prediction (PredLine) and projection (RegScore) of the best fitting common allometric model across all eels (each dot is a single eel). Percentages in parentheses indicate the percentage of variation explained by the principal component. PC1 explains most of the variability and is associated with the jaw landmark. Confidence ellipses are set

at 95% confidence with equal frequencies. **A**: Life stage as response variable **B**: Lake of origin as response variable **C**: Salinity as response variable

3.4.4 A lack of morphological discontinuity among yellow eels

When implementing the allometry model only on yellow eel, the lake loses its effect on head morphology (P value > 0.05) and we find an effect of salinity and country of origin. The variance explained by the sum of the two principal components based on the trajectory model is below 50%. Water salinity (Rsq 0.068 P value <0.01) and country of origin (Rsq 0.029 P value < 0.01) have an effect on the head shape (**Figure 3-6A**). Eels living in brackish water exhibit a less pronounced variation, with mouth opening never reaching the extreme width found in freshwater animals. Yellow eels in Scotland tend to have a less extreme jaw configuration, meanwhile, yellow eels sampled in Ireland have a greater variation of the jaw landmark (**Figure 3-6B**).

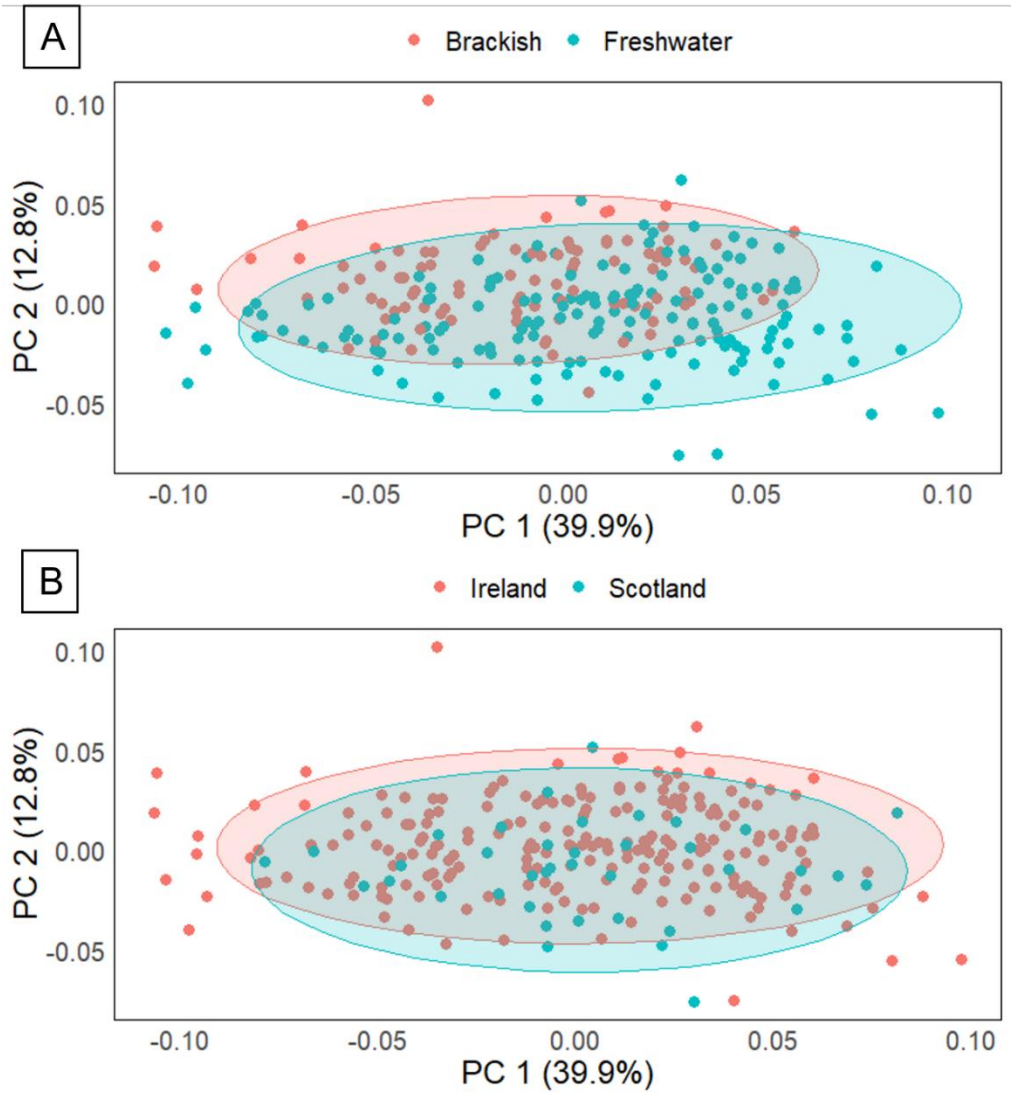

Figure 3-6 Principal component analysis based on the prediction (PredLine) and projection (RegScore) of the best fitting common allometric model only for yellow eels. Percentages in parentheses indicate the percentage of variation explained by the principal component. Confidence ellipses are set at 95% confidence with equal frequencies. **A**: Salinity as response variable **B**: Country of origin as response variable.

3.5 Discussion

The aim of the study was to implement the use of fixed landmark analysis to address morphological variation in the head shape of the European eel. Morphometric analysis revealed significant differences in head shape variation between life stage, study site and water salinity. We were not able to detect any evidence of clear bimodality in head shape consistent with broad or narrow head ecomorphs. To avoid the overpowering effect of salinity and site of sampling, we

ran the same analysis within lake of sampling and we didn't detect any bimodal distribution of head shape. Instead, head shape variation was continuous with all the populations' samples. When accounting only for yellow eels, which represents the feeding stage, again we did not find a bimodal distribution of cranial morphology but the characterizing feature shaping the head differences was the country of origin and the water salinity.

When yellow eels mature into non-feeding silver eels, their jaw size shifts towards smaller and narrower jaws, there were no broad jawed silver eels found in our data. This finding can have two possible explanations. Broad headed eels are silvering at a lower frequency, there is some evidence that narrow headed eels might acquire lipid faster and thus might migrate in higher numbers or the broad head ecotype is potentially lost as yellow eels mature into silver eels, with a jaw modification. Silver eels start a long migration journey with up to 47 km day speed and daily vertical dive of 1000m in the open ocean (Righton et al., 2016). During migration silver eels stop feeding and internal organs are remodelled as energy is invested in migration and gonadal development (C. Durif et al., 2009). The plastic remodelling to a more streamlined jaw is beneficial in reducing hydrodynamic drag and likely contributes to a successful migration. The jaw rearrangement also results from morphological changes associated with the increase of the eye size, which is positioned just above the jaw line (C. Durif et al., 2009). Eye size is associated with the complex environment with light variation, phytoplankton and dissolved organic matter, therefore an increase in the size of the eyes may favor increased visual sensitivity (Lisney et al., 2020). During the migration, eye size is considered an essential trait for success in reaching the spawning ground. Silver eels present enlargement of the eye with a visual sensitivity of the retina pigments shifting from green-sensitive to blue-sensitive for better vision during deep diving in the marine environment (van Ginneken & Maes, 2005). In anguillids, eye size is also associated with predator avoidance (Kaifu, Yokouchi, et al., 2013). In other diadromous fish like salmon, studies on juveniles have shown that feeding rates are 7.5 times higher during daylight (Perry et al., 2021). Larger eye size is likely due to the lower visibility and has been hypothesized to be an adaptation to locating and ingesting prey in low visibility conditions (Drinan et al., 2012). In mandarin fish, *Siniperca kneri*, eyes size is also associated with skull reshaping in

flowing water environment, same environmental condition which silver eels are exposed during migration (Cao et al., 2021).

Analysing only the feeding yellow stage we did not find a bimodal distribution of the head morphology but a continuum between different head morphologies. Traditionally broad head eels tend to feed on hard and large prey, such as fish and molluscs, whereas narrow-headed eels consume smaller and more soft-bodied prey (De Meyer et al., 2016). Eels with different head widths displayed significant patterns of trophic niche segregation (Cucherousset et al., 2011). Fish are more energetically profitable than invertebrates but are more costly to capture and handle, then it is likely that head morphology affects eel foraging performances where broader headed individuals forage more efficiently on fish as capture and handling times are reduced through increased mouth gape (Galarowicz & Wahl, 2005). This potential of food niche separation may be crucial when intraspecific competition for prey is high (De Meyer, Herrel, et al., 2017). Reduced competition for food increases the survival and fitness of the respective morphs (De Meyer et al., 2016). We were not able to detect a clear separation in the head differentiation, it is ecologically relevant that the whole spectrum of eel morphology occurs in the same lake (Ide et al., 2011). To support the diet driven differentiation theory of the head shape, eels raised in captivity are exclusively narrow headed (Proman & Reynolds, 2000). Our findings of a non-bimodal distribution in eels contrast with previous research. In Europe, there is a series of studies which report a bimodal distribution as in Germany (van Ginneken & Maes, 2005) and the Netherlands (Lammens & Visser, 1989) associated with varying feeding conditions. Bimodality in head shape has also been suggested for Japanese eels (S. H. Lee et al., 2018) but interestingly, such a head dimorphism has not been suggested for the American eel, despite the morphological resemblance, close phylogenetic relationship, similar life cycle and spawning grounds to the European eel (Barry et al., 2016; Frankowski et al., 2009; Jacobsen et al., 2014). The presence of ecomorphs might vary year-on-year with changing environmental conditions, as demonstrated for sex ratio in silver eels during migration that is liked to rainfall and river flow, the proportion of lacustrine habitat and pollution by oestrogen-like substances (Laffaille et al., 2006). Biomodality is not observed in our data but it does not mean feeding specialisation is not occurring within a shared habitat (Klemetsen et al., 2003). Our analysis shows that there is a

significant effect of jaw shape on head shape trajectory, but we did not investigate the relationship between head width and total length, which was reported to be a crude measure of the head size variation in relation to full body length in previous study (De Meyer et al., 2015). Unfortunately we did not measure full body length for all our individuals.

We found that one of the main factors of shaping head morphology is the water salinity. In Japanese eel, *Anguilla japonica*, a differentiation process of head-shape polymorphism is known in which slow and fast somatic growth lead to broad or narrow heads are associated with fresh and brackish water respectively (Kaifu, Yokouchi, et al., 2013). The differences in the hardness of the main food species might play a role in the head-shape transition process between morphs. Hard feeders develop broader heads and a broader adductor mandibulae region, whereas soft feeders develop narrow heads and a less broad adductor mandibulae region (De Meyer, Maes, et al., 2017). This theory also explains why the lake of origin has a strong impact on head morphology in our samples. Lough Feeagh, Bunavilla and Loch Lomond are oligotrophic freshwater lakes of different sizes and Lough Furnace the only brackish water lake with a wide connection to the ocean. Loch Lomond is one of the biggest Scottish water basins offering a wider range of ecological niches (Maitland & Adams, 2005). Instead Irish lakes are smaller, with a less complex environment variability and more exposed to drastic atmospheric changes (S. Kelly et al., 2020). The allometric models and the trajectory analysis we propose are not perfect. We were not able to record prey abundance or life history traits for all the fish we collect. We are only able to explain a small portion of the variance between the head shapes. Most of the head morphology variation and adaptations to different environments still remains unsolved and more study will need to be conducted to include prey availability, trophic niche specialization, ecological factors, diet preferences and stable isotope in gut content. The level of complexity in eels life history traits makes a study based on two populations comparison a simplistic representation of the complex adaptation of this animal. A final factor that we cannot exclude is the influence of genetics in morphological variation. Head shape can be influenced by differential gene expression levels and by exposure to different environmental conditions (De Meyer, Maes, et al., 2017). Eels populations are considered panmictic (van Ginneken & Maes, 2005), but there is already considerable non bimodal variation

in head width and snout bluntness of glass eels suggesting that differentiation in head morphology can be a genetic trait already differentiation from larval development (De Meyer et al., 2015). Further research on this subject is required to find out the genetic basis of phenotypic plasticity in head development. Including some habitat information and main prey availability and trophic status of lake can be beneficial in the resolution on the allometric model to explain variance of observed differences between head shapes.

In conclusion, in this study we present implemented the classic approach of fixed landmark to detect head morphology in European eels. We detected a continuous variation of head shapes within lakes, contrasting previous results showing a bimodal pattern of differentiation, but we also showed a strong effect of life stage, sites and water salinity in shaping the head morphology. We found a convergence towards the narrow morph in silver eels possibly related to the stop of feeding at the beginning of the migration. Yellow eels presented the most diverse head shape conformations driven by salinity and lake of sampling. Both those variables can correlate with prey availability and shift in diet. Further studies of yellow and silver eel behaviour and feeding habits can be the key to understanding the relationship between the plastic nature of head morphology.

4 Chapter 4 Metabolic rate and migratory phenotype in European eels, *Anguilla anguilla*.

Abstract

The oxygen consumption in fish reflects their basal metabolic status and can be useful to assess the physiological state of an organism, and correlates with the behaviour of the animal. The maintenance of metabolic costs in teleosts is limited by physiological and environmental factors. Evaluation of metabolic rate is essential to understand metabolic adaptation to body alteration, migration and parasitic infection. In this study we examined standard metabolic rate (SMR), maximum metabolic rate (MMR) and aerobic scope (AS) in 74 animals between 50 yellow and 24 silver eels using intermittent flow respirometry chambers from three lakes in Scotland and Ireland. Eels with higher lean mass have a higher standard metabolic rate (P value < 0.05). The nematode parasite, *A. crassus*, impacts SMR in both freshwater life stages (P value <0.05), but not MMR or AS. Salinity also had a significant effect on metabolic traits with eels fished in brackish water showing a higher SMR, potentially to cope with higher osmoregulatory demands. We found that in silver eels higher lean mass corresponds in lower MMR and AS, potential pointing to the importance of endurance, rather than burst, swimming during migration. Our data provide a first assessment on the relationship between parasite infections status, lipid content, migratory status and metabolic phenotype in European eels. The data lay the groundwork for understanding the physiological constraints on migration in this critically endangered species.

4.1 Introduction

4.1.1 Metabolic rate variation in fish

The capacity to provide oxygen for vital processes and important activities, such as reproduction or digesting or movement, is essential for animal fitness (Chabot, McKenzie, et al., 2016a). Oxygen consumption is often used as an indirect measure of metabolic rate (Nelson, 2016). An organism's metabolic rate is the amount of energy expended by that organism in a given time period (Deutsch et al., 2015) Metabolic rate can be influenced by environmental factors, such as temperature

and salinity, or individual factors, like body size and fat content (Norin & Clark, 2016a). Understanding how energy consumption and allocation in ectothermal animals, like fish, varies in response to external changes is crucial to address physiological adaptations (Cooke et al., 2014). The cost of basal metabolic function increases with the increase of temperature, especially in bigger fish where the changes in thermal sensitivity follow an allometric function with body size (Breau et al., 2011). Larger fish mechanism to cope with the energy required to sustain metabolism with the body size increase consists in having a smaller surface area to volume ratio making them more resistant to external temp change (Li et al., 2018) Standard metabolic rate (SMR) represents the minimum rate of energy use needed to maintain basal metabolism, whereas maximum metabolic rate (MMR) is the upper limit for the capacity to perform oxygen-consuming physiological activities (Killen et al., 2021). Aerobic scope (AS) is the difference between SMR and MMR and represents an individual's total capacity for simultaneous oxygen-consuming tasks above basal metabolism (Holt & Jørgensen, 2015). Metabolic rate has also a strong impact on fitness. Fitness, considered as the trade-off between growth, reproduction and survival, can take up to 50% of the daily energy expenditure, representing the highest maintaining cost but higher SMR is known to have a positive effect on survival (Auer et al., 2015). Differences in SMR have also been associated with growth, reproduction and survival in experimental conditions where the food was provided ad-libitum, with fish achieving the greatest growth recording the lowest SMR (Reid et al., 2011). SMR has also been linked with foraging, predator avoidance and intraspecific aggression (Metcalfe et al., 2016). Generally individuals with higher SMR or resting metabolic rates are more aggressive and more likely to become dominant over conspecifics, possibly driven by local variation in factors such as food availability as shown in brown trout, *Salmo trutta* (Lahti et al., 2002). Links between metabolic rate, physiology and behaviour observed under experimental conditions may not be replicated in the field, where interactions are more complex and trends do not always match the laboratory based observations (Farrell et al., 2008). Growth and reproduction can be negatively correlated with metabolic rate (Holt & Jørgensen, 2015; Norin & Malte, 2011). Aerobic scope and MMR and their relation with SMR is essential to understand the connection between metabolism and life history traits (Einum, 2014; Hayes, 2010). Variation in AS among individuals can be linked with the ability to cope with environmental changes and

migratory effort, often called "coping mechanisms" (Hayes, 2010). Individual variation in AS might be expected to have important consequences for fitness, but remains largely unexplored.

4.1.2 Metabolic rate and migration

Migration has evolved as an adaptation to exploit seasonal peaks in resource abundance, avoid predation and improve reproduction success, but it comes with a cost (Lok et al., 2015). The cost can be direct, reducing survival at the migration time or carried into next year reducing future reproduction event success and fitness (Klaassen et al., 2014). The cost of migration in terms of physiology and metabolism is high (Alves et al., 2013). Endurance during migration is a function of energy availability and thus the accumulation of fuel, in the form of fat, is an essential mechanism supporting migration (Lennox et al., 2016). Accessing food of sufficient quality and quantity may mitigate the energetic impact during migration (King et al., 2015). The cost of migration in physiological mechanisms needs to take into consideration also endurance, and sustained locomotory effort (Jachowski & Singh, 2015). Those are all activities requiring a high energetic level (Goossens et al., 2020) Metabolic rate has a strong impact on the potential for migration in the animal realm (Tudorache et al., 2007). Bird and mammal migratory species tend to exhibit a higher metabolic rate related to the high energy demand of a long distance migration (Jetz et al., 2008). Migratory species living in warmer areas of the planet have a lower metabolic rate, gradually increasing towards the pole to facilitate high rates of thermoregulatory heat production during rapid heat loss at low environmental temperatures (Lovegrove, 2003). More sedentary bird colonies also present a lower metabolic rate as shown in barnacle geese, *Branta leucopsis*, where in both adults and juveniles oxygen consumption is lower if living in a sedentary colony (Eichhorn et al., 2019). During their migration, birds exhibit considerable phenotypic flexibility and organs changes which needs to be taken into consideration when studying the effect of metabolic rate on migration (Mckechnie, 2019). In Great knots, *Calidris tenuirostris*, a decrease in metabolic rate at the end of a long distance migration, correlated with the alteration of the internal organs, especially kidneys, liver and heart, and a 42% reduction in resting metabolic rate (Phil et al., 2001) (Phil et al., 2001). The availability of stored fat along with a variety of environmental factors

influences the flight performance and could limit endurance, considering that long distance migrations require an great energy expenditure and can cause exhaustion (Bairlein et al., 2015).

4.1.3 Metabolism in anadromous fish and migratory fish

It is important to understand the energetic investment and metabolic profiles for different life history stages in migratory fish. Few studies report the effect of inter-individual variation in aerobic scope on migratory performance. It is suggested that fish experiencing strenuous migration in adverse conditions have a higher aerobic scope to sustain their journey (Crozier & Hutchings, 2013). In Sockeye salmon, *Oncorhynchus nerka*, river condition, especially temperature, and cardiac capacity during migration play an important role in defining their metabolic rate. Fish with larger heart and better coronary supply exhibit a greater aerobic scope but they are more susceptible to physiological limitations in aerobic performance due to cardiac collapse at high temperatures (Eliason et al., 2011). An increase in mortality during migration has also been reported this may be linked with a low aerobic scope and temperature in Sockeye salmon, Pink salmon, *Oncorhynchus gorbuscha*, and Coho salmon, *Oncorhynchus kisutch*. (Crozier & Hutchings, 2013). Diadromous fish, not only have to face migration exhaustion but the osmoregulation cost of switching between hypo and hyperosmotic aquatic environments (Chabot, McKenzie, et al., 2016b). The cost of gill metabolism and swimming speed is estimated to be higher in saltwater caused the cost of hyperosmotic regulation is higher (Wagner et al., 2006). Exposure to different salinity levels can also stimulate an adaptive increase in the activity of ion-translocating enzymes in the gills to promote salinity tolerance (McKenzie et al., 2001). Osmoregulation can modify the SMR and MMR in fishes, various salinities exposition in laboratory conditions altering the maximum oxygen consumption (Norin & Clark, 2016b). In salmonids, short-duration saltwater transfer causes a reduction in swimming performance, which can be directly related to plasma ion levels being significantly higher in the blood of fish in saltwater compared to freshwater (Brauner et al., 1996). Sockeye salmon have a significantly higher routine and active metabolic rates in saltwater compared to freshwater, mainly caused by the difference in ions concentration in the environment altering the sodium, chloride and potassium concentration in the blood (Wagner et al., 2006).

In Pacific salmon experiencing the transition from freshwater to saltwater, the same pattern was found, with adults having significantly higher routine and active metabolic rates in saltwater (Hinch & Farrell, 2015). Anadromous population of brown trout, *Salmo trutta*, have a higher MMR and aerobic scope compared to non-migratory populations, showing the importance of life history traits on the ability to migrate to sustain swimming performance and food availability (Archer et al., 2020). The same trend has been found in juvenile of Atlantic salmon, *Salmo salar*, where smolts ready to start the migration to sea present a higher SMR than those that are not (Seppänen et al., 2010). There are little data around the metabolic remodelling and costs involved with long range migrations in the marine phase of diadromous fish.

4.1.4 Importance of fat content in the eels' migration

European eels, *Anguilla anguilla*, undertake a long marine migration for their only breeding event in their lifetime, during which they cease feeding and undergo a substantial physical and physiological remodelling (van Ginneken & Maes, 2005). Among the physiological changes during migration, we see the skin pigmentation alteration, function of the skeletal muscles modification, digestive apparatus remodeling and changes in the density of chloride cells in the gills apparatus (Han et al., 2001). The digestive apparatus, no longer in use, is re-absorbed and atrophies. All energy is allocated towards the migration and gonad development for the final reproductive event (C. Durif et al., 2009; van den Thillart et al., 2009). Therefore, to sustain this remodelling, the European eels rely on the stored fat during the freshwater (‘yellow’) phase and the rearrangement of the internal organs (Righton et al., 2016). There is no study investigating the effect of fat mass on metabolic rate in eels. Fat is considered to not influence the metabolic rate because adipocytes are largely metabolically inactive, but fat stores are essential for a successful migration (Cooke et al., 2014). In the southern catfish, *Silurus meridionalis*, has been shown there is no effect of body fat content on their metabolic rate, increased body fat content did not decrease the resting metabolic rate (Luo & Xie, 2009). In Trinidadian guppies, *Poecilia reticulata*, had been shown a positive correlation between the increase of organ body mass and metabolic rate (Odell et al., 2003). Is brown trout on the other hand the trend has not been confirmed, with no significant effect of internal organs changes on metabolic rate

(Norin & Malte, 2011). In the European eel it has been shown that the sum of the organ mass (liver, heart, spleen and intestine) explains the 38% of the variation in SMR. Eels with larger liver and intestine have increased food assimilation efficiency, resulting in a higher growth rate but in turn increases the basic cost of living (SMR) (Boldsen et al., 2013). To our knowledge, the effect of fat accumulation and efficiency of energy conversion in different metabolic profiles in the European eel is still unknown.

4.1.5 Effect of *Anguillicoloides crassus* on migration

Anguillicoloides crassus is an invasive nematode parasite accidentally introduces in Northern Europe about 30years ago (Becerra-Jurado et al., 2014a). The parasitic infection can have detrimental physiological effects, can be linked with secondary bacterial infections, and can influence the eels silvering phase and it can alter immune response (Fazio et al., 2012; Kirk, 2003; Schneebauer et al., 2017). It has also been shown that the presence of the parasite can affect the adaptation to the marine phase, a different allocation of the gut mass and alteration of the sexual maturation (Fazio et al., 2012). *A. crassus* has also physiological effects on the swim bladder. The parasite can lead to a reduction of gas deposition and gas volume because it feeds on the swim bladder wall producing an immune response defence that creates scaring tissue making the wall thicker and less elastic. The parasite can also reduce swim bladder elasticity and increase the energetic demand for buoyancy (Henderson et al., 2012). During the freshwater stage the swim bladder is thought to possess a minimal impact on buoyance regulation because eels are primarily benthic animals, not experiencing critical depth changes (Barry et al., 2014). The effect of parasites on fish metabolism more generally is not clear, with ambiguous and contradictory studies published. Parasitism seems to not have a consistent effect on SMRs of fish hosts (Robar *et al.*, 2011). Brain parasites can cause alteration in behaviour, exposing the fish to more risks and it can disrupt the metabolism of their host both during parasite exposure and after infection, as shown in California killifish, *Fundulus parvipinnis* (L. E. Nadler et al., 2021). Ectoparasites, on the other hand, have a strong impact on the fish metabolism reducing swimming performance (Binning et al., 2012). In Atlantic salmon, the parasitic amoeba, *Paramoeba perurans*, is the cause of amoebic gill disease (AGD). AGD compromises gill function both in terms of gas

exchange and ion regulation, reducing the aerobic capacity with lower haematocrit, haemoglobin and higher plasma osmolality caused by the reduced capacity to maintain ionic homoeostasis (Hvas et al., 2017). Parasitic infection can also interfere with immune response caused by infection, inflammation and chronic stress from elevated cortisol (Balasch & Tort, 2019). The metabolic costs of mounting an immune response and its possible associated tissue repair can impact the aerobic scope (Robar et al., 2011b). In the mosquito fish, *Gambusia holbrooki,* immune challenged individuals have a long term diminishing of muscle gain as body condition decreases compromising their maximum metabolic rate (Bonneaud et al., 2016). Little is known about the effect of *A. crassus* on the European eel's metabolism in correlation with their migration.

4.1.6 Estimates metabolic rate

Measurement of fish oxygen consumption as a proxy for adaptation and resilience is increasingly undertaken in ecophysiology (Cooper et al., 2018; Pilakouta et al., 2020). Animal metabolic rates measurement is frequently applied to the study of physiology, behavioural ecology, and responses to environmental changes (Clark et al., 2013a; Clarke & Johnston, 1999). Oxygen consumption is used as a proxy for different measures of metabolic rate and the link between metabolic rate and multiple ecological and behavioural traits in fish is now well established (Killen et al., 2021). The tools to measure metabolic rate are various depending on the animal of interest or the research question (Butler et al., 2004). Many studies have used electrocardiograms as a proxy for metabolism because of the correlation between heart rate and oxygen consumption observed in many species (Forsman, 2015; Mercier et al., 2000; Zaremba & Smoleński, 2000). Measuring swimming speed is also considered a locomotor-related metabolic trait in fish as shown in Atlantic cod, *Gadus morhua*, and European sea bass, *Dicentrarchus labrax* (Steinhausen et al., 2007). A few studies have investigated the possibility of using opercular rate to monitor ventilatory activity as a means of monitoring oxygen demand and consumption in fish (Dalla Valle et al., 2003). Mitochondrial respiration and efficiency can provide key insights into fish metabolism, performance and stress when measuring respiration, reactive oxygen species (ROS) production and membrane potential (Gerber et al., 2020). When measuring mitochondrial function to address metabolic questions it had to be taken into

consideration the strong effect of temperature on enzymatic activities (Hunter-Manseau et al., 2019). In recent times the most widely used methodology to estimate metabolic rate in fish has been the rate of oxygen consumption ($\dot{M}O_2$) because all fishes are obligate aerobes (Nelson, 2016). The $\dot{M}O_2$ is influenced by environmental variables such as gas concentration, temperature, water chemistry and individual variables such as weight, length and health status (Neelima et al., 2016). The advantage of using oxygen consumption as a metabolic rate proxy is the possibility of controlling all the environmental variables in a laboratory setting, in acquiring the oxygen consumption of a fish in his entirety, it is not invasive and is an accurate indirect calorimetry measurement (Chabot, Steffensen, et al., 2016).

4.1.7 Aims of the study

Wild European eel metabolism is still a field that needs to be explored to understand the energy required during the growth face and the energy needed to succeed in the long migration. The amount of stored fat is essential for the success of migration in anadromous fish (Norin & Clark, 2016b). Parasitic infection plays also a key role in migration success and distributed energy expenditure (Robar et al., 2011a) The aims of this study are

1) to understand the relationship between physiological and ecological traits and metabolic profile in silver and yellow European eel

2) to discover the effect of *A. crassus* infection and parasitic load on the eel metabolism

3) to understand how the amount of fat stored in silver eels interacts with the aerobic scope and metabolic rate to ensure the success of the migration.

4.2 Materials and methods

4.2.1 Sample collection

Eels were collected across two sampling sites, the Burrishoole catchment in Ireland and Loch Lomond in Scotland (UK). All samples were collected in 2019.

4.2.1.1 *A. anguilla* collections in the UK

Yellow eels (n=28) were collected In Loch Lomond, UK, 56°07'21.5"N 4°37'43.1"W, with 10 unbaited fyke nets set in chains overnight in August 2019 at different lake depths ranging from 1 to 20 meters. Fish collection was carried out under licence. Yellow eels after the procedure were released in the wild (Appendix 3, Supplementary material 4.1).

4.2.1.2 *A. anguilla* collections in Ireland

Animals in Ireland were collected in the Burrishoole catchment, 53°55'27.6"N 9°34'27.0"W. Yellow eel were collected from Loughs Feeagh (freshwater)(n=12) and Furnace (tidal brackish water) (n=12) using unbaited fyke nets deployed overnight in chains of 10 nets set at different lake depths, ranging from 1 to 15 meters, respectively in June and July of 2019. Eels during the silvering process were collected in September 2019 using permanent downstream river Wolf-type traps (n=24). Silver eels were identified by the eye size, silver abdomen colouration and presence of neuromasts in the lateral line (Acou et al., 2005). The study was carried out under a Health Products Regulatory Authority (HPRA) license number AE19130-P096. Yellow eels after the procedure were euthanized while silver eels were released in the wild (Appendix 3, Supplementary material 4.2).

4.2.1.3 Eels husbandry and maintenance

After the capture, all the eels were starved in holding tanks of approx. 25 m3 in groups of 12 for 24 h with an air stone to keep the water oxygenated and a chiller to keep the temperature constant at 13.5°C ± 1°C. Tanks were filled with plastic pipes for shelter. Animals were weighed to 5 g precision scale.

4.2.2 Establishment of parasitological status

4.2.2.1 Molecular detection via targeted PCR

After respirometry fish were mildly anaesthetized with MS-222. Weight (g) and length (cm) was measured. A colonic irrigation using the rapid test described in chapter 2 was collected for *A. crassus* parasite detection (De Noia et al., 2020). Parasite presence/absence was detected using the protocol described by De Noia

at al, 2020. PCR was executed in triplicate per colonic irrigation, if at least one of the amplification gave a positive result the animal was considered infected.

4.2.2.2 Dissection of Anguilla's swim bladders

Yellow eels from Ireland were euthanized with an overdose of MS-222 (10 min in a 100 mg/L Tricaine methane sulfonate solution, FVG Ireland) followed by a cervical separation of the spinal cord. Dissection was undertaken and the status of the organs was recorded like any evident state of infection, organ color alteration and unexpected organs size. The swim bladder was removed from the animal, opened longitudinally and inspected under a stereomicroscope to detect *A. crassus* presence. If at least one parasite, independently life stage, was identified, the animal was considered infected.

4.2.3 Lipid analysis

We recorded yellow and silver eels fat content using a Distell Fatmeter Model - FM 692 (Distell LTD) for the Burroshoole catchment while they were mildly anaesthetized. Fat content was measured four times per fish side (total = eight) and the average reading was recorded as final fat content (% of body mass). The four points alongside the body are: after the gills, before the anus, after the anus and halfway between the anus and the caudal fin. Lean mass was calculated by subtracting the % of fat recorded from the overall body weight (**Table 5**).

Table 5. Summary of numbers of eels fished per location and relative variables recorded.

Lake	Life Stage	Individuals	Fat	Load	Infection	Lean mass	Salinity
Feeagh	Yellow	12	Yes	Yes	Yes	Yes	Yes
	Silver	16	Yes	Yes	Yes	Yes	Yes
Furnace	Yellow	12	Yes	Yes	Yes	Yes	Yes
	Silver	12	Yes	Yes	Yes	Yes	Yes
Loch Lomond	Yellow	24	No	No	Yes	No	Yes

4.2.4 Respirometry

4.2.4.1 Standard Metabolic Rate (SMR)

We used intermittent flow respirometry to estimate the metabolic rate of individual eels using oxygen consumption. Four cylindrical glass respirometry chambers were used at the same time (inner diameter: 6.5cm, length: 70cm).

These chambers were submerged in a 25m^3 tank of oxygen saturated water with constant 13.5°C ± 1°C temperature using a chiller. Oxygen concentration (mg O_2 L^{-1}) was measured every second using a four-channel FireSting (PyroScience GmbH) with PyroScience (PyroScience GmbH) oxygen sensors. To account for bacterial and background respiration, oxygen was monitored two hours before the fish were put in the chambers. To sterilize the water flowing in the respirometry chambers and minimize bacterial respiration a UV filter was connected to the experimental bath tank. Bacterial and background oxygen uptake was calculated assuming a linear increase over time. The calculated respiration was subtracted from the oxygen uptake measures of the individual fish within the respective respirometer. Eel oxygen uptake was measured in five minutes intermittent flow intervals over a 24h period using a peristaltic pump. The flushing period consisted of five minutes interval of oxygenated water versus the closed circle where eels oxygen consumption was measured. Oxygen concentration data obtained from Firesting software were analysed in LabChart 7 (ADInstruments Pty Ltd). Oxygen consumption rate was calculated using the average slope of each five minute cycle measurement period derived from the linear regressions between oxygen consumption over time (Killen et al., 2021). Oxygen consumption rate was corrected for the volume of the chamber, for the mass of the eels and for the volume of the closed circle tubing material measured in cm^3. SMR was estimated as the lowest 10th percentile of estimated oxygen consumption during the recording period (Rosewarne et al., 2016b). During the measurement period, the external ambient photoperiod was replicated with artificial light. The experimental tanks were isolated from staff to avoid external disturbance. Fish were removed from the respirometry chambers after 24h. The water in the experimental bath tank was replaced every 72h, between batches of animals, to minimise ammonia accumulation.

4.2.4.2 Maximum Metabolic Rate (MMR) and Aerobic Scope (AS)

Fish were exhausted, defined as being non-responsive and would not correct themselves if turned upside down, by chasing for approximately five minutes in a circular bucket under HPRA license. Fish were placed in individual respirometry chambers and oxygen content was quantified till oxygen concentration in the chamber reached less than 60% of saturation or overseed a period of 4 minutes of

oxygen depletion. The MMR (in mg O_2 h^{-1}) was calculated using the slope of oxygen decline in each chamber accounted for the chamber water volume (and associated tubing), minus the volume of the fish (assuming 1 g of fish approximates 1 ml). After MMR measurement fish were left to recover in the oxygenated respirometry chambers for 2h before starting the SMR measurement. Aerobic scope (AS) was calculated as MMR minus SMR (Norin et al., 2014; Reid et al., 2011).

4.2.5 Statistical analysis

All statistical analyses were conducted in R version 4.1.0.

4.2.5.1 Modelling the correlates of parasite (*Anguilicola crassus*) infectious status in silver and yellow eels.

We used a linear mixed model (GLM) to test the predictive value of environmental factors and eel lipid context with eel parasite load or prevalence. Correlation between variables was assessed using likelihood-ratio tests (ANOVA). Length, weight, month of sampling, condition factor, lipid content and salinity were considered as explanatory variables; the parasitic load was considered the independent variable. Fat was corrected with a quadratic factor to best explain the model. Condition Factor (CF) was calculated using the formula CF= (weight(g)x100)/(length^3(cm)). The best fitting model was selected using dredge MuMIn package in R studio version 4.1.0 using Akaike's Information Criterion (AICc) and Bayesian Information Criterion (BIC) for selection criteria with package TmB in R (Kristensen et al., 2016).

4.2.5.2 Modelling the influence of lean mass and migratory status on energetic metabolism in silver and yellow eels.

The potential drivers of SMR, MMR and AS (response variables) in yellow and silver eels together were assessed using a generalized linear model (GLM). We used lean mass, length, lake of sampling (2 levels: Feeagh and Furnace), salinity of water (2 levels: FreshWater and BrackishWater), infection status (2 levels: Yes or No) and parasitic load as covariates (Appendix 3, Supplementary material 4,1). We used lean mass on the assumption that fat is metabolically inactive (Scharnweber et al., 2021). Collinearity between explanatory variables was tested with Pearson's product-moment correlation coefficients using R and variables with a coefficient higher than 0.5 were removed from the model. Interaction between explanatory

variables was taken into consideration in the model building process. Model assumptions were verified by examining residuals compared to the fitted values. Best fitted model was selected following the process described in the previous paragraph.

4.2.5.3 Modelling the drivers of energetic metabolism in yellow eels

We tested the effect of multiple covariates on SMR, MMR and AS in yellow eels using GLM. Considered covariates were weight, length, condition factor, lake of sampling (3 levels: Feeagh, Furnace and Loch Lomond), salinity of water (2 levels: Fresh Water and Brackish Water), location of sampling (2 levels: Ireland and Scotland), infection status (2 levels: Yes or No) (Appendix 3, Supplementary material 4.2). As previously described correlation within covariates was checked using Peason's method and same threshold was kept. The best fitting model was selected using dredge MuMIn package in R.

4.3 Results

4.3.1 Infection rate and parasite detection in Ireland

Using a minimally invasive molecular rapid test we detected the infection rate per sampling site (De Noia et al., 2020). Lough Feeagh had the highest infection rate, almost 80% of eels infected. Lough Furnace (Ireland) had the lowest infection rate with only 52% of the population infected. 58% of eels were infected in Loch Lomond. Silver eels had a significantly higher infection rate compared to yellow eels (87% vs 56%) (two-way ANOVA $p < 0.05$). Eels sampled in brackish water have a lower infection incidence compared to eels in freshwater (52% vs 76%). The number of counted parasites in the swim bladder averaged from 0 to 24 in Lough Furnace, and from 0 to 48 in Lough Feeagh. As such, not only did Lough Feeagh has the highest infection rate but also the highest parasitic load.

4.3.2 Correlates of parasite (*Anguilicola crassus*) infectious status in yellow eels in Ireland.

Statistical analysis to explore the drivers of infection prevalence was undertaken for samples collected in the Burrishoole system. Among all the variables taken into consideration for the model, only eel life stage, length, weight, fat and lake were identified on the basis they showed no signs of collinearity using variance

inflator factor (VIF). The GLM that best fitted the data shows that fat and length as the most reliable predictors of the parasitic load (AIC=488, p-value <0.001). Fat best explained infection prevalence with a quadratic function based on the AIC score with the highest infection rate for those of around average fat content. Fat was corrected with a quadratic factor and then tested with an ANOVA, with length kept as a linear factor (**Figure 4-1**). The parasitic load was found to increase linearly with the length of the animal. Longer animals have a higher parasitic load.

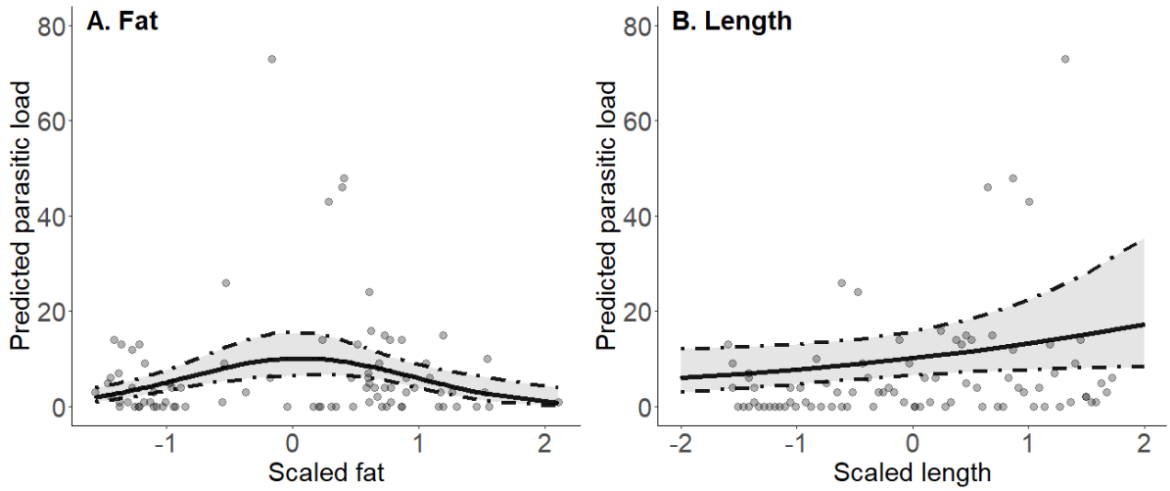

Figure 4-1 Observed *A. crassus* parasite load data super-imposed on that model-predicted for different *A. anguilla* phenotypes . The lines represent model predictions and the points represent experimental data. On x axis scaled fat and length for graphic purpose. The parasite load is predicted to increase with longer animals (P value < 0.05) and with animals recorded with a mean fat content (P value < 0.05). The model fitted was Parasitic Load ~ Fat+I(Fat^2) +Length +(1|Eel)

4.3.3 Factors shaping energetic metabolism across all yellow and silver eels

4.3.3.1 Lean mass influences the standard metabolic rate in the different life stages

The best fitting GLM having SMR as response variable has 414,74 AIC score (MMR ~ Life stage + Water + Lean Mass + Infection + Parasitic Load + Lean Mass * Infection + Lean Mass * Life Stage). Weight and infection rate were removed from the

models because highly correlated with other explanatory variables with a Pearson's product-moment correlation coefficients higher than 0.5. Residuals of the model followed a normally distributed curve so GLM was kept as best fitting model. Standard metabolic rate is positively correlated with lean mass ($p<0.05$). In contrast, length is negatively associated with SMR: longer eels have a lower SMR (**Table 6**). With the same amount of lean mass infected animals have a lower SMR compared to non-infected (**Figure 4-2**) and silver eels have a lower SMR compared to yellow eels (**Figure 4-3**). All samples used in this analysis are listed in Appendix 3, Supplementary material 4.2.

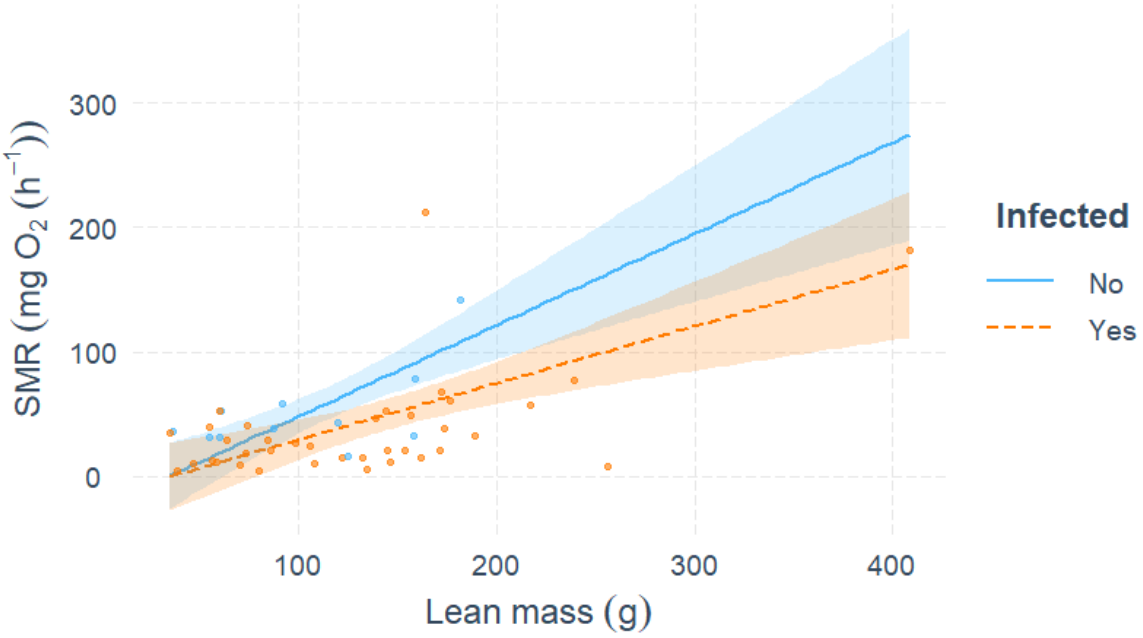

Figure 4-2 Observed and predicted SMR in relation to lean mass and infection across all samples eels. Each dots represent SMR against lean mass. The shade around the linear regression lines represents 95% confidence interval. Infected fish with the same lean mass have a lower SMR (p value < 0.05).

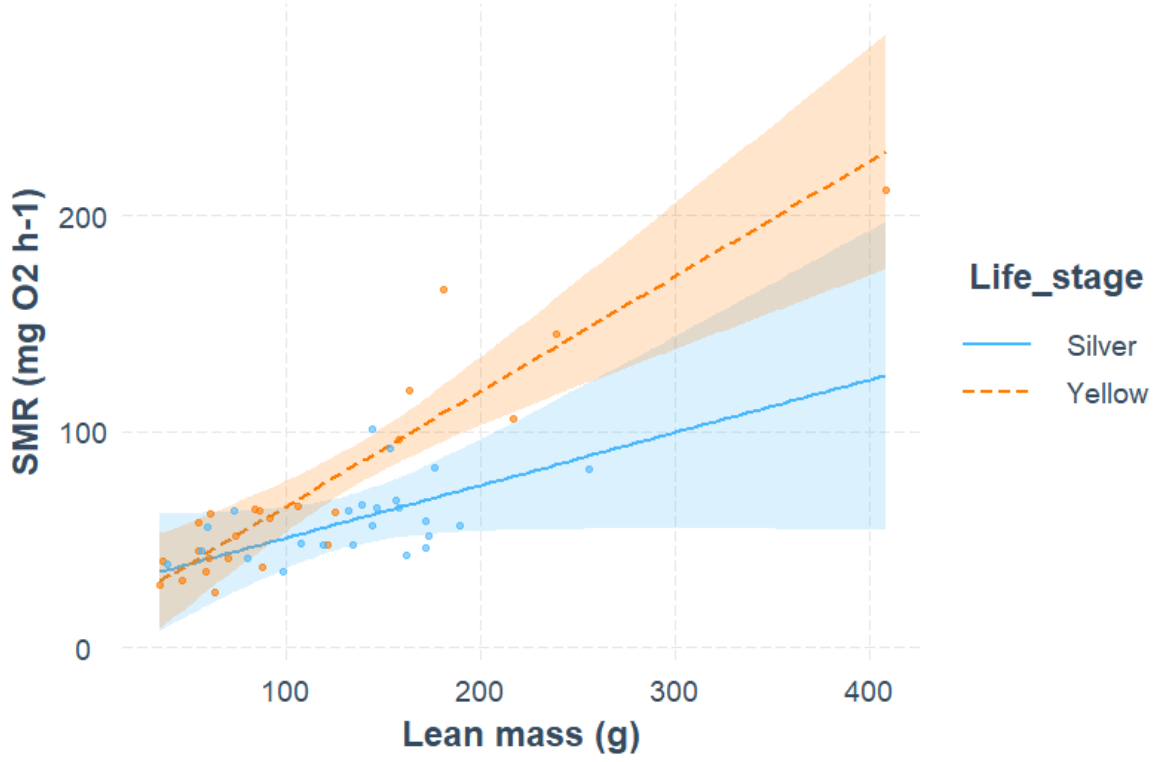

Figure 4-3 Observed and predicted SMR in relation to lean mass and eels life stage across all samples eels. Each dots represent SMR against lean mass. The shade around the linear regression lines represents 95% confidence interval. At the same lean mass, silver eels have a lower SMR compared to yellow eels (p value < 0.05).

4.3.3.2 Maximum aerobic metabolism across all eels (yellow and silver)

The best fitting GLM having MMR as response variable has 666.88 AIC score (SMR ~ Life stage + Water + Lean Mass + Infection + Parasitic Load + Length * Infection + Lean Mass * Life Stage). Weight and infection rate were removed from the model because highly correlated with other explanatory variables The maximum metabolic rate is solely influenced by the life stage and the interaction between the life stage and the amount of lean mass. Overall yellow eels have a higher MMR compared to silver eels. Silver eels with a higher lean mass have a lower MMR compared to yellow eels of similar lean mass ($p<0.05$) (**Figure 4-4**) (**Table 6**).

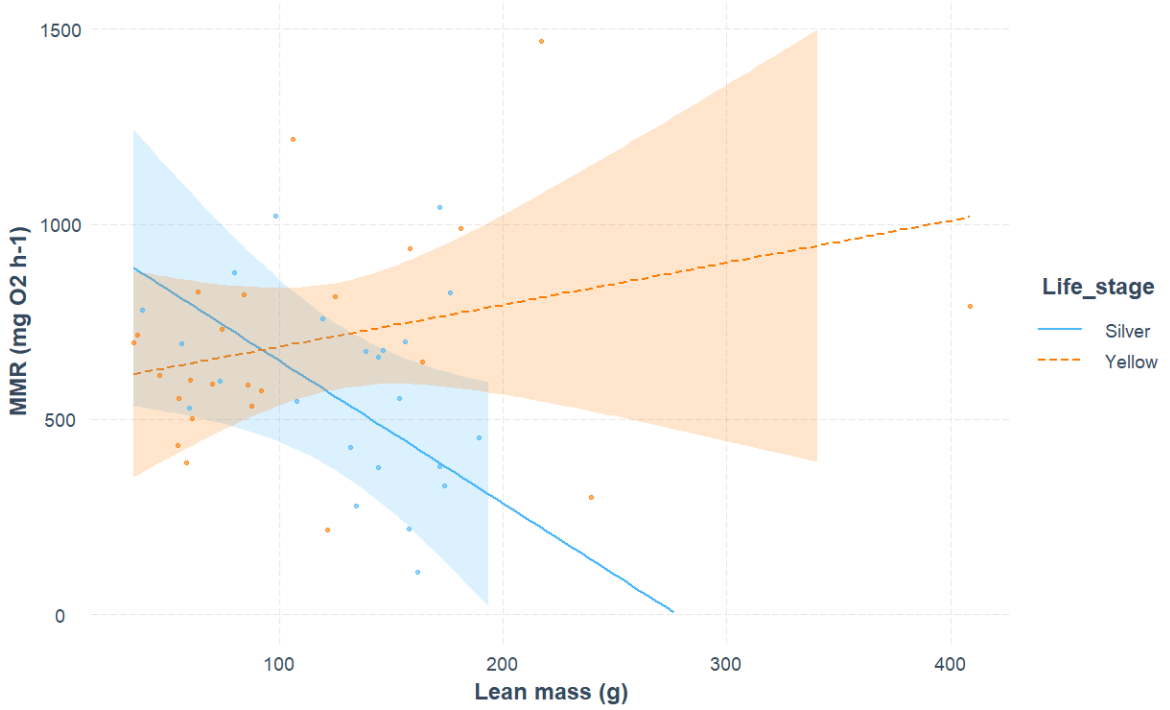

Figure 4-4 Observed and predicted MMR in relation to lean mass and life stage across all sampled eels. Each dots represent SMR against lean mass. The shade around the linear regression lines represents 95% confidence interval.

4.3.3.3 Aerobic scope in migratory silver eels and yellow eels

The best fitting GLM having AS as response variable has 666.28 AIC score (AS ~ Life stage + Water + Lean Mass + Infection + Parasitic Load + Lean Mass * Infection + Lean Mass * Life Stage). Based on the GLM, the aerobic scope in silver and yellow eels is affected by the lean mass, the life stage and the interaction between the two covariates, following the same trends as MMR. Yellow eels have a higher AS compared to silver eels. When considering all eels together, despite life stage, the fish with more lean mass have a lower AS. Trends in yellow and silver eels are the opposite. Silver eels with high lean mass have a lower AS, yellow eels with a higher lean mass have a higher AS ($p<0.05$) (**Figure 4-5**) (**Table 6**).

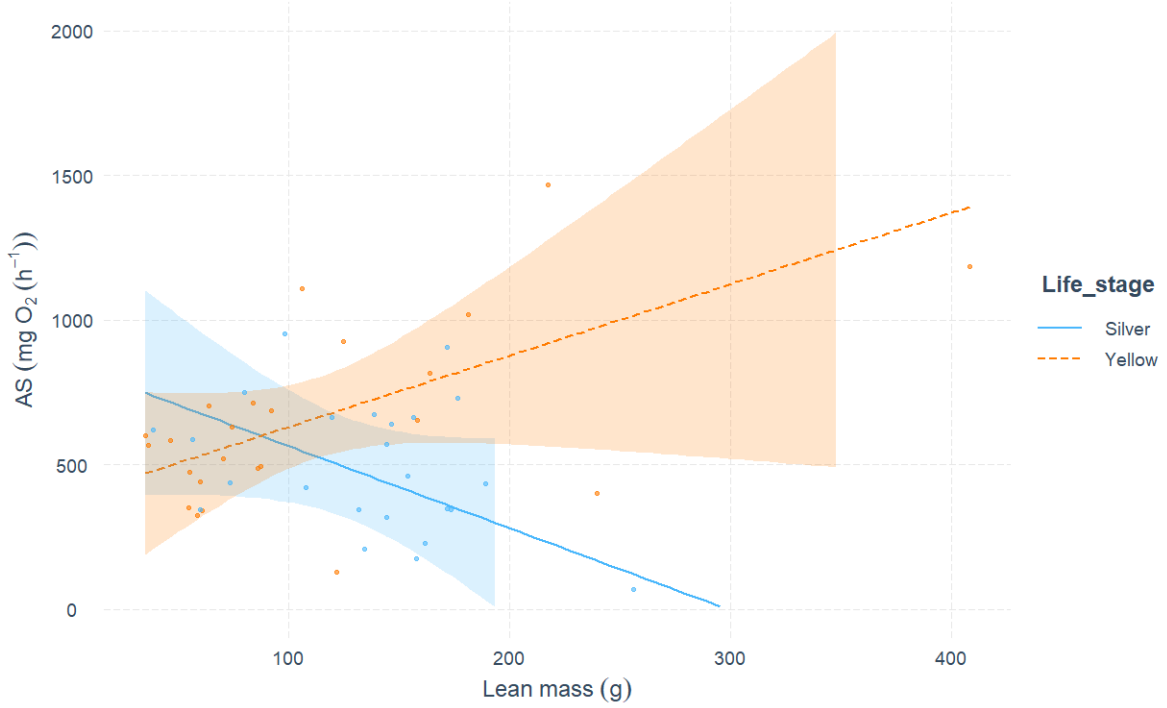

Figure 4-5 Observed and predicted AS in relation to lean mass and life stage across all European eel. Each dots represent SMR against lean mass. The shade around the linear regression lines represents 95% confidence interval.

Table 6 Results of the best-fit generalized linear model describing the factors influencing respectively SMR, MMR and AS in silver and yellow eels. AIC (Akaike's Information Criteria), Asterisks indicate significant difference * p value < 0.05

Indipendent Variable	AIC	Explanatory variables	Estimate	Std. Error	t value	P value
SMR	414.74	Life Stage	-14.33	13.58	-1.06	0.298
		Water	-16.54	9.22	-1.79	0.081
		Lean Mass	0.73	0.21	3.34	0.002*
		Length	-0.25	1.25	-2.49	0.017*
		Infection	9.13	16.27	0.56	0.577
		Parasitic load	0.39	0.27	1.35	0.185
		Lean mass * Infection	-0.28	0.12	-2.09	0.043*
		Lean Mass *Life stage	0.23	0.09	2.45	0.018*
MMR	666.88	Life Stage	-437.91	198.55	-2.21	0.033*
		Water	212.11	136.69	1.55	0.129
		Lean Mass	-3.67	Feb-49	-1.46	0.151
		Length	31.69	19.61	1.61	0.114
		Infection	500.54	624.88	0.8	0.428
		Parasitic load	1.93	3.98	0.48	0.631
		Length * Infection	-15.29	14.57	-1.05	0.301
		Life Stage * Lean Mass	4.73	1.38	3.41	0.002*
AS	666.28	Life Stage	-486.95	288.69	-2.12	0.039*
		Water	171.73	211.96	0.81	0.422
		Lean Mass	-5.28	2.52	-2.11	0.042*
		Length	22.82	19.32	1.18	0.254
		Infection	-128.38	112.94	-1.12	0.263
		Parasitic load	1.69	3.98	0.42	0.672
		Lean mass * Infection	5.26	1.71	3.09	0.003*
		Lean Mass *Life stage	0.92	1.61	0.57	0.571

4.3.4 Metabolism variability in yellow eels in the Burrishoole and Loch Lomond

4.3.4.1 Weight and salinity effect SMR in yellow eels

The infection rate was excluded from the GLM because it was collinear with the year of sampling, including infection rate instead of the year of sampling was reducing the model power decreasing the AIC score. (Best fitting model formula SMR ~ Origin + Water + Weight + Length + Infected). Yellow eels sampled in Loch Lomond have a higher SMR compared to Irish yellow eels (two way ANOVA $p<0.05$). The standard metabolic rate is driven by eel weight and the salinity of the water they inhabit. Animals living in brackish water have a higher metabolic rate and the bigger the eels are the greater is the SMR ($p < 0.05$) (**Table 7**). All samples included in the analysis are listed in Appendix 3, Supplementary material 4.1 and 4.2.

4.3.4.2 Upper constrain of aerobic capacity in yellow eels

The maximum energetic effort yellow eel can make is shaped by multiple covariates (MMR ~ Origin + Water + Weight + Length + Infected + Infected*Length + Infected*Weight + Infected*Origin) (**Table 7**). Longer animals had a higher MMR but heavier animals had a lower MMR. Infected animals tend to have a higher MMR. Looking at the interaction between weight, length and infection the model prediction shows clear patterns of metabolic allocation. Infected eels have a slow increase in MMR with the increase of their total body length, meanwhile, in parasite free animals, the energetic availability raises faster with their length (**Figure 4-6**). A similar trend is found when looking at the interaction between infected animals and the body weight. Infected eels seem to have a constant MMR, while there is a decline in energy availability in bigger non infected eels (**Figure 4-7**). The same findings are valid for the Aerobic scope (**Table 7**).

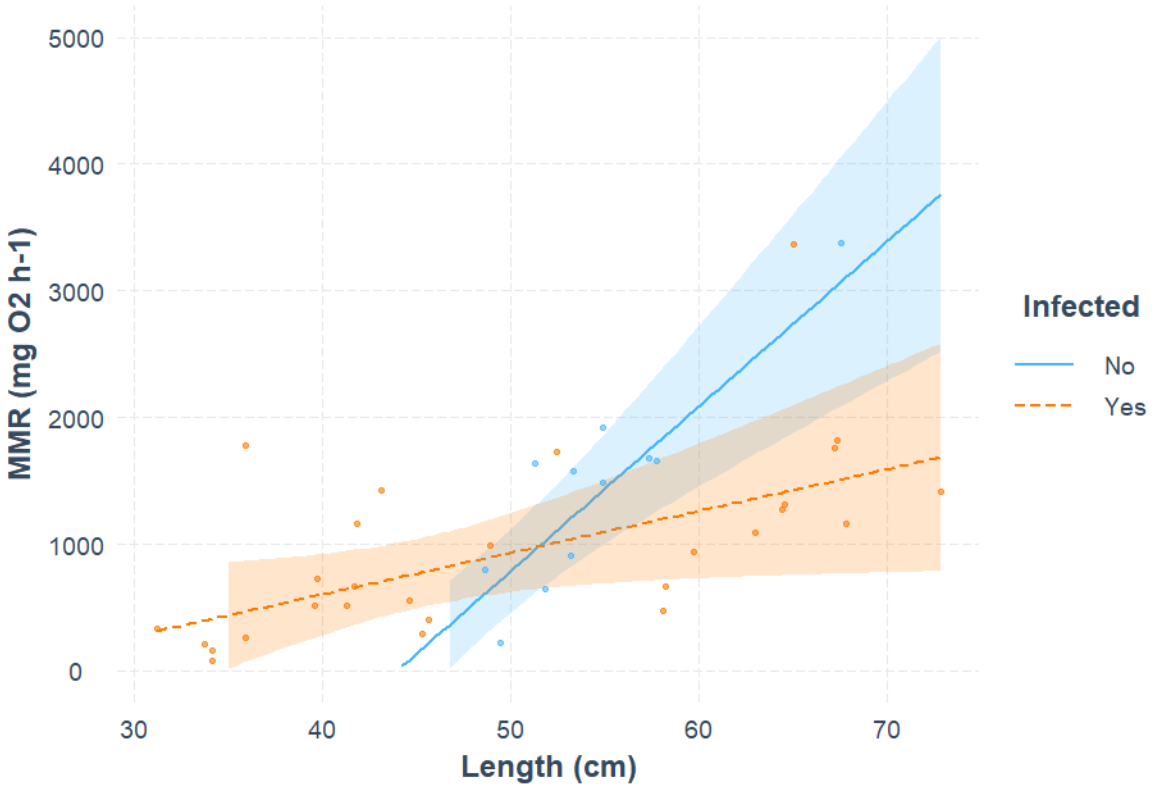

Figure 4-6 Observed and predicted MMR in relation to length and infection in yellow eels. Each dots represent MMR against lean mass. The shade around the linear regression lines represents 95% confidence interval. At the same length, infected fish have a lower maximum metabolic rate (p value < 0.05).

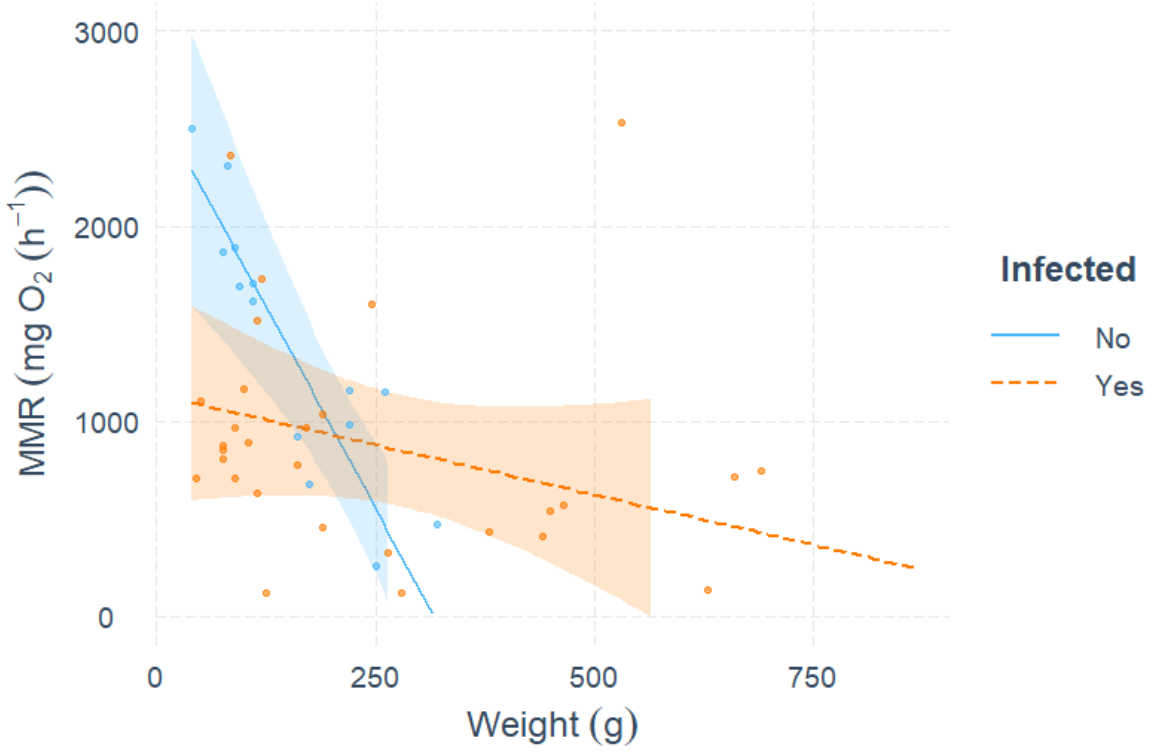

Figure 4-7 Observed and predicted MMR in relation to weight and infection in yellow eel. Each dots represent MMR against weight. The shade around the linear

regression lines represents 95% confidence interval**.** Weight in non infected eels is negatively correlated with MMR (p value < 0.05), while in infected animals is constant across heavy or light fish (p value < 0.05)

Table 7 Results of the best-fit generalized linear model describing the factors influencing respectively SMR, MMR and AS in yellow eels. AIC (Akaike's Information Criteria), Asterisks indicate significant difference * p value < 0.05

Indipendent Variable	AIC	Exlanatory Varibales	Estimate	Std. Error	t value	P value
SMR	520.750	Origin	29.616	17.787	1.665	0.104
		Water	-42.703	18.683	-2.286	0.027*
		Weight	0.472	0.097	4.890	1.6E-05 *
		Length	-0.941	1.630	-0.578	0.567
		Infected	13.297	13.749	0.967	0.339
MMR	734.230	Sample origin	425.058	349.798	1.215	0.232
		Water	-63.987	248.727	-0.257	0.798
		Weight	-8.269	2.790	-2.964	0.005*
		Length	130.103	39.079	3.329	0.001*
		Infected	3237.140	1571.799	2.060	0.046*
		Weight*Infected	7.245	3.043	2.381	0.022*
		Length*Infected	-97.164	44.888	-2.165	0.036*
		Sample origin*Infected	-704.619	412.953	-1.706	0.096
AS	735.290	Origin	416.088	353.747	1.176	0.247
		Water	-19.629	251.535	-0.078	0.938
		Length	131.672	39.520	3.332	0.001*
		Weight	-8.851	2.821	-3.138	0.003*
		Infected	3279.538	1589.542	2.063	0.045*
		Weight*Infected	7.517	3.077	2.443	0.019*
		Length*Infected	-99.171	45.395	-2.185	0.035*
		Sample origin*Infected	-729.962	417.614	-1.748	0.089

4.4 Discussion

We demonstrated a strong impact of lean mass on metabolic rate in the European eel. Animals with more lean mass have a higher SMR because lean mass is the active tissue contributing to the basal energetic requirements. SMR in yellow and silver eels is highly influenced by the length of the animal too, with longer animals presenting a lower SMR. We also prove that the nematode parasite, *A. crassus*, impacts energetic in both life stages. When looking at the interaction between length, lean mass and infection, we found infected eels to exhibit a lower SMR having an equal amount of lean mass. With the same level of lean mass, silver eels also have a lower SMR. Looking into their MMR and AS, we find the same pattern for both. Silver eels with a higher lean mass have a lower MMR and AS compared to the yellow eel, and overall yellow eels have a higher aerobic scope. Within

yellow eels we were not able to calculate the lean mass across all samples because we didn't have a fat meter available in Scotland, therefore we considered net weight. Yellow eels, collected in Scotland and Ireland, with a higher mass have a higher SMR, especially if living in brackish water. When considering AS and MMR we find again the same pattern between both. Longer eels have a higher MMR and AS but the trend is the opposite for heavier eels. The parasite also has an effect on the energetic allowance. Infected animals have a constant MMR and AS despite their body mass, instead heavier non infected animals have a lower MMR and AS. The same relationship was found for length.

Anguillicoloides crassus has multiple effects on the eels, from a physiological, immunological and pathological point of view (Laetsch et al., 2012b). Post infection the swim bladder becomes increasingly thickened and opaque as a result of fibrosis (Kirk, 2003). The blood-feeding activities of *A. crassus* cause degenerative and inflammatory changes compromising the buoyancy of the animal during their freshwater stage, but more importantly during their ocean migration to the spawning grounds (Righton et al., 2016). Our GLMM shows how the length of the eels is related to the level of infection, with higher levels of parasites in longer fish. Longer animals are mostly older animals and they have more chances to encounter the parasite (Weclawski et al., 2013). The interpretation of the correlation between fat and infection rate is unclear. Eels entering the catchment are low in fat and present a low infection rate because they have not encountered the parasite in their saltwater stage; *A. crassus* infectious stages do not tolerate the marine environment (Laetsch et al., 2012b). When eels fatten during the yellow stage of the life cycle the possibility of being infected increases as their fat level increases because both processes are related to the time of the growing phase. Peculiar is the reduction of the infection in eels with high levels of fat. Possibly fatter fish have a healthier status or a different feeding strategy and they are starting to clear out from the parasite (Iwanowicz, 2011). A link between fish health and parasite infection is been found in salmonids recovering from PKD (proliferative kidney disease) infection, with salmon in poorer health conditions showing enhanced inflammatory response and difficulties to recover (Bailey et al., 2018). In juvenile of European perch, *Perca fluviatilis*, infection from tapeworm is linked with lower growth and reduction in fat storage, with fish in a poor

nutritional status having a higher infection rate (Frantz et al., 2018). This relationship in eels needs to be investigated further.

An increase in *A. crassus* prevalence in *A. anguilla* is recorded all over Europe, where the parasite has established and has been fast to colonizing all the freshwater basins (Aguilar et al., 2005b; Mossali et al., 2010; Schabuss, Kennedy, Konecny, Grillitsch, Schiemer, et al., 2005a; Selim & El-ashram, 2012). *A. crassus* has a very recent history in the Burrishoole catchment. First detection occurred in 2010 in a yellow eel in brackish water and in 2016 for the first time in a silver eel from freshwater (R. Poole, pers. comm.). In contrast to the rising burdens across much of Europe, in some lakes where the parasite had been detected since first discovery, there is stabilization and even a slight decline in nematode abundance and intensities (Wielgoss et al., 2008). There is a possibility of an increased resistance towards the parasites in the long term (Schabuss, Kennedy, Konecny, Grillitsch, Schiemer, et al., 2005a). Although some evidence of increasing tolerance of *A. anguilla* to parasite infection, the overall impact of the parasite on the eel's mortality has been severe and is likely a contributor to the European population's steep decline impeding a recovery (Kirk, 2003; Molnar et al., 1993). Treatment of infected eels with anti-helminthic has not been trialed and a single study exploring a vaccination test to reduce the development of adults from irradiated L3 larvae showed that the antibody response is not a key element in the resistance of eels against *A. crassus* (Knopf & Lucius, 2008).

Understanding the effect of the parasite and fat on metabolic rate and energetic allowance is crucial for the success of the species and its migration. We found an effect of length and lean mass in silver and yellow eel on their standard metabolic rate, especially when interacting with infection rate. In our study, independently from their life stage, eels with a higher lean mass had a higher standard metabolic rate. It is known that lean mass is the main active metabolic component in fish (Boldsen et al., 2013; Hayes, 2010; Urbina & Glover, 2013), and this strong correlation between mass and SMR is observed across multiple species (Naya, Lardies and Bozinovic, 2007; Auer *et al.*, 2015; Cooper, Adriaenssens and Killen, 2018). We were also able to find a significant correlation between SMR and length, showing longer animals to have lower SMR for a given mass. Longer animals seem to be less active in the wild, as has been shown for *G. aculeatus*, where the

increased activity and risk-taking of shorter fishes may be associated with higher metabolic demands (Polverino et al., 2016). Also, longer animals are likely to have more energy reserve in their body, exhibiting fewer exploring behaviours slowing down their overall standard metabolic demand (Klefoth et al., 2012). Our efforts to disentangle the specific effect of lean mass and parasite infection status on SMR in the two different life stages results provided interesting results. For the same lean mass, silver eels had a lower SMR than yellow eels. Yellow eels are in the active feeding stage, and significant energy is likely invested in growing, which could explain their higher energy demands (C. Durif et al., 2009). It is common in fish to have a higher energetic demand in growing stages of the life cycle, as shown in Atlantic salmon and white sturgeon (Boucher et al., 2018; Reid et al., 2011). The silver eel stage is the migratory stage animals stop foraging and feeding, reduce and eliminate their intestines, and become reliant on stored fat during their long migration (C. M. F. Durif et al., 2013). The reduction in basal metabolism we observed is consistent with this state. In Atlantic salmon parr, increases in size due to ontogenesis leads mass specific metabolic rates decrease, partly due to a decrease in the proportion of metabolically demanding tissues (Rossignol et al., 2011). In Pacific salmon during upriver spawning migration and reproductive maturation SMR is higher in females due to elevated reproductive costs (Kraskura et al., 2020). In actively spawning eels, metabolic rates may again increase alongside gamete development and mating behaviour. The gametes development coincide with the starting of the silvering process and can be influenced by swimming behaviour and hydrostatic pressure (Palstra et al., 2010). Interestingly, when looking at the effect of parasites on SMR given the same lean mass, infected animals have a lower SMR. Across species, there is a lack of consistent directionality in the effects of parasites of metabolic rate on the host. Generally, ectoparasites are more likely to increase the energy demand, while endoparasites are had no effect (Robar et al., 2011b). In our case, infected eels presented a lower SMR, possibly caused by the parasite altering their behaviour, increasing the stress level and reducing normal metabolic activities (Muñoz et al., 2015). In our study, large fish (>300g) are rarely non infected. Most likely there is a sex bias to consider into the infection rate and prevalence because smaller eels with high fat content are likely to be males, while larger fish are likely to be all female. Sex determination in eels is still under debate (Laffaille et al., 2006) and

can be further investigated in relation to differential parasite exposure and effect on lipid accumulation and capacity to migrate.

Our findings on the influence of life stage for SMR are mirrored by our findings for maximum metabolic rate (MMR, the maximum rate of aerobic metabolism of an animal at a given temperature (Downs et al., 2016)), and aerobic scope (AS, the capacity of a fish to sustain metabolic activities at a given temperature (Norin et al., 2014; Norin & Clark, 2016b)). As such MMR and AR in eels are influenced by the life stage, the amount of lean mass and their interaction. Yellow eels present a higher MMR and AS, for a given mass than silver eels. Other studies in migratory fish have also revealed a reduction of metabolic allowance and expenditure (Archer et al., 2020; Bairlein et al., 2015). We did not detect a direct effect of the presence of parasite on MMR and AS in silver and yellow eels but we were able to show an effect of it for the SMR in both resident and migratory lifecycle stages. From a conservation point of view the parasite is reducing the energetic availability by reducing the fat content in silver eels (Laffaille et al., 2006). As mentioned before, the amount of fat stored is a key feature to sustain the endurance of the long migration (Jousseaume et al., 2021). Reduction in the migration success can deplete even more the size of the eel population, which in the past 30 years already has been drastically declining (Jacoby & Gollock, 2014). Therefore is important to control the spread of the parasite across eels populations to guarantee the survival of the species.

It is important to consider the effect of life history traits and environmental factors on metabolism in the yellow growing phase. Yellow eels spend various amounts of time in freshwater before maturing into the silver migratory phase based on food availability, growth rate and the amount of fat they are able to store (van Ginneken & Maes, 2005). Yellows eels may undertake daily migration to brackish or saltwater environment for food hunting (C. M. F. Durif et al., 2013). From our study we found SMR in yellow eels is affected by their overall weight, including lean mass and fat, and the salinity of the water. Eels samples in brackish water exhibit a higher SMR, an observation is established in many diadromous fish (Tudorache et al., 2007). The cost of osmoregulation is higher when transitioning to higher salinity may result in higher basal metabolic rate demands (Cooke et al., 2014; Van Leeuwen et al., 2017). We can’t state the same for silver eels, because

all our catch is from a freshwater lake, where they spend the last part of the yellow process before starting the migration. In addition, silver eels undergo a physiological transformation to compensate for the change in osmoregulation from fresh to saltwater (van den Thillart et al., 2009). The size of the animals also plays an important role in establishing the basal metabolism. In our study we found heavier eels having a higher SMR. In fish is an established trait that the cost of sustaining a bigger metabolic active body increases with the size of it (Clark et al., 2013b; Killen et al., 2016; Odell et al., 2003). The effect of body size on SMR has been proven in brown trout (Norin & Malte, 2011), threespine stickleback (Walker, 1997), juvenile and adult of Atlantic cod (Tirsgaard et al., 2015), zebra fish (Polverino et al., 2016), Atlantic salmon (Rossignol et al., 2011) and many more (Clarke & Johnston, 1999).

More complex relations were found in the effect of body weight, length and *A. crassus* parasitic infection on MMR and AS. Both of those two metabolic features revealed the same pattern so we will discuss them together. Aerobic scope and MMR have an important effect on growth rate in *ad libitum* experimental situations (Auer et al., 2015). In a variable environmental context, metabolic rates have more complex interactions with components of fitness which still needs to be explored. Longer eels present a higher AS and MMR, probably caused by a higher amount of caudal muscles which represents one of the most metabolic active tissue. Contrarily, bigger eels have a lower MMR and AS probably caused by the presence of more fat which is not a metabolic active tissue. When looking at the interaction between length, weight and the presence of the nematode parasite we found a strong effect of the parasite on their energetic metabolism. Ectoparasites have a strong impact on fish swimming ability and therefore energetic (Binning et al., 2012). Endoparasite don't have a direct physical effect on the metabolic rate in fish but they can alter their behaviour (L. E. Nadler et al., 2021) and fitness (Marino et al., 2014), which has a secondary effect on the energetic allowance. In eels we found that infection was affecting their MMR and AS both in relation to length and weight. Longer non infected animals have a higher MMR and AS compared to infected fish, where the parasite is draining the energy of the eels. *A crassus* produces an inflammatory response, increased thickness of the swim bladder altering the buoyancy ability and can cause long term effects on fitness (Barry et al., 2014). Infected animals have a constant MMR

and AS, instead bigger non infected animals have a lower MMR. Considering that bigger animals have a lower SMR, is expected that bigger non infected eels have the same trend in AS and MMR because they have more fat stored to start the migratory process. Meanwhile bigger infected animals are more likely to have less fat because of the presence of the parasite which is draining their energy. Their growing stage is extended, causing a higher exposure to predation and risk factors that can lead to a higher decline of the population.

In conclusion, we highlight the importance of fat content, lean mass and parasite burden in the eel's metabolism in relation to their growth and migration. The amount of lean mass is positively correlated with a higher metabolic rate, being the most active metabolic tissue. For the same lean mass, silver eels have a lower SMR than yellow eels, since yellow eels are in the active feeding and growing stage. *A. crassus* has a strong impact on the yellow eel life stage, reducing their energetic capacity during the growing phase. It is essential for the survival of the species to reach silvering with an adequate fat amount. It is important to consider parasite monitoring and food availability to better understand the ecology of the eels and their migratory success.

5 Chapter 5 Body mass, salinity and *Anguillicola crassus* infection induce microbial community changes in European eel, *Anguilla anguilla*.

Abstract

The study of fish microbiome is an emerging means to understand the role of commensal microbes in modulating immune responses, improving digestion and pathogen colonisation resistance. Fish are constantly surrounded by the aquatic microbes that shape their gut and skin microbial composition, along with diet intake and pathogenic infection. The eel gut microbiome has only been studied in farm-reared fish under experimental conditions. This study provides characterization and association with life history traits, physiology and environmental drivers shaping the wild European eel microbiome. We sequenced sixty-two gut compartment samples from eels and 16 environmental samples using 16S rRNA gene from two lakes in Ireland over three consecutive years. We measured microbial species richness, diversity and variation between samples linking them with environmental and physiological factors. Effective Richness and Shannon Effective were strongly influenced by the health status of the fish, using weight and fat as a proxy. Diversity and richness were also influenced by infection the nematode *A. crassus* infection. Parasite burden reduces microbial diversity and richness (P value < 0.05). In healthier (heavier and fatter) eels we found an increase of diversity positively correlated with *Oxyphotobacteria* (P value < 0.05). The environment also plays a role in shaping the microbial community showing a core gut microbiome differing from the environment microbiome, the latter characterized mainly by free living bacteria. We didn't detect any significant difference between microbial community diversity and composition and metabolic traits, although we found *Staphylococcus* and *Oxyphotobacteria* positively correlated with maximum metabolic rate. Our study opens a new field of study to investigate further the environmental and ecological factors driving the microbial composition and the connection between specific bacterial taxa and their function in fish heath, metabolism and ecology.

5.1 Introduction

5.1.1 Importance of the microbiome

The microbiome consists of symbiotic microbial cells hosted by each leaving creature, primarily bacteria in the gut (Thorn et al., 2012). The gut microbiome represents a dynamic microbial community that plays an active role in vertebrate immunity and physiology (Xiang et al., 2020). Bacteria can play an important role in the digestion process, nutrient absorption and disease control (Sekirov et al., 2010). They are important in carbohydrates digestion, especially in the anaerobic fermentation process and production of short chain fatty acids and gases (Rowland et al., 2018). The products of the bacterial fermentation can be directly used by the host for energy production and gasses can further oxidise organic material (Bratlie et al., 2021; Suarez et al., 1998). Bacteria are also essential in the digestion of protein, they have different proteolytic capabilities specific to each species (Diether & Willing, 2019). The gut microbiome can also synthesize certain vitamins, notably vitamin K, and B which are important to prevent haemorrhages, to stimulate brain function and cell metabolism (Yoshii et al., 2019). Bacteria are not only important during the digestion process but they can also maintain the intestinal homeostasis and prevent the propagation of pathogenic microbes by competition (W. J. Lee & Hase, 2014). The intestinal microbiota in continuous direct contact with the gut mucosa and can influence the tolerance and induce an immune response against harmful foreign pathogens (Pérez et al., 2010). The skin microbiota is the first barrier against pathogens and in the development and maintenance of physiology and immunity (Krotman et al., 2020). Microbial community living on the skin surface has been well adapted to protect against pathogenic infections via competition or antagonistic interaction mechanisms (C. Hu et al., 2021).

5.1.2 Fish microbiome

The gut microbiome in teleost is an understudied topic compared to humans or mice. However, with the rise of Next Generation Sequencing (NGS), more studies are revealing the importance of fish gut microbiota in all life functions (Estensoro et al., 2018). Many factors can influence the abundance of certain microbial species and their composition, such as diet and stress (Sandoval-Motta et al.,

2018). It is important to study which environmental factors alter the health status of fish microbiome for his essential role in modulating immune responses, improving metabolic digestion and parasite barrier prevention (Adamovsky et al., 2018; Kokou et al., 2020). In recent years many studies have explored the correlation between environmental factor, taxa composition and their role in the ecological process, only a few studies underpin the cause of it (Cheaib et al., 2020; Heys et al., 2020). To study causation in microbiome systems more ecological models have been proposed (Zeng et al., 2015). Neutral model measures the migration rate from the source community into the microbial community, revealing which taxa are transient and environmentally influenced and which is taxa can be considered core, stable and hence adapted to the intestinal environment (Cheaib et al., 2020). Experimental exposure to different stressors or environmental gradient exposure can help to assess the deterministic process of microbial composition shift and function (Burns et al., 2016). In nature is not always possible to test causation, therefore correlative studies still remain of great value to understand ecological, physiological and environmental drivers in the fish microbiota community. Such correlations can be used to frame ecological and biological hypotheses that can then be tested under controlled conditions in the laboratory.

5.1.2.1 Salinity shaping the microbiome composition

Fish are constantly surrounded by the water environment which plays a key role in the microbiome composition (Yoshii et al., 2019). Changes in environment and diet can affect the microbiome by changing the relative abundance of individual groups of microorganisms (Dulski, Kujawa, et al., 2020). A study in the Baltic Sea shows how, along the salinity gradient the number of marine microbial species declines and the number of FW microbial species increases with decreasing salinity while the alpha diversity stays constant (Herlemann et al., 2011). In anadromous species such as the Atlantic salmon, *Salmo salar*, salinity gradients are one of the main drivers of change in the microbiome composition and richness. Freshwater fish had a richer intestinal microbiome and a higher number of unique OTUs, with *Proteobacteria* representing the most abundant phyla (60.8%), whereas saltwater fish had *Firmicutes* representing their major phyla (55.6%) (Dehler et al., 2017). The impact of salinity on the microbiome is consistent across different Atlantic

salmon populations (Llewellyn et al., 2016). Also in farmed Chinook salmon (*Oncorhynchus tshawytscha*) salinity plays an important role in the gut microbial composition, confirming the trends of phyla abundance and differences between freshwater and saltwater with salinity representing a significant environmental barrier for salmon gut microbiota colonization (Zhao et al., 2020). It is hard to separate the effects of lifecycle change from fresh to salt migration because during the smoltification stage there are lots of associated physiological changes (Caballero et al., 2013; Rossignol et al., 2011).

5.1.2.2 The effect of diet on the microbiome

Fish diet is linked with gut microbial composition and equilibrium, with the potential of altering the capacity of enzyme production and, digestion and fatty acid production (Perry et al., 2020). In general carnivorous fish present a less diverse microbiota because their digestive systems are shorter and more proteolytic with less carbohydrates digestive capacity, little is known about wild fish shift in microbiome with their diet change (Hamilton et al., 2019). Numerous studies have been conducted of fish reared in an aquaculture setting, where diet manipulation can be done in a controlled environment. A plant based diet can impact the digesta and mucosa microbiota with a decrease of Shannon's diversity index characterized by a lower microbial richness and a decrease of microbial diversity in farmed European seabass (*Dicentrarchus labrax*) (Serra et al., 2021). Although the change in diet has an effect on the overall community composition, the plant based diet may have a greater impact on transient microorganisms without affecting autochthonous microbiota closely associated with the gut mucosa (Rimoldi et al., 2020; Serra et al., 2021). In first feeding Atlantic Salmon, *Salmo salar*, no effect on the microbial community was observed when shifting from a fish to vegetable oil feed, with life stage appearing to be the main factor affecting the structure of gut microbiota (Nikouli et al., 2021). The mentioned study is supporting previous ones where life stage was recognised to be one of the main drivers of microbial composition in *Sparus aurata* (Piazzon et al., 2017), *Danio rerio* (Stephens et al., 2016) and *Gadus morhus* (Bakke et al., 2013). Though the complex interplay between host diet and the gut microbiota has been examined in many contexts the reproducibility is poor and the definition of the diet-host-microbiota relationship remain a challenge.

5.1.2.3 Host metabolism interaction with microbiome

A recent field of interest is the examination of the influence of the gut microbiota on host metabolic rate (Ayayee et al., 2020; E. C. Lindsay et al., 2020). The gut microbiota can adapt to changes in the host diet altering the production of microbial metabolites affecting the host metabolic rate (W. Huang et al., 2018a). The connection between the gut microbiota and host metabolism appears to be bidirectional. The potential effect of the gut microbiome on metabolism has been examined in a few fish species (Butt & Volkoff, 2019). In juveniles of Atlantic salmon a significant positive association was observed between lipid carbon metabolism and *Bradyrhizobium* and *Pseudoalteromonas* which are known to produce antimicrobial compounds and important proteases for host smolification (Dvergedal et al., 2020). In grass carp (*Ctenopharyngodon idella*) the gut microbiota was linked with the digestion of polysaccharose, otherwise undigested, and also help the grass carp to achieve physiological homeostasis (Ni et al., 2014). In zebrafish, *Danio renio*, the presence of food drives the enrichment of intestinal bacteria with the phylum *Firmicutes* which in turn improves fatty acid absorption and energy balance (Semova et al., 2012). In the rainbow trout, *Oncorhynchus mykiss*, although overall microbiota differences were not found to be significantly associated with the fish growth rate, there was an association between specific taxa and growth speed. *Bacillales* and *Clostridiales* were associated with fast growing animals because of their nature of inhibiting pathogens and inducing the barrier function in the host epithelium (Chapagain et al., 2019).

5.1.2.4 Pathogenic bacteria and fish immune responses

The microbiome has an important connection with immunity in fish because they are in constant contact with the water environment which is a source of opportunistic and obligate pathogens commensal microbes (Ellis, 2001). Pathogenic bacteria are normally present at low abundance in healthy teleost gut microbial communities and they can emerge as pathogens under stressful circumstances (Llewellyn et al., 2014). Furthermore, it is increasingly thought that fish diseases may be caused by a pathobiome instead of a single pathogen (Bass et al., 2019). In salmonids no evidence was found of a decrease in microbial diversity in the gut compartments in relation to disease, instead was found that the richness in the microbial community increased with the myxozoan,

Tetracapsuoides bryosalmonae, parasitic load (Anti Vasemägi et al., 2017). In sea bream, *Sparus aurata*, changes in diet can lead to a higher parasitic infection with infected animals showing a reduction in growth and changes in the gut mucus proteins essential for metabolism (Estensoro et al., 2018; Piazzon et al., 2017). Fish mucosal microbiome can also be associated with parasitic infection ad demonstrated for Southern Bluefin Tuna, *Thunnus maccoyii,* where the microbial community was indirectly affected by promoting secondary infections (Minich et al., 2020). The microbiota is known to enable colonization resistance by inhibiting the over-growth of potential opportunistic pathogens (Bastos Gomes et al., 2019). Parasites can perturb the microbiome and allow these communities to be invaded by opportunistic pathogens. In some cases that parasite can directly modulate the immune system and make them more susceptible to parasitic colonization and microbial pathogen infection (Lhorente et al., 2014). In Atlantic salmon, *salmo salar*, it has been demonstrated the influence that salmon lice, *Lepeophtheirus salmonis,* has on salmon skin microbiota. The perturbation of the mucosal microbiome caused by the feeding of the parasite can decrease colonization resistance and promote the proliferation of endogenous pathogens (Llewellyn et al., 2017a). Gut microbiota can be associated with parasite exposure, as demonstrated in *Gasterosteus aculeatus* experimentally exposed to their natural parasite, *Schistocephalus solidus*. Fish infected had a significant shift in the bacteria community with an increase of *Clostridiales* and *Rhodobacterales* (Ling et al., 2020). Also in zebrafish was found a shift in gut microbiota community of fish infected with the intestinal helminth, *Pseudocapillaria tomentosa*. The helminth parasite uncovered microbial general as *Plesiomonas* and *Pseudomonas* that can influence parasite success and virulence from disturbed gut microbiota (Gaulke et al., 2019).

5.1.3 Microbiome composition and function in anguillids

Little is known about anguillid microbiomes. Studies to date are preliminary and descriptive. A recent paper showed the differences in gut microbiome composition based on the 16S rDNA sequencing in three different species of wild anguillids (Hsu et al., 2018). The gut microbiome of Japanese eels, *Anguilla japonica*, were characterized by Gram-negative bacteria (Bradyrhizobium, Cetobacterium) recognized as important for nitrogen fixation, vitamin B12 and acetic acid

production, and Gram-positive bacteria (Clostridium) used in aquaculture as probiotics to suppress inflammation and act as an anti-oxidant (Hsu et al., 2018; Sandoval-Motta et al., 2018). In the Giant Mottled eel, *A. marmorata*, and Shortfin eel, *A. bicolor pacifica*, the most represented genus in the gut microbiome were Acinetobacter, Mycoplasma, Shewanella and Bacteroides. Bacterioides are thought to produce anti-inflammatory substances to maintain the balance of the immune system (Gerhauser, 2018). Acinetobacter has the ability to produce inhibitory substances against *Vibrio* species (Yoshii et al., 2019). Shewanella is associated with the prevention of pathogens infection producing the digestive enzymes (Ramírez & Romero, 2017). The mucus secreted by the eels is one of the most important compartments acting as the first protection from external factors, improving hydrodynamic and exchange with the environment (Schneebauer et al., 2017). The microbiome in the mucus can attract and select concentrates of specific members of the aquatic microbiome, with higher alpha in the resident bacteria living on the section of the mucus closer to the skin showing particular abilities to attach to a substrate and resistance innate genes (Carda-Diéguez et al., 2017). There is only one study that investigated the gut bacterial composition in European eels. The study, undertaken in an aquaculture setting, revealed differences in the gut microbiome during different life stages is highly influenced by the diet composition, showing how both diet and life cycle can impact microbiome composition (W. Huang et al., 2018a). The main group of bacteria characterizing the elver stage are Proteobacteria (*Aeromonas*), the yellow stage *Cetobacterium* and *Plesiomonas* in yellow eel and *Aeromons* in the silver eel (Huang et al. 2018).

5.1.4 Aims of this study

Little is known about the gut microbiome of wild European eels, how this microbial community interacts with the environment, and how the gut microbiota might influence, or be influenced by, host physiology and immune status. In particular, the invasive nematode parasite *Anguilicola crassus*, represents a major threat to *A. anguilla*, and the influence of this parasite on gut microbiome homeostasis should be explored. In this chapter, this aim is addressed via several objectives:

1) Collect eels gut samples and environmental samples, extract DNA, prepare library and sequence the microbiome using 16S rRNA gene molecular marker.

2) Characterize microbial richness and composition using Alpha diversity matrix and link them with parasitic infection, ecological and physiological traits.

3) Study the ecological and physiological drivers of dissimilarities between microbial community across infected eels and their life stages.

4) Correlate changes in OTUs diversity and richness with parasitic infection, salinity changes and eels physiological features.

5.2 Material and methods

5.2.1 Sample collection

Eels were collected during three samples season in the Burrishoole catchment in Ireland in July. The Burrishoole catchment is described in chapter 2, we collected eels from both the FW lake Feeagh and the brackish water lake Furnace. We collected 14, 23 and 25 yellow eels respectively in 2017, 2018 and 2019. Collection methods are described in Chapter 1. Eels were terminally euthanized using MS222 anaesthetic. Weight (g), length (cm) and fat (%) was recorded as mentioned in chapter 2. Eels were dissected, a 5g piece of stomach (ST), mid gut (MG) and hind gut (HG) was collected and flash frozen in liquid nitrogen. The swim bladder was also inspected for parasite detection as described in Chapter 1. For animals sampled in 2019 before sample collection, metabolic rate was recorded as described in Chapter 3. Environmental water samples were taken by passing 500 ml of water from the 2 lakes where eels were collected through a 0.2um nitro-cellulose filter (Minisart single use filter, 16534-K, CE 0120) using a peristaltic pump. Each filter paper was manually removed from the filter and immediately placed into a cryotube (Cryo-Vial Int Thd FS, Ref:LW3534) and stored in liquid nitrogen.

5.2.2 DNA extraction and Library preparation

A piece of tissue of 1g was taken from each gut compartment to extract bacterial DNA. DNA extraction followed the QIAamp DNA Stool Mini Kit (Qiagen) according to the manufacturer's protocol with modifications described in chapter 1. The same extraction method was used for environmental samples. DNA quality was

assessed with gel electrophoresis and DNA quantification using Qubit. Amplicon library were prepared using two different methodologies.

5.2.2.1 Library preparation, protocol 1 for 2017 and 2018

For samples collected in 2017 and 2018 first round of PCR reaction targeted the V1 hypervariable region of the 16S rRNA gene with the primer pair CS1_27F and CS2_338R (Gajardo et al., 2016). Primers were modified with tag sequences, CS1 tag was attached to the forward sequence and CS2 to the revers (**Table 8**). PCR reaction consisted in 1 µl of each forward and reverse adapted primer (10µM), 10µl of Q5 Hot Start High-Fidelity 2X Master Mix (New England BioLabs Inc.), 6 µl of pure water and 2µl of DNA template, for a total volume of 20 µl. PCR conditions were as follows: 95˚C for 10 minutes; 30 cycles of 0:30 at 95˚C, 0:30 at 55˚C and 0:30 at 72˚C; final extension step for 10 minutes at 72˚C. The PCR product was verified on a 1% agarose gel using TBE buffer. PCR products were used as templates for 2nd round PCR, consisting in attaching a specific barcode per sample in the reverse fragment and universal adaptor in the forward fragment. Reaction volume (25µl) for second round PCR was consisting of 12.5µl Q5 Hot Start High-Fidelity 2X Master Mix (New England BioLabs Inc.), 1µl forward universal primer, 1µl specific barcode, 8,5 µl of water and 2µl of first Round PCR product. PCR conditions were as follows: initial denaturation of 95˚C for 10 minutes; 8 cycles of 0:30 at 95˚C, 0:30 at 60˚C and 1:00 at 72˚C; 3 minutes at 72˚C. The barcoded PCR products were visualized on a 1% agarose gel using TBE buffer. Individual second round amplification was purified using the Agencourt paramagnetic bead clean-up (Agencourt AMPure XP, Beckman Coulter) using 0.75x ration of Beads and product to remove fragments below 300bp. Concentration of each product was determined with a Qubit fluorometer and final amplicons were pooled equimolar, the final library was sequenced using PE250 Novaseq provided by NovaGene.

Table 8 Sequences of V1 16s rRNA primers and Illumina adapters used to prepare amplicon library with protocol 1 for samples collected in 2017 and 2018

27F_Adapter	ACA CTG ACG ACA TGG TTC TAC AAG AGT TTG ATC MTG GCT CAG
338R_Adapter	TAC GGT AGC AGA GAC TTG GTC TGC TGC CTC CCG TAG GAG T
V1_Nextover_REV	GTC TCG TGG GCT CGG AGA TGT GTA TAA GAG ACA GCA AGC AGA AGA CGG CAT ACGAGAT
V1_Nextover_FWD	TCG TCG GCA GCG TCA GAT GTG TAT AAG AGA CAG NNN AGA GTT TGA TCM TGG CTC AG
i7 Bases in Adapter	CGCTCAGT
i5 Bases in adapter	CTCTCTAT

5.2.2.2 Library preparation, protocol 2 for 2019

For samples collected in 2019 extracted DNA was amplified using tagged V1 region primers of the 16S rRNA gene. First round PCR primers were designed with an internal tag (**Table 9**). Mastermix, total volume 15 µl, consisted in 0.7 µl Internal Rev, 0.7 µl Internal Fwd, 5.6 µl H2O 7µl Q5 Hot Start High-Fidelity 2X Master Mix and 1µl DNA. First Round PCR reaction was as follow: 95˚C for 5 minutes; 30 cycles of 0:30 at 95˚C, 0:30 at 55˚C and 0:30 at 72˚C; final extension step for 5 minutes at 72˚C. PCR products were visualized on a 1% gel electrophoresis. The second round PCR enabled the addition of sample specific barcodes integrated in the primers (Table 2). PCR reaction consisted in 1.25 µl of External Rev (10µM), 1.25 µl External Fwd (10µM), 12.5µl of Q5 Hot Start High-Fidelity 2X Master Mix (New England BioLabs Inc.), 8.7 µl of pure water and 1.3µl of DNA template for a total volume of 25µl. PCR condition was the same as above described. The barcoded PCR products were visualized on a 1% agarose gel using TBE buffer. Library purification and pooling followed the same method ad previous samples. Libraries were sequenced in the same run ad previous samples, using PE250 Novaseq.

Table 9 Sequences of V1 16s rRNA primers and Illumina adapters used to prepare amplicon library for samples collected in 2019. The highlighted section in External Fwd and External Rev sequence represents the external barcode, while the highlighted section of the sequence in Internal Fwd and Internal Rev is the internal tag. The Internal Fwd contains also a spacer (NNNNN).

External Fwd	AAT GAT ACG GCG ACC ACC GAG ATC TAC AC **ACTGCACTA** CAC TCT TTC CCT ACA CGA CGC TC
External Rev	CAA GCA GAG ACG GCA TAC GAG ATA CTG C **ACTGTGACT** GGA GTT CAG ACG TGT GCTC
Internal Fwd	ACA CTC TTT CCC TAA CGA CGC TCT TCC GAT CT **CTAGTACG** NNNNN
Internal Rev	GTG ACT GGA GTT CAG ACG TGT GCT CTT CCG ATC T **CTAGTACG**

5.2.3 Bioinformatic analyses

Sequencing data from all sample cohorts were processed together. Quality filtering and trimming (>Q27 quality score) was performed on all the reads using Sickle version V1.2 software (Joshi and Fass 2011). Reads error correction was performed SPAdes V2.5.0 software to obtain high-quality assemblies (Bankevich et al., 2012; Nikolenko et al., 2013). Third, paired-end reads were merged (overlap length 70bp) using PANDAseq v2.11 software with simple bayesian read merging algorithm (Masella et al., 2012). After overlapping, paired-end reads merged reads were dereplicated, sorted, and filtered chimaeras using GOLD SILVA reference dataset (Quast et al., 2013) and singletons were removed by using VSEARCH version 2.3.4 tool (Rognes et al., 2016). Merged pair-end filtered reads were clustered into operational taxonomic units (OTUs) using VSEARCH software at 97% identity. Taxonomic assignment of OTUs was achieved using the Naïve Bayesian Classifier (Pedregosa et al., 2011) implemented in the QIIME 2 platform using SILVA 132 database (Bolyen et al., 2019). Phylogenetic trees of OTUs were

generated using FastTree (Price et al., 2010) software after using MAFFT for multiple sequence alignment (Katoh & Standley, 2013). The resultant OTU table was converted to a biological observation matrix (BIOM) format for the post-OTUs statistical analysis (Cleary et al., 2019).

5.2.4 Post-OTU statistical analysis

5.2.4.1 Alpha diversity metrics

All statistical analysis post OTU calling were performed by using RStudio v 1.3.959 (R studio Team 2019). To assess the alpha diversity of OTUs within each sample, we used species Richness (an estimate number of observed OTUs) and the Effective Shannon index to estimate diversity. (Leinster, 2020). Generalized Linear Model (GLM) was used to explore relationships between microbial alpha diversity traits and ecological variables recorded during sampling as weight, length, fat, salinity, lake of origin, metabolic traits and library preparation method. Species richness or Shannon effective were used as the response variable. The best fitting model was selected on lowest AICc.

5.2.4.2 Beta diversity Metrics

To assess similarity between different microbiome compositions, beta diversity was assessed using UniFrac, which takes into account both species abundance and phylogenetic diversity (Chen et al., 2012). Distance-based redundancy analysis (dbRDA) was used to assess how different explanatory variables contributed to variation among microbial communities. Redundancy analysis with forward selection was performed to specifically select the environmental variables that explained variation within the microbial communities (Nikolova et al., 2021). A PERMANOVA was calculated based on pairwise Unifrac distances using the *adonis2* function within the *vegan* package to assay the role of covariables (e.g. lifecycle stage, infection status etc) in driving microbiome composition. To provide an overall visualisation of microbial composition across all samples, a principal Coordinates Analysis (PCoA) was performed using the microbiomeSeq (Ssekagiri et al., 2017) package based on phyloseq package (McMurdie & Holmes, 2013) with Bray-Curtis dissimilarity measures.

5.2.4.3 Correlation and OTUs differential abundance

Differential abundance of OTUs and variables was calculated by using microbiomeSeq based on DESeq2 package (Ssekagiri et al., 2017). BIOM generated OTU table was used as an input to calculate differentially abundant OTUs between selected groups based on the Negative Binomial (Gamma-Poisson) distribution. Bayesian shrinkage was applied to obtain shrunken log fold changes before the Wald test was used for obtaining significance in each pairwise comparison (Ijaz et al., 2018). Pearson correlation coefficients were calculated across the variables to detect any correlation between OTUs and metavariables. Correlation was performed using Rhea in R. To remove the effect of overpowering bacteria OTUs that were present in <20% of the samples were removed and the minimum number of pairs necessary to support a correlation was set to 3.

5.3 Results

5.3.1 OTUs Samples, sequences and Operational Taxonomic Units (OTUs)

We sequenced 217 samples in total, including gut compartments, environmental samples and control samples across the 3 years. Using a 2x300bp Illumina Novaseq sequencing run we generated 82,018,469 raw reads. We then overlapped the pair end sequences and applied all filtering steps leaving 66,728,009 pair end reads for an average of 307,502 pair end reads per sample. We assigned 15038 OTUs in total, but we removed the OTUs present in less than the 3% of the samples (6 samples), leaving 9454 OTUs that were used for the following steps.

5.3.2 Impact of library preparation on microbial composition

We detected a strong impact of the library preparation approach (Sections 2.2.1 and 2.2.2) on the overall dataset. This effect is clearly discernible based on pairwise Unifrac measures and is shown clearly in the PERMANOVA (p value < 0.001) (**Table 10**) and supported by a dbRDA graphical interpretation of the PERMANOVA (**Figure 5-1**). A principal coordinate analysis (PCoA) based on Bray-Curtis dissimilarity measures shows the same pattern (**Figure 5-2**). For the motivations listed above, we decided to subset the dataset in two biological

replicates based on the library preparation technique. The rest of the results will be presented also as two replicas based on library protocol.

Table 10 PERMANOVA coefficient with permutation test for capscale under reduced model across all sequencing samples and recorded variables. Significance codes: 0 '***' 0.001 '**' 0.01 '*' 0.05 '.'.

	Df	SumOfSqs	F	Pr(>F)	
Environment	2	0.652	0.9512	0.53	
Worms	1	0.341	0.9947	0.339	
Condition Factor	1	0.351	1.0243	0.3	
Fat	1	0.37	1.0797	0.204	
Infected	1	0.399	1.1641	0.154	
Lake	1	0.445	1.2987	0.07	
Protocol	1	9.485	27.6676	0.001	***

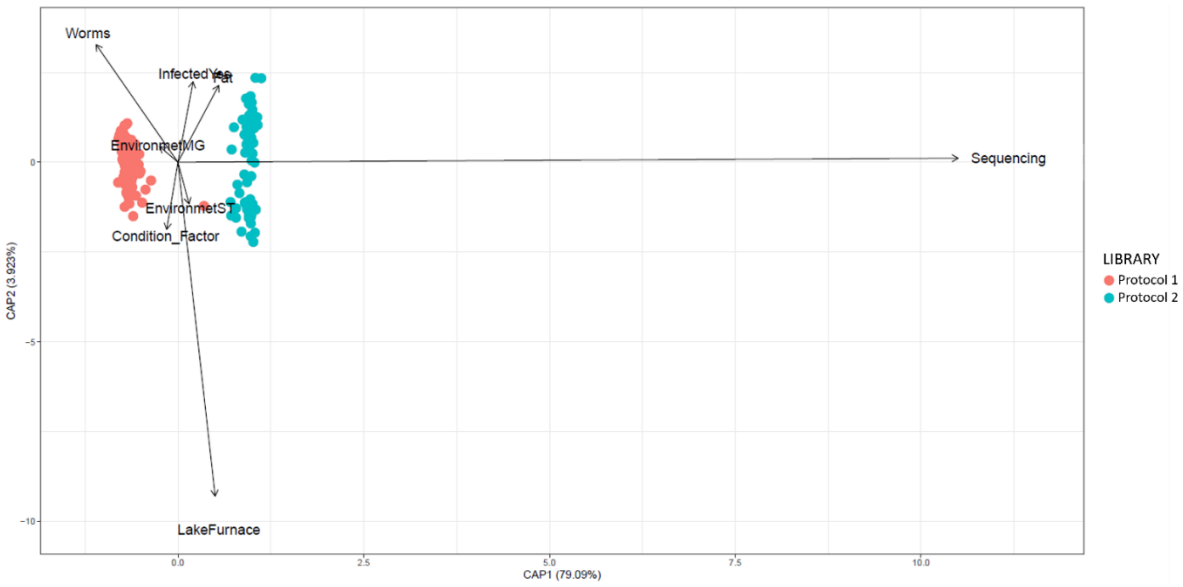

Figure 5-1 Distance-based redundancy analysis (dbRDA) illustrates the drivers of differences in library preparation on beta diversity in European Eel gut microbiota. Blue and red points represent samples processed with protocol 1 and Blue dots samples processed with protocol 2. Arrows in the plot denote the magnitudes and directions of the effects of explanatory variables. The total variance (in per cent) explained by each axis is indicated.

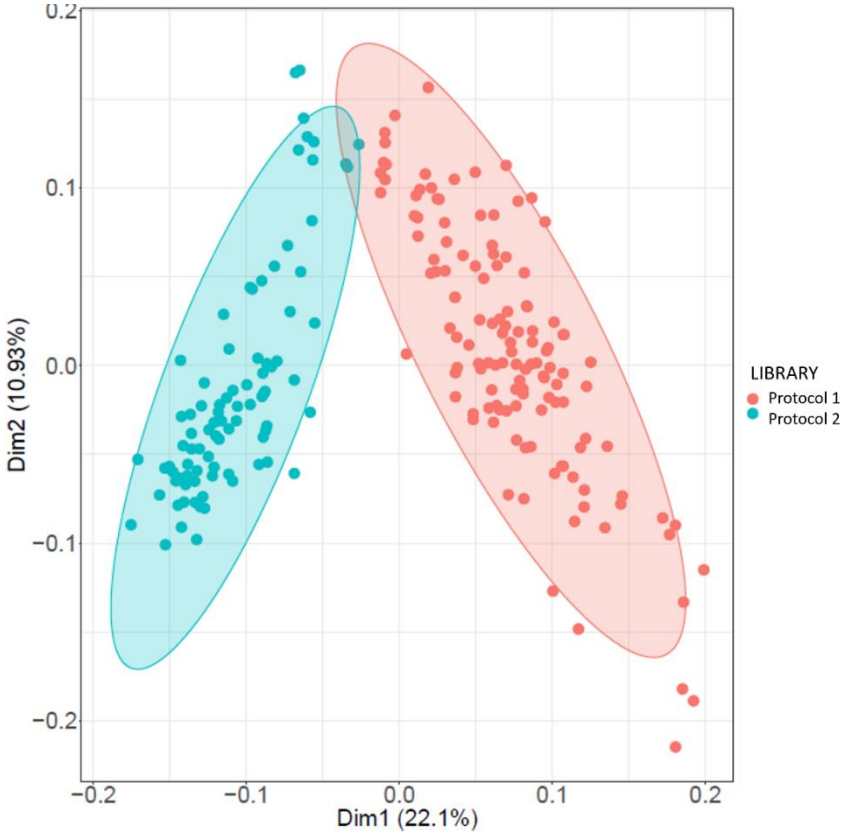

Figure 5-2 PCoA plot visualising European Eel bacterial community diversity across all samples. Displays principal-coordinate analysis (PCoA) plot for Bray-Curtis dissimilarity measures for the different protocols of library preparation. Each dot represents a sample, colour coded based on the library preparation protocol. Dim 1 is principal coordinate 1 and Dim 2 is principle coordinate 2

5.3.3 Influence of parasite on Alpha diversity

5.3.3.1 Protocol 1, 2017 and 2018

To understand the drivers of microbial differentiation across our samples we ran a GLM using Shannon effective or Effective Richness as response variables and covariates we used all the listed recorded covariates in materials and methods. The best model for Shannon Effective (AIC = 986.01, df = 103, Null Deviance = 216700). We detected an effect of weight, year, fat, parasitic load and condition factor on the Shannon effective parameter (p value < 0.05) (**Table 11**). Eels from the 2017 sampling season had a higher diversity. Model prediction also shows how parasitic load in inversional correlated with diversity, with heavily infected animals showing lower microbial diversity (**Table 12**) (**Figure 5-3**). Animals with more fat and a heavier body present a more diverse microbiome. Considering

Effective richness the best model (AIC = 873,65, df = 103, null deviance = 30960) lake, weight and year have an effect. Results for species richness follow Shannon diversity with 2017 representing a more diverse community, FW lake Feaagh having a richer microbiome and heavier animals showing a richer bacterial community (**Figure 5-4**).

Table 11 Best GLM showing the effect of categorical variables on Shannon Effective index in samples processed with protocol 1. GLM = Shannon.Effective ~ (Environment+ Weight+ Length+ Year+ Fat+ Worms+ Condition factor+ Lake+ (Year*Weight)+ (Year*Worms)+ (Year*Fat)+ (Year*Condition factor)). Significance codes for p value: 0 '***' 0.001 '**' 0.01 '*' 0.05 '.'.

	Estimate	Std. Error	t value	Pr(>|t|)	
Environment_MG	-0.26638	6.1091412	-0.043603	0.9653174	
Environment_ST	7.794685	6.2466951	1.2478094	0.2153377	
Weight	0.345876	0.1618954	2.1364173	0.0353591	*
Length	-1.51598	1.743863	-0.869321	0.3869843	
Year_2018	-157.333	63.398819	-2.481641	0.0149347	*
Fat	2.802851	0.8580687	3.266465	0.0015419	**
Worms	-0.7357	0.2293728	-3.20745	0.0018552	**
Condition factor	-1007.26	327.1495	-3.07889	0.0027545	**
Lake_Furnace	-0.96354	5.7390519	-0.167891	0.8670456	
Weight*Year_2018	-0.23181	0.0607481	-3.815998	0.0002485	***
Year_2018*Worms	1.474931	0.8967349	1.6447788	0.103504	
Year_2018*Fat	-2.94551	1.0059917	-2.927964	0.0043207	*
Year_2018*Condition factor	907.4686	386.54384	2.3476472	0.0210845	*

Table 12 Best GLM showing the effect of categorical variables on Effective Richness index in samples processed with protocol 1. GLM = Effective Richness ~ (Environment+ Weight+ Length+ Year+ Fat+ Worms+ Condition factor+ Lake+ (Year*Lake)). Significance codes for p value: 0 '***' 0.001 '**' 0.01 '*' 0.05 '.'.

	Estimate	Std. Error	t value	Pr(>|t|)	
Environment_MG	1.133515334	3.61155865	0.313857656	0.754332069	
Environment_ST	3.253747679	3.693799581	0.880867412	0.380660372	
Weight	0.16964129	0.079182525	2.142408193	0.034772408	*
Length	-1.49187507	0.943434585	-1.581323278	0.117199306	
Year_2018	22.80783974	18.26517353	1.248706436	0.214906683	
Fat	-0.103183418	0.261074971	-0.395225238	0.693581747	
Worms	0.031723421	0.12661829	0.250543752	0.80271955	
Condition factor	-239.0829245	123.6124178	-1.93413355	0.056136793	.
Lake_Furnace	-8.937380858	3.106951274	-2.876575804	0.004985083	**
Length*Year_2018	-0.819520517	0.395785549	-2.070617586	0.041165862	*

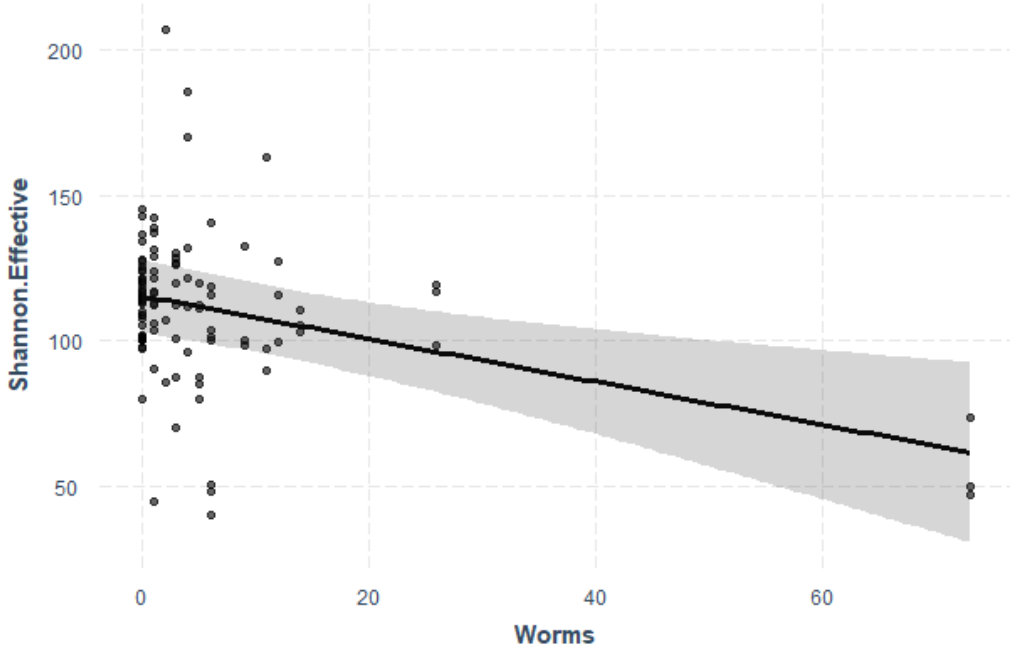

Figure 5-3 GLM visualization of the relationship between parasite burden and Shannon effective index in the European eel. Each dot represents an eel sample, the black line represents the model prediction and the grey shadow 95% confidence interval. Shannon Effective diversity index model prediction decreases with the increase of parasite load (Worms).

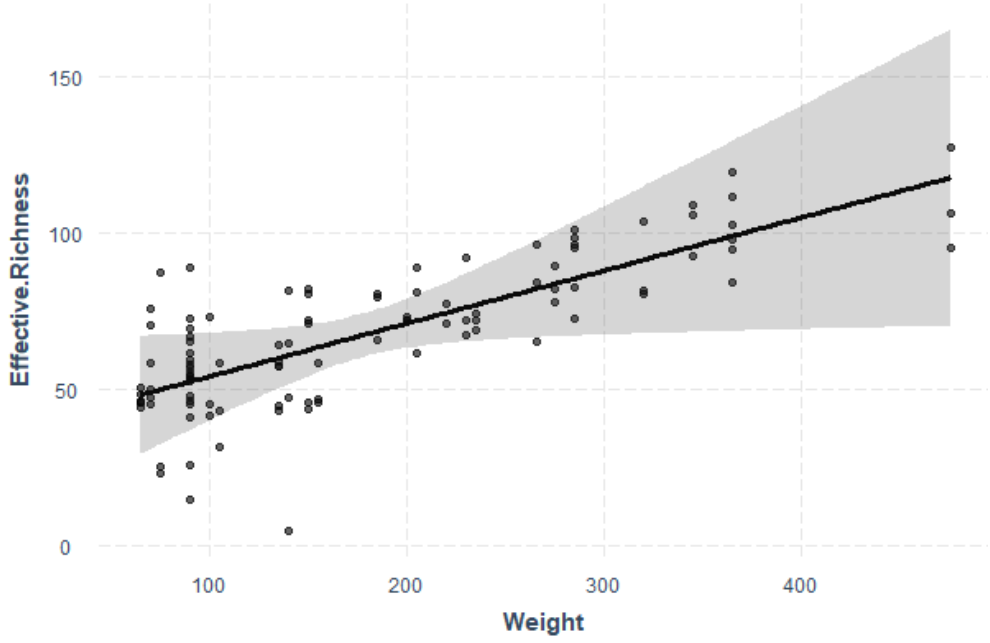

Figure 5-4 GLM visualization of the relationship between respectively weight and Effective Richness in the European eel. Each dot represents an eel sample, the black line represents the model prediction and the grey shadow 95% confidence interval. Effective Richness diversity index model prediction increases with the increase of eel weight (g).

We then visualized using boxplot the average difference in Effective Richness and Shannon Effective diversity in relation to our categorical variables (Environment, Weight, Length, Year, Fat, Worms burden, Infection status, Lake, Year). On average non infected animals have a higher diversity (**Figure 5-5A**). We also visualised the 25 most abundant taxa to genus level across infected and not infected animals (**Figure 5-6**). Although there is no evidence of differentiation, Proteobacteria as *Actinobacter* and *Aeromonas* are more abundant in non-infected animals, while Firmicutes as *Staphylococcus* and *Clostridium* are more abundant in infected animals. Considering differences in alpha diversity between lakes, the freshwater lake Feeagh has a higher richness and Shannon effective with a higher abundance of *Acinetobacter*, *Aeromonas* and *Cetobacterium*. Meanwhile, brackish water samples have a higher abundance of unclassified species, *Flavobacterium* and *Micrococcus* (**Figure 5-5**B, **Figure 5-7**).

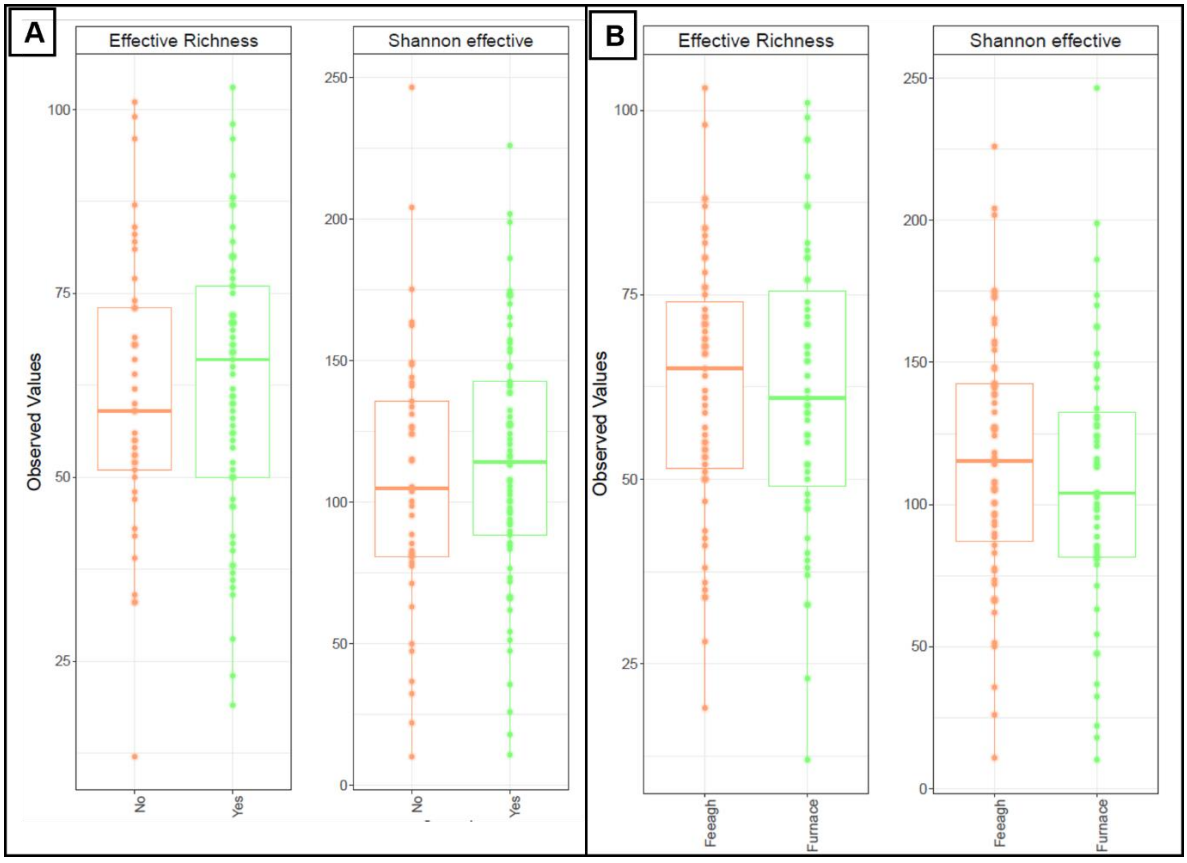

Figure 5-5 Boxplot showing differences in alpha-diversity metrics within infection and salinity in sampled processed with protocol 1 in eels. **A:** Effective Richness and Shannon Effective observed values plotted in relation to *A. crassus* infection (yes/no). **B**: Effective Richness and Shannon Effective observed values plotted in relation to salinity and lake of collection (Feeagh/Furnace)

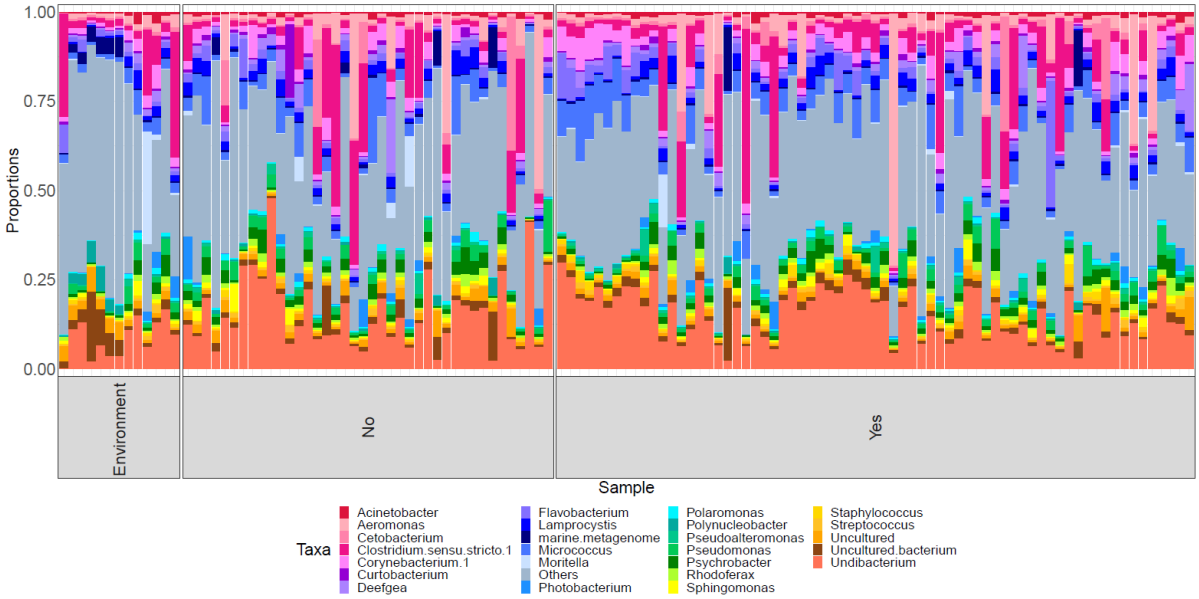

Figure 5-6 Boxplot visualization of the microbial composition (25 most common genus) amongst infected and not infected eels processed with protocol 1. Each column represents a sample. The different infection status is labelled on the x-axis (yes/no).

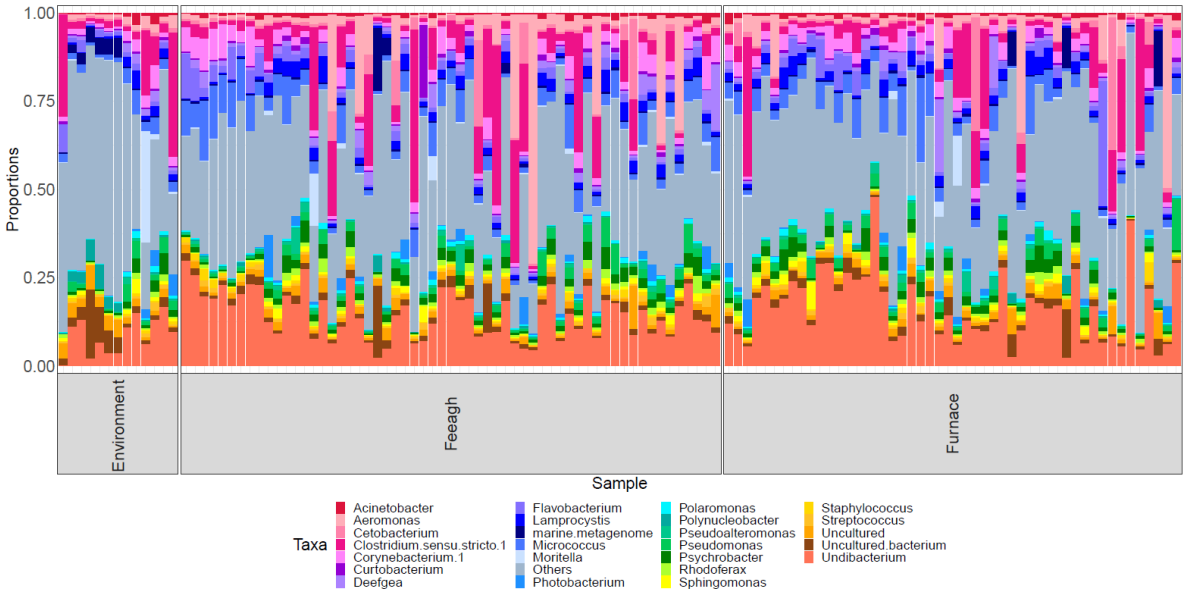

Figure 5-7 Boxplot visualization of the microbial composition (25 most common genus) amongst samples, including eels and environment, collected in fresh/brackish water processed with protocol 1. The different lake of collection is labelled in the x axes (Feeagh and Furnace).

5.3.3.2 Protocol 2, 2019

Based on the GLM analysis, the best model to explain the difference is Effective Richness (AIC= 647.2, df = 71, null deviance 30735) shows that the parasitic load and the interaction between parasitic load and lake have an impact on the

diversity of the bacterial community (**Table 13**). Prediction of the model based on the interaction between the number of recorded worms and lake shows that in Furnace there is a decrease in richness with an increase of worms, while in lake Feeagh it is almost constant the richness across the samples (**Figure 5-8**). Considering Shannon Effective as the response variable, in our best GLM (AIC= 783.4, df= 71, null deviance = 214729) the only variable impacting the variability is the parasitic load (**Table 14**). Animals with more parasites present a lower bacterial diversity (**Figure 5-9**). We did not find any significant interaction between alpha diversity and metabolic phenotype in our analysis.

Table 13 Best GLM showing the effect of categorical variables on Effective Richness index in samples processed with protocol 2 from 2019. GLM = Effective Richness ~ (Environment+ Weight+ Length+ Fat+ Worms+ Condition factor+ Infection + Lake+ (Worms*Lake)+ (Worms*Condition factor). Significance codes for p value: 0 '***' 0.001 '**' 0.01 '*' 0.05 '.'.

	Estimate	Std. Error	t value	Pr(>|t|)	
Environment_MG	-1.791666667	5.718185545	-0.31332783	0.755118249	
Environment_ST	-0.791666667	5.718185545	-0.138447181	0.890350629	
Weight	0.092546523	0.114333943	0.809440485	0.421460274	
Length	0.021011334	1.268310212	0.0165664	0.986837496	
Fat	0.578592699	0.395297203	1.463690344	0.148498161	
Worms	-15.0783202	4.976222771	-3.03007339	0.003604266	**
Lake_Furnace	16.12366888	11.90719036	1.35411196	0.180778938	
Infected_Yes	8.969632032	10.31773489	0.8693412	0.388124975	
Condition factor	-281.9300028	141.7672835	-1.988681703	0.051302803	.
Worms*Lake_Furnace	-7.521595892	3.081246818	-2.441088409	0.017610612	*
Worms*Condition factor	97.30372391	33.22750568	2.928408917	0.004809421	**

Table 14 Best GLM showing the effect of categorical variables on Shannon Effective index in samples processed with protocol 2 from 2019. GLM = Shannon Effective ~ (Environment+ Fat+ Worms+ Lake). Significance codes for p value: 0 '***' 0.001 '**' 0.01 '*' 0.05 '.'.

	Estimate	Std. Error	t value	Pr(>|t|)	
Environment_MG	-10.07	15.25928216	-0.659926194	0.51159766	
Environment_ST	15.34708333	15.25928216	1.005753952	0.318207146	
Fat	0.678401334	0.747231323	0.90788664	0.367241262	
Worms	-2.767455867	1.25092606	-2.212325696	0.030409537	*
Lake_Furnace	-24.59054307	13.68930885	-1.796331965	0.077018219	.

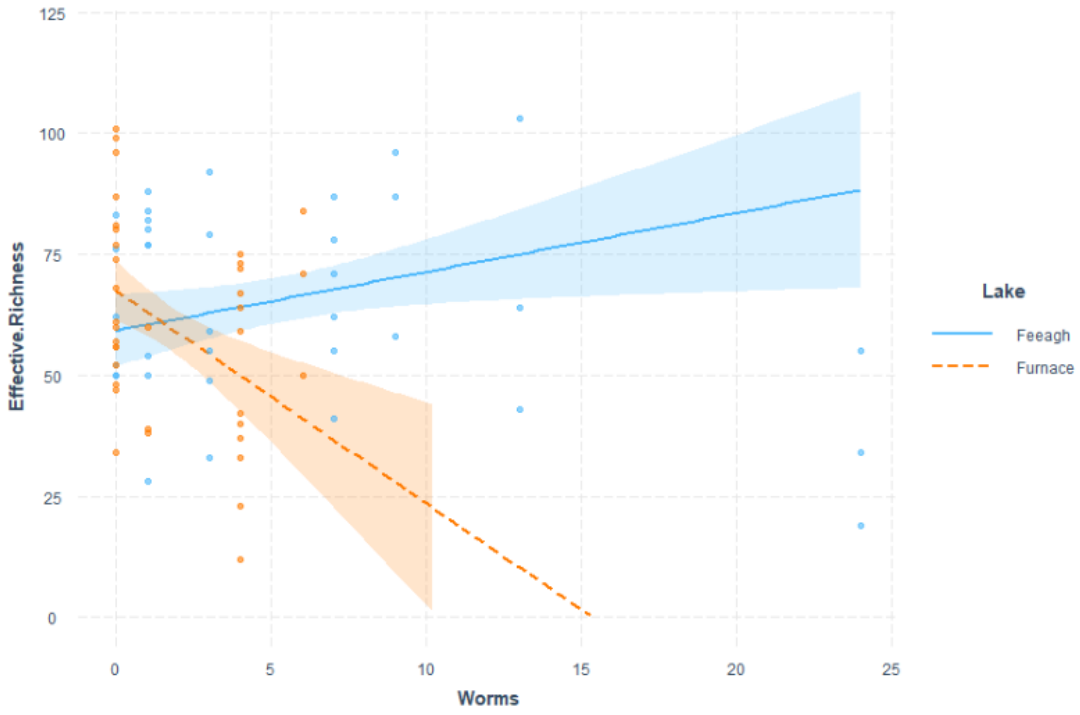

Figure 5-8 GLM model prediction in relation to parasite burden on Effective Richness in the European eel samples in different lakes and processed with protocol 2 in 2019. Each dot represents an eel sample. The continuous and dotted lines represent the linear prediction and shadows 95% interval confidence. There is a trend inversion in microbial richness and parasitic load in eels samples in FW compare to brackish water.

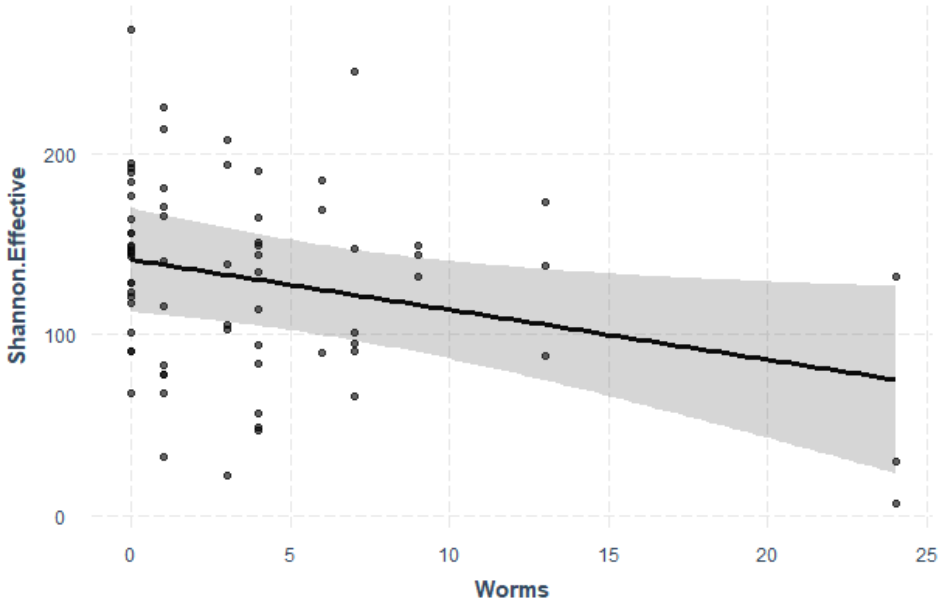

Figure 5-9 GLM model prediction in relation to parasite burden on Shannon Effective in the European eel processed with protocol 2 in 2019. Each dot represents an eel sample. The continuous line represents the linear prediction and shadows 95% interval confidence.

We performed the same analyses as in 2017/18 (Section 5.3.3.1) for samples collected in 2019. For those samples, we also included in the analysis the recorded SMR, MMR and AS. Reassuringly, the results obtained follow similar trends. Effective richness and Shannon effective are higher in infected animals (**Figure 5-10A**) Taxa plot based on the most 25 abundant genus visually provide the prevalence of *Proteobacterium*, *Mycoplasma* and *Pseudomonas* in infected animals. While non infected animals have a higher proportion of unknown bacteria (**Figure 5-11**). Considering the differences between alpha diversity and lakes of sampling, as previously found, Lough Feeagh has a higher Richness and Shannon Effective as graphically presented in Figure 10B. Furnace bacterial community presents a higher abundance of *Photobacterium*, *Staphylococcus*, *Acynetobacter* and *Shewanella*, while Feeagh presents more *Mycoplasma*, *Pseudomonas* and *Aeromonas* (**Figure 5-10B**, **Figure 5-12**).

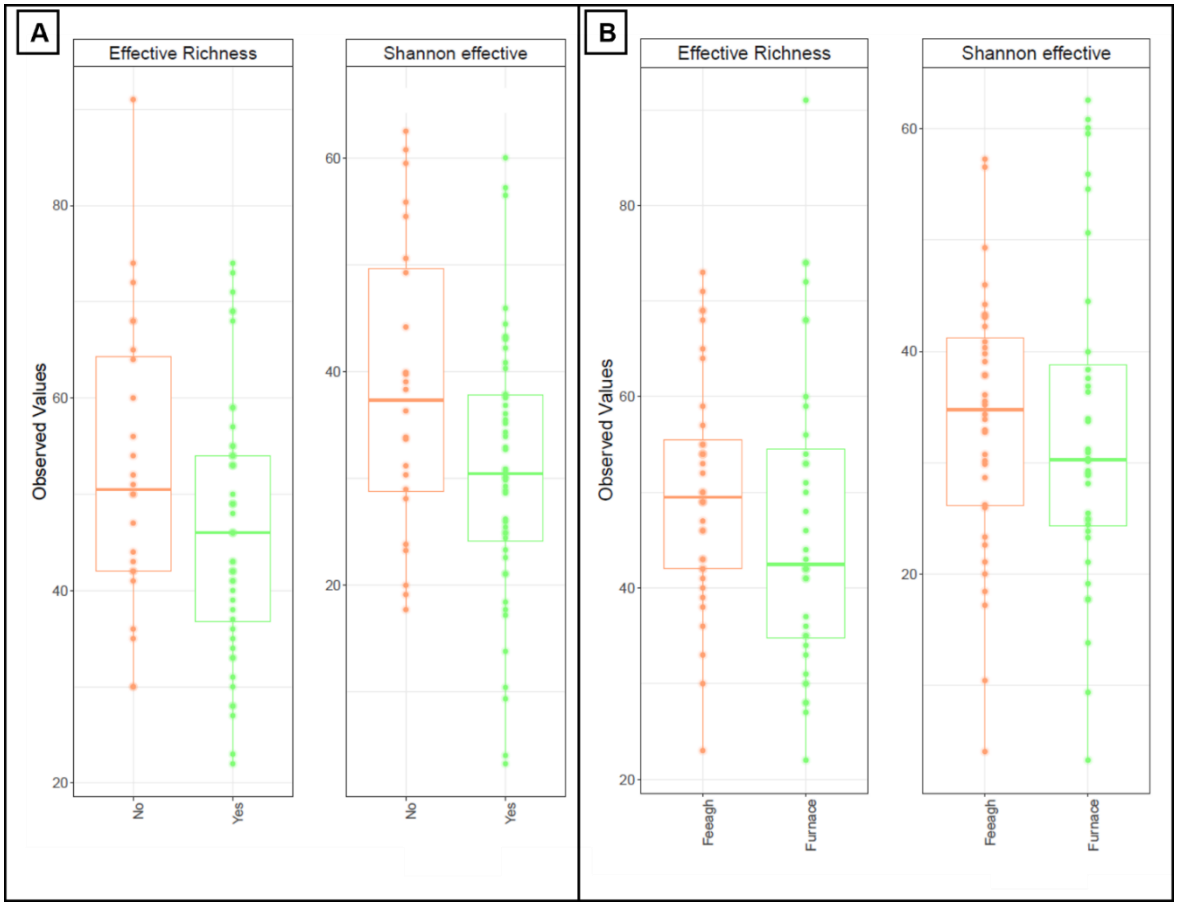

Figure 5-10 Boxplot showing differences in alpha-diversity metrics within infection and salinity in sampled processed with protocol 2 in the European eels. A Effective Richness and Shannon Effective observed values plotted in

relation to *A. crassus* infection (yes/no). B Effective Richness and Shannon Effective observed values plotted in relation to salinity and lake of collection (Feeagh/Furnace)

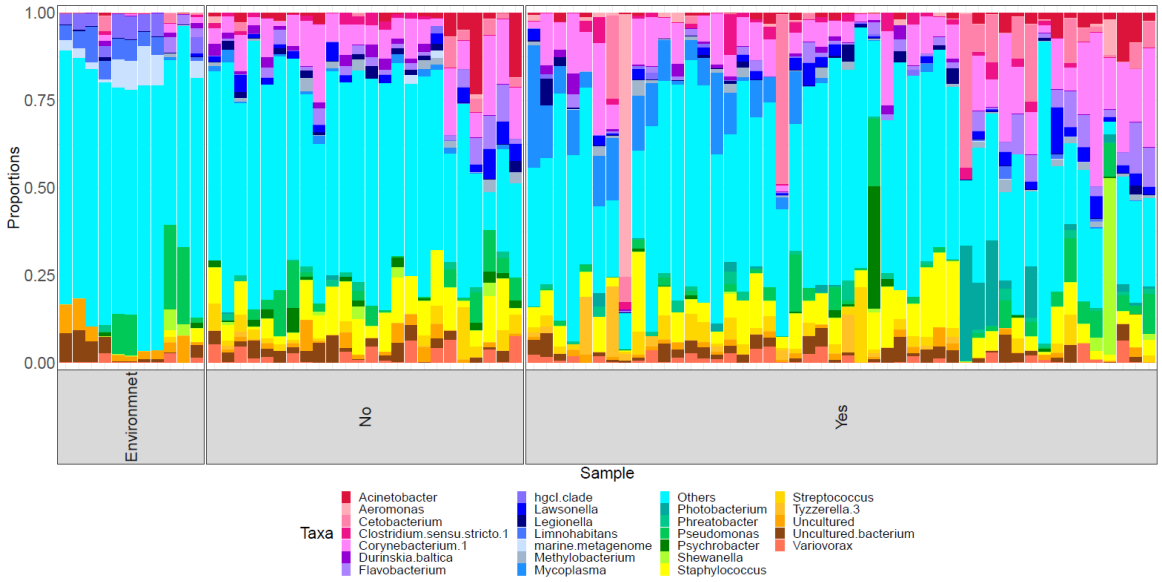

Figure 5-11 Boxplot visualization of the microbial composition (25 most common genus) amongst infected and not infected eels processed with protocol 2 in 2019. The different infection status is labeled on the x-axis (yes/no). Each column represents a sample.

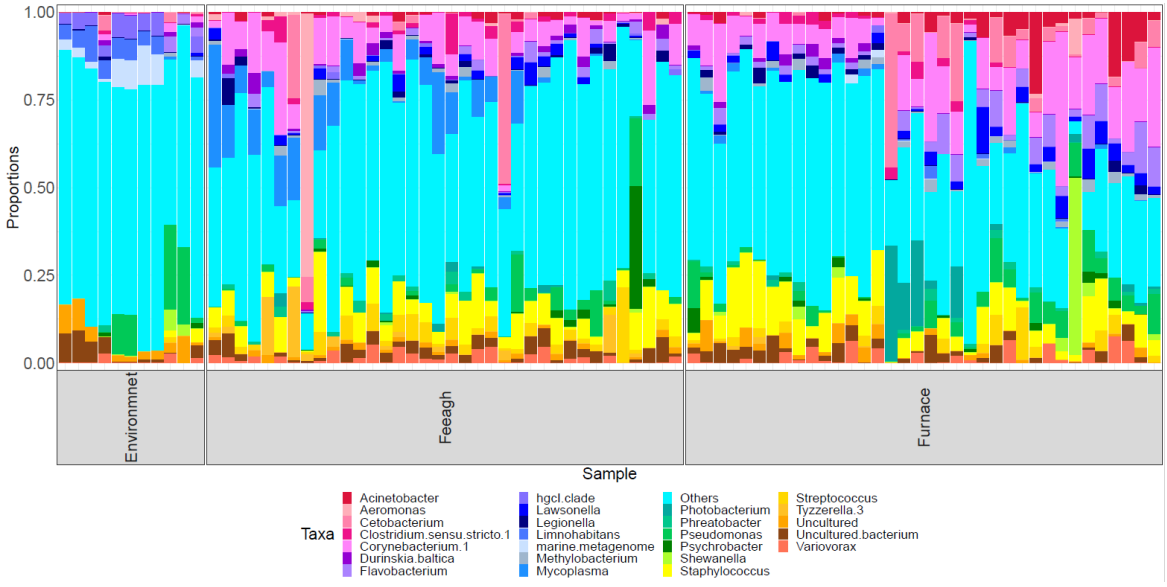

Figure 5-12 Boxplot visualization of the microbial composition (25 most common genus) amongst samples, including eels and environment, collected in fresh/brackish water processed with protocol 2. The different lake of collection is labeled in the x axes (Feeagh and Furnace). Each column represents a sample.

5.3.4 Similarity between microbial communities using Beta diversity

5.3.4.1 Protocol 1, 2017 and 2018

Statistical comparisons based on PERMANOVA show there is an effect of year of sampling and parasitic load on beta diversity (**Table 15**). A dbRDA was used as an overall graphical representation of all the variables influencing beta-diversity in the data (**Figure 5-13**). A PCoA (Principal coordinates Analysis) based on Bray-Curtis distance was performed to illustrate the impact of variables identified as significant by the PERMANOVA (**Figure 5-14**).

Table 15 PERMANOVA coefficient with permutation test for capscale under reduced model across samples processed with protocol 1 to discover beta diversity differences between categorical variables. There is a significant effect of year of sampling and parasitic load on beta diversity. Significance codes: 0 '***' 0.001 '**' 0.01 '*' 0.05 '.'.

	Df	SumOfSqs	F	Pr(>F)	
Environment	2	0.6197	0.9709	0.729	
Condition factor	1	0.3205	1.0043	0.417	
Fat	1	0.326	1.0216	0.307	
Lake	1	0.3301	1.0343	0.267	
Infected	1	0.332	1.0405	0.229	
Weight	1	0.336	1.0529	0.212	
Length	1	0.3395	1.0639	0.165	
Worms	1	0.3943	1.2356	0.018	*
Year	1	0.5667	1.7758	0.001	***

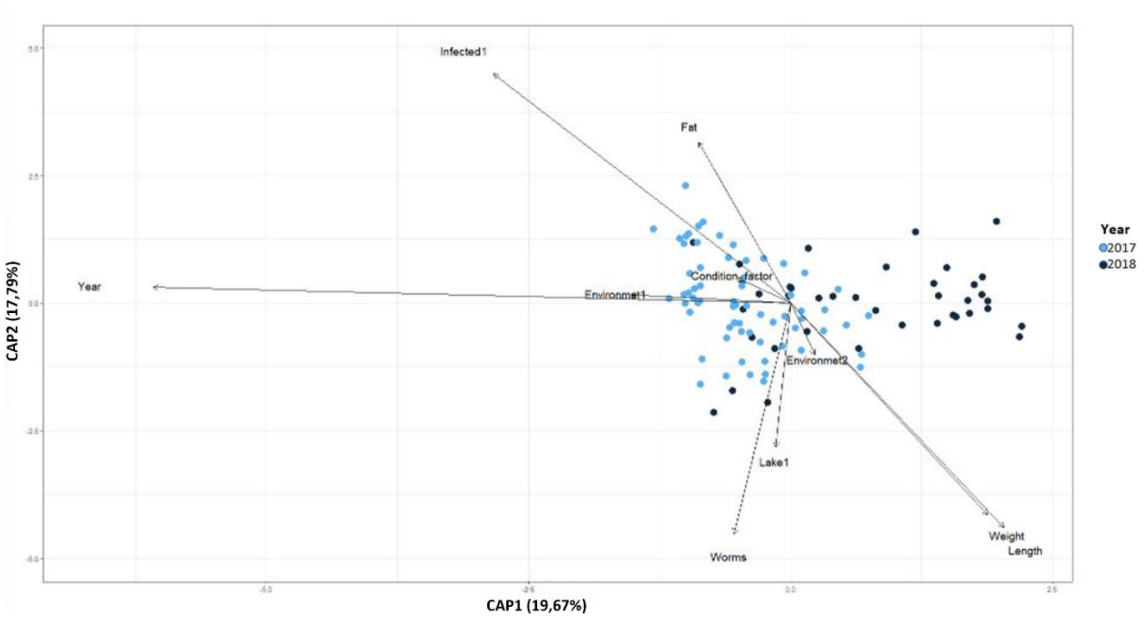

Figure 5-13 Distance-based redundancy analysis (dbRDA) illustrating the drivers of differences between eels processed with protocol 1 (2017 and 2018). Light blue dots are samples collected in 2017 and dark blue in 2018. Arrows in the plot denote the magnitudes and directions of the effects of explanatory variables. The total variance (in per cent) explained by each axis is indicated.

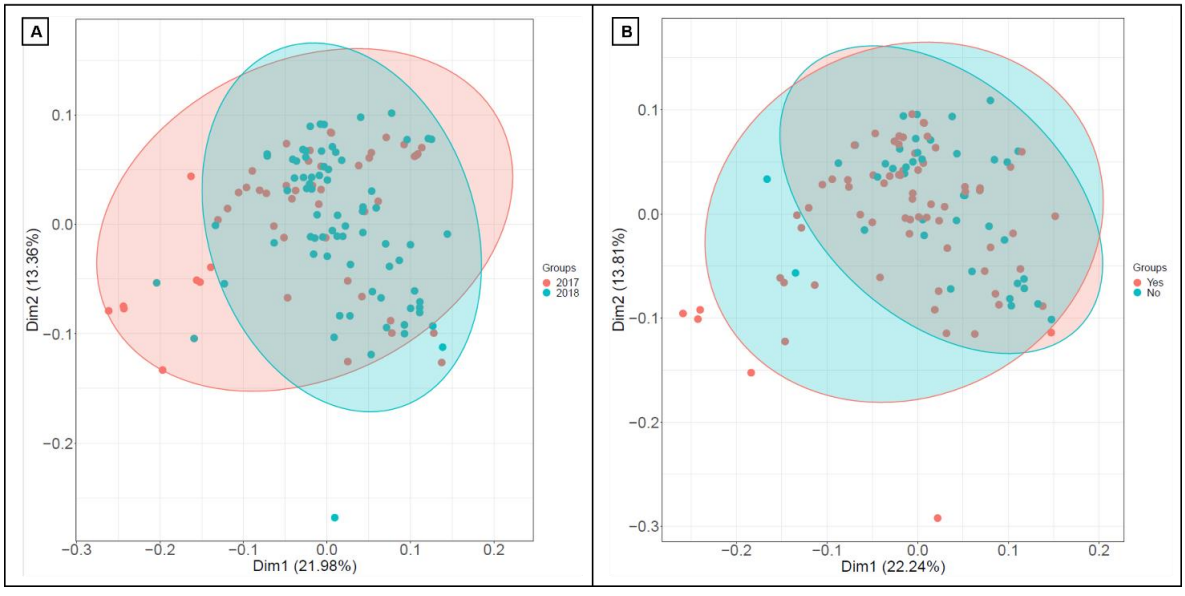

Figure 5-14 PCoA analysis for eels and environmental samples processed with protocol 1. Figure displays two principal-coordinate analysis (PCoA) plots for Bray-Curtis dissimilarity measures, each dot represents a sample. Dim 1 is principal coordinate 1, and Dim 2 is principle coordinate 2, oval represent 95% interval confidence. **A**: PCoA grouped by year of sampling, 2017 in red dots and 2018 in blue dots **B**: PCoA grouped by different infectious status, with infected eels represented by red dots and parasite free eels by blue dots

5.3.4.2 Protocol 2, 2019 data

The PERMANOVA performed on samples collected in 2019 showed an impact of the parasite, lake of origin and fat microbial diversity (**Table 16**) (p value < 0.05). dbRDA graphical representation supported this result (**Figure 5-15**). As before, a PCoA (Principal coordinates Analysis) based on Bray-Curtis distance was conducted to illustrate the significant relationships between beta diversity and categorical variables (i.e. lake origin and parasite infection status)(**Figure 5-16**). A PCoA describing the clear distinction between eel gut and environmental microbiota is also provided (**Figure 5-17**).

Table 16 PERMANOVA coefficient with permutation test for capscale under reduced model across eels processed with protocol 2 to discover beta diversity differences between categorical variables. There is a significant effect of the lake of sampling, parasitic infection and fat content on beta diversity. Significance codes: 0 '***' 0.001 '**' 0.01 '*' 0.05 '.'.

	Df	SumOfSqs	F	Pr(>F)	
Environment	2	0.701	0.9636	0.746	
SMR	1	0.702	0.9872	0.479	
MMR	1	0.682	1.021	0.486	
Weight	1	0.3876	1.0656	0.157	
Length	1	0.3901	1.0725	0.133	
Aerobic Scope	1	0.437	1.1138	0.265	
Worms	1	0.3902	1.0727	0.119	
Condition factor	1	0.4125	1.1342	0.054	.
Infected	1	0.4525	1.2441	0.009	**
Fat	1	0.4531	1.2456	0.004	**
Lake	1	0.519	1.4269	0.002	**

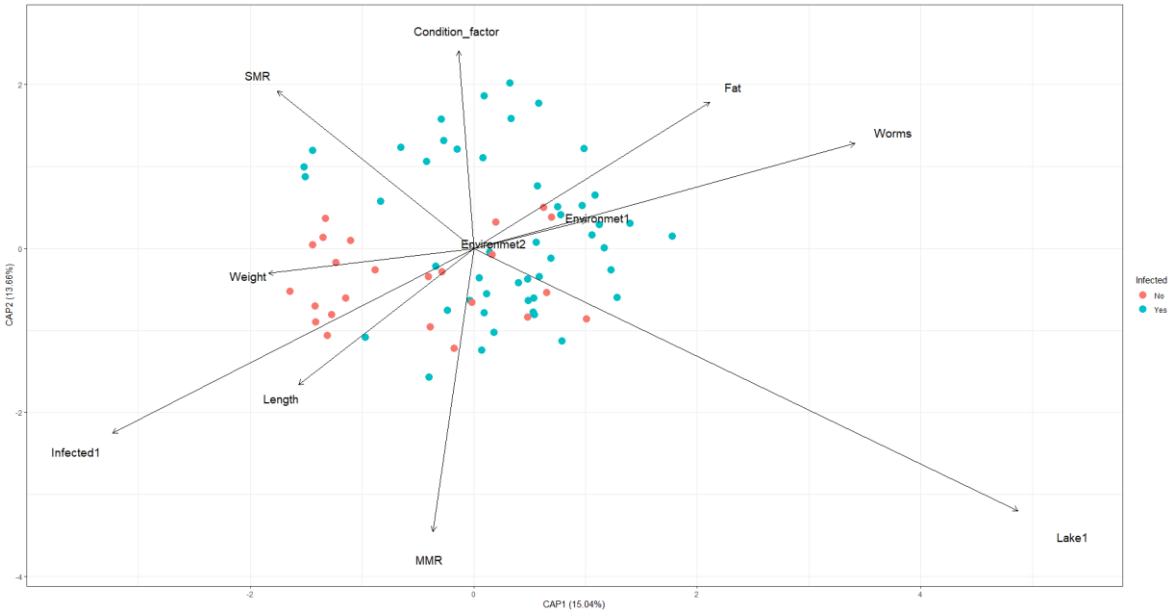

Figure 5-15 Distance-based redundancy analysis (dbRDA) illustrating the drivers of differences between infected and not infected eels. Blue dots are infected eels and red dots are parasite-free. Arrows in the plot denote the magnitudes and directions of the effects of explanatory variables. The total variance (in per cent) explained by each axis is indicated.

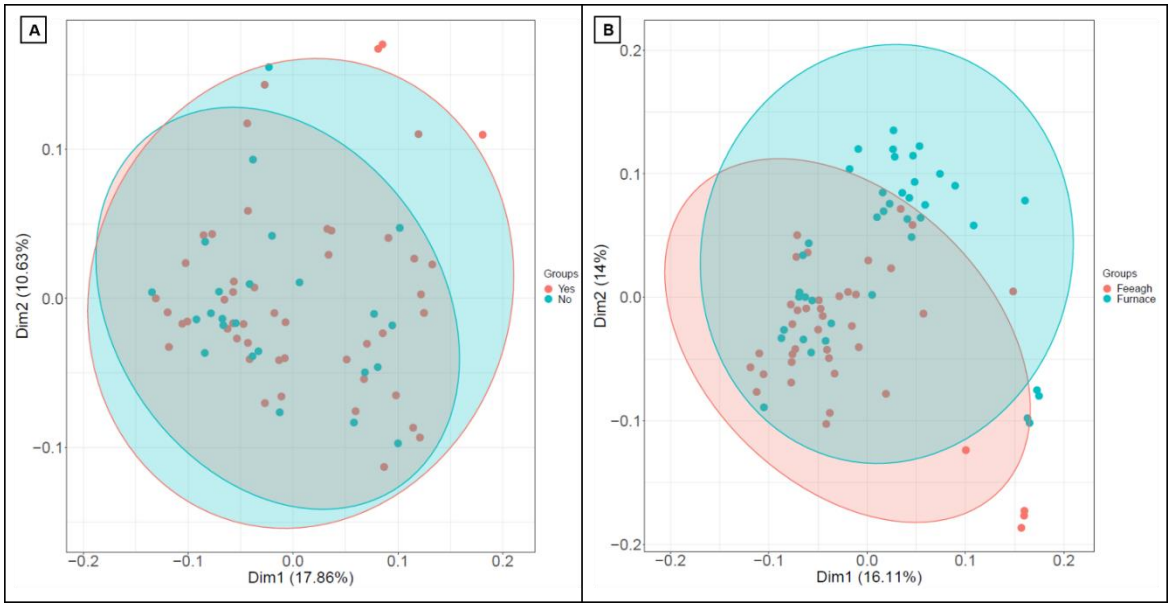

Figure 5-16 PCoA analysis for eels and environmental samples processed with protocol 2. The figure displays two principal-coordinate analysis (PCoA) plots for Bray-Curtis dissimilarity measures, each dot represents a sample. Dim 1 is principal coordinate 1, and Dim 2 is principle coordinate 2, oval represent 95% interval confidence. **A**: PCoA grouped by different infectious status, with infected eels represented by red dots and parasite free eels by blue dots. **B**: PCoA grouped by lake of collection with samples from Feeagh represented by red dots and samples from Furnace by blue dots.

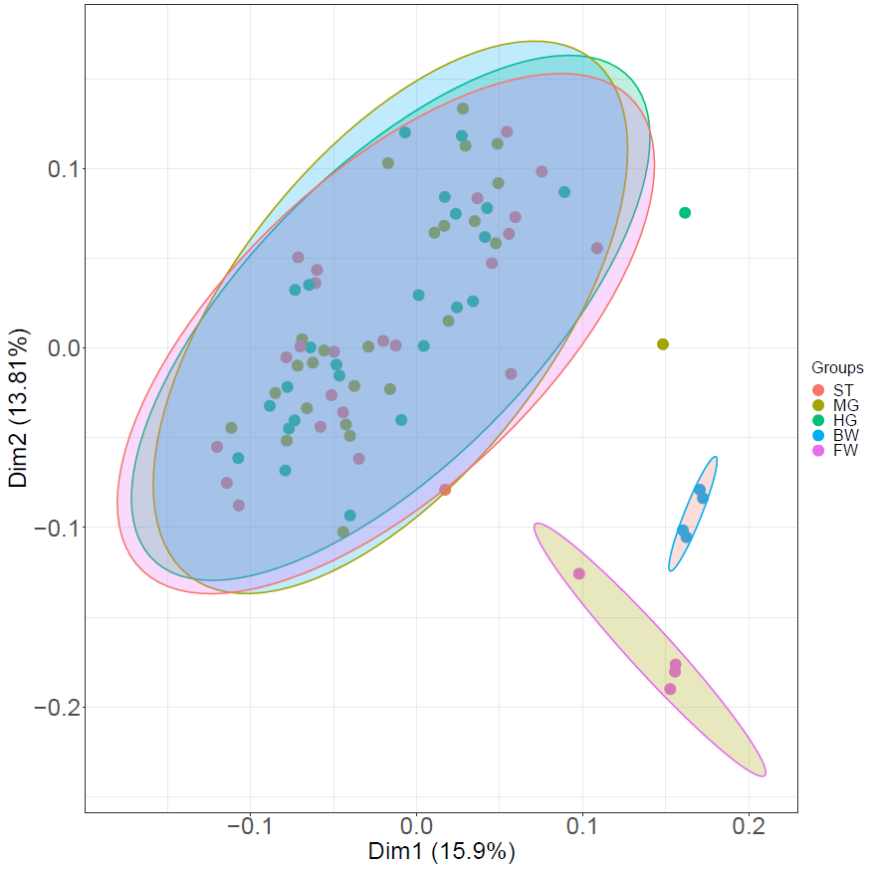

Figure 5-17 PCoA analysis for eels and environmental samples processed with protocol 2. The figure displays two principal-coordinate analysis (PCoA) plots for Bray-Curtis dissimilarity measures, each dot represents a sample. Dim 1 is principal coordinate 1, and Dim 2 is principle coordinate 2, oval represent 95% interval confidence. Dots are divided in stomach (ST), mid gut (MD), hind hut (HD), Freshwater (FW) and brackish water (BW)

5.3.5 Correlation and differential abundance with OTUs

5.3.5.1 In protocol 1, 2017 and 2018

For correlation analysis we focussed on linear covariates. We found a significant positive correlation (p value < 0.05) between Effective Richness, Shannon Effective, Parasitic burden (Worms), Fat and Year of sampling with OTU76, OUT25, OTU243, OTU17, OTU66 and OTU319 which are respectively *Psychrobacter, Polynucleobacter, Clostridium, Undibacterium, Lamprocystis* and *Photobacterium*. We found a significant negative correlation (p value < 0.05) between Effective Richness, Shannon Effective, Condition factor, Length and Year

with OTU76, OTU25, OTU243, OTU26 and OTU18 which are respectively *Psychrobacter*, *Polynucleobacter*, *Clostridium*, uncultured Alphaproteobacteria and *Undibacterium*. OTUs with a significant p value and their correlation direction are highlighted in **Figure 5-18**. We only found two bacterial taxa having a statistically different abundance between infected and not infected eels (*Proteiniphilum* and *Candidatus arthromitus*), and one taxa between samples collected in the two different lakes (*Dysgonomonas*).

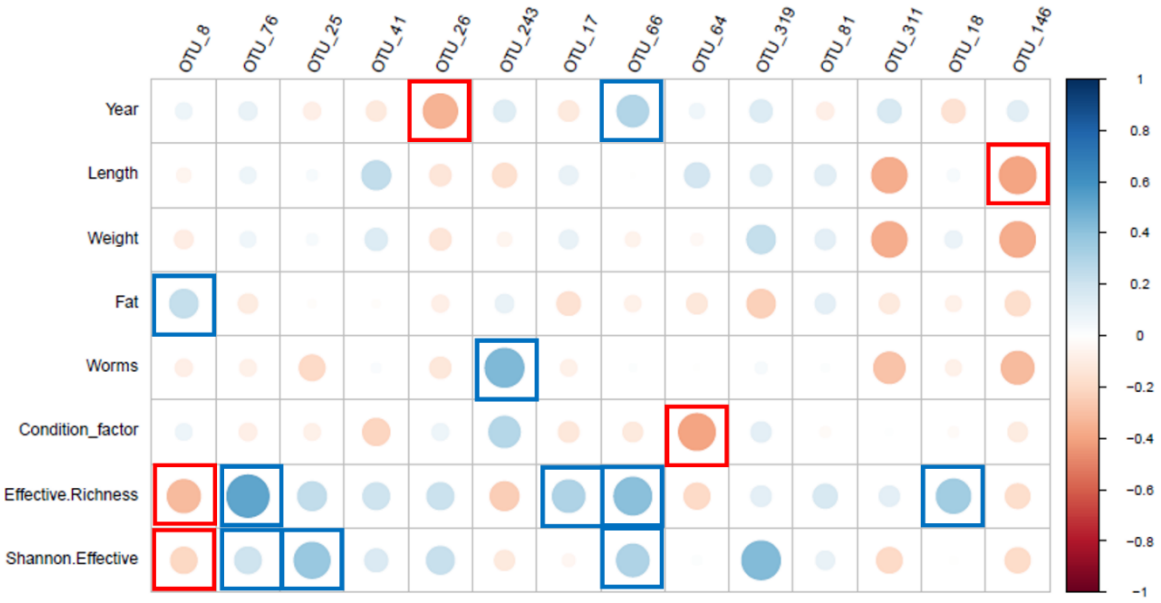

Figure 5-18 Correlations plot showing the correlations between metavariables and OTUs across eels processed with protocol 1. Each correlation is shown as a circle that is coloured to indicate the direction of the correlation coefficient, where red is negative, and blue is positive. The size of each circle relates to the uncorrected p-value of the corresponding relationship, with larger circles indicating lower uncorrected p-values. Significant p value associated with OTUs are highlighted with squares around the circle following the same colour coding

5.3.5.2 In protocol 2, 2019

We found a significant positive correlation (p value < 0.05) between Length, MMR, Aerobic Scope, Shannon Effective with OTU11 and OTU1929 which are respectively *Oxyphotobacteria* and *Staphylococcus*. We found a significant negative correlation between Length, Fat, Parasitic burden (Worms), SMR, MMR, AS, Effective Richness and Shannon Diversity with OTU16, OTU5, OTU33, OTU1, OTU11, OTU30, OTU6, OTU4, OTU13, OTU22 and OTU588 which are respectively *Mycoplasma*, *Lawsonella*, *Oxyphotobacteria* sp., *Staphylococcus*, *Oxyphotobacteria sp.*,

Methylobacterium, *Corynebacterium*, *Streptococcus*, *Pseudomonas*, *Durinskia baltica* and *Oxyphotobacteria* sp. OTUs with a significant p value and their correlation direction are highlighted in **Figure 5-19**. We found 54 significantly different abundant OTUs between infected and not infected eels (Appendix 4, Supplementary material 5.1), and 52 between samples collected in Feeagh vs Furnace (Appendix 4. Supplementary material 5.2). Since we detected a strong difference in beta diversity between gut microbiota and environment we run a Wald test for pairwise comparison in different abundance between the 2 categories. 204 OTUs were significantly different between gut and environment (p value < 0.05), revealing a strong difference in microbial composition. *Aphanizomenon*, *Aquiluna*, *Solibacter*, *Fluviicola*, *Magnetospira* and *Polynucleobacter* were among the most different bacterial taxa to drive the differences. The gut microbiota difference was mainly driven by *Peptoniphilus*, a bacteria belonging to the Streptococcus family, *Staphylococcus*, *Cetobacterium* and *Mycoplasma*.

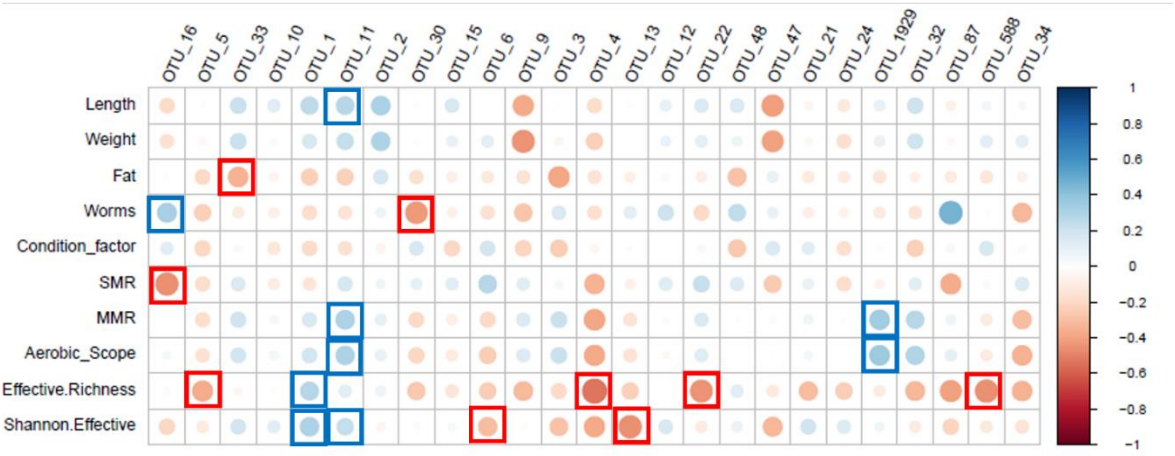

Figure 5-19 Correlations plot showing the correlations between metavariables and OTUs across eels processed with protocol 2. Each correlation is shown as a circle that is coloured to indicate thedirection of the correlation coefficient, where red is negative, and blue is positive. The size of each circle relates to the uncorrected p-value of the corresponding relationship, with larger circles indicating lower uncorrected p-values. Significant p values associated with OTUs are highlighted with squares around the circle following the same colour coding.

5.4 Discussion

To our knowledge, this study is the first to investigate the gut microbiota of wild European eel and their interaction with environmental and physiological factors. The method of 16S rDNA sequencing allows us to characterize the microbiome in the intestines of eels and to understand the main drivers of its compositions. We recorded a strong effect of library preparation in the taxonomic assignment and beta diversity, therefore we split the data into the two parts reflecting the protocol of processing and we considered them as biological replicates (2017/18 samples and 2019 samples respectively). Encouragingly, the different datasets produced comparable findings, showing the same trends in shaping the microbial diversity across and within samples. We detected a strong annual effect on alpha diversity based on richness and bacterial diversity. Effective Richness and Shannon Effective were strongly influenced by health status of the fish, using weight and fat as a proxy for it, and also influenced by the nematode *A. crassus* infection. We recorded a strong reduction in bacterial richness and diversity with an increase of the parasitic load. Considering dissimilarity between communities, measured with beta diversity, we found concurring results with alpha diversity. In eels processed with protocol 2 we also detected the important role environment plays in shaping the microbial community showing a core gut microbiome differing from the environment microbiome. We were not able to detect any significant influence of metabolic traits on microbial diversity and composition.

We know very little about the interactions between the gut microbiota and diseases in fish, our limited knowledge is mostly based on farmed fish (Vasemägi et al., 2017). Disease and parasites can be the cause of infection and inflammation resulting in weaker homeostasis in infected fish with a higher degree of colonization (transient environmental effects) (Q. Huang et al., 2020). Contrasting are the results available in the literature about the effect of parasites on fish health and microbiome (Rimoldi et al., 2020; Sehnal et al., 2021; Tarnecki et al., 2017; Wang et al., 2020). Our study is the first one to show the evidence that *A. crassus* parasitic infection has an impact on microbial community in wild European eels. We found a reduction in richness and diversity of the microbial community with an increase of the parasitic load of *Anguillicola crassus*. The nematode survives in the swim bladder which becomes increasingly thickened and opaque as

a result of fibrosis, can cause degenerative, inflammatory and proliferative changes in the surrounding tissue and acute inflammatory responses (Kirk, 2003). The parasite can also reduce swimming performance and decreased resistance to stress, altering eels' normal behavior (Aguilar et al., 2005b). Our results have a similar pattern as what was found in Atlantic salmon affected by yellow mouth (*Tenacibauclosis*), with a significant reduction of the microbial community in infected animals with an increased abundance of *Aeromonas* and *Vibrio,* which may act as an opportunistic pathogen (Wynne et al., 2020). *Vibrio* has been shown to affect many aquatic species as either the primary or opportunistic pathogen (Austin & Austin, 2007). In Atlantic salmon infected with salmon lice, was recorded a perturbation of microbiome structure and composition with a putative reduction in the colonization resistance (Llewellyn et al., 2017b). In yellow perch, *Perca flavescens*, with high parasitic infection was detected and associated with opportunistic invaders such as *Mycoplasma* and other genera related to fish pathogens like *Aeromonas*, *Pseudomonas* and *Flavobacterium* (Cheaib et al., 2021). Our results agree with previous studies that show a reduction in diversity caused by dysbiosis, defined as a condition caused by an imbalance in the bacterial community, in parasitized animals (Cadena et al., 2018; George Hajishengallis et al., 2012). The eels nematode parasite doesn't cause external lesions and the swim bladder alteration are not connected with the intestinal tract, which can explain the absence of dysbiosis in infected eels. The impact of the parasite on the microbiome could be indirect, perhaps mediated via the immune system, as may be the case in salmon (Lhorente et al., 2014). The nematode may also alter the feeding behaviour of the eels as discussed in chapter 3 changing lipid content and affecting vertical movement, therefore altering the gut microbial community, in light of the importance of diet in the microbial composition (Naya et al., 2007).

Several previous studies have revealed that the gut microbiota of FW and seawater fish are different (Dulski, Kujawa, et al., 2020; Pan et al., 2019; Rennison et al., 2019). Variation in fish gut bacteria composition is correlated with water salinity and our results are following the same trend. There is a difference in microbial community driven by salinity in our data both in Richness based on GLM and beta diversity based on PERMANOVA. Lough Feeagh (FW) and Furnace (brackish) represent two different environments, which are reflected in the different microbial communities. FW most abundant phyla we found are *Mycoplasma*,

Pseudomonas and *Aeromonas*. *Mycoplasma* is a recurrent bacteria present in the gut microbiome of FW fish, including farmed and wild salmon both in farming and not (Steury et al., 2019; Tarnecki et al., 2017). *Aeromonas* and *Pseudomonas* have been recorded in both farmed European and Japanese eels, as potential and opportunistic pathogens (W. Huang et al., 2018b; Joh et al., 2013). We also detected this abundant bacteria in our study, giving a warning on the potential threat those animals are facing. Brackish water microbial composition has more unassigned OTUs showing the lack of assigned classification of saltwater bacteria. We found that *Staphylococcus*, *Photobacterium* and *Corynebacterium* were differing from the freshwater community the most. In Atlantic cod, *Gadus morua*, closely related *Photobacterium* strains represent almost 40% of the gut microbiome and it was associated with breaking down biomass consisting of materials that contain a broad range of fibrous proteins and carbohydrates (Le Doujet et al., 2019). In Atlantic salmon transitioning from salt to FW *Photobacterium* is the genus indicating more apparent separation with fish from the two salinity clines (Wang et al., 2020). *Staphylococcus*, and in general Firmicutes, are often associated with skin or mucosal microbiome because they have increased protein repair and replication mechanisms that potentially allow them to survive in adverse conditions as found in European seabass (Kokou et al., 2020), *Anguilla marmorata* (Lin et al., 2019) and wild *Seriola lalandi* (Ramírez & Romero, 2017). Looking into specific different bacterial from gut microbiota and environmental microbiota we were able to detect multiple OTUs which are constituting the core differences. Most of the bacteria found in water are free living organisms such as *Aphanizomenon*, *Aquiluna*, *Solibacter*, *Fluviicola*, *Magnetospira* and *Polynucleobacter*. Most of those bacterial are freshwater organism associated with catabolism of urea and reduction of nitrate, organic material digestion or emerging motile FW taxa (Challacombe et al., 2012; Volynets et al., 2017). In contrast, gut microbiota was associated with *Staphylococcus*, *Cetobacterium* and *Mycoplasma*, which are common gut bacteria in fish (Holben et al., 2002; Lin et al., 2019; Osimani et al., 2019).

The gut microbiota impacts energy harvest from the diet, resulting in host physiological changes which will likely impact the host metabolic rate and energy availability (Hao et al., 2017). We did not find any indication that changes in microbiome effect, or is effected by, standard metabolic rate and maximum

metabolic rate, in contrast with what is found in other animals as cockroaches (Ayayee et al., 2018) and opiliones (Naya et al., 2007). Also in juveniles of Atlantic salmon a correlation between *Rhodobacteraceae* and low metabolic rate was recorded (E. C. (2021) Lindsay, 2021). Although we didn't detect any effect of SMR and MMR differences in richness and bacterial diversity, we found interesting results on OTUs correlated with metabolic rate. We detected the negative effect of beta microbial diversity on the aerobic scope of eels. We found a is a positive correlation between MMR and AS with Staphylococcus and *Oxyphotobacteria*. *Staphylococcus* can be a potential contributor to lipase, cellulase, protease, and chitinase production (Q. Huang et al., 2020). Improving digestion can be beneficial for energy production and maximum metabolic rate (Adeolu & Gupta, 2014; Nikouli et al., 2021). *Oxyphotobacteria* are associated with fish from eutrophic waters, where feeding is abundant and digestion needs to be efficient (Sehnal et al., 2021). We found a negative correlation between SMR and *Mycoplasma*. Despite the observed dominance of *Mycoplasma* in fish, especially salmonids, very little is known about *Mycoplasma* and its functional potential in teleosts (Rasmussen et al., 2021; Sellyei et al., 2021)

The importance of temporal variation and environment in the microbial composition is well established (Hamilton et al., 2019). In our study both alpha and beta-diversity analysis, based on the results from PERMANOVA and GLM, reveal an effect in annual changes. This finding is consistent with previous studies on freshwater and marine fish, showing how important is the external environment where fish are surrounded into shaping the microbial community (Schmidt et al., 2015). Similar results were found in tench, *Tinca tinca*, where the gut microbiome followed seasonal changes of the farming ponds with *Verrucomicrobia* being the main variable taxa (Dulski, Kozłowski, et al., 2020). The bacteria that mostly were correlated with year changes in microbial composition in our study are *Mycoplasma, Staphylococcus, Corynebacterium and Pseudomonas*. The increase in their overall abundance reduces the richness and diversity of the community, because they are over-represented in the taxonomic assignment. *Mycoplasma* is a well known commensal bacterial present in a wide range of teleosts, where constitutes the dominant bacteria (Egerton et al., 2018). *Mycoplasma* is also one of the main species colonizing the gut microbiome in Atlantic salmon and various species of eels (Hsu et al., 2018; Llewellyn et al., 2016). *Corynebacterium* is found

in diadromous fish, such as rainbow trout and *Anguilla marmorata*, which is associated with disease (Chapagain et al., 2019; Friberg et al., 2019; Lin et al., 2019). As *Corynebacterium*, also *Pseudomonas* is associated with microbiome perturbation and is often recognized as pathogenic genera in farmed fish (Andree et al., 2013; Llewellyn et al., 2017a). The presence of pathogenic bacteria driving the difference in microbial composition in specific years can be a warning of the health status of the eel population and their susceptibility to diseases and external agents.

In conclusion, we reported for the first time a clear impact of *A. crassus* has on the European eel microbiome, reducing its diversity and richness. We also detected an increase of bacterial richness linked with eels' health status measured with fat and weight as proxy. We were also able to address changes caused by salinity differences, probably linked to diet, food availability and digestion capacity. We did not find any link between microbiome and metabolic traits. To date, all our findings are preliminary and correlative in nature. Nonetheless, the clarity and repeatability of our findings, especially in the context of parasite infection, represent a strong motivation to explore the biological drivers of the effects observed. Such studies could involve controlled experiments, artificial rearing and controlled infections to understand the causal directionalities and consequences for *A. anguilla*. As such, this study sets the mark for future investigations about the link between physiology, ecology, environmental drivers and changes in the gut microbiome of the European eel.

6 General discussion

6.1 General findings

The thesis comprised four chapters aimed at exploring ecological and physiological traits in the European eel, *Anguilla anguilla*, in the context of phenotypic plasticity, gut microbiome, parasite infection status and metabolic phenotype. In chapter one, we developed a sensitive, non-lethal and in situ test to establish *A. crassus* infection in *A. anguilla* via the detection of parasite DNA in faecal material. High values for NPV (87%) and PPV (95%) suggest the test may have a useful role in both veterinary and fisheries management contexts. In chapter two we investigated the head shape variation and head phenotypic plasticity. Eels appear to have two different ecomorphs in many catchments, but we did not see any bimodal distribution of narrow and broad head. We implemented the existing methodology of fixed landmark and we found significant differences in head shape variation between life stage, sites of sampling and water salinity. All silver eels appeared to have a narrow head configuration. Differences in head shape in yellow eels were mainly explained by the jaw position and environmental factor as country of origin and the water salinity, shaping the food availability. In chapter three we highlight the impact of fat content, lean mass and parasite burden on the eels' metabolism in relation to their growth and migration. We found that silver eels had a lower SMR compared to yellow eels and infected eels. Fish with a higher general body mass have a higher SMR, especially if living in brackish water. We found that health status, measured in body mass and fat content, and parasite presence is impacting energetic metabolism in eels, potentially reducing their chance to endure swimming during the long migration. In chapter four we characterize the eel gut microbiome using 16S rDNA and we linked microbial richness and diversity with ecological, physiological factors and parasite infection. We detected a strong annual effect on microbial diversity. Bacterial richness and diversity were strongly influenced by the health status of the fish, using weight and fat as a proxy, as well as, importantly by *A. crassus* infection. Microbial diversity in the eel's gut was reduced overall and associated with the increase of opportunistic and potentially pathogenic bacterial like *Mycoplasma*.

6.2 Opportunities and remaining gaps in knowledge

6.2.1 Implementation of a rapid *Anguillicola crassus* screen for infected eels

We developed a rapid test to screen for *A. crassus* presence in the European eel. The test can be performed in the field because all the equipment can be powered by a battery and the result is 97% specific and 91% sensitive. Our test is a first approach to conduct a mass screening of the parasitic infection in the European waters and offers the opportunity to engage in efficient infection control by assessing the disease status of eels before allowing transfers between river systems. The test can contribute to the conservation and management of the European eel and restocking programs in catchment free from infection. Unfortunately, the rapid test may remain untested in glass eels and elvers. Screening the elvers would be essential to stop *A. crassus* from entering the catchment. Faecal samples from elvers could be collected using a smaller and more flexible cannula. Similarly, the costs of screening thousands of eels are likely to be prohibitive. Bulk screening of eels via interpooling can be considered as an alternative approach (Thierry-Mieg & Bailly, 2008). The interpool is an algorithm that enables a large number of individuals to be individually screened using a limited number of pools, reducing the overall cost of the screening but not sample collection. Pooling is a technique that is widely spread helminths detection in stool samples, reducing logistic cost and epidemiological factors (Papaiakovou et al., 2019). Non-molecular diagnostic tools also have a potential role. Fourier transformed infrared spectroscopy, for example, is an efficient, versatile and non-invasive technique that is used to identify human disease and parasites (Elsheikha et al., 2019; Sheng et al., 2016). In a pilot study in a malaria-endemic country has been used as malaria diagnostic tool with 92% sensitivity and 97% specificity providing the efficiency of the technique (Heraud et al., 2019). Similar level of detection was also found in experimental of early-stage laboratory based infection of erythrocytes with the aim to improve earlier detection and treatment of malaria (Khoshmanesh et al., 2014). Few studies have used Fourier spectroscopy in fish and not for parasite detection (Santana et al., 2015). The approach could potentially be deployed to detect the chemical signatures of parasite infection in the skin mucus, for example. High-end ultrasonic imaging to detect the presence

of *A. crassus* in the European eel is been proposed but the level of sensitivity of the diagnostic imaging tool alone can provide enough information (Frisch et al., 2016). Another approach that can be implemented for parasite detection is antibodies testing. Monoclonal antibody probes against parasitic fish pathogens have provided useful tools for the rapid immune diagnosis and control of disease (A. Adams et al., 1995). Indirect enzyme-linked immunosorbent assay (ELISA) has been used to detect the immunological response against the dinoflagellate, *Amyloodinium ocellatum*, in the blood of the European sea bass developing partial resistance against the parasitic infection (Cecchini et al., 2001). In gilthead sea bream the myxozoa parasite *Enteromyxum leei* alters the regulation of cytokines, which can be detected using immunohistochemical analysis (Piazzon et al., 2018). In yellow European eel, the presence of *A. crassus* upregulates genes involved in the swim bladder metabolism and extracellular matrix production as mucin genes, suggesting increased mucus production as a defence reaction against the parasite (Schneebauer et al., 2017). Genes involved in parasitic response, as the one found by Schneebauer *et al,*. can be candidate to develop immunohistochemistry or Fourier spectroscopy assay for parasite detection in the mucus or blood.

6.2.2 Genetic component and diet effect on phenotypic plasticity

Phenotypic plasticity is the ability of one genotype to produce multiple phenotypes in response to environmental variation (Oufiero & Whitlow, 2016b). In some fish species, head morphology differentiation can be considered a plastic trait often associated with diet availability (Stauffer & van Snik Gray, 2004). The drivers in eels head differentiation are still vague. The dimorphic shape occurs independently in different lakes across Europe, North Africa and East Asia, while some other lakes don't present a bimodal distribution of the two ecomorphs (Barry et al., 2016; De Meyer, Herrel, et al., 2017; Ide et al., 2011; Proman & Reynolds, 2000). We found differentiation in head shape between life stages with silver eels always presenting a narrow head and yellow eels a continuum between the two opposite morphs reported by others. Narrow head accumulate lipid faster (Barry et al., 2016), therefore are more prone to silver since the amount of lipid stored is one of the discovered characteristics essential to start the migration (C. Durif et al., 2009). Broad head eels have a slower lipid accumulation and may prolong the longevity of the freshwater stage of their life cycle. The exploitation of the

distinctive trophic niches by broad and narrow head eels may limit intraspecific competition. However, whether the morph emerge as a result of genetics and mortality of intermediates, as in *A. rostrata*, is unclear (Pavey et al., 2015). Epigenetic modifications may underpin phenotypic divergence between morphs In the coral reef fish, *Acanthochromis polyacanthus,* epigenetic signatures have been associated with plasticity in thermal adaptation indicating that distinct gene upregulation may be used for generational plasticity to ocean warming (Ryu et al., 2020). In eels investigation of methylation of specific genes across different life stages might pick up signs of genetic regulation and genes associated with jaw development, bone structuring and digestive capabilities. Any such study should include juvenile eels, because environmental conditions during development can alter patterns of methylation, as observed in embryos of rainbow trout (Lallias et al., 2021), Chinook salmon (Venney et al., 2021) and Atlantic salmon (Jonsson & Jonsson, 2019). In parallel with epigenetic variation across morphs a laboratory experimental approach can be conducted to see the effect of diet. In experiments on brown trout fed with different pray items showed that the adoption of a piscivorous diet may be a factor contributing to the extension of lifespan (Hoffmann et al., 2020; Hughes et al., 2019). A similar experiment can be conducted in eels, where environmental conditions can be standardized with different feeds administered. We know that broad-headed eels favour a piscivorous diet and feeding at a higher trophic level and narrow-headed eels favour invertebrates and benthic animals and the bite force of broad-heads are higher compared with narrow-heads (Barry et al., 2016; De Meyer, Herrel, et al., 2017). Via a controlled rearing experiments it may be possible to establish if the head morphology can shift with different diets or it is a genetically defined traits.

6.2.3 Metabolism, parasite infection status and migration in eels

We found that *A. crassus* parasitic infection impacts the standard metabolic rate in yellow eels. As such, infected eels with the same lean mass as un-infected eels exhibit a lower SMR and parasitic infection is known to delay the lipid accumulation and the starting of the silvering process (C. Durif et al., 2009). We found a metabolic rate decline in silver eels, supporting and adaptation to endurance swimming or as a result of reduced core metabolic demand from atrophied organs (C. Durif et al., 2005, 2009). Lower AS and MMR may also support

the long endurance silver eels have to face to reach spawning grounds (Righton et al., 2016; Simon et al., 2018). A promising technique for evaluating how fishes utilize their maximum aerobic capacity in the natural environment is the use of tagging because it can provide information on acceleration, behavioural thermoregulation, depth preferences and heart rate (Norin & Clark, 2016b). Metabolic profiling of eels prior to release and tracking can help to understand the importance of MMR and AS in migration. Parasite infection in eels also reduced SMR but the reasons are not clear and metabolic data on other parasite-fish interactions are equivocal. In California killifish, *Fundulus parvipinnis*, infection with cercariae of the trematode brain parasite, *Euhaplorchis californiensis*, increase both metabolic rate and activity are affected (L. Nadler et al., 2020). Experiments involving infection of sticklebacks with *Schistocephalus solidus* demonstrate how the parasite can alter movement ability and social interaction, with highly infected fish presenting continuous and predictable movement, swimming slower and modified social behaviour (Jolles et al., 2020). Contrasting pattern was found in Eastern Baltic cod, *Gadus morhua*, infected with the parasitic nematode, *Contracaecum osculatum*, where fish with a high infection rate present a reduction in nutritional condition and reduction of standard metabolic rate and organ mass (Ryberg et al., 2020). Experimental infections in eels can help to understand if the standard metabolic rate can be experimentally reduced by the increase of the parasitic load. We also identified an effect of *A. crassus* on silver eels metabolism linked with lean mass and lipid stored. Infected silver eels present changes to haematological parameters with decreased numbers of red blood cells and an increase in serum cortisol levels (Kirk, 2003). The cortisol has a major role as a primary messenger of stress response in teleost fish, repressing immune response (Fast et al., 2008) and in eels' cortisol is the key hormone produced during fasting, which induces the mobilization of lipid and protein stores (Fazio et al., 2012). The presence of the parasite could have indirect stimulatory effects on silvering mechanisms inducing the migration too early when the eels have not reached the required amount of fat to reach the spawning ground. Screening silver eels for *A. crassus* with the non-invasive test developed in chapter one, recording their metabolic profile and then testing their swimming capacity at different speeds (Killen et al., 2015) can provide answers on the effect of the parasite on silver eels migration and metabolic rate.

6.2.4 Causation in microbiome characterization via transplant experiments

We investigated the gut microbiota of wild European using 16S rDNA and discovered environmental and physiological factors shaping the microbial community. We recorded a strong reduction in bacterial richness and diversity with the increase of the parasitic load and a shift in the microbial community across different years and salinity profiles. Several challenges exist with the interpretation of microbiome data, beyond the technical. Firstly, it is not always clear which members of the gut microbial community are resident and adapted to the host environment and those that are transient and passing through. This is especially for fish, which continually collect microbes from the aquatic environment. Models of microbiome colonisation might distinguish between resident and transient gut microbes and might be applied to future analysis in wild eels (Woodcock et al., 2007). In Atlantic salmon neutral community models have been used to address the importance of random drift and selection to identify 'core' microbes that may have long term relationships with their hosts (Heys et al., 2020). The identification of such 'core' microbes in healthy eels, for example, and their potential disturbance as a result of parasitism may help understand how colonisation resistance breaks down (Llewellyn et al., 2017b). A second challenge with microbiome studies lies in establishing the causal directionally of correlations uncovered. To follow up correlations between gut microbial diversity, parasite infection status and host metabolism and health status multiple experiments in a laboratory setting are possible. Experimental exposure to parasites can be undertaken, as described previously. Dual challenge experiments, first with the parasite, then with an opportunistic pathogen, can establish the link between dysbiosis and colonisation resistance (Lhorente et al., 2014). To study the impacts of microbiomes on host physiology, microbial transplant experiments are possible in gnotobiotic animals. Rearing of germ-free individuals is not always possible to generate for non-model species, especially for eels, where efforts continue to close the lifecycle in captivity (Butts et al., 2016). Instead is the possibility of trans-species microbiome transplant as has been demonstrated in brown bears whose microbiome has been transplanted in mice to study hibernation processes (F. Sommer et al., 2016). Protocols to rear germ-free zebrafish exist and could be a possible recipients of eel microbiomes.

6.3 Conclusions

The thesis provides preliminary data on the effect of the *Anguillicola crassus* on the European eel ecology, metabolism and microbiome. The thesis also provides a test for screening the eels for the presence of the parasite in a non-lethal way, contributing to the conservation management and parasite control of this specie. Our findings highlight the possible negative effect the parasite has on eels' capacity of storing lipids and alteration in richness and diversity of the microbiome. We also detected an impact of the health status of eels, measured as fat content and lean mass, on standard and maximum metabolic rate. Our findings open more research lines to better understand the eel ecology, physiology and microbiome function in lipid metabolism and parasitic resistance. Different experiments have been proposed to investigate the importance of diet and DNA methylation in head phenotypic plasticity, to investigate the effect of *A. crassus* on swimming capacity, metabolic profiles and lipid storage in yellow and silver eels, experiments to understand the impact microbiome changes causation using transplants. We also suggested multiple ways to improve the rapid test detection, based on antibodies presence or Fourier spectroscopy, to reduce the cost per sample and have a test for a mass eel's screening. All the work conducted in the thesis aims to fill a gap of knowledge and contribute to the conservation management and restoration of the critically endangered the European eel, a fascinating animal, whose life cycle and ecology, despite my best efforts, still remains a mystery.

Appendices

Appendix 1: Chapter 2 Supplementary materials

Supplementary material 2.1. Data collection for chapter 2. Location: Bo = Burrishoole, N_Ir = Northern Ireland; Lake: Fe = Lough Feeagh, Fu = Lough Furnace, Ne = Lough Neagh, Extraction method: Q = Qiagen, W = Whatman; Life stage: Y = Yellow, S = Silver.

Eel	Year	Location	Lake	Nematode counted	Infection rate	Extraction method	Life stage	Length (cm)	Weight (g)	Fat
1	2017	Bu	Fe	0	0.67	Q	Y	31.3	55	N/A
2	2017	Bu	Fe	26	0.67	Q	Y	38.3	90	12.5
3	2017	Bu	Fe	6	0.67	Q	Y	40	105	15.4
4	2017	Bu	Fe	1	0.67	Q	Y	42.3	140	7.6
5	2017	Bu	Fe	1	0.67	Q	Y	36.6	90	12.3
6	2017	Bu	Fu	73	0.67	Q	Y	53.9	275	15.5
7	2017	Bu	Fu	4	0.67	Q	Y	47.6	185	21.7
8	2017	Bu	Fu	4	0.67	Q	Y	36.2	70	9.6
9	2017	Bu	Fu	0	0.67	Q	Y	36.7	75	9.1
10	2017	Bu	Fu	2	0.67	Q	Y	58.1	320	5
11	2017	Bu	Fe	0	0.67	Q	Y	58.1	320	5
12	2017	Bu	Fu	0	0.67	Q	Y	36.6	90	12.3
13	2018	Bu	Fu	0	0.52	Q	Y	49	200	6.6

14	2018	Bu	Fu	0	0.52	Q	Y	43.2	135	6.9
15	2018	Bu	Fu	5	0.52	Q	Y	37.8	90	8.9
16	2018	Bu	Fu	0	0.52	Q	Y	33.7	70	18.2
17	2018	Bu	Fu	0	0.52	Q	Y	34.3	65	20.8
18	2018	Bu	Fu	6	0.52	Q	Y	33.7	65	25.8
19	2018	Bu	Fe	14	0.52	Q	Y	57.3	365	5.2
20	2018	Bu	Fe	5	0.52	Q	Y	59.9	365	4.8
21	2018	Bu	Fe	12	0.52	Q	Y	50.7	205	6.4
22	2018	Bu	Fe	1	0.52	Q	Y	59	285	5.6
23	2018	Bu	Fe	0	0.52	Q	Y	47.8	150	7.5
24	2018	Bu	Fe	3	0.52	Q	Y	64.2	475	4
25	2018	Bu	Fe	0	0.52	Q	Y	36.1	90	19.7
26	2018	Bu	Fe	0	0.52	Q	Y	35.4	90	16.5
27	2018	Bu	Fe	9	0.52	Q	Y	55.8	285	27.2
28	2018	Bu	Fe	1	0.52	Q	Y	46.5	230	22.8
29	2018	Bu	Fe	3	0.52	Q	Y	51.1	235	20.9
30	2018	Bu	Fu	0	0.52	Q	Y	33.2	65	18.7
31	2018	Bu	Fu	0	0.52	Q	Y	43.2	140	7.2
32	2018	Bu	Fu	1	0.52	Q	Y	54.2	250	23.3

33	2018	Bu	Fu	0	0.52	Q	Y	37.6	85	29.4
34	2018	Bu	Fu	0	0.52	Q	Y	35.8	75	18.5
35	2018	Bu	Fu	13	0.52	Q	Y	52.1	225	8.2
36	2019	Bu	Fe	7	0.67	W and Q	Y	52.4	245	5.5
37	2019	Bu	Fe	3	0.67	W and Q	Y	41.3	105	13.8
38	2019	Bu	Fe	3	0.67	W and Q	Y	45.3	190	34.2
39	2019	Bu	Fe	1	0.67	W and Q	Y	41.8	115	7.8
40	2019	Bu	Fe	0	0.67	W and Q	Y	51.8	160	19.4
41	2019	Bu	Fe	13	0.67	W and Q	Y	31.2	50	6.9
42	2019	Bu	Fe	1	0.67	W and Q	Y	34.1	75	21.9
43	2019	Bu	Fe	24	0.67	W and Q	Y	39.6	90	21.9
44	2019	Bu	Fe	1	0.67	W and Q	Y	58.2	265	6.1
45	2019	Bu	Fe	0	0.67	W and Q	Y	51.3	260	28.9
46	2019	Bu	Fe	9	0.67	W and Q	Y	39.7	100	12.4
47	2019	Bu	Fe	7	0.67	W and Q	Y	33.7	75	21.8
48	2019	Bu	Fu	0	0.67	W and Q	Y	32	40	18.7
49	2019	Bu	Fu	1	0.67	W and Q	Y	35.9	85	7.15
50	2019	Bu	Fu	0	0.67	W and Q	Y	38.4	75	18.6
51	2019	Bu	Fu	0	0.67	W and Q	Y	38.3	95	7.8

52	2019	Bu	Fu	0	0.67	W and Q	Y	49.4	175	6.8
53	2019	Bu	Fu	4	0.67	W and Q	Y	41.7	170	6.4
54	2019	Bu	Fu	4	0.67	W and Q	Y	31.5	45	22.2
55	2019	Bu	Fu	4	0.67	W and Q	Y	35.9	75	9
56	2019	Bu	Fu	0	0.67	W and Q	Y	34.9	80	26.4
57	2019	Bu	Fu	4	0.67	W and Q	Y	34.1	90	24.8
58	2019	Bu	Fu	0	0.67	W and Q	Y	40.1	110	8
59	2019	Bu	Fu	10	0.67	W and Q	Y	N/A	N/A	N/A
60	2019	Bu	Fu	2	0.67	W and Q	Y	N/A	N/A	N/A
61	2019	Bu	Fe	0	0.67	W and Q	Y	N/A	N/A	N/A
62	2019	Bu	Fe	0	0.67	W and Q	Y	N/A	N/A	N/A
63	2019	Bu	Fu	6	0.67	W and Q	Y	64.5	465	5
64	2019	Bu	Fe	13	0.85	W	S	42,7	185	18.8
65	2019	Bu	Fe	0	0.85	W	S	38,5	105	22.7
66	2019	Bu	Fe	16	0.85	W	S	46,8	190	22
67	2019	Bu	Fe	48	0.85	W	S	50.7	215	20.2
68	2019	Bu	Fe	15	0.85	W	S	48.4	190	22.9
69	2019	Bu	Fe	4	0.85	W	S	51.6	210	22.9
70	2019	Bu	Fe	2	0.85	W	S	58.1	330	22.4

71	2019	Bu	Fe	9	0.85	W	S	31.5	50	22.5
72	2019	Bu	Fe	5	0.85	W	S	47.3	185	21.9
73	2019	Bu	Fe	4	0.85	W	S	51	230	23.3
74	2019	Bu	Fe	6	0.85	W	S	45.6	200	21.8
75	2019	Bu	Fe	43	0.85	W	S	51.2	215	19.2
76	2019	Bu	Fe	0	0.85	W	S	46.4	205	23
77	2019	Bu	Fe	0	0.85	W	S	43.6	165	27.6
78	2019	Bu	Fe	13	0.85	W	S	47.2	195	21.1
79	2019	Bu	Fe	14	0.85	W	S	47.4	190	24
80	2019	Bu	Fe	15	0.85	W	S	47.3	175	26.7
81	2019	Bu	Fe	3	0.85	W	S	40.9	130	24.3
82	2019	Bu	Fe	3	0.85	W	S	38.2	110	27.3
83	2019	Bu	Fe	6	0.85	W	S	49.7	250	24.3
84	2019	Bu	Fe	14	0.85	W	S	46.6	175	23.2
85	2019	Bu	Fe	9	0.85	W	S	42.4	145	25.6
86	2019	Bu	Fe	0	0.85	W	S	35.3	85	29.7
87	2019	Bu	Fe	6	0.85	W	S	44.2	175	20.7
88	2019	Bu	Fe	10	0.85	W	S	37.4	80	29.6
89	2019	Bu	Fe	3	0.85	W	S	38.8	100	26.5

90	2019	Bu	Fe	46	0.85	W	S	48.2	215	20.1
91	2018	N_Ir	Ne	3	0.68	Q	Y	57.1	340	N/A
92	2018	N_Ir	Ne	0	0.68	Q	Y	57.9	450	N/A
93	2018	N_Ir	Ne	0	0.68	Q	Y	61.3	370	N/A
94	2018	N_Ir	Ne	1	0.68	Q	Y	65.8	550	N/A
95	2018	N_Ir	Ne	4	0.68	Q	Y	48.7	230	N/A
96	2018	N_Ir	Ne	4	0.68	Q	Y	52.7	280	N/A
97	2018	N_Ir	Ne	3	0.68	Q	Y	47.9	250	N/A
98	2018	N_Ir	Ne	4	0.68	Q	Y	54	280	N/A
99	2018	N_Ir	Ne	5	0.68	Q	Y	58.2	410	N/A
100	2018	N_Ir	Ne	4	0.68	Q	Y	46.4	210	N/A
101	2018	N_Ir	Ne	0	0.68	Q	Y	48.2	230	N/A
102	2018	N_Ir	Ne	0	0.68	Q	Y	56.2	380	N/A
103	2018	N_Ir	Ne	1	0.68	Q	Y	55.7	350	N/A
104	2018	N_Ir	Ne	1	0.68	Q	Y	61.2	340	N/A
105	2018	N_Ir	Ne	0	0.68	Q	Y	51.2	280	N/A
106	2018	N_Ir	Ne	0	0.68	Q	Y	61.8	400	N/A
107	2018	N_Ir	Ne	0	0.68	Q	Y	49.1	270	N/A
108	2018	N_Ir	Ne	1	0.68	Q	Y	47.6	210	N/A

109	2018	N_Ir	Ne	4	0.68	Q	Y	50.7	250	N/A
110	2018	N_Ir	Ne	0	0.68	Q	Y	48.6	205	N/A
111	2018	N_Ir	Ne	2	0.68	Q	Y	50.1	280	N/A
112	2018	N_Ir	Ne	0	0.68	Q	Y	63.3	500	N/A
113	2018	N_Ir	Ne	7	0.68	Q	Y	52.2	250	N/A
114	2018	N_Ir	Ne	1	0.68	Q	Y	55.6	310	N/A
115	2018	N_Ir	Ne	4	0.68	Q	Y	52.5	270	N/A
116	2018	N_Ir	Ne	3	0.68	Q	Y	46.7	190	N/A
117	2018	N_Ir	Ne	2	0.68	Q	Y	48.7	210	N/A
118	2018	N_Ir	Ne	14	0.68	Q	Y	46	180	N/A
119	2018	N_Ir	Ne	11	0.68	Q	Y	40.9	150	N/A
120	2018	N_Ir	Ne	0	0.68	Q	Y	48.3	150	N/A
121	2018	N_Ir	Ne	6	0.68	Q	Y	58.6	350	N/A
122	2018	N_Ir	Ne	12	0.68	Q	Y	46.8	180	N/A
123	2018	N_Ir	Ne	9	0.68	Q	Y	60.8	410	N/A
124	2018	N_Ir	Ne	0	0.68	Q	Y	50	285	N/A
125	2018	N_Ir	Ne	1	0.68	Q	Y	48.2	180	N/A
126	2018	N_Ir	Ne	1	0.68	Q	Y	41.9	140	N/A
127	2018	N_Ir	Ne	0	0.68	Q	Y	44.8	160	N/A

128	2018	N_Ir	Ne	4	0.68	Q	Y	44.9	165	N/A
129	2018	N_Ir	Ne	0	0.68	Q	Y	45.9	130	N/A
130	2018	N_Ir	Ne	3	0.68	Q	Y	46.2	200	N/A
131	2018	N_Ir	Ne	6	0.68	Q	Y	61	N/A	N/A

Supplementary material 2.2. DNA extraction protocol from Whatman qualitative filter paper No. 1

1. Prepare a 1cm^2 cut of Whatman qualitative filter paper No. 1 in sterile condition
2. Deposit a drop of collected faecal material on the paper
3. Let air dry for approx. 5 min at room temperature
4. The piece can now be stored in -80◦C for long preservation or directly used to continue the extraction
5. Transfer each cut into a separate 1.5 ml Eppendorf and label with sample name
6. Add with 100 µl of FTA Purification Reagent
7. Incubate 5 min toom temperature
8. Remove the reagent and rinse with 200 µl of TE buffer
9. Remove carefully all TE buffer
10. Add 14 µl of Solution 1
11. Incubate at room temperature for 5 mins
12. Add 26 µl of Solution 2 to each Eppendorf
13. Incubate room temperature for 10 mins
14. Shake or votex for 10 sec
15. Centrifuge for 20 sec at 2000 rpm
16. Transfer 40 µl in a new sterile Eppendorf consisting in your final eluted DNA

Elution solutions

SOLUTION 1: 0.1N NaOH, 0.3mM EDTA, pH 13.0

- Start with 50ml of stock 0.5M EDTA pH 8.0. Add solid NaOH slowly until you reach pH 13. Make up to 250ml. This is now 0.1M EDTA pH13.
- Make up 0.5M NaOH (20g of NaOH per 1 litre)

- Add 200ml of 0.5M NaOH, 3ml 0.1M EDTA pH13, 797 ml H20.

SOLUTION 2: 0.1M Tris-HCl, pH7.0

- Dissolve 12.1g of anhydrous Tris in less than a litre. pH using HCl to 7.0 and make up to a litre.

Supplementary material 2.3. DNA concentration measured with Thermo Scientific™ NanoDrop 2000 for each faecal samples extracted with Qiagen method.

Eel	Name	Year	Concentration [ng/µl]	260/280	260/230
1	Ang17_0050	2017	2.7	1.06	1.09
2	Ang17_0051	2017	4.1	4.4	0.68
3	Ang17_0052	2017	6.2	2.01	0.41
4	Ang17_0053	2017	6.3	2.04	0.54
5	Ang17_0059	2017	5.1	10.6	0.56
6	Ang17_0062	2017	2	1.78	0.31
7	Ang17_0079	2017	23.2	1.81	2.04
8	Ang17_0080	2017	31	5.76	0.78
9	Ang17_0081	2017	5.3	1.51	0.45
10	Ang17_0082	2017	4.1	3.05	0.41
11	Ang17_0083	2017	6	3.15	0.68
12	Ang17_0085	2017	5.5	0.71	0.91
13	ANG18_1000	2018	1.5	3.82	1.01

14	ANG18_1001	2018	2.4	0.69	0.5
15	ANG18_1002	2018	0.2	0.78	0.81
16	ANG18_1003	2018	1.8	1.02	0.74
17	ANG18_1004	2018	1.4	0.22	1.05
18	ANG18_1005	2018	0.4	1.24	2.7
19	ANG18_1006	2018	1.4	0.78	0.32
20	ANG18_1007	2018	2.6	1.83	1.75
21	ANG18_1008	2018	4.3	0.53	0.9
22	ANG18_1009	2018	3	1.9	1.57
23	ANG18_1010	2018	2.5	2.73	7.32
24	ANG18_1011	2018	1.1	0.43	0.89
25	ANG18_1012	2018	3.2	1.92	1.43
26	ANG18_1013	2018	3.3	1.48	3.87
27	ANG18_1018	2018	12.4	1.9	1.84
28	ANG18_1019	2018	0.6	0.33	0.76
29	ANG18_1020	2018	0.8	0.69	0.94
30	ANG18_1023	2018	5.3	1.24	1.89
31	ANG18_1024	2018	20.3	1.65	2.65
32	ANG18_1025	2018	7.2	1.83	3.57

33	ANG18_1029	2018	0.8	1.79	2.95
34	ANG18_1030	2018	0.8	2.75	1.46
35	ANG18_1034	2018	1	0.46	0.71
36	ANG19_40	2019	2.6	2.36	2.45
37	ANG19_41	2019	0.8	0.92	0.41
38	ANG19_42	2019	0.3	0.9	0.81
39	ANG19_43	2019	0.5	0.89	0.88
40	ANG19_44	2019	2.9	0.47	1.62
41	ANG19_45	2019	3.8	1.78	1.43
42	ANG19_46	2019	0.2	2.3	2.54
43	ANG19_47	2019	0.9	2.71	4.34
44	ANG19_48	2019	17.3	7.31	1.98
45	ANG19_49	2019	2.7	0.44	6.41
46	ANG19_50	2019	14.1	1.36	1.82
47	ANG19_51	2019	0.5	0.77	0.38
48	ANG19_63	2019	2.4	0.91	1.43
49	ANG19_64	2019	0.4	1.76	1.1
50	ANG19_65	2019	15.2	3.54	4.56
51	ANG19_66	2019	7.4	2.2	1.9

52	ANG19_67	2019	1.3	1.21	1.23
53	ANG19_68	2019	1.2	1.91	1.21
54	ANG19_69	2019	1.3	1.08	1.01
55	ANG19_70	2019	0.7	0.53	0.71
56	ANG19_71	2019	1.2	1.31	1.45
57	ANG19_72	2019	1.6	1.2	1.32
58	ANG19_73	2019	3.3	2.21	4.4
59	ANG19_74	2019	3.7	0.45	0.43
60	NE2018_1	2018N	84	1.96	1.73
61	NE2018_2	2018N	153	2.03	1.88
62	NE2018_3	2018N	19	0.86	0.39
63	NE2018_4	2018N	74	1.91	1.92
64	NE2018_5	2018N	10.2	1.57	8.32
65	NE2018_6	2018N	73.5	1.77	2.52
66	NE2018_7	2018N	5.6	1.37	2.27
67	NE2018_8	2018N	5.3	1.83	0.53
68	NE2018_9	2018N	3.3	1.53	3.62
69	NE2018_10	2018N	58.7	1.57	0.35
70	NE2018_11	2018N	10.3	1.96	1.75

71	NE2018_12	2018N	14.8	1.75	4.28
72	NE2018_13	2018N	18.6	1.87	3.28
73	NE2018_14	2018N	47.2	1.97	1.86
74	NE2018_15	2018N	22.9	1.65	3.62
75	NE2018_16	2018N	68.2	1.82	1.87
76	NE2018_17	2018N	40.1	2.01	1.45
77	NE2018_18	2018N	12.1	2.5	1.74
78	NE2018_19	2018N	43.5	2.41	3.62
79	NE2018_20	2018N	65.4	1.03	2.7
80	NE2018_21	2018N	0.9	0.76	1.73
81	NE2018_22	2018N	1.4	0.91	0.77
82	NE2018_23	2018N	3.2	1.43	1.23
83	NE2018_24	2018N	19.7	1.54	1.9
84	NE2018_25	2018N	67.4	1.62	2.21
85	NE2018_26	2018N	43.7	1.73	2.4
86	NE2018_27	2018N	92.1	1.98	4.21
87	NE2018_28	2018N	8.2	2.9	2.5
88	NE2018_29	2018N	41.1	0.43	0.66
89	NE2018_30	2018N	16.4	0.96	0.9

90	NE2018_31	2018N	74.2	2.98	3.81
91	NE2018_32	2018N	32.4	2.75	0.57
92	NE2018_33	2018N	9.3	1.93	2.04
93	NE2018_34	2018N	13.3	1.95	4.21
94	NE2018_35	2018N	0.3	1.43	1.76
95	NE2018_36	2018N	75.4	1.89	1.5
96	NE2018_37	2018N	6.4	2.7	1.33
97	NE2018_38	2018N	92.3	2.35	4.43
98	NE2018_39	2018N	65.5	2.91	0.31
99	NE2018_40	2018N	21.4	2.08	2.57
101	NE2018_41	2018N	5.4	0.54	0.65

Appendix 2: Chapter 3 Supplementary materials

Supplementary material 3.1. European eel sample collection for head picture digitalization.

ID	Year	life stage	Country	Lake	Water
ANG17_FE_18	2017	Yellow	Ireland	Feeagh	Freshwater
ANG17_FE_19	2017	Yellow	Ireland	Feeagh	Freshwater
ANG17_FE_20	2017	Yellow	Ireland	Feeagh	Freshwater

ANG17_FE_21	2017	Yellow	Ireland	Feeagh	Freshwater
ANG17_FE_22	2017	Yellow	Ireland	Feeagh	Freshwater
ANG17_FE_23	2017	Yellow	Ireland	Feeagh	Freshwater
ANG17_FE_24	2017	Yellow	Ireland	Feeagh	Freshwater
ANG17_FE_25	2017	Yellow	Ireland	Feeagh	Freshwater
ANG17_FE_26	2017	Yellow	Ireland	Feeagh	Freshwater
ANG17_FE_27	2017	Yellow	Ireland	Feeagh	Freshwater
ANG17_FE_28	2017	Yellow	Ireland	Feeagh	Freshwater
ANG17_FE_29	2017	Yellow	Ireland	Feeagh	Freshwater
ANG17_FE_30	2017	Yellow	Ireland	Feeagh	Freshwater
ANG17_FE_31	2017	Yellow	Ireland	Feeagh	Freshwater
ANG17_FE_32	2017	Yellow	Ireland	Feeagh	Freshwater
ANG17_FE_33	2017	Yellow	Ireland	Feeagh	Freshwater
ANG17_FE_34	2017	Yellow	Ireland	Feeagh	Freshwater
ANG17_FE_35	2017	Yellow	Ireland	Feeagh	Freshwater
ANG17_FE_36	2017	Yellow	Ireland	Feeagh	Freshwater
ANG17_FE_37	2017	Yellow	Ireland	Feeagh	Freshwater
ANG17_FE_38	2017	Yellow	Ireland	Feeagh	Freshwater
ANG17_FE_39	2017	Yellow	Ireland	Feeagh	Freshwater

ANG18_FE_71	2018	Yellow	Ireland	Feeagh	Freshwater
ANG18_FE_72	2018	Yellow	Ireland	Feeagh	Freshwater
ANG18_FE_73	2018	Yellow	Ireland	Feeagh	Freshwater
ANG18_FE_74	2018	Yellow	Ireland	Feeagh	Freshwater
ANG18_FE_77	2018	Yellow	Ireland	Feeagh	Freshwater
ANG18_FE_78	2018	Yellow	Ireland	Feeagh	Freshwater
ANG18_FE_79	2018	Yellow	Ireland	Feeagh	Freshwater
ANG18_FE_80	2018	Yellow	Ireland	Feeagh	Freshwater
ANG18_FE_81	2018	Yellow	Ireland	Feeagh	Freshwater
ANG18_FE_82	2018	Yellow	Ireland	Feeagh	Freshwater
ANG18_FE_83	2018	Yellow	Ireland	Feeagh	Freshwater
ANG18_FE_84	2018	Yellow	Ireland	Feeagh	Freshwater
ANG18_FE_85	2018	Yellow	Ireland	Feeagh	Freshwater
ANG18_FE_86	2018	Yellow	Ireland	Feeagh	Freshwater
ANG18_FE_87	2018	Yellow	Ireland	Feeagh	Freshwater
ANG18_FE_88	2018	Yellow	Ireland	Feeagh	Freshwater
ANG18_FE_89	2018	Yellow	Ireland	Feeagh	Freshwater
ANG18_FE_90	2018	Yellow	Ireland	Feeagh	Freshwater
ANG18_FE_92	2018	Yellow	Ireland	Feeagh	Freshwater

ANG18_FE_93	2018	Yellow	Ireland	Feeagh	Freshwater
ANG18_FE_94	2018	Yellow	Ireland	Feeagh	Freshwater
ANG18_FE_96	2018	Yellow	Ireland	Feeagh	Freshwater
ANG18_FE_105	2018	Yellow	Ireland	Feeagh	Freshwater
ANG18_FE_106	2018	Yellow	Ireland	Feeagh	Freshwater
ANG18_FE_107	2018	Yellow	Ireland	Feeagh	Freshwater
ANG18_FE_108	2018	Yellow	Ireland	Feeagh	Freshwater
ANG18_FE_109	2018	Yellow	Ireland	Feeagh	Freshwater
ANG18_FE_110	2018	Yellow	Ireland	Feeagh	Freshwater
ANG18_FE_111	2018	Yellow	Ireland	Feeagh	Freshwater
ANG18_FE_112	2018	Yellow	Ireland	Feeagh	Freshwater
ANG18_FE_113	2018	Yellow	Ireland	Feeagh	Freshwater
ANG18_FE_114	2018	Yellow	Ireland	Feeagh	Freshwater
ANG19_FE_1000	2019	Yellow	Ireland	Feeagh	Freshwater
ANG19_FE_1001	2019	Yellow	Ireland	Feeagh	Freshwater
ANG19_FE_1002	2019	Yellow	Ireland	Feeagh	Freshwater
ANG19_FE_1003	2019	Yellow	Ireland	Feeagh	Freshwater
ANG19_FE_1004	2019	Yellow	Ireland	Feeagh	Freshwater
ANG19_FE_1005	2019	Yellow	Ireland	Feeagh	Freshwater

ANG19_FE_1006	2019	Yellow	Ireland	Feeagh	Freshwater
ANG19_FE_1007	2019	Yellow	Ireland	Feeagh	Freshwater
ANG19_FE_1008	2019	Yellow	Ireland	Feeagh	Freshwater
ANG19_FE_1009	2019	Yellow	Ireland	Feeagh	Freshwater
ANG19_FE_1010	2019	Yellow	Ireland	Feeagh	Freshwater
ANG19_FE_1011	2019	Yellow	Ireland	Feeagh	Freshwater
ANG19_FE_1012	2019	Yellow	Ireland	Feeagh	Freshwater
ANG19_FE_1013	2019	Yellow	Ireland	Feeagh	Freshwater
ANG19_FE_1014	2019	Yellow	Ireland	Feeagh	Freshwater
ANG19_FE_1015	2019	Yellow	Ireland	Feeagh	Freshwater
ANG19_FE_1016	2019	Yellow	Ireland	Feeagh	Freshwater
ANG19_FE_1017	2019	Yellow	Ireland	Feeagh	Freshwater
ANG19_FE_1018	2019	Yellow	Ireland	Feeagh	Freshwater
ANG19_FE_1019	2019	Yellow	Ireland	Feeagh	Freshwater
ANG19_FE_1020	2019	Yellow	Ireland	Feeagh	Freshwater
ANG19_FE_1021	2019	Yellow	Ireland	Feeagh	Freshwater
ANG19_FE_1022	2019	Yellow	Ireland	Feeagh	Freshwater
ANG19_FE_1023	2019	Yellow	Ireland	Feeagh	Freshwater
ANG19_FE_1024	2019	Yellow	Ireland	Feeagh	Freshwater

ANG19_FE_1025	2019	Yellow	Ireland	Feeagh	Freshwater
ANG19_FE_1026	2019	Yellow	Ireland	Feeagh	Freshwater
ANG19_FE_1027	2019	Yellow	Ireland	Feeagh	Freshwater
ANG19_FE_1028	2019	Yellow	Ireland	Feeagh	Freshwater
ANG19_FE_1029	2019	Yellow	Ireland	Feeagh	Freshwater
ANG19_FE_1030	2019	Yellow	Ireland	Feeagh	Freshwater
ANG19_FE_1031	2019	Yellow	Ireland	Feeagh	Freshwater
ANG19_FE_1032	2019	Yellow	Ireland	Feeagh	Freshwater
ANG19_FE_1033	2019	Yellow	Ireland	Feeagh	Freshwater
ANG19_FE_1034	2019	Yellow	Ireland	Feeagh	Freshwater
ANG19_FE_1035	2019	Yellow	Ireland	Feeagh	Freshwater
ANG19_FE_1036	2019	Yellow	Ireland	Feeagh	Freshwater
ANG19_FE_1037	2019	Yellow	Ireland	Feeagh	Freshwater
ANG19_FE_1038	2019	Yellow	Ireland	Feeagh	Freshwater
ANG19_FE_1039	2019	Yellow	Ireland	Feeagh	Freshwater
ANG19_FE_1040	2019	Yellow	Ireland	Feeagh	Freshwater
ANG19_FE_1041	2019	Yellow	Ireland	Feeagh	Freshwater
ANG19_FE_1042	2019	Yellow	Ireland	Feeagh	Freshwater
ANG19_FE_1043	2019	Yellow	Ireland	Feeagh	Freshwater

ANG19_FE_1044	2019	Yellow	Ireland	Feeagh	Freshwater
ANG19_FE_1045	2019	Yellow	Ireland	Feeagh	Freshwater
ANG19_FE_1046	2019	Yellow	Ireland	Feeagh	Freshwater
ANG19_FE_1047	2019	Yellow	Ireland	Feeagh	Freshwater
ANG19_FE_1048	2019	Yellow	Ireland	Feeagh	Freshwater
ANG19_FE_1049	2019	Yellow	Ireland	Feeagh	Freshwater
ANG19_FE_1050	2019	Yellow	Ireland	Feeagh	Freshwater
ANG19_FE_1051	2019	Yellow	Ireland	Feeagh	Freshwater
ANG17_FU_1	2017	Yellow	Ireland	Furnace	Brackish
ANG17_FU_10	2017	Yellow	Ireland	Furnace	Brackish
ANG17_FU_11	2017	Yellow	Ireland	Furnace	Brackish
ANG17_FU_2	2017	Yellow	Ireland	Furnace	Brackish
ANG17_FU_3	2017	Yellow	Ireland	Furnace	Brackish
ANG17_FU_4	2017	Yellow	Ireland	Furnace	Brackish
ANG17_FU_5	2017	Yellow	Ireland	Furnace	Brackish
ANG17_FU_6	2017	Yellow	Ireland	Furnace	Brackish
ANG17_FU_7	2017	Yellow	Ireland	Furnace	Brackish
ANG17_FU_8	2017	Yellow	Ireland	Furnace	Brackish
ANG17_FU_9	2017	Yellow	Ireland	Furnace	Brackish

ANG18_FU_42	2018	Yellow	Ireland	Furnace	Brackish
ANG18_FU_21	2018	Yellow	Ireland	Furnace	Brackish
ANG18_FU_46	2018	Yellow	Ireland	Furnace	Brackish
ANG18_FU_49	2018	Yellow	Ireland	Furnace	Brackish
ANG18_FU_62	2018	Yellow	Ireland	Furnace	Brackish
ANG18_FU_72	2018	Yellow	Ireland	Furnace	Brackish
ANG18_FU_75	2018	Yellow	Ireland	Furnace	Brackish
ANG18_FU_56	2018	Yellow	Ireland	Furnace	Brackish
ANG18_FU_60	2018	Yellow	Ireland	Furnace	Brackish
ANG18_FU_58	2018	Yellow	Ireland	Furnace	Brackish
ANG18_FU_33	2018	Yellow	Ireland	Furnace	Brackish
ANG18_FU_71	2018	Yellow	Ireland	Furnace	Brackish
ANG18_FU_39	2018	Yellow	Ireland	Furnace	Brackish
ANG18_FU_68	2018	Yellow	Ireland	Furnace	Brackish
ANG18_FU_50	2018	Yellow	Ireland	Furnace	Brackish
ANG18_FU_59	2018	Yellow	Ireland	Furnace	Brackish
ANG18_FU_41	2018	Yellow	Ireland	Furnace	Brackish
ANG18_FU_26	2018	Yellow	Ireland	Furnace	Brackish
ANG18_FU_48	2018	Yellow	Ireland	Furnace	Brackish

ANG18_FU_19	2018	Yellow	Ireland	Furnace	Brackish
ANG18_FU_44	2018	Yellow	Ireland	Furnace	Brackish
ANG18_FU_16	2018	Yellow	Ireland	Furnace	Brackish
ANG18_FU_55	2018	Yellow	Ireland	Furnace	Brackish
ANG18_FU_29	2018	Yellow	Ireland	Furnace	Brackish
ANG18_FU_65	2018	Yellow	Ireland	Furnace	Brackish
ANG18_FU_31	2018	Yellow	Ireland	Furnace	Brackish
ANG18_FU_32	2018	Yellow	Ireland	Furnace	Brackish
ANG18_FU_70	2018	Yellow	Ireland	Furnace	Brackish
ANG18_FU_69	2018	Yellow	Ireland	Furnace	Brackish
ANG18_FU_22	2018	Yellow	Ireland	Furnace	Brackish
ANG18_FU_13	2018	Yellow	Ireland	Furnace	Brackish
ANG18_FU_64	2018	Yellow	Ireland	Furnace	Brackish
ANG18_FU_52	2018	Yellow	Ireland	Furnace	Brackish
ANG18_FU_38	2018	Yellow	Ireland	Furnace	Brackish
ANG18_FU_25	2018	Yellow	Ireland	Furnace	Brackish
ANG18_FU_54	2018	Yellow	Ireland	Furnace	Brackish
ANG18_FU_27	2018	Yellow	Ireland	Furnace	Brackish
ANG18_FU_45	2018	Yellow	Ireland	Furnace	Brackish

ANG18_FU_40	2018	Yellow	Ireland	Furnace	Brackish
ANG18_FU_37	2018	Yellow	Ireland	Furnace	Brackish
ANG18_FU_14	2018	Yellow	Ireland	Furnace	Brackish
ANG18_FU_12	2018	Yellow	Ireland	Furnace	Brackish
ANG18_FU_24	2018	Yellow	Ireland	Furnace	Brackish
ANG18_FU_23	2018	Yellow	Ireland	Furnace	Brackish
ANG18_FU_28	2018	Yellow	Ireland	Furnace	Brackish
ANG18_FU_63	2018	Yellow	Ireland	Furnace	Brackish
ANG18_FU_35	2018	Yellow	Ireland	Furnace	Brackish
ANG18_FU_15	2018	Yellow	Ireland	Furnace	Brackish
ANG18_FU_61	2018	Yellow	Ireland	Furnace	Brackish
ANG18_FU_73	2018	Yellow	Ireland	Furnace	Brackish
ANG18_FU_34	2018	Yellow	Ireland	Furnace	Brackish
ANG18_FU_43	2018	Yellow	Ireland	Furnace	Brackish
ANG18_FU_18	2018	Yellow	Ireland	Furnace	Brackish
ANG18_FU_67	2018	Yellow	Ireland	Furnace	Brackish
ANG18_FU_53	2018	Yellow	Ireland	Furnace	Brackish
ANG18_FU_17	2018	Yellow	Ireland	Furnace	Brackish
ANG18_FU_30	2018	Yellow	Ireland	Furnace	Brackish

ANG18_FU_47	2018	Yellow	Ireland	Furnace	Brackish
ANG18_FU_51	2018	Yellow	Ireland	Furnace	Brackish
ANG18_FU_36	2018	Yellow	Ireland	Furnace	Brackish
ANG18_FU_20	2018	Yellow	Ireland	Furnace	Brackish
ANG18_FU_57	2018	Yellow	Ireland	Furnace	Brackish
ANG18_FU_74	2018	Yellow	Ireland	Furnace	Brackish
ANG19_FU_1052	2019	Yellow	Ireland	Furnace	Brackish
ANG19_FU_1053	2019	Yellow	Ireland	Furnace	Brackish
ANG19_FU_1054	2019	Yellow	Ireland	Furnace	Brackish
ANG19_FU_1055	2019	Yellow	Ireland	Furnace	Brackish
ANG19_FU_1056	2019	Yellow	Ireland	Furnace	Brackish
ANG19_FU_1057	2019	Yellow	Ireland	Furnace	Brackish
ANG19_FU_1058	2019	Yellow	Ireland	Furnace	Brackish
ANG19_FU_1059	2019	Yellow	Ireland	Furnace	Brackish
ANG19_FU_1060	2019	Yellow	Ireland	Furnace	Brackish
ANG19_FU_1061	2019	Yellow	Ireland	Furnace	Brackish
ANG19_FU_1062	2019	Yellow	Ireland	Furnace	Brackish
ANG19_FU_1063	2019	Yellow	Ireland	Furnace	Brackish
ANG19_FU_1064	2019	Yellow	Ireland	Furnace	Brackish

ANG19_FU_1065	2019	Yellow	Ireland	Furnace	Brackish
ANG19_FU_1066	2019	Yellow	Ireland	Furnace	Brackish
ANG19_FU_1067	2019	Yellow	Ireland	Furnace	Brackish
ANG19_FU_1068	2019	Yellow	Ireland	Furnace	Brackish
ANG19_FU_1069	2019	Yellow	Ireland	Furnace	Brackish
ANG19_FU_1070	2019	Yellow	Ireland	Furnace	Brackish
ANG19_FU_1071	2019	Yellow	Ireland	Furnace	Brackish
ANG19_FU_1072	2019	Yellow	Ireland	Furnace	Brackish
ANG19_FU_1073	2019	Yellow	Ireland	Furnace	Brackish
ANG19_FU_1074	2019	Yellow	Ireland	Furnace	Brackish
ANG19_LOMOND_A_5	2019	Yellow	Scotland	Lomond	Freshwater
ANG19_LOMOND_A_6	2019	Yellow	Scotland	Lomond	Freshwater
ANG19_LOMOND_A_7	2019	Yellow	Scotland	Lomond	Freshwater
ANG19_LOMOND_A_8	2019	Yellow	Scotland	Lomond	Freshwater
ANG19_LOMOND_A_9	2019	Yellow	Scotland	Lomond	Freshwater
ANG19_LOMOND_A_10	2019	Yellow	Scotland	Lomond	Freshwater
ANG19_LOMOND_A_11	2019	Yellow	Scotland	Lomond	Freshwater
ANG19_LOMOND_A_12	2019	Yellow	Scotland	Lomond	Freshwater
ANG19_LOMOND_A_16	2019	Yellow	Scotland	Lomond	Freshwater

ANG19_LOMOND_A_15	2019	Yellow	Scotland	Lomond	Freshwater
ANG19_LOMOND_A_14	2019	Yellow	Scotland	Lomond	Freshwater
ANG19_LOMOND_A_13	2019	Yellow	Scotland	Lomond	Freshwater
ANG19_LOMOND_A_18	2019	Yellow	Scotland	Lomond	Freshwater
ANG19_LOMOND_A_17	2019	Yellow	Scotland	Lomond	Freshwater
ANG19_LOMOND_A_19	2019	Yellow	Scotland	Lomond	Freshwater
ANG19_LOMOND_A_20	2019	Yellow	Scotland	Lomond	Freshwater
ANG19_LOMOND_A_24	2019	Yellow	Scotland	Lomond	Freshwater
ANG19_LOMOND_A_21	2019	Yellow	Scotland	Lomond	Freshwater
ANG19_LOMOND_A_22	2019	Yellow	Scotland	Lomond	Freshwater
ANG19_LOMOND_A_23	2019	Yellow	Scotland	Lomond	Freshwater
ANG19_LOMOND_A_25	2019	Yellow	Scotland	Lomond	Freshwater
ANG19_LOMOND_A_26	2019	Yellow	Scotland	Lomond	Freshwater
ANG19_LOMOND_A_27	2019	Yellow	Scotland	Lomond	Freshwater
ANG19_LOMOND_A_28	2019	Yellow	Scotland	Lomond	Freshwater
ANG19_LOMOND_J_1	2019	Yellow	Scotland	Lomond	Freshwater
ANG19_LOMOND_J_2	2019	Yellow	Scotland	Lomond	Freshwater
ANG19_LOMOND_J_3	2019	Yellow	Scotland	Lomond	Freshwater
ANG19_LOMOND_J_4	2019	Yellow	Scotland	Lomond	Freshwater

ANG19_LOMOND_J_5	2019	Yellow	Scotland	Lomond	Freshwater
ANG19_LOMOND_J_6	2019	Yellow	Scotland	Lomond	Freshwater
ANG19_LOMOND_J_7	2019	Yellow	Scotland	Lomond	Freshwater
ANG19_LOMOND_J_8	2019	Yellow	Scotland	Lomond	Freshwater
ANG19_LOMOND_J_9	2019	Yellow	Scotland	Lomond	Freshwater
ANG19_LOMOND_J_10	2019	Yellow	Scotland	Lomond	Freshwater
ANG19_LOMOND_J_11	2019	Yellow	Scotland	Lomond	Freshwater
ANG19_LOMOND_J_12	2019	Yellow	Scotland	Lomond	Freshwater
ANG19_LOMOND_J_13	2019	Yellow	Scotland	Lomond	Freshwater
ANG19_LOMOND_J_14	2019	Yellow	Scotland	Lomond	Freshwater
ANG19_LOMOND_J_15	2019	Yellow	Scotland	Lomond	Freshwater
ANG17_SIL_1	2017	Silver	Ireland	Feeagh	Freshwater
ANG17_SIL_2	2017	Silver	Ireland	Feeagh	Freshwater
ANG17_SIL_3	2017	Silver	Ireland	Feeagh	Freshwater
ANG17_SIL_4	2017	Silver	Ireland	Feeagh	Freshwater
ANG17_SIL_5	2017	Silver	Ireland	Feeagh	Freshwater
ANG17_SIL_6	2017	Silver	Ireland	Feeagh	Freshwater
ANG17_SIL_7	2017	Silver	Ireland	Feeagh	Freshwater
ANG17_SIL_8	2017	Silver	Ireland	Feeagh	Freshwater

ANG17_SIL_9	2017	Silver	Ireland	Feeagh	Freshwater
ANG17_SIL_10	2017	Silver	Ireland	Feeagh	Freshwater
ANG17_SIL_11	2017	Silver	Ireland	Feeagh	Freshwater
ANG17_SIL_12	2017	Silver	Ireland	Feeagh	Freshwater
ANG17_SIL_13	2017	Silver	Ireland	Feeagh	Freshwater
ANG17_SIL_14	2017	Silver	Ireland	Feeagh	Freshwater
ANG17_SIL_15	2017	Silver	Ireland	Feeagh	Freshwater
ANG17_SIL_17	2017	Silver	Ireland	Feeagh	Freshwater
ANG17_SIL_18	2017	Silver	Ireland	Feeagh	Freshwater
ANG17_SIL_19	2017	Silver	Ireland	Feeagh	Freshwater
ANG17_SIL_20	2017	Silver	Ireland	Feeagh	Freshwater
ANG17_SIL_21	2017	Silver	Ireland	Feeagh	Freshwater
ANG17_SIL_22	2017	Silver	Ireland	Feeagh	Freshwater
ANG19_SIL_6	2019	Silver	Ireland	Feeagh	Freshwater
ANG19_SIL_7	2019	Silver	Ireland	Feeagh	Freshwater
ANG19_SIL_4	2019	Silver	Ireland	Feeagh	Freshwater
ANG19_SIL_5	2019	Silver	Ireland	Feeagh	Freshwater
ANG19_SIL_8	2019	Silver	Ireland	Feeagh	Freshwater
ANG19_SIL_9	2019	Silver	Ireland	Feeagh	Freshwater

ANG19_SIL_10	2019	Silver	Ireland	Feeagh	Freshwater
ANG19_SIL_11	2019	Silver	Ireland	Feeagh	Freshwater
ANG19_SIL_13	2019	Silver	Ireland	Feeagh	Freshwater
ANG19_SIL_14	2019	Silver	Ireland	Feeagh	Freshwater
ANG19_SIL_15	2019	Silver	Ireland	Feeagh	Freshwater
ANG19_SIL_16	2019	Silver	Ireland	Feeagh	Freshwater
ANG19_SIL_17	2019	Silver	Ireland	Feeagh	Freshwater
ANG19_SIL_18	2019	Silver	Ireland	Feeagh	Freshwater
ANG19_SIL_19	2019	Silver	Ireland	Feeagh	Freshwater
ANG19_SIL_20	2019	Silver	Ireland	Feeagh	Freshwater
ANG19_SIL_21	2019	Silver	Ireland	Feeagh	Freshwater
ANG19_SIL_22	2019	Silver	Ireland	Feeagh	Freshwater
ANG19_SIL_23	2019	Silver	Ireland	Feeagh	Freshwater
ANG19_SIL_24	2019	Silver	Ireland	Feeagh	Freshwater
ANG19_SIL_25	2019	Silver	Ireland	Feeagh	Freshwater
ANG19_SIL_26	2019	Silver	Ireland	Feeagh	Freshwater
ANG19_SIL_27	2019	Silver	Ireland	Feeagh	Freshwater
ANG19_SIL_31	2019	Silver	Ireland	Feeagh	Freshwater
ANG19_SIL_29	2019	Silver	Ireland	Feeagh	Freshwater

ANG19_SIL_30	2019	Silver	Ireland	Feeagh	Freshwater
ANG19_SIL_28	2019	Silver	Ireland	Feeagh	Freshwater
ANG17_BUN_1	2017	Yellow	Ireland	Bunaveela	Freshwater
ANG17_BUN_2	2017	Yellow	Ireland	Bunaveela	Freshwater
ANG17_BUN_3	2017	Yellow	Ireland	Bunaveela	Freshwater
ANG17_BUN_4	2017	Yellow	Ireland	Bunaveela	Freshwater
ANG17_BUN_5	2017	Yellow	Ireland	Bunaveela	Freshwater
ANG17_BUN_6	2017	Yellow	Ireland	Bunaveela	Freshwater
ANG17_BUN_7	2017	Yellow	Ireland	Bunaveela	Freshwater
ANG17_BUN_8	2017	Yellow	Ireland	Bunaveela	Freshwater
ANG17_BUN_9	2017	Yellow	Ireland	Bunaveela	Freshwater
ANG17_BUN_10	2017	Yellow	Ireland	Bunaveela	Freshwater
ANG17_BUN_11	2017	Yellow	Ireland	Bunaveela	Freshwater
ANG17_BUN_12	2017	Yellow	Ireland	Bunaveela	Freshwater
ANG17_BUN_13	2017	Yellow	Ireland	Bunaveela	Freshwater
ANG17_BUN_14	2017	Yellow	Ireland	Bunaveela	Freshwater
ANG17_BUN_15	2017	Yellow	Ireland	Bunaveela	Freshwater
ANG17_BUN_16	2017	Yellow	Ireland	Bunaveela	Freshwater
ANG17_BUN_17	2017	Yellow	Ireland	Bunaveela	Freshwater

Appendix 3: Chapter 4 Supplementary materials

Supplementary material 4.1. Yellow eel collection in UK for chapter 4. Location: LL = Loch Lomond; Month: Aug = August; Water: FW = Freshwater; Life stage: Y = Yellow.

Name	Location	Month	Nation	Life stage	Water	Weight	Length	CF	Infected	Infection rate
ANG19_LOMOND_A_5	LL	Aug	Scot	Y	FW	505	65	0.193	Yes	0.58
ANG19_LOMOND_A_6	LL	Aug	Scot	Y	FW	210	53.3	0.145	No	0.58
ANG19_LOMOND_A_7	LL	Aug	Scot	Y	FW	190	48.9	0.162	Yes	0.58
ANG19_LOMOND_A_8	LL	Aug	Scot	Y	FW	110	42.8	0.159	Yes	0.58
ANG19_LOMOND_A_9	LL	Aug	Scot	Y	FW	305	57.3	0.165	No	0.58
ANG19_LOMOND_A_10	LL	Aug	Scot	Y	FW	550	67.5	0.185	No	0.58
ANG19_LOMOND_A_11	LL	Aug	Scot	Y	FW	435	64.4	0.168	Yes	0.58
ANG19_LOMOND_A_12	LL	Aug	Scot	Y	FW	660	67.3	0.226	Yes	0.58
ANG19_LOMOND_A_13	LL	Aug	Scot	Y	FW	620	67.8	0.202	Yes	0.58
ANG19_LOMOND_A_14	LL	Aug	Scot	Y	FW	270	58.1	0.143	Yes	0.58

ANG19_LOMOND_A_15	LL	Aug	Scot	Y	FW	205	48.6	0.192	No	0.58
ANG19_LOMOND_A_16	LL	Aug	Scot	Y	FW	225	53.2	0.166	No	0.58
ANG19_LOMOND_A_17	LL	Aug	Scot	Y	FW	120	45.6	0.121	Yes	0.58
ANG19_LOMOND_A_18	LL	Aug	Scot	Y	FW	90	36.2	0.19	No	0.58
ANG19_LOMOND_A_19	LL	Aug	Scot	Y	FW	110	41.6	0.153	No	0.58
ANG19_LOMOND_A_20	LL	Aug	Scot	Y	FW	650	67.2	0.217	Yes	0.58
ANG19_LOMOND_A_21	LL	Aug	Scot	Y	FW	365	59.7	0.179	Yes	0.58
ANG19_LOMOND_A_22	LL	Aug	Scot	Y	FW	240	57.7	0.18	No	0.58
ANG19_LOMOND_A_23	LL	Aug	Scot	Y	FW	845	72.8	0.224	Yes	0.58
ANG19_LOMOND_A_24	LL	Aug	Scot	Y	FW	430	63	0.176	Yes	0.58
ANG19_LOMOND_A_26	LL	Aug	Scot	Y	FW	315	54.9	0.193	No	0.58
ANG19_LOMOND_A_27	LL	Aug	Scot	Y	FW	380	54.9	0.23	No	0.58
ANG19_LOMOND_A_28	LL	Aug	Scot	Y	FW	155	44.6	0.18	Yes	0.58

ANG19_LOMOND_A_29	LL	Aug	Scot	Y	FW	115	43.1	0.15	Yes	0.58

Supplementary material 4.2. European eel collection in Ireland for chapter 4. Lake: Fe = Lough Feeagh, Fu = Lough Furnace; Month: Jun = June, Jul = July, Sep = September; Water: FW = Freshwater. BW = Brackish water; Life stage: Y = Yellow, S = Silver.

Name	Lake	Month	Life Stage	Water	Weight	Lean mass	Length	Infected	Parasitic load	Infection rate	Fat
Ang19_1040	Fe	Jun	Y	FW	230	217.35	52.4	Y	7	0.67	5.5
Ang19_1041	Fe	Jun	Y	FW	100	86.2	41.3	Y	3	0.67	13.8
Ang19_1042	Fe	Jun	Y	FW	185	121.73	45.3	Y	1	0.67	34.2
Ang19_1043	Fe	Jun	Y	FW	115	106.03	41.8	Y	3	0.67	7.8
Ang19_1044	Fe	Jun	Y	FW	155	124.93	51.8	N	0	0.67	19.4
Ang19_1045	Fe	Jun	Y	FW	50	46.55	31.2	Y	13	0.67	6.9

Ang19_1046	Fe	Jun	Y	FW	75	58.575	34.1	Y	1	0.67	21.9
Ang19_1047	Fe	Jun	Y	FW	90	70.29	39.6	Y	24	0.67	21.9
Ang19_1048	Fe	Jun	Y	FW	255	239.445	58.2	Y	1	0.67	6.1
Ang19_1049	Fe	Jun	Y	FW	255	181.305	51.3	N	0	0.67	28.9
Ang19_1050	Fe	Jun	Y	FW	96	84.096	39.7	Y	9	0.67	12.4
Ang19_1051	Fe	Jun	Y	FW	70	54.74	33.7	Y	7	0.67	21.8
Ang19_1063	Fu	Jul	Y	BW	45	36.585	32	N	0	0.67	18.7
Ang19_1064	Fu	Jul	Y	BW	80	74.28	35.9	Y	1	0.67	7.15
Ang19_1065	Fu	Jul	Y	BW	75	61.05	38.4	N	0	0.67	18.6
Ang19_1066	Fu	Jul	Y	BW	95	87.59	38.3	N	0	0.67	7.8

Ang19_1067	Fu	Jul	Y	BW	170	158.44	49.4	N	0	0.67	6.8
Ang19_1068	Fu	Jul	Y	BW	175	163.8	41.7	Y	4	0.67	6.4
Ang19_1069	Fu	Jul	Y	BW	45	35.01	31.5	Y	4	0.67	22.2
Ang19_1070	Fu	Jul	Y	BW	70	63.7	35.9	Y	4	0.67	9
Ang19_1071	Fu	Jul	Y	BW	75	55.2	34.9	N	0	0.67	26.4
Ang19_1072	Fu	Jul	Y	BW	80	60.16	34.1	Y	4	0.67	24.8
Ang19_1073	Fu	Jul	Y	BW	100	92	40.1	N	0	0.67	8
Ang19_1074	Fu	Jul	Y	BW	430	408.5	64.5	Y	6	0.67	5
SE2019_04	Fe	Sep	S	FW	215	171.57	50.7	Y	48	0.85	20.2
SE2019_05	Fe	Sep	S	FW	190	146.49	48.4	Y	15	0.85	22.9
SE2019_06	Fe	Sep	S	FW	210	161.91	51.6	Y	4	0.85	22.9

SE2019_07	Fe	Sep	S	FW	330	256.08	58.1	Y	2	0.85	22.4
SE2019_08	Fe	Sep	S	FW	50	38.75	31.5	Y	9	0.85	22.5
SE2019_09	Fe	Sep	S	FW	185	144.485	47.3	Y	5	0.85	21.9
SE2019_10	Fe	Sep	S	FW	230	176.41	51	Y	4	0.85	23.3
SE2019_11	Fe	Sep	S	FW	200	156.4	45.6	Y	6	0.85	21.8
SE2019_12	Fe	Sep	S	FW	215	173.72	51.2	Y	43	0.85	19.2
SE2019_13	Fe	Sep	S	FW	205	157.85	46.4	N	0	0.85	23
SE2019_14	Fe	Sep	S	FW	165	119.46	43.6	N	0	0.85	27.6
SE2019_15	Fe	Sep	S	FW	195	153.855	47.2	Y	13	0.85	21.1
SE2019_16	Fe	Sep	S	FW	190	144.4	47.4	Y	14	0.85	24
SE2019_17	Fe	Sep	S	FW	180	131.94	47.3	Y	15	0.85	26.7
SE2019_18	Fe	Sep	S	FW	130	98.41	40.9	Y	3	0.85	24.3
SE2019_19	Fe	Sep	S	FW	110	79.97	38.2	Y	3	0.85	27.3

SE2019_20	Fe	Sep	S	FW	250	189.25	49.7	Y	6	0.85	24.3
SE2019_21	Fe	Sep	S	FW	175	134.4	46.6	Y	14	0.85	23.2
SE2019_22	Fe	Sep	S	FW	145	107.88	42.4	Y	9	0.85	25.6
SE2019_23	Fe	Sep	S	FW	85	59.755	35.3	N	0	0.85	29.7
SE2019_24	Fe	Sep	S	FW	175	138.775	44.2	Y	6	0.85	20.7
SE2019_25	Fe	Sep	S	FW	80	56.32	37.4	Y	10	0.85	29.6
SE2019_26	Fe	Sep	S	FW	100	73.5	38.8	Y	3	0.85	26.5
SE2019_27	Fe	Sep	S	FW	215	171.785	48.2	Y	46	0.85	20.1

Appendix 4: Chapter 5 Supplementary materials

Supplementary material 5.1: List of bacteria with statistically significant difference in abundance between infected and not infected eels processes with protocol 2.

Bacteria	pvalue	Upregulated
D_5__Tyzzerella 3	6.63E-27	Yes
D_5__Hyphomicrobium	5.06E-24	No
D_5__Aeromonas	1.12E-17	Yes
D_5__hgcI clade	2.03E-17	Yes
D_5__Polaromonas	3.77E-17	No
D_5__Polynucleobacter	7.11E-17	Yes
D_5__Rickettsiella	3.28E-16	No
D_5__Burkholderia-Caballeronia-Paraburkholderia	1.09E-14	Yes
D_5__Deefgea	1.23E-14	Yes
D_5__Bosea	3.74E-12	Yes
D_5__candidate division TM7 bacterium	6.20E-12	No
D_5__Fusobacterium	7.05E-12	Yes
D_5__Lautropia	1.56E-11	Yes
D_5__Haemophilus	1.06E-10	Yes
D_5__Lactobacillus	4.51E-10	Yes
D_5__Limnohabitans	1.20E-09	Yes
D_5__Rhodococcus	1.55E-09	Yes
D_5__Methylotenera	2.02E-09	No
D_5__Leptospira	2.34E-09	Yes
D_5__Photobacterium	6.47E-09	Yes
D_5__Melosira varians	9.43E-09	Yes
D_5__Gemella	1.25E-08	Yes
D_5__Arenimonas	2.48E-08	Yes
D_5__Paracoccus	2.81E-08	Yes
D_5__Moritella	8.67E-08	Yes
D_5__Comamonas	9.84E-08	Yes
D_5__Roseomonas	1.40E-07	Yes
D_5__Arcicella	3.12E-07	No
D_5__Porphyromonas	3.71E-07	Yes
D_5__Flectobacillus	4.51E-07	Yes
D_5__Bergeyella	8.08E-07	Yes
D_5__Epulopiscium	9.90E-07	Yes
D_5__Fluviicola	1.27E-06	Yes
D_5__Candidatus Peribacteria bacterium	1.33E-06	Yes
D_5__Brevibacterium	2.44E-06	Yes
D_5__Pseudarcicella	9.16E-06	Yes
D_5__Mesorhizobium	4.01E-05	Yes
D_5__Lactococcus	4.69E-05	Yes
D_5__Pseudolabrys	7.44E-05	Yes
D_5__Carnobacterium	1.00E-04	Yes
D_5__groundwater metagenome	0.000104838	No
D_5__Enterovibrio	0.000110441	Yes
D_5__Rheinheimera	0.000113333	Yes
D_5__Devosia	0.000148296	Yes
D_5__Malikia	0.000150686	Yes
D_5__Aquabacterium	0.000156243	Yes
D_5__Peptoniphilus	0.000353974	Yes
D_5__Psychrobacter	0.000449643	No
D_5__Lamprocystis	0.00171581	No
D_5__Mycoplasma	0.002527363	Yes
D_5__Sphingobium	0.004967919	No
D_5__Bacillus	0.005028637	No

Supplementary material 5.2: List of bacteria with statistically significant difference in abundance between eels sampled in different lakes and processes with protocol

Bacteria	p value	Upregulated
D_5__Moritella	7.24E-29	Furnace
D_5__hgcI clade	1.01E-28	Feeagh
D_5__Fusobacterium	1.44E-27	Feeagh
D_5__Lactobacillus	1.37E-25	Feeagh
D_5__Limnohabitans	6.31E-23	Furnace
D_5__Carnobacterium	2.09E-22	Feeagh
D_5__Deefgea	6.73E-20	Feeagh
D_5__Arcicella	1.29E-18	Feeagh
D_5__Shewanella	1.87E-18	Furnace
D_5__Burkholderia-Caballeronia-Paraburkholderia	1.72E-17	Furnace
D_5__Rhodococcus	9.73E-15	Feeagh
D_5__Aquabacterium	2.28E-14	Feeagh
D_5__Melosira varians	3.00E-14	Feeagh
D_5__Bacteroides	1.29E-13	Feeagh
D_5__Mucilaginibacter	1.93E-13	Feeagh
D_5__Gemella	3.42E-13	Feeagh
D_5__Haemophilus	4.85E-13	Feeagh
D_5__Pelomonas	2.33E-12	Feeagh
D_5__Arenimonas	2.51E-12	Feeagh
D_5__Leptospira	9.89E-12	Feeagh
D_5__Flectobacillus	3.51E-11	Feeagh
D_5__Marinomonas	8.95E-11	Furnace
D_5__Epulopiscium	2.28E-10	Feeagh
D_5__Bergeyella	3.51E-10	Feeagh
D_5__Candidatus Peribacteria bacterium	3.41E-10	Feeagh
D_5__Roseomonas	6.14E-10	Feeagh
D_5__Pseudorhodobacter	1.07E-09	Furnace
D_5__Tyzzerella 3	3.73E-09	Feeagh
D_5__Agarivorans	9.44E-09	Feeagh
D_5__Frigoribacterium	1.65E-08	Furnace
D_5__candidate division TM7 bacterium	3.24E-08	Furnace
D_5__Lactococcus	5.77E-08	Feeagh
D_5__Sporolactobacillus	8.33E-08	Furnace
D_5__Dolosigranulum	8.15E-08	Furnace
D_5__Mycoplasma	1.14E-07	Feeagh
D_5__Rheinheimera	3.94E-07	Furnace
D_5__Malikia	4.22E-07	Feeagh
D_5__Enterovibrio	5.08E-07	Feeagh
D_5__Curvibacter	5.43E-07	Furnace
D_5__Methylotenera	1.69E-06	Feeagh
D_5__Devosia	2.31E-06	Feeagh
D_5__Ruminococcaceae UCG-014	3.92E-06	Feeagh
D_5__Acinetobacter	1.10E-05	Furnace
D_5__Photobacterium	2.05E-05	Furnace
D_5__groundwater metagenome	2.50E-05	Feeagh
D_5__Bacillus	3.79E-05	Feeagh
D_5__Sphingobium	0.000121	Furnace
D_5__Vibrio	0.000268	Furnace
D_5__Rhodoferax	0.000771	Feeagh
D_5__Polynucleobacter	0.001755	Furnace
D_5__Brevibacterium	0.003616	Feeagh
D_5__Fluviicola	0.008521	Furnace

Bibliography

Aalto, E., Capoccioni, F., Mas, J. T., Schiavina, M., Leone, C., Leo, G. De, & Ciccotti, E. (2016). Quantifying 60 years ofdeclining European eel (Anguilla anguilla L., 1758) fishery yields in Mediterranean coastal lagoons. *ICES Journal OfMarine Science*, *73*, 101–110.

Acou, A., Boury, P., Laffaille, P., Crivelli, A. J., & Feunteun, E. (2005). Towards a standardized characterization of the potentially migrating silver European eel (Anguilla anguilla, L.). *Archiv Fur Hydrobiologie*, *164*(2), 237–255. https://doi.org/10.1127/0003-9136/2005/0164-0237

Adamovsky, O., Buerger, A. N., Wormington, A. M., Ector, N., Griffitt, R. J., Bisesi, J. H., & Martyniuk, C. J. (2018). The gut microbiome and aquatic toxicology: An emerging concept for environmental health. *Environmental Toxicology and Chemistry*, *37*(11), 2758–2775. https://doi.org/10.1002/etc.4249

Adams, A., Thompson, K. D., Morris, D., & Farias, C. (1995). D e v e l o p m e n t and use of m o n o c l o n a l antibody probes for i m m u n o h i s t o c h e m i s t r y , ELISA and IFAT to detect bacterial and parasitic fish p a t h o g e n s. *Fish & Shellfish Immunology (1995)*, 537–547.

Adams, D. C., & Otárola-Castillo, E. (2013). Geomorph: An r package for the collection and analysis of geometric morphometric shape data. *Methods in Ecology and Evolution*, *4*(4), 393–399. https://doi.org/10.1111/2041-210X.12035

Adeolu, M., & Gupta, R. (2014). *Phylogenomics and molecular signatures for the order Neisseriales : Proposal for division of the order Neisseriales into the emended family Neisseriaceae Phylogenomics and molecular signatures for the order Neisseriales : proposal for division of the orde*. *April 2013*. https://doi.org/10.1007/s10482-013-9920-6

Affairs, R. (2018). *Implementation of UK Eel Management Plans Contents* (Issue December). www.gov.uk/defra

Aguilar, A., Álvarez, M. F., Leiro, J. M., & Sanmartín, M. L. (2005a). Parasite populations of the European eel (Anguilla anguilla L.) in the Rivers Ulla and Tea (Galicia, northwest Spain). *Aquaculture*, *249*(1–4), 85–94. https://doi.org/10.1016/j.aquaculture.2005.04.052

Aguilar, A., Álvarez, M. F., Leiro, J. M., & Sanmartín, M. L. (2005b). Parasite populations of the European eel (Anguilla anguilla L.) in the Rivers Ulla and Tea (Galicia, northwest Spain). *Aquaculture*, *249*(1–4), 85–94. https://doi.org/10.1016/j.aquaculture.2005.04.052

Alberdi, A., Aizpurua, O., Bohmann, K., Zepeda-Mendoza, M. L., & Gilbert, M. T. P. (2016). Do Vertebrate Gut Metagenomes Confer Rapid Ecological Adaptation? *Trends in Ecology and Evolution*, *31*(9), 689–699. https://doi.org/10.1016/j.tree.2016.06.008

Alves, J. A., Gunnarsson, T. G., Hayhow, D. B., Appleton, G. F., Potts, P. M., Sutherland, W. J., & Gill, J. A. (2013). Costs, benefits, and fitness consequences of different migratory strategies. *Ecology*, *94*(1), 11–17. https://doi.org/10.1890/12-0737.1

Amin, O. M., Thielen, F., Münderle, M., Taraschewski, H., & Sures, B. (2008). Description of a new echinorhynchid species (acanthocephala) from the European EEL, Anguilla anguilla, in Germany, with a key to species of Acanthocephalus in Europe. *Journal of Parasitology*, *94*(6), 1299–1304. https://doi.org/10.1645/GE-1561.1

Andree, K. B., Rodgers, C. J., Furones, D., & Gisbert, E. (2013). Co-Infection with Pseudomonas anguilliseptica and Delftia acidovorans in the European eel, Anguilla anguilla (L.): A case history of an illegally trafficked protected species. *Journal of Fish Diseases*, *36*(7), 647–656. https://doi.org/10.1111/jfd.12066

Anti Vasemägi, A., Visse, M., & Kisandd, V. (2017). Effect of Environmental Factors and an Emerging Parasitic Disease on Gut Microbiome of Wild Salmonid Fish. *MSphere*, *2*(6), 1–13.

Arai, T. (2014). Do we protect freshwater eels or do we drive them to extinction? *SpringerPlus*, *3*(1), 1–10. https://doi.org/10.1186/2193-1801-3-534

Archer, L. C., Hutton, S. A., Harman, L., Poole, W. R., Gargan, P., Mcginnity, P., & Reed, T. E. (2020). *Metabolic traits in brown trout (Salmo trutta) vary in response to food restriction and intrinsic factors*. *8*(1), 1–17. https://doi.org/10.1093/conphys/coaa096.....
.....
.....
.....

Artacho, P., & Nespolo, R. F. (2009). Natural selection reduces energy metabolism in the garden snail, helix aspersa (Cornu aspersum). *Evolution*, *63*(4), 1044–1050. https://doi.org/10.1111/j.1558-5646.2008.00603.x

Åström, M., & Dekker, W. (2007). When will the eel recover? A full life-cycle model. *ICES Journal of Marine Science*, *64*(7), 1491–1498. https://doi.org/10.1093/icesjms/fsm122

Aubret, F., Shine, R., & Bonnet, X. (2004). Adaptive developmental plasticity in snakes. *Nature*, *431*(7006), 261–262. https://doi.org/10.1038/431261a

Auer, S. K., Salin, K., Rudolf, A. M., Anderson, G. J., & Metcalfe, N. B. (2015). The optimal combination of standard metabolic rate and aerobic scope for somatic growth depends on food availability. *Functional Ecology*, *29*(4), 479–486. https://doi.org/10.1111/1365-2435.12396

Austin, B., & Austin, D. (2007). Bacterial Fish Pathogens: Diseases ofFarmed and Wild Fish. In *Springer*. https://doi.org/10.1007/978-1-4020-6069-4_2

Ayayee, P. A., Kinney, G., Yarnes, C., Larsen, T., Custer, G. F., Van Diepen, L. T. A., & Muñoz-Garcia, A. (2020). Role of the gut microbiome in mediating standard metabolic rate after dietary shifts in the viviparous cockroach, Diploptera punctata. *Journal of Experimental Biology*, *223*(11). https://doi.org/10.1242/jeb.218271

Ayayee, P. A., Ondrejech, A., Keeney, G., & Munõz-Garcia, A. (2018). The role of gut microbiota in the regulation of standard metabolic rate in female Periplaneta americana. *PeerJ*, *2018*(5), 1–22. https://doi.org/10.7717/peerj.4717

Bailey, C., Rubin, A., Strepparava, N., Segner, H., Rubin, J. F., & Wahli, T. (2018). Do fish get wasted? Assessing the influence of effluents on parasitic infection of wild fish. *PeerJ*, *2018*(11), 1–22. https://doi.org/10.7717/peerj.5956

Baillon, L., Oses, J., Pierron, F., Bureau du Colombier, S., Caron, A., Normandeau, E., Lambert, P., Couture, P., Labadie, P., Budzinski, H., Dufour, S., Bernatchez, L., & Baudrimont, M. (2015). Gonadal transcriptome analysis of wild contaminated female European eels during artificial gonad maturation. *Chemosphere*, *139*, 303–309. https://doi.org/10.1016/j.chemosphere.2015.06.007

Bairlein, F., Fritz, J., Scope, A., Schwendenwein, I., Stanclova, G., Dijk, G. Van, Meijer, H. A. J., & Verhulst, S. (2015). *Energy Expenditure and Metabolic Changes of Free-Flying Migrating Northern Bald Ibis*. 1–17. https://doi.org/10.1371/journal.pone.0134433

Bakke, I., Skjermo, J., Vo, T. A., & Vadstein, O. (2013). Live feed is not a major determinant of the microbiota associated with cod larvae (Gadus morhua). *Environmental Microbiology Reports*, *5*(4), 537–548. https://doi.org/10.1111/1758-2229.12042

Balasch, J. C., & Tort, L. (2019). Netting the stress responses in fish. *Frontiers in Endocrinology*, *10*(FEB), 1–12. https://doi.org/10.3389/fendo.2019.00062

Baltazar-Soares, M., Bracamonte, S. E., Bayer, T., Chain, F. J. J., Hanel, R., Harrod, C., & Eizaguirre, C. (2016). Evaluating the adaptive potential of the European eel: is the immunogenetic status recovering? *PeerJ*, *4*, e1868. https://doi.org/10.7717/peerj.1868

Bankevich, A., Nurk, S., Antipov, D., Gurevich, A. A., Dvorkin, M., Kulikov, A. S., Lesin, V. M., Nikolenko, S. I., Pham, S., Prjibelski, A. D., Pyshkin, A. V.,

Sirotkin, A. V., Vyahhi, N., Tesler, G., Alekseyev, M. A., & Pevzner, P. A. (2012). SPAdes: A new genome assembly algorithm and its applications to single-cell sequencing. *Journal of Computational Biology*, *19*(5), 455–477. https://doi.org/10.1089/cmb.2012.0021

Barry, J. (2015). *The Foraging Specialisms , Movement and Migratory Behaviour of the European Eel*. 1–195.

Barry, J., Mcleish, J., Dodd, J. A., Turnbull, J. F., Boylan, P., & Adams, C. E. (2014). Introduced parasite Anguillicola crassus infection significantly impedes swim bladder function in the European eel Anguilla anguilla (L.). *Journal of Fish Diseases*, *37*(10), 921–924. https://doi.org/10.1111/jfd.12215

Barry, J., Newton, M., Dodd, J. A., Hooker, O. E., Boylan, P., Lucas, M. C., & Adams, C. E. (2016). Foraging specialisms influence space use and movement patterns of the European eel Anguilla anguilla. *Hydrobiologia*, *766*(1), 333–348. https://doi.org/10.1007/s10750-015-2466-z

Bass, D., Stentiford, G. D., Wang, H. C., Koskella, B., & Tyler, C. R. (2019). The Pathobiome in Animal and Plant Diseases. *Trends in Ecology and Evolution*, *34*(11), 996–1008. https://doi.org/10.1016/j.tree.2019.07.012

Bastos Gomes, G., Hutson, K. S., Domingos, J. A., Infante Villamil, S., Huerlimann, R., Miller, T. L., & Jerry, D. R. (2019). Parasitic protozoan interactions with bacterial microbiome in a tropical fish farm. *Aquaculture*, *502*, 196–201. https://doi.org/10.1016/j.aquaculture.2018.12.037

Becerra-Jurado, G., Cruikshanks, R., O'Leary, C., Kelly, F., Poole, R., & Gargan, P. (2014a). Distribution, prevalence and intensity of Anguillicola crassus (Nematoda) infection in Anguilla anguilla in the Republic of Ireland. *Journal of Fish Biology*, *84*(4), 1046–1062. https://doi.org/10.1111/jfb.12344

Becerra-Jurado, G., Cruikshanks, R., O'Leary, C., Kelly, F., Poole, R., & Gargan, P. (2014b). Distribution, prevalence and intensity of Anguillicola crassus (Nematoda) infection in Anguilla anguilla in the Republic of Ireland. *Journal of Fish Biology*, *84*(4), 1046–1062. https://doi.org/10.1111/jfb.12344

Beregi, A., Molnár, K., Békési, L., & Székely, C. (1998). Radiodiagnostic method for studying swimbladder inflammation caused by Anguillicola crassus (Nematoda: Dracunculoidea). *Diseases of Aquatic Organisms*, *34*(2), 155–160. https://doi.org/10.3354/dao034155

Berger, C. S., & Aubin-Horth, N. (2018). An eDNA-qPCR assay to detect the presence of the parasite Schistocephalus solidus inside its threespine stickleback host. *Journal of Experimental Biology*, *221*(9). https://doi.org/10.1242/jeb.178137

Bilandžija, H., Hollifield, B., Steck, M., Meng, G., Ng, M., Koch, A. D., Gračan, R., Ćetković, H., Porter, M. L., Renner, K. J., & Jeffery, W. (2020). Phenotypic plasticity as a mechanism of cave colonization and adaptation. *ELife*, *9*, 1–27. https://doi.org/10.7554/eLife.51830

Binning, S. A., Roche, D. G., Layton, C., & Binning, S. A. (2012). *Ectoparasites increase swimming costs in a coral reef fish*.

Bitz-Thorsen, J., Häkli, K., Bhat, S., & Præbel, K. (2019). Allochrony as a potential driver for reproductive isolation in adaptive radiations of European whitefish ecomorphs. *Ecology of Freshwater Fish*.

Boldsen, M. M., Norin, T., & Malte, H. (2013). A Temporal repeatability of metabolic rate and the effect of organ mass and enzyme activity on metabolism in European eel (Anguilla anguilla). *Comparative Biochemistry and Physiology, Part A*, *165*(1), 22–29. https://doi.org/10.1016/j.cbpa.2013.01.027

Bolyen, E., Rideout, J. R., Dillon, M. R., Bokulich, N. A., Abnet, C. C., Al-Ghalith, G. A., Alexander, H., Alm, E. J., Arumugam, M., Asnicar, F., Bai, Y., Bisanz, J. E., Bittinger, K., Brejnrod, A., Brislawn, C. J., Brown, C. T., Callahan, B. J., Caraballo-Rodríguez, A. M., Chase, J., … Caporaso, J. G. (2019). Reproducible, interactive, scalable and extensible microbiome data science using QIIME 2. *Nature Biotechnology*, *37*(8), 852–857. https://doi.org/10.1038/s41587-019-0209-9

Bonneaud, C., Wilson, R. S., & Seebacher, F. (2016). Immune-challenged fish up-regulate their metabolic scope to support locomotion. *PLoS ONE*, *11*(11), 1–14. https://doi.org/10.1371/journal.pone.0166028

Boucher, M. A., Baker, D. W., Brauner, C. J., & Shrimpton, J. M. (2018). The effect of substrate rearing on growth, aerobic scope and physiology of larval white sturgeon Acipenser transmontanus. *Journal of Fish Biology*, *92*(6), 1731–1746. https://doi.org/10.1111/jfb.13611

Bratlie, M., Hagen, I. V., Helland, A., Erchinger, F., Midttun, Ø., Ueland, P. M., Rosenlund, G., Sveier, H., Mellgren, G., Hausken, T., & Gudbrandsen, O. A. (2021). Effects of high intake of cod or salmon on gut microbiota profile, faecal output and serum concentrations of lipids and bile acids in overweight adults: a randomised clinical trial. *European Journal of Nutrition*, *60*(4), 2231–2248. https://doi.org/10.1007/s00394-020-02417-8

Brauner, C. J., Shrimpton, M., & Randall, D. (1996). Effect of Short-Duration Seawater Exposure on Plasma Ion Concentrations and Swimming Performance in Coho Salmon (Oncorhynchus kisutch) Parr. *Can. 9. Fish. Aquat*, *Houston 1959*.

Breau, C., Cunjak, R. A., & Peake, S. J. (2011). Behaviour during elevated water temperatures: Can physiology explain movement of juvenile Atlantic salmon to cool water? *Journal of Animal Ecology*, *80*(4), 844–853. https://doi.org/10.1111/j.1365-2656.2011.01828.x

Bridcut, E. E., & Giller, P. S. (1995). Diet variability and foraging strategies in brown trout (Salmo trutta): an analysis from subpopulations to individuals. *Canadian Journal of Fisheries and Aquatic Sciences*, *52*(12), 2543–2552. https://doi.org/10.1139/f95-845

Burns, A. R., Stephens, W. Z., Stagaman, K., Wong, S., Rawls, J. F., Guillemin, K., & Bohannan, B. J. M. (2016). Contribution of neutral processes to the assembly of gut microbial communities in the zebrafish over host development. *ISME Journal*, *10*(3), 655–664.

https://doi.org/10.1038/ismej.2015.142

Butler, P. J., Green, J. A., Boyd, I. L., & Speakman, J. R. (2004). Measuring metabolic rate in the field: The pros and cons of the doubly labelled water and heart rate methods. *Functional Ecology*, *18*(2), 168–183. https://doi.org/10.1111/j.0269-8463.2004.00821.x

Butt, R. L., & Volkoff, H. (2019). Gut microbiota and energy homeostasis in fish. *Frontiers in Endocrinology*, *10*(JAN), 6–8. https://doi.org/10.3389/fendo.2019.00009

Butts, I. A. E., Sørensen, S. R., Politis, S. N., & Tomkiewicz, J. (2016). First-feeding by European eel larvae: A step towards closing the life cycle in captivity. *Aquaculture*, *464*, 451–458. https://doi.org/10.1016/j.aquaculture.2016.07.028

Caballero, P., Morán, P., & Marco-Rius, F. (2013). A review of the genetic and ecological basis of phenotypic plasticity in brown trout. *Trout: From Physiology to Conservation*, *January*, 9–26.

Cadena, A. M., Ma, Y., Ding, T., Bryant, M., Maiello, P., Geber, A., Lin, P. L., Flynn, J. L., & Ghedin, E. (2018). Profiling the airway in the macaque model of tuberculosis reveals variable microbial dysbiosis and alteration of community structure. *Microbiome*, *6*(1), 1–13. https://doi.org/10.1186/s40168-018-0560-y

Cao, X. Y., Zhao, J. L., Li, C. H., Zhu, S. Q., Hao, Y. Y., Cheng, Y. M., & Wu, H. Y. (2021). Morphological and skeletal comparison and ecological adaptability of Mandarin fish Siniperca chuatsi and big-eye Mandarin fish Siniperca kneri. *Aquaculture and Fisheries*, *6*(5), 455–464. https://doi.org/10.1016/j.aaf.2020.04.007

Carda-Diéguez, M., Ghai, R., Rodríguez-Valera, F., & Amaro, C. (2017). Wild eel microbiome reveals that skin mucus of fish could be a natural niche for aquatic mucosal pathogen evolution. *Microbiome*, *5*(1), 162. https://doi.org/10.1186/s40168-017-0376-1

Cavallero, S., Bruno, A., Arletti, E., Caffara, M., Fioravanti, M. L., Costa, A., Cammilleri, G., Graci, S., Ferrantelli, V., & D'Amelio, S. (2017). Validation of a commercial kit aimed to the detection of pathogenic anisakid nematodes in fish products. *International Journal of Food Microbiology*, *257*(March), 75–79. https://doi.org/10.1016/j.ijfoodmicro.2017.06.011

Cecchini, S., Saroglia, M., Terova, G., & Albanesi, F. (2001). Detection of antibody response against Amyloodinium ocellatum (Brown, 1931) in serum of naturally infected European sea bass by an enzyme-linked immunosorbent assay (ELISA). *Bulletin of the European Association of Fish Pathologists*, *21*(3), 104–108.

Chabot, D., McKenzie, D., & Craig, J. (2016a). Metabolic rate in fishes: Definitions, methods and significance for conservation physiology. *Journal of Fish Biology*, *88*(1), 1–9. https://doi.org/10.1111/jfb.12873

Chabot, D., McKenzie, D. J., & Craig, J. F. (2016b). Metabolic rate in fishes : definitions , methods and significance for conservation physiology There. *Journal OfFish Biology*, *88*, 1–9. https://doi.org/10.1111/jfb.12873

Chabot, D., Steffensen, J. F., & Farrell, A. P. (2016). The determination of standard metabolic rate in fishes. *Journal of Fish Biology*, *88*(1), 81–121. https://doi.org/10.1111/jfb.12845

Challacombe, J., Kuske, C., Challacombe, J. F., & Kuske, C. R. (2012). Mobile genetic elements in the bacterial phylum Acidobacteria. *Mobile Genetic Elements ISSN:*, *2:4*, 179–183. https://doi.org/10.4161/mge.21943

Chapagain, P., Arivett, B., Cleveland, B. M., Walker, D. M., & Salem, M. (2019). Analysis of the fecal microbiota of fast-and slow-growing rainbow trout (Oncorhynchus mykiss). *BMC Genomics*, *20*(1), 1–11. https://doi.org/10.1186/s12864-019-6175-2

Cheaib, B., Seghouani, H., Ijaz, U. Z., & Derome, N. (2020). Community recovery dynamics in yellow perch microbiome after gradual and constant metallic perturbations. *Microbiome*, *8*(1), 1–19. https://doi.org/10.1186/s40168-020-

0789-0

Cheaib, B., Seghouani, H., Llewellyn, M., Vandal-Lenghan, K., Mercier, P.-L., & Derome, N. (2021). The yellow perch (Perca flavescens) microbiome revealed resistance to colonisation mostly associated with neutralism driven by rare taxa under cadmium disturbance. *Animal Microbiome*, *3*(1). https://doi.org/10.1186/s42523-020-00063-3

Chen, J., Bittinger, K., Charlson, E. S., Hoffmann, C., Lewis, J., Wu, G. D., Collman, R. G., Bushman, F. D., & Li, H. (2012). Associating microbiome composition with environmental covariates using generalized UniFrac distances. *Bioinformatics*, *28*(16), 2106–2113. https://doi.org/10.1093/bioinformatics/bts342

Churcher, A. M., Pujolar, J. M., Milan, M., Huertas, M., Hubbard, P. C., Bargelloni, L., Patarnello, T., Marino, I. A. M., Zane, L., & Canário, A. V. M. (2015). Transcriptomic profiling of male European eel (Anguilla anguilla) livers at sexual maturity. *Comparative Biochemistry and Physiology - Part D: Genomics and Proteomics*, *16*, 28–35. https://doi.org/10.1016/j.cbd.2015.07.002

Clark, T. D., Sandblom, E., & Jutfelt, F. (2013a). Aerobic scope measurements of fishes in an era of climate change: respirometry, relevance and recommendations. *Journal of Experimental Biology*, *216*(15), 2771–2782. https://doi.org/10.1242/jeb.084251

Clark, T. D., Sandblom, E., & Jutfelt, F. (2013b). Aerobic scope measurements of fishes in an era of climate change: Respirometry, relevance and recommendations. *Journal of Experimental Biology*, *216*(15), 2771–2782. https://doi.org/10.1242/jeb.084251

Clarke, A., & Johnston, N. M. (1999). Scaling of metabolic rate with body mass and temperature in teleost fish. *Journal of Animal Ecology*, *68*(5), 893–905. https://doi.org/10.1046/j.1365-2656.1999.00337.x

Cleary, D. F. R., Swierts, T., Coelho, F. J. R. C., Polónia, A. R. M., Huang, Y. M., Ferreira, M. R. S., Putchakarn, S., Carvalheiro, L., van der Ent, E., Ueng, J.

P., Gomes, N. C. M., & de Voogd, N. J. (2019). The sponge microbiome within the greater coral reef microbial metacommunity. *Nature Communications*, *10*(1). https://doi.org/10.1038/s41467-019-09537-8

Cogliati, K. M., Noakes, D. L. G., Unrein, J. R., Stewart, H. A., & Schreck, C. B. (2018). *Egg size and emergence timing affect morphology and behavior in juvenile Chinook Salmon , Oncorhynchus tshawytscha*. *July 2017*, 778–789. https://doi.org/10.1002/ece3.3670

Cooke, S. J., Killen, S. S., Metcalfe, J. D., McKenzie, D. J., Mouillot, D., Jørgensen, C., & Peck, M. A. (2014). Conservation physiology across scales: Insights from the marine realm. *Conservation Physiology*, *2*(1), 1–15. https://doi.org/10.1093/conphys/cou024

Cooper, B., Adriaenssens, B., & Killen, S. S. (2018). Individual variation in the compromise between social group membership and exposure to preferred temperatures. *Proceedings of the Royal Society B: Biological Sciences*, *285*(1880). https://doi.org/10.1098/rspb.2018.0884

Crawley, J. A. H., Chapman, S. N., Lummaa, V., & Lynsdale, C. L. (2016). Testing storage methods of faecal samples for subsequent measurement of helminth egg numbers in the domestic horse. *Veterinary Parasitology*, *221*, 130–133. https://doi.org/10.1016/j.vetpar.2016.03.012

Crean, S. R., Dick, J. T. A., Evans, D. W., Elwood, R. W., & Rosell, R. S. (2003). Anal redness in European eels as an indicator of infection by the swimbladder nematode, Anguillicola crassus. *Journal of Fish Biology*, *62*(2), 482–485. https://doi.org/10.1046/j.1095-8649.2003.00034.x

Cresci, A., Durif, C. M., Paris, C. B., Shema, S. D., Skiftesvik, A. B., & Browman, H. I. (2019). Glass eels (Anguilla anguilla) imprint the magnetic direction of tidal currents from their juvenile estuaries. *Communications Biology*, *2019*. https://doi.org/10.1038/s42003-019-0619-8

Crozier, L. G., & Hutchings, J. A. (2013). *Plastic and evolutionary responses to climate change in fish*. https://doi.org/10.1111/eva.12135

Cucherousset, J., Acou, A., Blanchet, S., Britton, J. R., Beaumont, W. R. C., & Gozlan, R. E. (2011). Fitness consequences of individual specialisation in resource use and trophic morphology in European eels. *Oecologia*, *167*(1), 75–84. https://doi.org/10.1007/s00442-011-1974-4

Dagenais, P., Blanchoud, S., Pury, D., Pfefferli, C., Aegerter-Wilmsen, T., Aegerter, C. M., & Jazwinska, A. (2021). Hydrodynamic stress and phenotypic plasticity of the zebrafish regenerating fin. *Journal of Experimental Biology*, *224*(15). https://doi.org/10.1242/jeb.242309

Dalla Valle, A. Z., Rivas-Diaz, R., & Claireaux, G. (2003). Opercular differential pressure as a predictor of metabolic oxygen demand in the starry flounder. *Journal of Fish Biology*, *63*(6), 1578–1588. https://doi.org/10.1111/j.1095-8649.2003.00268.x

Dangel, K. C., Keppel, M., Le, T. T. Y., Grabner, D., & Sures, B. (2015). Competing invaders: Performance of two Anguillicola species in Lake Bracciano. *International Journal for Parasitology: Parasites and Wildlife*, *4*(1), 119–124. https://doi.org/10.1016/j.ijppaw.2014.12.010

Davey, A. J. H., & Jellyman, D. J. (2005). Sex determination in freshwater eels and management options for manipulation of sex. *Reviews in Fish Biology and Fisheries*, *15*(1–2), 37–52. https://doi.org/10.1007/s11160-005-7431-x

Day, S. W., Higham, T. E., Holzman, R., & Van Wassenbergh, S. (2015). Morphology, Kinematics, and Dynamics: The Mechanics of Suction Feeding in Fishes. *Integrative and Comparative Biology*, *55*(1), 21–35. https://doi.org/10.1093/icb/icv032

de Eyto, E., White, J., Boylan, P., Clarke, B., Cotter, D., Doherty, D., Gargan, P., Kennedy, R., McGinnity, P., O'Maoil??idigh, N., & O'Higgins, K. (2015). The fecundity of wild Irish Atlantic salmon Salmo salar L. and its application for stock assessment purposes. *Fisheries Research*, *164*, 159–169. https://doi.org/10.1016/j.fishres.2014.11.017

De Meyer, J., Christiaens, J., & Adriaens, D. (2016). Diet-induced phenotypic

plasticity in European eel (Anguilla anguilla). *Journal of Experimental Biology*, *219*(3), 354–363. https://doi.org/10.1242/jeb.131714

De Meyer, J., Herrel, A., Belpaire, C., Goemans, G., Ide, C., De Kegel, B., Christiaens, J., & Adriaens, D. (2017). Broader head, stronger bite: In vivo bite forces in European eel Anguilla anguilla. *Journal of Fish Biology*, 268–273. https://doi.org/10.1111/jfb.13511

De Meyer, J., Ide, C., Belpaire, C., Goemans, G., & Adriaens, D. (2015). Head shape dimorphism in European glass eels (Anguilla anguilla). *Zoology*, *118*(6), 413–423. https://doi.org/10.1016/j.zool.2015.07.002

De Meyer, J., Maes, G. E., Dirks, R. P., & Adriaens, D. (2017). Differential gene expression in narrow- and broad-headed European glass eels (Anguilla anguilla) points to a transcriptomic link of head shape dimorphism with growth rate and chemotaxis. *Molecular Ecology*, *26*(15), 3943–3953. https://doi.org/10.1111/mec.14155

De Noia, M., Poole, R., Kaufmann, J., Waters, C., Adams, C., McGinnity, P., & Llewellyn, M. (2020). In-situ non-lethal rapid test to accurately detect the presence of the nematode parasite, Anguillicoloides crassus, in European eel, Anguilla anguilla. *BioRxiv*, *1*. https://doi.org/10.1101/2020.06.16.155002

Dean, A., Collyer, M., Baken, E., & Adams, M. D. (2021). *Package ‘ geomorph .’*

Dehler, C. E., Secombes, C. J., & Martin, S. A. M. (2017). Seawater transfer alters the intestinal microbiota profiles of Atlantic salmon (Salmo salar L.). *Scientific Reports*, *7*(1), 1–11. https://doi.org/10.1038/s41598-017-13249-8

Deutsch, C., Ferrel, A., Seibel, B., Pörtner, H.-O., & Huey, R. B. (2015). Climate change tightens a metabolic constraint on marine habitats. *ECOPHYSIOLOGY*, *348*(6239), 1132–1136.

Di Biase, A., Lokman, P. M., Govoni, N., Casalini, A., Emmanuele, P., Parmeggiani, A., & Mordenti, O. (2017). Co-treatment with androgens during artificial induction of maturation in female eel, Anguilla anguilla: Effects on egg

production and early development. *Aquaculture*, *479*(November 2016), 508–515. https://doi.org/10.1016/j.aquaculture.2017.06.030

Didžiulis, V. (2013). *NOBANIS – Invasive Alien Species Fact Sheet – Anguillicoloides crassus*. *Weber 2000*, 1–11. http://www.nobanis.org/files/factsheets/Pacifastacus_leniusculus.pdf

Diether, N. E., & Willing, B. P. (2019). Microbial fermentation of dietary protein: An important factor in diet-microbe–host interaction. *Microorganisms*, *7*(1). https://doi.org/10.3390/microorganisms7010019

Doenz, C. J., Krähenbühl, A. K., Walker, J., Seehausen, O., & Brodersen, J. (2019). Ecological opportunity shapes a large Arctic charr species radiation. *Proceedings of the Royal Society B: Biological Sciences*, *286*(1913). https://doi.org/10.1098/rspb.2019.1992

Downs, C. J., Brown, J. L., Wone, B. W. M., Donovan, E. R., & Hayes, J. P. (2016). Speeding up growth: Selection for mass-independent maximal metabolic rate alters growth rates. *American Naturalist*, *187*(3), 295–307. https://doi.org/10.1086/684837

Drinan, T. J., McGinnity, P., Coughlan, J. P., Cross, T. F., & Harrison, S. S. C. (2012). Morphological variability of Atlantic salmon Salmo salar and brown trout Salmo trutta in different river environments. *Ecology of Freshwater Fish*, *21*(3), 420–432. https://doi.org/10.1111/j.1600-0633.2012.00561.x

Dulski, T., Kozłowski, K., & Ciesielski, S. (2020). Habitat and seasonality shape the structure of tench (Tinca tinca L.) gut microbiome. *Scientific Reports*, *10*(1), 1–11. https://doi.org/10.1038/s41598-020-61351-1

Dulski, T., Kujawa, R., Godzieba, M., & Ciesielski, S. (2020). Effect of salinity on the gut microbiome of pike fry (Esox lucius). *Applied Sciences (Switzerland)*, *10*(7). https://doi.org/10.3390/app10072506

Durif, C., Dufour, S., & Elie, P. (2005). The silvering process of Anguilla anguilla: A new classification from the yellow resident to the silver migrating stage.

Journal of Fish Biology, *66*(4), 1025–1043. https://doi.org/10.1111/j.0022-1112.2005.00662.x

Durif, C., Guibert, A., & Pierre, E. (2009). Morphological discrimination of the silvering stages of the European eel. *Eels at the Edge. Science, Status, and Conservation Concerns. American Fisheries Society Symposium 58*, *January*, 103–111. https://doi.org/10.1111/j.1095-8649.2010.02758.x

Durif, C. M. F., Browman, H. I., Phillips, J. B., Skiftesvik, A. B., Vøllestad, L. A., & Stockhausen, H. H. (2013). Magnetic Compass Orientation in the European Eel. *PLoS ONE*, *8*(3). https://doi.org/10.1371/journal.pone.0059212

Dvergedal, H., Sandve, S. R., Angell, I. L., Klemetsdal, G., & Rudi, K. (2020). Association of gut microbiota with metabolism in juvenile Atlantic salmon. *Microbiome*, *8*(1), 1–8. https://doi.org/10.1186/s40168-020-00938-2

Egerton, S., Culloty, S., Whooley, J., Stanton, C., & Ross, R. P. (2018). The gut microbiota of marine fish. *Frontiers in Microbiology*, *9*(MAY), 1–17. https://doi.org/10.3389/fmicb.2018.00873

Eichhorn, G., Enstipp, M. R., Georges, J.-Y., Enstipp, M. R., & Nolet, B. A. (2019). *Resting metabolic rate in migratory and non-migratory geese following range expansion: go south, go low*. *May*, 1424–1434. https://doi.org/10.1111/oik.06468

Einum, S. (2014). Ecological modeling of metabolic rates predicts diverging optima across food abundances. *American Naturalist*, *183*(3), 410–417. https://doi.org/10.1086/674951

Eliason, E. J., Clark, T. D., Hague, M. J., Hanson, L. M., Gallagher, Z. S., Jeffries, K. M., Gale, M. K., Patterson, D. A., Hinch, S. G., & Farrell, A. P. (2011). Differences in thermal tolerance among sockeye salmon populations. *Science*, *332*(6025), 109–112. https://doi.org/10.1126/science.1199158

Ellis, A. E. (2001). Innate host defense mechanisms of fish against viruses and bacteria. *Developmental and Comparative Immunology*, *25*(8–9), 827–839.

https://doi.org/10.1016/S0145-305X(01)00038-6

Elsheikha, H. M., Elsaied, N. A., Chan, K. L. A., Brignell, C., Harun, M. S. R., Wehbe, K., & Cinquee, G. (2019). Label-free characterization of biochemical changes within human cells under parasite attack using synchrotron based micro-FTIR. *Analytical Methods*, *11*(19), 2518–2530. https://doi.org/10.1039/c8ay02777c

Estensoro, I., Pérez-Cordón, G., Sitjà-Bobadilla, A., & Piazzon, M. C. (2018). Bromodeoxyuridine DNA labelling reveals host and parasite proliferation in a fish-myxozoan model. *Journal of Fish Diseases*, *41*(4), 651–662. https://doi.org/10.1111/jfd.12765

European Council. (2007). Establishing measures for the recovery of the stock of European eel. In *Official Journal of the European Union* (Vol. 248, Issue 1100).

Farrell, A. A. P., Hinch, S. G., Cooke, S. J., Patterson, D. A., Crossin, G. T., Mathes, M. T., & December, N. N. (2008). Comparative Biology Pacific Salmon in Hot Water : Applying Aerobic Scope Models and Biotelemetry to Predict the Success of Spawning Migrations Pacific Salmon in Hot Water : Applying Aerobic Scope Models and Biotelemetry to Predict the Success of Spawning. *The University of Chicago Press*, *81*(6), 697–708. https://doi.org/10.1086/592057

Fast, M. D., Hosoya, S., Johnson, S. C., & Afonso, L. O. B. (2008). Cortisol response and immune-related effects of Atlantic salmon (Salmo salar Linnaeus) subjected to short- and long-term stress. *Fish and Shellfish Immunology*, *24*(2), 194–204. https://doi.org/10.1016/j.fsi.2007.10.009

Fazio, G., Sasal, P., Mouahid, G., Lecomte-Finiger, R., & Moné, H. (2012). Swim Bladder Nematodes (Anguillicoloides crassus) Disturb Silvering In European Eels (Anguilla anguilla). *Journal of Parasitology*, *98*(4), 695–705. https://doi.org/10.1645/GE-2700.1

Forsman, A. (2015). Rethinking phenotypic plasticity and its consequences for individuals, populations and species. *Heredity*, *115*(4), 276–284. https://doi.org/10.1038/hdy.2014.92

Frankowski, J., Jennerich, S., Schaarschmidt, T., Ubl, C., Jürss, K., & Bastrop, R. (2009). Validation of the occurrence of the American eel Anguilla rostrata (Le Sueur, 1817) in free-draining European inland waters. *Biological Invasions*, *11*(6), 1301–1309. https://doi.org/10.1007/s10530-008-9337-8

Frantz, A., Perga, M. E., & Guillard, J. (2018). Parasitic versus nutritional regulation of natural fish populations. *Ecology and Evolution*, *8*(17), 8713–8725. https://doi.org/10.1002/ece3.4391

Friberg, I. M., Taylor, J. D., & Jackson, J. A. (2019). Diet in the driving seat: Natural diet-immunity-microbiome interactions in wild fish. *Frontiers in Immunology*, *10*(FEB), 1–13. https://doi.org/10.3389/fimmu.2019.00243

Frisch, K., Davie, A., Schwarz, T., & Turnbull, J. F. (2016). Comparative imaging of European eels (Anguilla anguilla) for the evaluation of swimbladder nematode (Anguillicoloides crassus) infestation. *Journal of Fish Diseases*, *39*(6), 635–647. https://doi.org/10.1111/jfd.12383

Gajardo, K., Rodiles, A., Kortner, T. M., Krogdahl, Å., Bakke, A. M., Merrifield, D. L., & Sørum, H. (2016). A high-resolution map of the gut microbiota in Atlantic salmon (Salmo salar): A basis for comparative gut microbial research. *Scientific Reports*, *6*(April), 1–10. https://doi.org/10.1038/srep30893

Galarowicz, T. L., & Wahl, D. H. (2005). Foraging by a young-of-the-year piscivore: The role of predator size, prey type, and density. *Canadian Journal of Fisheries and Aquatic Sciences*, *62*(10), 2330–2342. https://doi.org/10.1139/f05-148

Gaulke, C. A., Martins, M. L., Watral, V. G., Humphreys, I. R., Spagnoli, S. T., Kent, M. L., & Sharpton, T. J. (2019). A longitudinal assessment of host-microbe-parasite interactions resolves the zebrafish gut microbiome's link to Pseudocapillaria tomentosa infection and pathology. *Microbiome*, *7*(1), 1–16. https://doi.org/10.1186/s40168-019-0622-9

George Hajishengallis, Darveau, R. P., & Curtis, M. A. (2012). The Keystone Pathogen Hypothesis George. *Nat Rev Microbioliology*, *10*(10), 4.

https://doi.org/10.1038/nrmicro2873.The

Gerber, L., Clow, K. A., Mark, F. C., & Gamperl, A. K. (2020). Improved mitochondrial function in salmon (Salmo salar) following high temperature acclimation suggests that there are cracks in the proverbial 'ceiling.' *Scientific Reports*, *10*(1), 1–12. https://doi.org/10.1038/s41598-020-78519-4

Gerhauser, C. (2018). Impact of dietary gut microbial metabolites on the epigenome. *Philosophical Transactions of the Royal Society B: Biological Sciences*, *373*(1748), 20170359. https://doi.org/10.1098/rstb.2017.0359

Gilbey, J., Verspoor, E., Mo, T. A., Sterud, E., Olstad, K., Hytterød, S., Jones, C., & Noble, L. (2006). Identification of genetic markers associated with Gyrodactylus salaris resistance in Atlantic salmon Salmo salar. *Diseases of Aquatic Organisms*, *71*(2), 119–129. https://doi.org/10.3354/dao071119

Glazier, D. S. (2005). Beyond the "3/4-power law": Variation in the intra- and interspecific scaling of metabolic rate in animals. *Biological Reviews of the Cambridge Philosophical Society*, *80*(4), 611–662. https://doi.org/10.1017/S1464793105006834

Godínez-González, C., Roca-Geronès, X., Cancino-Faure, B., Montoliu, I., & Fisa, R. (2017). Quantitative SYBR Green qPCR technique for the detection of the nematode parasite Anisakis in commercial fish-derived food. *International Journal of Food Microbiology*, *261*(May), 89–94. https://doi.org/10.1016/j.ijfoodmicro.2017.05.012

Godoy-Vitorino, F., Rodriguez-Hilario, A., Alves, A. L., Gonçalves, F., Cabrera-Colon, B., Mesquita, C. S., Soares-Castro, P., Ferreira, M., Marçalo, A., Vingada, J., Eira, C., & Santos, P. M. (2017). The microbiome of a striped dolphin (Stenella coeruleoalba) stranded in Portugal. *Research in Microbiology*, *168*(1), 85–93. https://doi.org/10.1016/j.resmic.2016.08.004

Goossens, S., Wybouw, N., Van Leeuwen, T., & Bonte, D. (2020). The physiology of movement. *Movement Ecology*, *8*(1), 1–14. https://doi.org/10.1186/s40462-020-0192-2

Grabner, D. S., Dangel, K. C., & Sures, B. (2012). Merging species? Evidence for hybridization between the eel parasites Anguillicola crassus and A. novaezelandiae (Nematoda, Anguillicolidea). *Parasites and Vectors*, *5*(1), 1. https://doi.org/10.1186/1756-3305-5-244

Gunter, H., & Meyer, A. (2014). Molecular investigation of mechanical strain-induced phenotypic plasticity in the ecologically important pharyngeal jaws of cichlid fish. *J. Appl. Ichthyol*, *30*.

Haenen, O., Grisez, L., De Charleroy, D., Belpaire, C., & Ollevier, F. (1989). Experimentally induced infections of European eel Anguilla angutila with Anguillicola crassus (Nematoda, Dracunculoidea) and subsequent migration of larvae. *Diseases of Aquatic Organisms*, *7*, 97–101. https://doi.org/10.3354/dao007097

Hamilton, E. F., Element, G., van Coeverden de Groot, P., Engel, K., Neufeld, J. D., Shah, V., & Walker, V. K. (2019). Anadromous arctic char microbiomes: Bioprospecting in the high arctic. *Frontiers in Bioengineering and Biotechnology*, *7*(FEB), 1–13. https://doi.org/10.3389/fbioe.2019.00032

Han, Y., Huang, Y., Wann-Nian, T., & Chiu, L. (2001). *Silvering in the eel : changes in morphology , body fat content and gonadal development*. *January*.

Hao, Y. T., Wu, S. G., Jakovlić, I., Zou, H., Li, W. X., & Wang, G. T. (2017). Impacts of diet on hindgut microbiota and short-chain fatty acids in grass carp (Ctenopharyngodon idellus). *Aquaculture Research*, *48*(11), 5595–5605. https://doi.org/10.1111/are.13381

Hayes, J. P. (2010). Metabolic rates, genetic constraints, and the evolution of endothermy. *Journal of Evolutionary Biology*, *23*(9), 1868–1877. https://doi.org/10.1111/j.1420-9101.2010.02053.x

Hein, J. L., Buron, I. De, Roumillat, W. A., Post, W. C., Hazel, A. P., & Arnott, S. A. (2016). Infection of newly recruited American eels (Anguilla rostrata) by the invasive swimbladder parasite Anguillicoloides crassus in a US Atlantic tidal creek. *ICES Journal of Marine Science*, *73*, 14–21.

Heitlinger, E. G., Laetsch, D. R., Weclawski, U., Han, Y. S., & Taraschewski, H. (2009). Massive encapsulation of larval Anguillicoloides crassus in the intestinal wall of Japanese eels. *Parasites and Vectors*, *2*(1), 1–11. https://doi.org/10.1186/1756-3305-2-48

Henderson, P. A., Plenty, S. J., Newton, L. C., & Bird, D. J. (2012). Evidence for a population collapse of European eel (Anguilla anguilla) in the Bristol Channel. *Journal of the Marine Biological Association of the United Kingdom*, *92*(4), 843–851. https://doi.org/10.1017/S002531541100124X

Heraud, P., Chatchawal, P., Wongwattanakul, M., Tippayawat, P., Doerig, C., Jearanaikoon, P., Perez-Guaita, D., & Wood, B. R. (2019). Infrared spectroscopy coupled to cloud-based data management as a tool to diagnose malaria: A pilot study in a malaria-endemic country. *Malaria Journal*, *18*(1), 1–12. https://doi.org/10.1186/s12936-019-2945-1

Herlemann, D. P. R., Labrenz, M., Jürgens, K., Bertilsson, S., Waniek, J. J., & Andersson, A. F. (2011). Transitions in bacterial communities along the 2000 km salinity gradient of the Baltic Sea. *ISME Journal*, *5*(10), 1571–1579. https://doi.org/10.1038/ismej.2011.41

Herrero, B., Vieites, J. M., & Espiñeira, M. (2011). Detection of anisakids in fish and seafood products by real-time PCR. *Food Control*, *22*(6), 933–939. https://doi.org/10.1016/j.foodcont.2010.11.028

Heys, C., Cheaib, B., Busetti, A., Kazlauskaite, R., Maier, L., Sloan, W. T., Ijaz, U. Z., Kaufmann, J., McGinnity, P., & Llewellyn, M. S. (2020). Neutral Processes Dominate Microbial Community Assembly in Atlantic Salmon, Salmo salar. *Applied and Environmental Microbiology*, *April*, 1–17.

Hinch, S. G., & Farrell, A. P. (2015). Routine and Active Metabolic Rates of Migrating Adult Wild Sockeye Salmon (Oncorhynchus nerka Walbaum) in Seawater and Freshwater. *The University of Chicago Press*, *79*(1), 100–108.

Hoffmann, L., Rawski, M., Nogales-Merida, S., & Mazurkiewicz, J. (2020). Dietary Inclusion of Tenebrio Molitor Meal in Sea Trout Larvae Rearing: Effects on Fish

Growth Performance, Survival, Condition, and GIT and Liver Enzymatic Activity. *Annals of Animal Science*, *20*(2), 579–598. https://doi.org/10.2478/aoas-2020-0002

Holben, W. E., Williams, P., Saarinen, M., Särkilahti, L. K., & Apajalahti, J. H. A. (2002). Phylogenetic analysis of intestinal microflora indicates a novel Mycoplasma phylotype in farmed and wild salmon. *Microbial Ecology*, *44*(2), 175–185. https://doi.org/10.1007/s00248-002-1011-6

Hole, K., & Nfon, C. (2019). Foot-and-mouth disease virus detection on a handheld real-time polymerase chain reaction platform. *Transboundary and Emerging Diseases*, *66*(4), 1789–1795. https://doi.org/10.1111/tbed.13227

Holt, R. E., & Jørgensen, C. (2015). Climate change in fish: Effects of respiratory constraints on optimal life history and behaviour. *Biology Letters*, *11*(2). https://doi.org/10.1098/rsbl.2014.1032

Hsu, H., Wang, F. C. Y., Lin, S. C. Y., & Han, C. L. Y. (2018). Revealing the compositions of the intestinal microbiota of three Anguillid eel species using 16S rDNA sequencing. *Aquaculture Research*, 2404–2415. https://doi.org/10.1111/are.13700

Hu, C., Huang, Z., Liu, M., Sun, B., Tang, L., & Chen, L. (2021). Shift in skin microbiota and immune functions of zebrafish after combined exposure to perfluorobutanesulfonate and probiotic Lactobacillus rhamnosus. *Ecotoxicology and Environmental Safety*, *218*, 112310. https://doi.org/10.1016/j.ecoenv.2021.112310

Hu, Y., Ghigliotti, L., Vacchi, M., Pisano, E., Iii, H. W. D., & Albertson, R. C. (2016). Evolution in an extreme environment : developmental biases and phenotypic integration in the adaptive radiation of antarctic notothenioids. *BMC Evolutionary Biology*, 1–13. https://doi.org/10.1186/s12862-016-0704-2

Huang, Q., Sham, R. C., Deng, Y., Mao, Y., Wang, C., Zhang, T., & Leung, K. M. Y. (2020). Diversity of gut microbiomes in marine fishes is shaped by host-related factors. *Molecular Ecology*, *29*(24), 5019–5034.

https://doi.org/10.1111/mec.15699

Huang, W., Cheng, Z., Lei, S., Liu, L., Lv, X., Chen, L., Wu, M., Wang, C., Tian, B., & Song, Y. (2018a). Community composition, diversity, and metabolism of intestinal microbiota in cultivated European eel (Anguilla anguilla). *Applied Microbiology and Biotechnology*, 4143–4157. https://doi.org/10.1007/s00253-018-8885-9

Huang, W., Cheng, Z., Lei, S., Liu, L., Lv, X., Chen, L., Wu, M., Wang, C., Tian, B., & Song, Y. (2018b). Community composition, diversity, and metabolism of intestinal microbiota in cultivated European eel (Anguilla anguilla). *Applied Microbiology and Biotechnology*. https://doi.org/10.1007/s00253-018-8885-9

Hughes, M. R., Hooker, O. E., Van Leeuwen, T. E., Kettle-White, A., Thorne, A., Prodöhl, P., & Adams, C. E. (2019). Alternative routes to piscivory: Contrasting growth trajectories in brown trout (Salmo trutta) ecotypes exhibiting contrasting life history strategies. *Ecology of Freshwater Fish*, *28*(1), 4–10. https://doi.org/10.1111/eff.12421

Hunter-Manseau, F., Desrosiers, V., Le François, N. R., Dufresne, F., Detrich, H. W., Nozais, C., & Blier, P. U. (2019). From Africa to Antarctica: Exploring the Metabolism of Fish Heart Mitochondria Across a Wide Thermal Range. *Frontiers in Physiology*, *10*(October), 1–11. https://doi.org/10.3389/fphys.2019.01220

Hvas, M., Karlsbakk, E., Mæhle, S., Wright, D. W., & Oppedal, F. (2017). The gill parasite Paramoeba perurans compromises aerobic scope, swimming capacity and ion balance in Atlantic salmon. *Conservation Physiology*, *5*(1), 1–12. https://doi.org/10.1093/conphys/cox066

ICES. (2020). European eel (Anguilla anguilla) throughout its natural range. *ICES Advice on Fishing Opportunities, Catch, and Effort*, *October*, 1–5. https://doi.org/10.17895/ices.advice.5898

Ide, C., De Schepper, N., Christiaens, J., Van Liefferinge, C., Herrel, A., Goemans, G., Meire, P., Belpaire, C., Geeraerts, C., & Adriaens, D. (2011). Bimodality

in head shape in European eel. *Journal of Zoology*, *285*(3), 230–238. https://doi.org/10.1111/j.1469-7998.2011.00834.x

Ijaz, U. Z., Sivaloganathan, L., McKenna, A., Richmond, A., Kelly, C., Linton, M., Stratakos, A. C., Lavery, U., Elmi, A., Wren, B. W., Dorrell, N., Corcionivoschi, N., & Gundogdu, O. (2018). Comprehensive longitudinal microbiome analysis of the chicken cecum reveals a shift from competitive to environmental drivers and a window of opportunity for Campylobacter. *Frontiers in Microbiology*, *9*(OCT), 1–14. https://doi.org/10.3389/fmicb.2018.02452

Ivanović, A., & Arntzen, J. W. (2014). Evolution of skull and body shape in Triturus newts reconstructed from three-dimensional morphometric data and phylogeny. *Biological Journal of the Linnean Society*, *113*(1), 243–255. https://doi.org/10.1111/bij.12314

Iwanowicz, D. D. (2011). Overview On The Effects Of Parasites On Fish Health. *Proceedings of the Third Bilateral Conference between Russia and the United States. Bridging America and Russia with Shared Perspectives on Aquatic Animal Health.*, *June*, 176–184.

Jachowski, D. S., & Singh, N. J. (2015). Toward a mechanistic understanding of animal migration: Incorporating physiological measurements in the study of animal movement. *Conservation Physiology*, *3*(1), 1–12. https://doi.org/10.1093/conphys/cov035

Jacobsen, M. W., Pujolar, J. M., Gilbert, M. T. P., Moreno-Mayar, J. V., Bernatchez, L., Als, T. D., Lobon-Cervia, J., & Hansen, M. M. (2014). Speciation and demographic history of Atlantic eels (Anguilla anguilla and A. rostrata) revealed by mitogenome sequencing. *Heredity*, *113*(5), 432–442. https://doi.org/10.1038/hdy.2014.44

Jacoby, D., & Gollock, M. (2014). Anguilla anguilla. *The IUCN Red List of Threatened Species 2014*, *8235*. https://doi.org/e.T60344A45833138

Jessop, B. M. (2010). Geographic effects on American eel (Anguilla rostrata) life

history characteristics and strategies. *Canadian Journal of Fisheries and Aquatic Sciences*, *67*(2), 326–346. https://doi.org/10.1139/F09-189

Jetz, W., Freckleton, R. P., & Mckechnie, A. E. (2008). *Environment , Migratory Tendency , Phylogeny and Basal Metabolic Rate in Birds*. *3*(9). https://doi.org/10.1371/journal.pone.0003261

Joh, S. J., Ahn, E. H., Lee, H. J., Shin, G. W., Kwon, J. H., & Park, C. G. (2013). Bacterial pathogens and flora isolated from farm-cultured eels (Anguilla japonica) and their environmental waters in Korean eel farms. *Veterinary Microbiology*, *163*(1–2), 190–195. https://doi.org/10.1016/j.vetmic.2012.11.004

Jolles, J. W., Mazué, G. P. F., Davidson, J., Behrmann-Godel, J., & Couzin, I. D. (2020). Schistocephalus parasite infection alters sticklebacks' movement ability and thereby shapes social interactions. *Scientific Reports*, *10*(1), 1–11. https://doi.org/10.1038/s41598-020-69057-0

Jonsson, B., & Jonsson, N. (2019). Phenotypic plasticity and epigenetics of fish: Embryo temperature affects later-developing life-history traits. *Aquatic Biology*, *28*(April), 21–32. https://doi.org/10.3354/ab00707

Jousseaume, T., Roussel, J. M., Beaulaton, L., Bardonnet, A., Faliex, E., Amilhat, E., Acou, A., Feunteun, E., & Launey, S. (2021). Molecular detection of the swim bladder parasite Anguillicola crassus (Nematoda) in fecal samples of the endangered European eel Anguilla anguilla. *Parasitology Research*, *120*(5), 1897–1902. https://doi.org/10.1007/s00436-021-07100-3

Kaifu, K., Miyazaki, S., Aoyama, J., Kimura, S., & Tsukamoto, K. (2013). Diet of Japanese eels Anguilla japonica in the Kojima Bay-Asahi River system, Japan. *Environmental Biology of Fishes*, *96*(4), 439–446. https://doi.org/10.1007/s10641-012-0027-0

Kaifu, K., Yokouchi, K., Miller, M. J., Aoyama, J., & Tsukamoto, K. (2013). Head-shape polymorphism in Japanese eels Anguilla japonica in relation to differences of somatic growth in freshwater and brackish habitats. *Journal of*

Fish Biology, *82*(4), 1308–1320. https://doi.org/10.1111/jfb.12070

Katoh, K., & Standley, D. M. (2013). MAFFT multiple sequence alignment software version 7: Improvements in performance and usability. *Molecular Biology and Evolution*, *30*(4), 772–780. https://doi.org/10.1093/molbev/mst010

Kelley, J. L., Davies, P. M., Collin, S. P., & Grierson, P. F. (2017). *Morphological plasticity in a native freshwater fish from semiarid Australia in response to variable water flows*. *April*, 6595–6605. https://doi.org/10.1002/ece3.3167

Kelly, S. A., Panhuis, T. M., & Stoehr, A. M. (2012). Phenotypic plasticity: Molecular mechanisms and adaptive significance. *Comprehensive Physiology*, *2*(2), 1417–1439. https://doi.org/10.1002/cphy.c110008

Kelly, S., Doyle, B., de Eyto, E., Dillane, M., McGinnity, P., Poole, R., White, M., & Jennings, E. (2020). Impacts of a record-breaking storm on physical and biogeochemical regimes along a catchment-to-coast continuum. *PLoS ONE*, *15*(7 July), 1–24. https://doi.org/10.1371/journal.pone.0235963

Khoshmanesh, A., Dixon, M. W. A., Kenny, S., Tilley, L., McNaughton, D., & Wood, B. R. (2014). Detection and quantification of early-stage malaria parasites in laboratory infected erythrocytes by attenuated total reflectance infrared spectroscopy and multivariate analysis. *Analytical Chemistry*, *86*(9), 4379–4386. https://doi.org/10.1021/ac500199x

Killen, S. S., Christensen, E. A. F., Cortese, D., Závorka, L., Norin, T., Cotgrove, L., Crespel, A., Munson, A., Nati, J. J. H., Papatheodoulou, M., & McKenzie, D. J. (2021). Guidelines for reporting methods to estimate metabolic rates by aquatic intermittent-flow respirometry. *Journal of Experimental Biology*, *224*(18). https://doi.org/10.1242/jeb.242522

Killen, S. S., Glazier, D. S., Rezende, E. L., Clark, T. D., Atkinson, D., Willener, A. S. T., & Halsey, L. G. (2016). Ecological influences and morphological correlates of resting and maximal metabolic rates across teleost fish species. *American Naturalist*, *187*(5), 592–606. https://doi.org/10.1086/685893

Killen, S. S., Nati, J. J. H., & Suski, C. D. (2015). Vulnerability of individual fish to capture by trawling is influenced by capacity for anaerobic metabolism. *Proceedings of the Royal Society B: Biological Sciences*, *282*(1813). https://doi.org/10.1098/rspb.2015.0603

King, M. O., Zhang, Y., Carter, T., Johnson, J., Harmon, E., & Swanson, D. L. (2015). Phenotypic flexibility of skeletal muscle and heart masses and expression of myostatin and tolloid-like proteinases in migrating passerine birds. *Journal of Comparative Physiology B: Biochemical, Systemic, and Environmental Physiology*, *185*(3), 333–342. https://doi.org/10.1007/s00360-015-0887-7

Kirk, R. S. (2003). The impact of Anguillicola crassus on European eels. *Fisheries Management and Ecology*, *10*(6), 385–394. https://doi.org/10.1111/j.1365-2400.2003.00355.x

Klaassen, R. H. G., Hake, M., Strandberg, R., Koks, B. J., Trierweiler, C., Exo, K. M., Bairlein, F., & Alerstam, T. (2014). When and where does mortality occur in migratory birds? Direct evidence from long-term satellite tracking of raptors. *Journal of Animal Ecology*, *83*(1), 176–184. https://doi.org/10.1111/1365-2656.12135

Klefoth, T., Skov, C., Krause, J., & Arlinghaus, R. (2012). The role of ecological context and predation risk-stimuli in revealing the true picture about the genetic basis of boldness evolution in fish. *Behavioral Ecology and Sociobiology*, *66*(4), 547–559. https://doi.org/10.1007/s00265-011-1303-2

Klemetsen, a, Amundsen, P. -a., Dempson, J. B., Jonsson, B., Jonsson, N., O'Connell, M. F., & Mortensen, E. (2003). Atlantic salmon Salmo salar L., brown trout Salmo trutta L. and Arctic charr Salvelinus alpinus (L.): a review of aspects of their life histories. *Ecology of Freshwater Fish*, *12*(1), 1–59. https://doi.org/10.1034/j.1600-0633.2003.00010.x

Knopf, K., & Lucius, R. (2008). Vaccination of eels (Anguilla japonica and Anguilla anguilla) against Anguillicola crassus with irradiated L3. *Parasitology*, *135*(5),

633–640. https://doi.org/10.1017/S0031182008004162

Kokou, F., Sasson, G., Mizrahi, I., & Cnaani, A. (2020). Antibiotic effect and microbiome persistence vary along the European seabass gut. *Scientific Reports*, *10*(1), 1–12. https://doi.org/10.1038/s41598-020-66622-5

Kraskura, K., Hardison, E. A., Little, A. G., Dressler, T., Prystay, T. S., Hendriks, B., Farrell, A. P., Cooke, S. J., Patterson, D. A., Hinch, S. G., & Eliason, E. J. (2020). Sex-specific differences in swimming, aerobic metabolism and recovery from exercise in adult coho salmon (Oncorhynchus kisutch) across ecologically relevant temperatures. *Conservation Physiology*, *9*(1), 1–22. https://doi.org/10.1093/conphys/coab016

Kristensen, K., Nielsen, A., Berg, C. W., Skaug, H., & Bell, B. M. (2016). TMB: Automatic differentiation and laplace approximation. *Journal of Statistical Software*, *70*(5). https://doi.org/10.18637/jss.v070.i05

Krotman, Y., Yergaliyev, T. M., Alexander Shani, R., Avrahami, Y., & Szitenberg, A. (2020). Dissecting the factors shaping fish skin microbiomes in a heterogeneous inland water system. *Microbiome*, *8*(1), 1–16. https://doi.org/10.1186/s40168-020-0784-5

Kuwahara, N. & I. (1999). Anguillicola crassus DAISIE (Delivering, Alien Invasive Species Inventories for Europe). *DAISIE*, *34*(2), 81–82.

Laetsch, D. R., Heitlinger, E. G., Taraschewski, H., Nadler, S. A., & Blaxter, M. L. (2012a). The phylogenetics of Anguillicolidae (Nematoda: Anguillicoloidea), swimbladder parasites of eels. *BMC Evolutionary Biology*, *12*(1). https://doi.org/10.1186/1471-2148-12-60

Laetsch, D. R., Heitlinger, E. G., Taraschewski, H., Nadler, S. A., & Blaxter, M. L. (2012b). The phylogenetics of Anguillicolidae (Nematoda: Anguillicoloidea), swimbladder parasites of eels. *BMC Evolutionary Biology*, *12*(1). https://doi.org/10.1186/1471-2148-12-60

Laffaille, P., Acou, A., Guillouët, J., Mounaix, B., & Legault, A. (2006). Patterns

of silver eel (Anguilla anguilla L.) sex ratio in a catchment. *Ecology of Freshwater Fish*, *15*(4), 583–588. https://doi.org/10.1111/j.1600-0633.2006.00195.x

Lahti, K., Huuskonen, H., Laurila, A., & Piironen, J. (2002). Metabolic rate and aggressiveness between Brown Trout populations. *Functional Ecology*, *16*(2), 167–174. https://doi.org/10.1046/j.1365-2435.2002.00618.x

Lallias, D., Bernard, M., Ciobotaru, C., Dechamp, N., Labbé, L., Goardon, L., Le Calvez, J. M., Bideau, M., Fricot, A., Prézelin, A., Charles, M., Moroldo, M., Cousin, X., Bouchez, O., Roulet, A., Quillet, E., & Dupont-Nivet, M. (2021). Sources of variation of DNA methylation in rainbow trout: combined effects of temperature and genetic background. In *Epigenetics* (Vol. 16, Issue 9, pp. 1031–1052). https://doi.org/10.1080/15592294.2020.1834924

Lammens, E. H. R. R., & Visser, J. T. (1989). Variability of mouth width in European eel, Anguilla anguilla, in relation to varying feeding conditions in three Dutch lakes. *Environmental Biology of Fishes*, *26*(1), 63–75. https://doi.org/10.1007/BF00002476

Lapointe, D., Cooperman, M. S., Chapman, L. J., Clark, T. D., Val, A. L., Ferreira, M. S., Balirwa, J. S., Mbabazi, D., Mwanja, M., Chhom, L., Hannah, L., Kaufman, L., Farrell, A. P., & Cooke, S. J. (2018). Predicted impacts of climate warming on aerobic performance and upper thermal tolerance of six tropical freshwater fishes spanning three continents. *Conservation Physiology*, *6*(1), 1–19. https://doi.org/10.1093/conphys/coy056

Le Doujet, T., De Santi, C., Klemetsen, T., Hjerde, E., Willassen, N. P., & Haugen, P. (2019). Closely-related Photobacterium strains comprise the majority of bacteria in the gut of migrating Atlantic cod (Gadus morhua). *Microbiome*, *7*(1). https://doi.org/10.1186/s40168-019-0681-y

Lee, S. H., Lee, Y. K., Katya, K., Park, J. K., & Bai, S. C. (2018). Natural dietary additive yellow loess as potential antibiotic replacer in Japanese eel, Anguilla japonica: Effects on growth, immune responses, serological characteristics

and disease resistance against Edwardsiella tarda. *Aquaculture Nutrition*, *24*(3), 1034–1040. https://doi.org/10.1111/anu.12641

Lee, W. J., & Hase, K. (2014). Gut microbiota-generated metabolites in animal health and disease. *Nature Chemical Biology*, *10*(6), 416–424. https://doi.org/10.1038/nchembio.1535

Lefebvre, F. S., & Crivelli, A. J. (2004). Anguillicolosis: Dynamics of the infection over two decades. *Diseases of Aquatic Organisms*, *62*(3), 227–232. https://doi.org/10.3354/dao062227

Lefebvre, F., Wielgoss, S., Nagasawa, K., & Moravec, F. (2012). On the origin of Anguillicoloides crassus, the invasive nematode of anguillid eels. *Aquatic Invasions*, *7*(4), 443–453. https://doi.org/10.3391/ai.2012.7.4.001

Leinster, T. (2020). *Entropy and Diversity: The Axiomatic Approach*. http://arxiv.org/abs/2012.02113

Lennox, R. J., Chapman, J. M., Souliere, C. M., Tudorache, C., Wikelski, M., Metcalfe, J. D., & Cooke, S. J. (2016). Conservation physiology of animal migration. *Conservation Physiology*, *4*(1), 1–15. https://doi.org/10.1093/conphys/cov072

Levsen, A., Svanevik, C. S., Cipriani, P., Mattiucci, S., Gay, M., Hastie, L. C., Bušelić, I., Mladineo, I., Karl, H., Ostermeyer, U., Buchmann, K., Højgaard, D. P., González, Á. F., Pascual, S., & Pierce, G. J. (2018). A survey of zoonotic nematodes of commercial key fish species from major European fishing grounds—Introducing the FP7 PARASITE exposure assessment study. *Fisheries Research*, *202*(September 2017), 4–21. https://doi.org/10.1016/j.fishres.2017.09.009

Lhorente, J. P., Gallardo, J. A., Villanueva, B., Carabaño, M. J., & Neira, R. (2014). Disease Resistance in Atlantic Salmon (Salmo salar): Coinfection of the Intracellular Bacterial Pathogen Piscirickettsia salmonis and the Sea Louse Caligus rogercresseyi. *PLoS ONE*, *9*(4), e95397. https://doi.org/10.1371/journal.pone.0095397

Li, G., Lv, X., Zhou, J., Shen, C., Xia, D., Xie, H., & Luo, Y. (2018). Are the surface areas of the gills and body involved with changing metabolic scaling with temperature? *Journal of Experimental Biology*, *221*(8), 1–6. https://doi.org/10.1242/jeb.174474

Lin, M., Zeng, C. X., Jia, X. Q., Zhai, S. W., Li, Z. Q., & Ma, Y. (2019). The composition and structure of the intestinal microflora of Anguilla marmorata at different growth rates: a deep sequencing study. *Journal of Applied Microbiology*, *126*(5), 1340–1352. https://doi.org/10.1111/jam.14174

Lindsay, E. C. (2021). (2021). Ecophysiological exploration: the microbiota, metabolic rate and behaviour of juvenile Atlantic salmon (Salmo salar). *PhD Thesis*.

Lindsay, E. C., Metcalfe, N. B., & Llewellyn, M. S. (2020). The potential role of the gut microbiota in shaping host energetics and metabolic rate. *Journal of Animal Ecology*, *89*(11), 2415–2426. https://doi.org/10.1111/1365-2656.13327

Ling, F., Steinel, N., Weber, J., Ma, L., Smith, C., Correa, D., Zhu, B., Bolnick, D., & Wang, G. (2020). The gut microbiota response to helminth infection depends on host sex and genotype. *ISME Journal*, *14*(5), 1141–1153. https://doi.org/10.1038/s41396-020-0589-3

Lisney, T. J., Collin, S. P., & Kelley, J. L. (2020). The effect of ecological factors on eye morphology in the western rainbowfish, Melanotaenia australis. *Journal of Experimental Biology*, *223*(10). https://doi.org/10.1242/jeb.223644

Llewellyn, M. S., Boutin, S., Hoseinifar, S. H., & Derome, N. (2014). Teleost microbiomes: The state of the art in their characterization, manipulation and importance in aquaculture and fisheries. *Frontiers in Microbiology*, *5*(JUN), 1–1. https://doi.org/10.3389/fmicb.2014.00207

Llewellyn, M. S., Leadbeater, S., Garcia, C., Sylvain, F. E., Custodio, M., Ang, K. P., Powell, F., Carvalho, G. R., Creer, S., Elliot, J., & Derome, N. (2017a).

Parasitism perturbs the mucosal microbiome of Atlantic Salmon. *Scientific Reports*, *7*, 1–10. https://doi.org/10.1038/srep43465

Llewellyn, M. S., Leadbeater, S., Garcia, C., Sylvain, F. E., Custodio, M., Ang, K. P., Powell, F., Carvalho, G. R., Creer, S., Elliot, J., & Derome, N. (2017b). Parasitism perturbs the mucosal microbiome of Atlantic Salmon. *Scientific Reports*, *7*, 1–10. https://doi.org/10.1038/srep43465

Llewellyn, M. S., McGinnity, P., Dionne, M., Letourneau, J., Thonier, F., Carvalho, G. R., Creer, S., & Derome, N. (2016). The biogeography of the atlantic salmon (Salmo salar) gut microbiome. *ISME Journal*, *10*(5), 1280–1284. https://doi.org/10.1038/ismej.2015.189

Lok, T., Overdijk, O., & Piersma, T. (2015). The cost of migration: Spoonbills suffer higher mortality during trans-Saharan spring migrations only. *Biology Letters*, *11*(1), 0–3. https://doi.org/10.1098/rsbl.2014.0944

Lovegrove, B. G. (2003). *The influence of climate on the basal metabolic rate of small mammals : a slow-fast metabolic continuum*. 87–112. https://doi.org/10.1007/s00360-002-0309-5

Luo, Y., & Xie, X. (2009). Comparative Biochemistry and Physiology , Part A Effects of body lipid content on the resting metabolic rate and postprandial metabolic response in the southern cat fi sh Silurus meridionalis. *Comparative Biochemistry and Physiology, Part A*, *154*(4), 547–550. https://doi.org/10.1016/j.cbpa.2009.08.020

Magnusson, A. K., & Dekker, W. (2021). Economic development in times of population decline - A century of European eel fishing on the Swedish west coast. *ICES Journal of Marine Science*, *78*(1), 185–198. https://doi.org/10.1093/icesjms/fsaa213

Maitland, P. S., & Adams, C. E. (2005). The aquatic fauna of the Loch Lomond area: what have we got; why is it important; how do we look after its future? *Glasgow Naturalist*, *24*(January), 23–28.

Marić, S., Nikolić, V., Tomović, L., & Simonović, P. (2011). Morphological differentiation of trout (subf. Salmoninae) based on characteristics of head skeleton. *Italian Journal of Zoology*, *78*(4), 455–463. https://doi.org/10.1080/11250003.2011.575405

Marino, J. A., Holland, M. P., & Middlemis Maher, J. (2014). Predators and trematode parasites jointly affect larval anuran functional traits and corticosterone levels. *Oikos*, *123*(4), 451–460. https://doi.org/10.1111/j.1600-0706.2013.00896.x

Masella, A. P., Bartram, A. K., Truszkowski, J. M., Brown, D. G., & Neufeld, J. D. (2012). PANDAseq: Paired-end assembler for illumina sequences. *BMC Bioinformatics*, *13*(1), 31. https://doi.org/10.1186/1471-2105-13-31

Mckechnie, A. E. (2019). *Phenotypic flexibility in basal metabolic rate and the changing view of avian physiological diversity : A review Phenotypic X exibility in basal metabolic rate and the changing view of avian physiological diversity : a review*. *April 2008*. https://doi.org/10.1007/s00360-007-0218-8

McKenzie, D. J., Cataldi, E., Romano, P., Taylor, E. W., Cataudella, S., & Bronzi, P. (2001). Effects of acclimation to brackish water on tolerance of salinity challenge by young-of-the-year Adriatic sturgeon (*Acipenser naccarii*). *Canadian Journal of Fisheries and Aquatic Sciences*, *58*(6), 1113–1121. https://doi.org/10.1139/cjfas-58-6-1113

McMurdie, P. J., & Holmes, S. (2013). Phyloseq: An R Package for Reproducible Interactive Analysis and Graphics of Microbiome Census Data. *PLoS ONE*, *8*(4). https://doi.org/10.1371/journal.pone.0061217

Melchers, W. J. G., Kuijpers, J., Sickler, J. J., & Rahamat-Langendoen, J. (2017). Lab-in-a-tube: Real-time molecular point-of-care diagnostics for influenza A and B using the cobas® Liat® system. *Journal of Medical Virology*, *89*(8), 1382–1386. https://doi.org/10.1002/jmv.24796

Mercier, C., Aubin, J., Lefrançois, C., & Claireaux, G. (2000). Cardiac disorders in farmed adult brown trout, Salmo trutta L. *Journal of Fish Diseases*, *23*(4),

243–249. https://doi.org/10.1046/j.1365-2761.2000.00237.x

Metcalfe, N. B., Leeuwen, T. E. Van, & Killen, S. S. (2016). *Does individual variation in metabolic phenotype predict fish behaviour and performance ?* 298–321. https://doi.org/10.1111/jfb.12699

Meyer, J. De, Maes, G. E., Dirks, R. P., & Adriaens, D. (2017). Differential gene expression in narrow- and broad-headed European glass eels (Anguilla anguilla) points to a transcriptomic link of head shape dimorphism with growth rate and chemotaxis. *ARPN Journal of Engineering and Applied Sciences*, *12*(10), 3218–3221. https://doi.org/10.1111/ijlh.12426

Minich, J. J., Power, C., Melanson, M., Knight, R., Webber, C., Rough, K., Bott, N. J., Nowak, B., & Allen, E. E. (2020). The Southern Bluefin Tuna Mucosal Microbiome Is Influenced by Husbandry Method, Net Pen Location, and Anti-parasite Treatment. *Frontiers in Microbiology*, *11*(August), 1–16. https://doi.org/10.3389/fmicb.2020.02015

Moczek, A. P., & Emlen, D. J. (1999). Proximate determination of male horn dimorphism in the beetle Onthophagus taurus (Coleoptera: Scarabaeidae). *Journal of Evolutionary Biology*, *12*(1), 27–37. https://doi.org/10.1046/j.1420-9101.1999.00004.x

Molnar, P., England, P., & Martinod, J. (1993). Mantle dynamics, uplift of the Tibetan Plateau, and the Indian Monsoon. *Reviews of Geophysics*, *31*(4), 357–396. https://doi.org/10.1029/93RG02030

Moreno, J., Cantarero, A., Plaza, M., & López-Arrabé, J. (2019). Phenotypic plasticity in breeding plumage signals in both sexes of a migratory bird: responses to breeding conditions. *Journal of Avian Biology*, *50*(3). https://doi.org/10.1111/jav.01855

Mossali, C., Palermo, S., Capra, E., Piccolo, G., Botti, S., Bandi, C., D'Amelio, S., & Giuffra, E. (2010). Sensitive detection and quantification of anisakid parasite residues in food products. *Foodborne Pathogens and Disease*, *7*(00), 391–397. https://doi.org/10.1089/fpd.2009.0428

Muñoz, P., Peñalver, J., Ruiz de Ybañez, R., & Garcia, J. (2015). Influence of adult Anguillicoloides crassus load in European eels swimbladder on macrophage response. *Fish and Shellfish Immunology*, *42*(2), 221–224. https://doi.org/10.1016/j.fsi.2014.11.011

Musing, L., Shiraishi, H., Crook, V., Gollock, M., Levy, E., & Kecse-Nagy, K. (2018). Implementation of the CITES Appendix II listing of European eel (Anguilla anguilla). In *CITES Annex 1* (Vol. 1, Issue November). https://cites.org/sites/default/files/eng/com/ac/30/E-AC30-18-01-A1.pdf

Nadler, L., Bengston, E., Hassibi, E., Hassibi, C., Øverli, Ø., & Hechinger, R. (2020). A brain-infecting parasite impacts host metabolism both during exposure and after infection is established. *Functional Ecology*.

Nadler, L. E., Bengston, E., Eliason, E. J., Hassibi, C., Ida, S. H. H., Garfield, B. J., Martin, T. K., Turner, A. V, Weinersmith, K. L., Øverli, Ø., & Hechinger, R. F. (2021). *A brain-infecting parasite impacts host metabolism both during exposure and after infection is established*. *March 2020*, 105–116. https://doi.org/10.1111/1365-2435.13695

Naya, D. E., Lardies, M. A., & Bozinovic, F. (2007). The effect of diet quality on physiological and life-history traits in the harvestman Pachylus paessleri. *Journal of Insect Physiology*, *53*(2), 132–138. https://doi.org/10.1016/j.jinsphys.2006.11.004

Neelima, P., Rao, N. G., Rao, G. S., & Sekhara Rao, J. C. (2016). A Study on Oxygen Consumption in a Freshwater Fish Cyprinus carpio Exposed to Lethal and Sublethal Concentrations of Cypermethrin (25%Ec). *International Journal of Current Microbiology and Applied Sciences*, *5*(4), 338–346. https://doi.org/10.20546/ijcmas.2016.504.040

Nelson, J. A. (2016). Oxygen consumption rate v. rate of energy utilization of fishes: A comparison and brief history of the two measurements. *Journal of Fish Biology*, *88*(1), 10–25. https://doi.org/10.1111/jfb.12824

Newbold, L. R., Hockley, F. A., Williams, C. F., Cable, J., Reading, A. J.,

Auchterlonie, N., & Kemp, P. S. (2015). Relationship between European eel Anguilla anguilla infection with non-native parasites and swimming behaviour on encountering accelerating flow. *Journal of Fish Biology*, *86*(5), 1519–1533. https://doi.org/10.1111/jfb.12659

Ni, J., Yan, Q., Yu, Y., & Zhang, T. (2014). Factors influencing the grass carp gut microbiome and its effect on metabolism. *FEMS Microbiology Ecology*, *87*(3), 704–714. https://doi.org/10.1111/1574-6941.12256

Nikolenko, S. I., Korobeynikov, A. I., & Alekseyev, M. A. (2013). BayesHammer: Bayesian clustering for error correction in single-cell sequencing. *BMC Genomics*, *14*(June 2014). https://doi.org/10.1186/1471-2164-14-S1-S7

Nikolova, C., Ijaz, U. Z., & Gutierrez, T. (2021). Exploration of marine bacterioplankton community assembly mechanisms during chemical dispersant and surfactant-assisted oil biodegradation. *Ecology and Evolution*, *11*(20), 13862–13874. https://doi.org/10.1002/ece3.8091

Nikouli, E., Kormas, K. A., Jin, Y., Olsen, Y., Bakke, I., & Vadstein, O. (2021). Dietary Lipid Effects on Gut Microbiota of First Feeding Atlantic Salmon (Salmo salar L.). *Frontiers in Marine Science*, *8*(May), 1–10. https://doi.org/10.3389/fmars.2021.665576

Norin, T., & Clark, T. D. (2016a). Measurement and relevance of maximum metabolic rate in fishes. In *Journal of Fish Biology* (Vol. 88, Issue 1, pp. 122–151). https://doi.org/10.1111/jfb.12796

Norin, T., & Clark, T. D. (2016b). Measurement and relevance of maximum metabolic rate in fishes. *Journal of Fish Biology*, *88*(1), 122–151. https://doi.org/10.1111/jfb.12796

Norin, T., & Malte, H. (2011). Repeatability of standard metabolic rate, active metabolic rate and aerobic scope in young brown trout during a period of moderate food availability. *Journal of Experimental Biology*, *214*(10), 1668–1675. https://doi.org/10.1242/jeb.054205

Norin, T., Malte, H., & Clark, T. D. (2014). Aerobic scope does not predict the performance of a tropical eurythermal fish at elevated temperatures. *Journal of Experimental Biology*, *217*(2), 244–251. https://doi.org/10.1242/jeb.089755

Odell, J. P., Chappell, M. A., & Dickson, K. A. (2003). *Morphological and enzymatic correlates of aerobic and burst performance in different populations of Trinidadian guppies Poecilia reticulata*. 3707–3718. https://doi.org/10.1242/jeb.00613

Osimani, A., Ferrocino, I., Agnolucci, M., Cocolin, L., Giovannetti, M., Cristani, C., Palla, M., Milanović, V., Roncolini, A., Sabbatini, R., Garofalo, C., Clementi, F., Cardinali, F., Petruzzelli, A., Gabucci, C., Tonucci, F., & Aquilanti, L. (2019). Unveiling hákarl: A study of the microbiota of the traditional Icelandic fermented fish. *Food Microbiology*, *82*, 560–572. https://doi.org/10.1016/j.fm.2019.03.027

Oufiero, C. E., & Whitlow, K. R. (2016a). The evolution of phenotypic plasticity in fish swimming. *Current Zoology*, *62*(5), 475–488. https://doi.org/10.1093/cz/zow084

Oufiero, C. E., & Whitlow, K. R. (2016b). The evolution of phenotypic plasticity in fish swimming. In *Current Zoology* (Vol. 62, Issue 5, pp. 475–488). https://doi.org/10.1093/cz/zow084

Pakkasmaa, S., Ranta, E., Piironen, J., Pakkasmaa, S., Ranta, E., & Ecology, I. (1998). A morphometric study on four land-locked salmonid species. *Finnish Zoological and Botanical Publishing Board*, *35*(3), 131–140.

Palstra, A. P., Schnabel, D., Nieveen, M. C., Spaink, H. P., & van den Thillart, G. (2010). Swimming suppresses hepatic vitellogenesis in European female silver eels as shown by expression of the estrogen receptor 1, vitellogenin1 and vitellogenin2 in the liver. *Reproductive Biology and Endocrinology*, *8*(March 2010). https://doi.org/10.1186/1477-7827-8-27

Pan, H., Li, Z., Xie, J., Liu, D., Wang, H., Yu, D., Zhang, Q., Hu, Z., & Shi, C.

(2019). Berberine influences blood glucose via modulating the gut microbiome in grass carp. *Frontiers in Microbiology*, *10*(MAY), 1–10. https://doi.org/10.3389/fmicb.2019.01066

Paoletti, M., Mattiucci, S., Colantoni, A., Levsen, A., Gay, M., & Nascetti, G. (2018). Species-specific Real Time-PCR primers/probe systems to identify fish parasites of the genera Anisakis, Pseudoterranova and Hysterothylacium (Nematoda: Ascaridoidea). *Fisheries Research*, *202*(February 2017), 38–48. https://doi.org/10.1016/j.fishres.2017.07.015

Papaiakovou, M., Wright, J., Pilotte, N., Chooneea, D., Schär, F., Truscott, J. E., Dunn, J. C., Gardiner, I., Walson, J. L., Williams, S. A., & Littlewood, D. T. J. (2019). Pooling as a strategy for the timely diagnosis of soil-transmitted helminths in stool: Value and reproducibility. *Parasites and Vectors*, *12*(1), 1–14. https://doi.org/10.1186/s13071-019-3693-3

Parata, L., Mazumder, D., Sammut, J., & Egan, S. (2020). Diet type influences the gut microbiome and nutrient assimilation of Genetically Improved Farmed Tilapia (Oreochromis niloticus). *PLoS ONE*, *15*(8 August), 1–16. https://doi.org/10.1371/journal.pone.0237775

Pavey, S. A., Gaudin, J., Normandeau, E., Dionne, M., Castonguay, M., Audet, C., & Bernatchez, L. (2015). RAD Sequencing Highlights Polygenic Discrimination of Habitat Ecotypes in the Panmictic American Eel. *Current Biology*, *25*(12), 1666–1671. https://doi.org/10.1016/j.cub.2015.04.062

Pedregosa, F., Varoquaux, G., Gramfort, A., Michel, V., Thirion, B., Grisel, O., Blondel, M., Prettenhofer, P., Weiss, R., Dubourg, V., Vanderplas, J., Passos, A., Cournapeau, D., Brucher, M., Perrot, M., & Duchesnay, É. (2011). Scikit-learn: Machine learning in Python. *Journal of Machine Learning Research*, *12*(January), 2825–2830.

Pelster, B. (2015). Swimbladder function and the spawning migration of the European eel Anguilla anguilla. *Frontiers in Physiology*, *6*(JAN), 1–10. https://doi.org/10.3389/fphys.2014.00486

Pérez, T., Balcázar, J. L., Ruiz-Zarzuela, I., Halaihel, N., Vendrell, D., De Blas, I., & Múezquiz, J. L. (2010). Host-microbiota interactions within the fish intestinal ecosystem. *Mucosal Immunology*, *3*(4), 355–360. https://doi.org/10.1038/mi.2010.12

Perry, W. B., Kaufmann, J., Solberg, M. F., Phillips, K. P., Egan, F., Leseur, F., Ryan, S., Poole, R., Rogan, G., Ryder, E., Schaal, P., Waters, C., Wynne, R., Taylor, M., Paulo, P., Simon, C., Martin, L., McGinnity, P., Carvalho, G., & Glover, K. A. (2021). Domestication-induced reduction in eye size revealed in multiple common garden experiments: The case of Atlantic salmon (Salmo salar L.). *Evolutionary Applications*, *14*, 2319–2332.

Perry, W. B., Lindsay, E., Payne, C. J., Brodie, C., & Kazlauskaite, R. (2020). The role of the gut microbiome in sustainable teleost aquaculture. *Proceedings of the Royal Society B: Biological Sciences*, *287*(1926). https://doi.org/10.1098/rspb.2020.0184

Perry, W. B., Solberg, M. F., Besnier, F., Dyrhovden, L., Matre, I. H., Fjelldal, P. G., Ayllon, F., Creer, S., Llewellyn, M., Taylor, M. I., Carvalho, G., & Glover, K. A. (2019). Evolutionary drivers of kype size in atlantic salmon (salmo salar): domestication, age and genetics. *Royal Society Open Science*, *6*(4). https://doi.org/10.1098/rsos.190021

Phil, B., DEKINGA, A., DIETZ, M. W., PIERSMA, T., TANG, S., & HULSMAN, A. K. (2001). BASAL METABOLIC RATE DECLINES DURING LONG-DISTANCE MIGRATORY FLIGHT IN GREAT KNOTS. *The Cooper Ornithologica*, *103*(4), 838–845.

Piazzon, M. C., Calduch-Giner, J. A., Fouz, B., Estensoro, I., Simó-Mirabet, P., Puyalto, M., Karalazos, V., Palenzuela, O., Sitjà-Bobadilla, A., & Pérez-Sánchez, J. (2017). Under control: how a dietary additive can restore the gut microbiome and proteomic profile, and improve disease resilience in a marine teleostean fish fed vegetable diets. *Microbiome*, *5*(1), 164. https://doi.org/10.1186/s40168-017-0390-3

Piazzon, M. C., Estensoro, I., Calduch-Giner, J. A., Del Pozo, R., Picard-Sánchez, A., Pérez-Sánchez, J., & Sitjà-Bobadilla, A. (2018). Hints on T cell responses in a fish-parasite model: Enteromyxum leei induces differential expression of T cell signature molecules depending on the organ and the infection status. *Parasites and Vectors*, *11*(1), 1–18. https://doi.org/10.1186/s13071-018-3007-1

Pilakouta, N., Killen, S. S., Kristjánsson, B. K., Skúlason, S., Lindström, J., Metcalfe, N. B., & Parsons, K. J. (2020). Multigenerational exposure to elevated temperatures leads to a reduction in standard metabolic rate in the wild. *Functional Ecology*, *34*(6), 1205–1214. https://doi.org/10.1111/1365-2435.13538

Polverino, G., Bierbach, D., Killen, S. S., Uusi-Heikkilä, S., & Arlinghaus, R. (2016). Body length rather than routine metabolic rate and body condition correlates with activity and risk-taking in juvenile zebrafish Danio rerio. *Journal of Fish Biology*, *89*(5), 2251–2267. https://doi.org/10.1111/jfb.13100

Pouder, D. B., Curtis, E. W., & Yanong, R. P. E. (2009). *Common Freshwater Fish Parasites Pictorial Guide*. 109–112.

Price, M. N., Dehal, P. S., & Arkin, A. P. (2010). FastTree 2 - Approximately maximum-likelihood trees for large alignments. *PLoS ONE*, *5*(3). https://doi.org/10.1371/journal.pone.0009490

Proman, J. M., & Reynolds, J. D. (2000). Differences in head shape of the European eel, Anguilla anguilla (L.). *Fisheries Management and Ecology*, *7*(4), 349–354. https://doi.org/10.1046/j.1365-2400.2000.00207.x

Pujolar, J. M., Bevacqua, D., Andrello, M., Capoccioni, F., Ciccotti, E., De Leo, G. A., & Zane, L. (2011). Genetic patchiness in European eel adults evidenced by molecular genetics and population dynamics modelling. *Molecular Phylogenetics and Evolution*, *58*(2), 198–206. https://doi.org/10.1016/j.ympev.2010.11.019

Quast, C., Pruesse, E., Yilmaz, P., Gerken, J., Schweer, T., Yarza, P., Peplies, J.,

& Glöckner, F. O. (2013). The SILVA ribosomal RNA gene database project: Improved data processing and web-based tools. *Nucleic Acids Research*, *41*(D1), 590–596. https://doi.org/10.1093/nar/gks1219

Ramírez, C., & Romero, J. (2017). The Microbiome of Seriola lalandi of Wild and Aquaculture Origin Reveals Differences in Composition and Potential Function. *Frontiers in Microbiology*, *8*(SEP), 1–10. https://doi.org/10.3389/fmicb.2017.01844

Rasmussen, J. A., Villumsen, K. R., Duchêne, D. A., Puetz, L. C., Delmont, T. O., Sveier, H., Jørgensen, L. von G., Præbel, K., Martin, M. D., Bojesen, A. M., Gilbert, M. T. P., Kristiansen, K., & Limborg, M. T. (2021). Genome-resolved metagenomics suggests a mutualistic relationship between Mycoplasma and salmonid hosts. *Communications Biology*, *4*(1), 1–10. https://doi.org/10.1038/s42003-021-02105-1

Reid, D., Armstrong, J. D., & Metcalfe, N. B. (2011). Estimated standard metabolic rate interacts with territory quality and density to determine the growth rates of juvenile Atlantic salmon. *Functional Ecology*, *25*(6), 1360–1367. https://doi.org/10.1111/j.1365-2435.2011.01894.x

Reid, D., Armstrong, J. D., & Metcalfe, N. B. (2012). The performance advantage of a high resting metabolic rate in juvenile salmon is habitat dependent. *Journal of Animal Ecology*, *81*(4), 868–875. https://doi.org/10.1111/j.1365-2656.2012.01969.x

Rennison, D. J., Rudman, S. M., & Schluter, D. (2019). Parallel changes in gut microbiome composition and function during colonization, local adaptation and ecological speciation. *Proceedings of the Royal Society B: Biological Sciences*, *286*(1916). https://doi.org/10.1098/rspb.2019.1911

Righton, D., & Walker, A. M. (2013). Anguillids: Conserving a global fisherya. *Journal of Fish Biology*, *83*(4), 754–765. https://doi.org/10.1111/jfb.12157

Righton, D., Westerberg, H., Feunteun, E., Økland, F., Gargan, P., Amilhat, E., Metcalfe, J., Lobon-Cervia, J., Sjöberg, N., Simon, J., Acou, A., Vedor, M.,

Walker, A., Trancart, T., Brämick, U., & Aarestrup, K. (2016). Empirical observations of the spawning migration of European eels: The long and dangerous road to the Sargasso Sea. *Science Advances*, *2*(10), 1–14. https://doi.org/10.1126/sciadv.1501694

Rimoldi, S., Torrecillas, S., Montero, D., Gini, E., Makol, A., Victoria Valdenegro, V., Izquierdo, M., & Terova, G. (2020). Assessment of dietary supplementation with galactomannan oligosaccharides and phytogenics on gut microbiota of European sea bass (Dicentrarchus Labrax) fed low fishmeal and fish oil based diet. *PLoS ONE*, *15*(4), 1–30. https://doi.org/10.1371/journal.pone.0231494

Robar, N., Murray, D., & Burness, G. (2011a). Effects of parasites on host energy expenditure: The resting metabolic rate stalemate. *Canadian Journal of Zoology*, *89*(11), 1146–1155. https://doi.org/10.1139/z11-084

Robar, N., Murray, D. L., & Burness, G. (2011b). *Effects of parasites on host energy expenditure : the resting metabolic rate stalemate*. *April 2015*. https://doi.org/10.1139/z11-084

Robertsen, G., Reid, D., Einum, S., Aronsen, T., Fleming, I. A., Sundt-Hansen, L. E., Karlsson, S., Kvingedal, E., Ugedal, O., & Hindar, K. (2019). Can variation in standard metabolic rate explain context-dependent performance of farmed Atlantic salmon offspring? In *Ecology and Evolution* (Vol. 9, Issue 1, pp. 212–222). https://doi.org/10.1002/ece3.4716

Rognes, T., Flouri, T., Nichols, B., Quince, C., & Mahé, F. (2016). VSEARCH: A versatile open source tool for metagenomics. *PeerJ*, *2016*(10), 1–22. https://doi.org/10.7717/peerj.2584

Rohlf, F. J. (2015). The tps series of software. *Hystrix*, *26*(1), 1–4. https://doi.org/10.4404/hystrix-26.1-11264

Rohlf, F. J., & Slice, D. (1990). Extensions of the procrustes method for the optimal superimposition of landmarks. *Systematic Zoology*, *39*(1), 40–59. https://doi.org/10.2307/2992207

Rosenfeld, J., Van Leeuwen, T., Richards, J., & Allen, D. (2015). Relationship between growth and standard metabolic rate: Measurement artefacts and implications for habitat use and life-history adaptation in salmonids. *Journal of Animal Ecology*, *84*(1), 4–20. https://doi.org/10.1111/1365-2656.12260

Rosewarne, P. J., Wilson, J. M., & Svendsen, J. C. (2016a). Measuring maximum and standard metabolic rates using intermittent-flow respirometry: A student laboratory investigation of aerobic metabolic scope and environmental hypoxia in aquatic breathers. *Journal of Fish Biology*, *88*(1), 265–283. https://doi.org/10.1111/jfb.12795

Rosewarne, P. J., Wilson, J. M., & Svendsen, J. C. (2016b). Measuring maximum and standard metabolic rates using intermittent-flow respirometry: A student laboratory investigation of aerobic metabolic scope and environmental hypoxia in aquatic breathers. *Journal of Fish Biology*, *88*(1), 265–283. https://doi.org/10.1111/jfb.12795

Rossignol, O., Dodson, J. J., & Guderley, H. (2011). Relationship between metabolism, sex and reproductive tactics in young Atlantic salmon (Salmo salar L.). *Comparative Biochemistry and Physiology - A Molecular and Integrative Physiology*, *159*(1), 82–91. https://doi.org/10.1016/j.cbpa.2011.01.023

Rowland, I., Gibson, G., Heinken, A., Scott, K., Swann, J., Thiele, I., & Tuohy, K. (2018). Gut microbiota functions: metabolism of nutrients and other food components. *European Journal of Nutrition*, *57*(1), 1–24. https://doi.org/10.1007/s00394-017-1445-8

Ryberg, M. P., Skov, P. V., Vendramin, N., Buchmann, K., Nielsen, A., & Behrens, J. W. (2020). Physiological condition of Eastern Baltic cod, Gadus morhua, infected with the parasitic nematode Contracaecum osculatum. *Conservation Physiology*, *8*(1), 1–14. https://doi.org/10.1093/conphys/coaa093

Ryu, T., Veilleux, H. D., Munday, P. L., Jung, I., Donelson, J. M., & Ravasi, T. (2020). An Epigenetic Signature for Within-Generational Plasticity of a Reef

Fish to Ocean Warming. *Frontiers in Marine Science*, *7*(April), 1–15. https://doi.org/10.3389/fmars.2020.00284

Sancho, E., Andreau, O., Villarroel, M. J., Fernández-Vega, C., Tecles, F., Martínez-Subiela, S., Cerón, J. J., & Ferrando, M. D. (2017). European eel (anguilla anguilla) plasma biochemistry alerts about propanil stress. *Journal of Pesticide Science*, *42*(1), 7–15. https://doi.org/10.1584/jpestics.D16-062

Sandlund, O. T., Diserud, O. H., Poole, R., Bergesen, K., Dillane, M., Rogan, G., Durif, C., Thorstad, E. B., & Vøllestad, L. A. (2017). Timing and pattern of annual silver eel migration in two European watersheds are determined by similar cues. In *Ecology and Evolution* (Vol. 7, Issue 15, pp. 5956–5966). https://doi.org/10.1002/ece3.3099

Sandoval-Motta, S., Aldana, M., & Frank, A. (2018). Evolving Ecosystems: Inheritance and Selection in the Light of the Microbiome. *Archives of Medical Research*, 1–10. https://doi.org/10.1016/j.arcmed.2018.01.002

Sandoval, C. P. (1994). Plasticity in Web Design in the Spider Parawixia bistriata: A Response to Variable Prey Type. *Functional Ecology*, *8*(6), 701. https://doi.org/10.2307/2390229

Santana, C. A., Andrade, L. H. C., Súarez, Y. R., Yukimitu, K., Moraes, J. C. S., & Lima, S. M. (2015). Fourier transform-infrared photoacoustic spectroscopy applied in fish scales to access environmental integrity: A case study of Astyanax altiparanae species. *Infrared Physics and Technology*, *72*(July 2015), 84–89. https://doi.org/10.1016/j.infrared.2015.07.005

Santos, A. T., Sasal, P., Verneau, O., & Lenfant, P. (2006). A method to detect the parasitic nematodes from the family Anisakidae, in Sardina pilchardus, using specific primers of 18 S DNA gene. *European Food Research and Technology*, *222*(1–2), 71–77. https://doi.org/10.1007/s00217-005-0052-8

Schabuss, M., Kennedy, C. R., Konecny, R., Grillitsch, B., Reckendorfer, W., Schiemer, F., & Herzig, a. (2005). Dynamics and predicted decline of Anguillicola crassus infection in European eels, Anguilla anguilla, in

Neusiedler See, Austria. *Journal of Helminthology*, *79*(2), 159–167. https://doi.org/10.1079/JOH2005281

Schabuss, M., Kennedy, C. R., Konecny, R., Grillitsch, B., Schiemer, F., & Herzig, A. (2005a). Long-term investigation of the composition and richness of intestinal helminth communities in the stocked population of eel, Anguilla anguilla, in Neusiedler See, Austria. *Parasitology*, *130*(2), 185–194. https://doi.org/10.1017/S0031182004006444

Schabuss, M., Kennedy, C. R., Konecny, R., Grillitsch, B., Schiemer, F., & Herzig, A. (2005b). Long-term investigation of the composition and richness of intestinal helminth communities in the stocked population of eel, Anguilla anguilla, in Neusiedler See, Austria. *Parasitology*, *130*(2), 185–194. https://doi.org/10.1017/S0031182004006444

Scharnweber, K., Chaguaceda, F., & Eklöv, P. (2021). Fatty acid accumulation in feeding types of a natural freshwater fish population. *Oecologia*, *196*(1), 53–63. https://doi.org/10.1007/s00442-021-04913-y

Schmidt, V. T., Smith, K. F., Melvin, D. W., & Amaral-Zettler, L. A. (2015). Community assembly of a euryhaline fish microbiome during salinity acclimation. *Molecular Ecology*, *24*(10), 2537–2550. https://doi.org/10.1111/mec.13177

Schneebauer, G., Dirks, R. P., & Pelster, B. (2017). Anguillicola crassus infection affects mRNA expression levels in gas gland tissue of European yellow and silver eel. *PLoS ONE*, *12*(8), 1–26. https://doi.org/10.1371/journal.pone.0183128

Sehnal, L., Brammer-robbins, E., Wormington, A. M., & Grim, C. J. (2021). *Microbiome Composition and Function in Aquatic Vertebrates : Small Organisms Making Big Impacts on Aquatic Animal Health*. *12*(March). https://doi.org/10.3389/fmicb.2021.567408

Sekirov, I., Russell, S. L., Caetano M Antunes, L., & Finlay, B. B. (2010). Gut microbiota in health and disease. *Physiological Reviews*, *90*(3), 859–904.

https://doi.org/10.1152/physrev.00045.2009

Selim, K. M., & El-ashram, A. M. (2012). *STUDIES ON ANGUILLICOLIASIS OF CULTURED EEL (ANGUILLA ANGUILLA) IN EGYPT*. *5*, 409–425.

Sellyei, B., Varga, Z., Cech, G., Varga, Á., & Székely, C. (2021). Mycoplasma infections in freshwater carnivorous fishes in Hungary. *Journal of Fish Diseases*, *44*(3), 297–304. https://doi.org/10.1111/jfd.13283

Semova, I., Carten, J. D., Stombaugh, J., MacKey, L. C., Knight, R., Farber, S. A., & Rawls, J. F. (2012). Microbiota regulate intestinal absorption and metabolism of fatty acids in the zebrafish. *Cell Host and Microbe*, *12*(3), 277–288. https://doi.org/10.1016/j.chom.2012.08.003

Seppänen, E., Piironen, J., & Huuskonen, H. (2009). Standard metabolic rate, growth rate and smolting of the juveniles in three Atlantic salmon stocks. *Boreal Environment Research*, *14*(3), 369–381.

Seppänen, E., Piironen, J., & Huuskonen, H. (2010). Comparative Biochemistry and Physiology , Part A Consistency of standard metabolic rate in relation to life history strategy of juvenile Atlantic salmon Salmo salar. *Comparative Biochemistry and Physiology, Part A*, *156*(2), 278–284. https://doi.org/10.1016/j.cbpa.2010.02.014

Serra, C. R., Oliva-Teles, A., Enes, P., & Tavares, F. (2021). Gut microbiota dynamics in carnivorous European seabass (Dicentrarchus labrax) fed plant-based diets. *Scientific Reports*, *11*(1), 1–13. https://doi.org/10.1038/s41598-020-80138-y

Sheng, M., Gorzsás, A., & Tuck, S. (2016). Fourier transform infrared microspectroscopy for the analysis of the biochemical composition of C. elegans worms . *Worm*, *5*(1), e1132978. https://doi.org/10.1080/21624054.2015.1132978

Shental, N., Levy, S., Wuvshet, V., Skorniakov, S., Shalem, B., Ottolenghi, A., Greenshpan, Y., Steinberg, R., Edri, A., Gillis, R., Goldhirsh, M., Moscovici,

K., Sachren, S., Friedman, L. M., Nesher, L., Shemer-Avni, Y., Porgador, A., & Hertz, T. (2020). Efficient high-throughput SARS-CoV-2 testing to detect asymptomatic carriers. *Science Advances*, *6*(37). https://doi.org/10.1126/sciadv.abc5961

Simon, J., Westerberg, H., Righton, D., Sjöberg, N. B., & Dorow, M. (2018). Diving activity of migrating silver eel with and without Anguillicola crassus infection. *Journal of Applied Ichthyology*, *December 2017*, 1–10. https://doi.org/10.1111/jai.13626

Simonsen, M. K., Siwertsson, A., Adams, C. E., Amundsen, P. A., Præbel, K., & Knudsen, R. (2017). Allometric trajectories of body and head morphology in three sympatric Arctic charr (Salvelinus alpinus (L.)) morphs. *Ecology and Evolution*, *7*(18), 7277–7289. https://doi.org/10.1002/ece3.3224

Sleezer, L. J., Angermeier, P. L., Frimpong, E. A., & Brown, B. L. (2021). A new composite abundance metric detects stream fish declines and community homogenization during six decades of invasions. *Diversity and Distributions*, *27*(11), 2136–2156. https://doi.org/10.1111/ddi.13393

Solem, O., & Berg, O. K. (2011). Morphological differences in parr of Atlantic salmon Salmo salar from three regions in Norway. *Journal of Fish Biology*, *78*(5), 1451–1469. https://doi.org/10.1111/j.1095-8649.2011.02950.x

Sommer, F., Ståhlman, M., Ilkayeva, O., Arnemo, J. M., Kindberg, J., Josefsson, J., Newgard, C. B., Fröbert, O., & Bäckhed, F. (2016). The Gut Microbiota Modulates Energy Metabolism in the Hibernating Brown Bear Ursus arctos. *Cell Reports*, *14*(7), 1655–1661. https://doi.org/10.1016/j.celrep.2016.01.026

Sommer, R. J. (2020). Phenotypic plasticity: From theory and genetics to current and future challenges. *Genetics*, *215*(1), 1–13. https://doi.org/10.1534/genetics.120.303163

Ssekagiri, A., T. Sloan, W., & Zeeshan Ijaz, U. (2017). microbiomeSeq: An R package for analysis of microbial communities in an environmental context. *ISCB Africa ASBCB Conference*, *December*.

https://doi.org/10.13140/RG.2.2.17108.71047

Stauffer, J. R., & van Snik Gray, E. (2004). Phenotypic plasticity: Its role in trophic radiation and explosive speciation in cichlids (Teleostei: Cichlidae). *Animal Biology*, *54*(2), 137–158. https://doi.org/10.1163/1570756041445191

Steinhausen, M. F., Steffensen, J. F., & Andersen, N. G. (2007). The relationship between caudal differential pressure and activity of Atlantic cod: A potential method to predict oxygen consumption of free-swimming fish. *Journal of Fish Biology*, *71*(4), 957–969. https://doi.org/10.1111/j.1095-8649.2007.01563.x

Stephens, W. Z., Burns, A. R., Stagaman, K., Wong, S., Rawls, J. F., Guillemin, K., & Bohannan, B. J. M. (2016). The composition of the zebrafish intestinal microbial community varies across development. *ISME Journal*, *10*(3), 644–654. https://doi.org/10.1038/ismej.2015.140

Steury, R. A., Currey, M. C., Cresko, W. A., & Bohannan, B. J. M. (2019). Population genetic divergence and environment influence the gut microbiome in oregon threespine stickleback. *Genes*, *10*(7). https://doi.org/10.3390/genes10070484

Stojanović, M., Apostolović, M., Stojanović, D., Milošević, Z., Toplaović, A., Lakušić, V. M., & Golubović, M. (2014). Understanding sensitivity, Specificity and predictive values. *Vojnosanitetski Pregled*, *71*(11), 1062–1065. https://doi.org/10.2298/VSP1411062S

Suarez, F. L., Springfield, J., & Levitt, M. D. (1998). Identification of gases responsible for the odour of human flatus and evaluation of a device purported to reduce this odour. *Gut*, *43*(1), 100–404. https://doi.org/10.1136/gut.43.1.100

Tarnecki, A. M., Burgos, F. A., Ray, C. L., & Arias, C. R. (2017). Fish intestinal microbiome: diversity and symbiosis unravelled by metagenomics. *Journal of Applied Microbiology*, *123*(1), 2–17. https://doi.org/10.1111/jam.13415

Thapana, C., Sothorn, A., & Thanawan, T. (2018). The rapid detection method by

polymerase chain reaction for minute intestinal trematodes: Haplorchis taichui in intermediate snail hosts based on 18s ribosomal DNA. *Journal of Parasitic Diseases*, *42*(3), 423–432. https://doi.org/10.1007/s12639-018-1020-0

Thierry-Mieg, N., & Bailly, G. (2008). Interpool: Interpreting smart-pooling results. *Bioinformatics*, *24*(5), 696–703. https://doi.org/10.1093/bioinformatics/btn001

Thomas A. Hall. (2017). BioEdit: user-friendly biological sequebce alignment editor and analysis program for windows 95/98/NT. In *Nucleic Acid Symposium* (Vol. 4, Issue 11, pp. 1881–1887). https://doi.org/10.1039/c7qi00394c

Thorn, G. W., Goldstein, J. L., Scriver, C. R., Eisen, H. N., Kunkel, H. G., Rich, A., & Steiner, D. F. (2012). Defining the Human Microbiome. *New England Journal of Medicine*, *299*(23), 1278–1280. https://doi.org/10.1056/nejm197812072992304

Tirsgaard, B., Behrens, J. W., & Steffensen, J. F. (2015). The effect of temperature and body size on metabolic scope of activity in juvenile Atlantic cod Gadus morhua L. *Comparative Biochemistry and Physiology -Part A : Molecular and Integrative Physiology*, *179*(September 2018), 89–94. https://doi.org/10.1016/j.cbpa.2014.09.033

Tudorache, C., Blust, R., & De Boeck, G. (2007). Swimming capacity and energetics of migrating and non-migrating morphs of three-spined stickleback Gasterosteus aculeatus L. and their ecological implications. *Journal of Fish Biology*, *71*(5), 1448–1456. https://doi.org/10.1111/j.1095-8649.2007.01612.x

Tudorache, C., Burgerhout, E., Brittijn, S., & van den Thillart, G. (2015). Comparison of swimming capacity and energetics of migratory European eel (Anguilla anguilla) and New Zealand short-finned eel (A. australis). *Frontiers in Physiology*, *6*(SEP), 1–7. https://doi.org/10.3389/fphys.2015.00256

Urbina, M. A., & Glover, C. N. (2013). Relationship between fish size and metabolic rate in the oxyconforming inanga Galaxias maculatus reveals size-dependent strategies to withstand hypoxia. *Physiological and Biochemical Zoology*, *86*(6), 740–749. https://doi.org/10.1086/673727

van den Thillart, G., Dufour, S., & Rankin, J. C. (2009). Spawning Migration of the European Eel. In *Fish & Fisheries Series volume 30*. http://fishlarvae.org/common/SiteMedia/durif et al_2009.pdf

van Ginneken, V. J. T., & Maes, G. E. (2005). The European eel (Anguilla anguilla, Linnaeus), its lifecycle, evolution and reproduction: A literature review. *Reviews in Fish Biology and Fisheries*, *15*(4), 367–398. https://doi.org/10.1007/s11160-006-0005-8

Van Leeuwen, T. E., Killen, S. S., Metcalfe, N. B., & Adams, C. E. (2017). Differences in early developmental rate and yolk conversion efficiency in offspring of trout with alternative life histories. *Ecology of Freshwater Fish*, *26*(3), 371–382. https://doi.org/10.1111/eff.12281

Vasemägi, A., Visse, M., & Kisandd, V. (2017). Effect of Environmental Factors and an Emerging Parasitic Disease on Gut Microbiome of Wild Salmonid Fish. *MSphere*, *2*(6), 1–13.

Venney, C. J., Wellband, K. W., & Heath, D. D. (2021). Rearing environment affects the genetic architecture and plasticity of DNA methylation in Chinook salmon. *Heredity*, *126*(1), 38–49. https://doi.org/10.1038/s41437-020-0346-4

Vieira, M. L. C., Santini, L., Diniz, A. L., & Munhoz, C. de F. (2016). Microsatellite markers: What they mean and why they are so useful. *Genetics and Molecular Biology*, *39*(3), 312–328. https://doi.org/10.1590/1678-4685-GMB-2016-0027

Volff, J. N. (2005). Genome evolution and biodiversity in teleost fish. *Heredity*, *94*(3), 280–294. https://doi.org/10.1038/sj.hdy.6800635

Volynets, V., Louis, S., Pretz, D., Lang, L., Ostaff, M. J., Wehkamp, J., & Bischoff,

S. C. (2017). Intestinal Barrier Function and the GutMicrobiome Are Differentially Affected in MiceFed a Western-Style Diet or Drinking WaterSupplemented with Fructose. *The Journal of Nutrition*.

Wagner, G. N., Kuchel, L. J., Lotto, A., Patterson, D. A., Shrimpton, J. M., Hinch, S. G., & Farrell, A. P. (2006). Routine and active metabolic rates of migrating adult wild sockeye salmon (Oncorhynchus nerka Walbaum) in seawater and freshwater. *Physiological and Biochemical Zoology*, *79*(1), 100–108. https://doi.org/10.1086/498186

Walker, J. A. (1997). Ecological morphology of lacustrine threespine stickleback Gasterosteus aculeatus L. (Gasterosteidae) body shape. *Biological Journal of the Linnean Society*, *61*(1), 3–50. https://doi.org/10.1006/bijl.1996.9999

Wang, J., Kortner, T. M., Chikwati, E. M., Li, Y., Jaramillo-Torres, A., Jakobsen, J. V., Ravndal, J., Brevik, Ø. J., Einen, O., & Krogdahl, Å. (2020). Gut immune functions and health in Atlantic salmon (Salmo salar) from late freshwater stage until one year in seawater and effects of functional ingredients: A case study from a commercial sized research site in the Arctic region. *Fish and Shellfish Immunology*, *106*, 1106–1119. https://doi.org/10.1016/j.fsi.2020.09.019

Weclawski, U., Heitlinger, E. G., Baust, T., Klar, B., Petney, T., Han, Y. S., & Taraschewski, H. (2013). Evolutionary divergence of the swim bladder nematode Anguillicola crassus after colonization of a novel host, Anguilla anguilla. *BMC Evolutionary Biology*, *13*(1). https://doi.org/10.1186/1471-2148-13-78

Westley, P. A. H., Stanley, R., & Fleming, I. A. (2013). Experimental tests for heritable morphological color plasticity in non-native brown trout (Salmo trutta) populations. *PLoS ONE*, *8*(11). https://doi.org/10.1371/journal.pone.0080401

Wielgoss, S., Taraschewski, H., Meyer, A., & Wirth, T. (2008). Population structure of the parasitic nematode Anguillicola crassus, an invader of declining North

Atlantic eel stocks. *Molecular Ecology*, *17*(15), 3478–3495. https://doi.org/10.1111/j.1365-294X.2008.03855.x

Wintzer, A. P., & Motta, P. J. (2005). A comparison of prey capture kinematics in hatchery and wild Micropterus salmoides floridanus: Effects of ontogeny and experience. *Journal of Fish Biology*, *67*(2), 409–427. https://doi.org/10.1111/j.0022-1112.2005.00748.x

Woodcock, S., Van Der Gast, C. J., Bell, T., Lunn, M., Curtis, T. P., Head, I. M., & Sloan, W. T. (2007). Neutral assembly of bacterial communities. *FEMS Microbiology Ecology*, *62*(2), 171–180. https://doi.org/10.1111/j.1574-6941.2007.00379.x

Wynne, J. W., Thakur, K. K., Slinger, J., Samsing, F., Milligan, B., Powell, J. F. F., McKinnon, A., Nekouei, O., New, D., Richmond, Z., Gardner, I., & Siah, A. (2020). Microbiome Profiling Reveals a Microbial Dysbiosis During a Natural Outbreak of Tenacibaculosis (Yellow Mouth) in Atlantic Salmon. *Frontiers in Microbiology*, *11*(October), 1–12. https://doi.org/10.3389/fmicb.2020.586387

Xiang, Z., Zhu, H., Yang, B., Fan, H., Guo, J., Liu, J., Kong, Q., Teng, Q., Shang, H., Su, L., & Qin, C. (2020). A glance at the gut microbiota of five experimental animal species through fecal samples. *Scientific Reports*, *10*(1), 1–11. https://doi.org/10.1038/s41598-020-73985-2

Yoshii, K., Hosomi, K., Sawane, K., & Kunisawa, J. (2019). Metabolism of dietary and microbial vitamin b family in the regulation of host immunity. *Frontiers in Nutrition*, *6*(April), 1–12. https://doi.org/10.3389/fnut.2019.00048

Zaremba, L. S., & Smoleński, W. H. (2000). Optimal portfolio choice under a liability constraint. *Annals of Operations Research*, *97*(1–4), 131–141. https://doi.org/10.1023/A

Zeng, Q., Sukumaran, J., Wu, S., & Rodrigo, A. (2015). Neutral Models of Microbiome Evolution. *PLoS Computational Biology*, *11*(7), 1–18. https://doi.org/10.1371/journal.pcbi.1004365

Zenimoto, K., Sasai, Y., Sasaki, H., & Kimura, S. (2011). Estimation of larval duration in Anguilla spp., based on cohort analysis, otolith microstructure, and Lagrangian simulations. *Marine Ecology Progress Series*, *438*(June 2007), 219–228. https://doi.org/10.3354/meps09255

Zhao, R., Symonds, J. E., Walker, S. P., Steiner, K., Carter, C. G., Bowman, J. P., & Nowak, B. F. (2020). Salinity and fish age affect the gut microbiota of farmed Chinook salmon (Oncorhynchus tshawytscha). *Aquaculture*, *528*(February), 735539. https://doi.org/10.1016/j.aquaculture.2020.735539

Zou, Y., Mason, M. G., Wang, Y., Wee, E., Turni, C., Blackall, P. J., Trau, M., & Botella, J. R. (2017). Nucleic acid purification from plants, animals and microbes in under 30 seconds. *PLoS Biology*, *15*(11), 1–22. https://doi.org/10.1371/journal.pbio.2003916